AN ANALYSIS OF THE SPIRAL SPRING

by

W. A. C. SWIFT, B.Sc., M.Eng.

A thesis submitted to the University of Sheffield
for the degree of Doctor of Philosophy

Department of Mechanical Engineering,
The University of Sheffield.

July, 1971.

ACKNOWLEDGEMENTS

The research reported in this thesis arose out of discussions with Dr. Siegfried Gross in 1962 regarding the short-comings of clock-spring theory. It is a pity that Dr. Gross died a few months before this thesis was submitted. I am sure that he would have derived much pleasure from perusing its contents as, indeed, he did when I published a short paper verifying the theory in 1965.+

My thanks are due to Mr. J. D. Trott and the workshop staff of the Department of Mechanical Engineering at the University of Sheffield for help over the years in building and modifying experimental rigs, to my Head of Department, Professor J. K. Royle, for his frequent reminders regarding my Ph.D. project, to Mrs. P. M. Windle for the typing of the thesis and to Mr. A. D. Butler for his assistance in assembling it. Also, I have to thank the Spring Research Association and its staff for arranging the supply of springs for testing and of strip material for the winding experiments.

W. A. C. Swift,

July 1971.

+ SWIFT, W. A. C. Verification of the Gross Theory for Clock-type springs - Wire; 77; 1965.

SUMMARY

This thesis reports what is believed to be a new approach to the analysis of the spiral (clock-type) spring based on a re-thinking of the fundamental equations.

Detailed examination of this type of spring has led to the discovery that the free spiral form approximates to a logarithmic spiral. Methods of examining the free spiral form are described and what are thought to be unique methods of determining its equation are presented.

Knowledge of the spiral equation enables the moment-rotation characteristic to be constructed which is then compared with experimental results obtained on a testing machine designed by the author. This machine allows measurements of torque to be obtained without introducing machine friction. It has been designed to allow autographic recordings to be made of the spring test.

Prediction of the spiral equation from consideration of the elastic-plastic behaviour of an idealised material has been achieved and charts have been produced which will facilitate this prediction. The relationship between the back-tension during winding and the free spiral form has also been investigated.

A further research programme has been outlined which, together with the present findings, should lead to a complete understanding of the mechanics of the spiral-spring forming process however performed.

CONTENTS

CONTENTS (continued)

CONTENTS (continued)

CONTENTS (continued)

CONTENTS (continued)

PREFACE

The spring industry is seldom given the credit it deserves for the part it plays in modern technology. Its products often disappear into the remote inaccessible regions of complex mechanisms, sometimes never to reappear but never-the-less to function as they were designed to do throughout their working lives. Some of the products of the spring industry spend their lives exposed for all to see but subjected to an environment in which no other mechanical device would be expected to function.

Mechanisms in which springs find a use appear to be designed specially to frustrate the spring manufacturer who, at this stage, is usually given the credit of being the expert. In the majority of new designs it appears that the springs are the last components to be considered and, apparently with no malice aforethought, the space available is always insufficient to allow the spring to meet its specification. Furthermore the supply of the springs for the prototype always falls in the category 'urgent'. There is little wonder that the spring designer tends to rely on his past experience when designing a new spring. It seems inevitable that he is forced into designing for higher and higher working stresses and faster working cycles.

This thesis forms part of a more extensive field of research in which the effects of prestressing of springs is being investigated. The aim of the prestressing is to produce within the material residual stresses which are of the opposite sense to the normal working stresses. There are, in fact, two advantages

to be gained if the residual stress pattern is as desired. First, the working load can be increased without increasing the maximum permissible stresses. Unfortunately, the penalty paid for this concession is that operation must be unidirectional; for example a pre-strained torsion bar must be loaded in the direction of pre-straining if the material is to be utilized to its full extent. The second advantage is derived from the fact that over-straining usually leads to a raising of the elastic limit of the material in the direction of loading and, therefore, a higher working stress can be employed with a resultant saving in the cost of material.

This thesis is concerned with the clock-type spiral spring, its method of manufacture, the residual stresses encountered, methods of analysis and predicted performance. Whilst it is recognised that power springs of this type are no longer used in record players and other devices in which they used to be employed, it is true to say that this type of spring still finds extensive applications.

The work covered by this thesis really falls into three parts:

Part 1 re-examines the theory of the working of this type of spring as a result of which some knowledge of the mathematical form of the spiral is required.

Part 2 examines methods of determining the mathematical equation of the spiral relating this to the theory of part 1, and validating the theory.

Part 3 examines the reasons for the spiral form, the consequent residual stress pattern and a method of determining the residual stress pattern in a real spring.

CHAPTER 1

INTRODUCTION

1.1. Preamble

Springs have played, and still do play, an important role in the development of many of the mechanical contrivances which characterise our present technological attainments. Had it not been for the development of the hair-spring and the power spring for use in clocks and watches it is doubtful that our scientific knowledge would have reached its present high level. The high performance of the modern internal combustion engine is seriously impaired if the many springs built into it do not function faultlessly. A brief study of the paraphernalia associated with modern technology will reveal the use of a multitude of springs of various shapes and sizes and materials. The materials currently employed for springing include solids, liquids and gases, metals and non-metals and also fibre reinforced materials.

At the present time the vast majority of springs are made of metal, steel being the most widely used of these. Wahl(R1 Ch.2)* compares a wide variety of spring materials on a cost basis and also on the basis of physical properties. Table I summarises the properties of some of the materials commonly used in the manufacture of clock-type springs.

The clock-type spring is only one of a whole range of special shapes into which metals are formed so as to produce a spring. The basic function of a spring

---

* R1 Ch.2 refers to Bibliography in appendix B1.1 Ref. 1 Chapter 2.

Table 1

MATERIAL	ANALYSIS	TENSILE PROPERTIES			*Rockwell Hardness
		Ultimate Strength Lb. per sq. in.	Elastic Limit Lb. per sq. in.	Modulus of Elasticity, p.s.i.	
CLOCK SPRING STEEL A.S. 100 S.A.E. 1095 E.N.44 b/d	Carbon .90–1.05% Mn. .30–.50%	180,000 to 340,000	150,000 to 310,000	30,000,000	Annealed B75–90 Temp'd C40–52
FLAT SPRING STEEL A.S. 101 S.A.E. 1074 E.N42, E.N42c	Carbon .70–.80% Mn. .50–.80%	160,000 to 320,000	125,000 to 280,000	30,000,000	Annealed B70–85 Temp'd C38–50
18-8 TYPE STAINLESS A.S. 35 S.A.E. 30302 E.N 58a	Chrome 17–20% Nickel 6–10% Carbon .08–.15% Mn. 2% Max. Si. .30–.75%	160,000 to 330,000	60,000 to 260,000	28,000,000	C35–45
NI-SPAN "C"	Ni 42% Cr. 5.2% Ti. 2.3% Fe. bal.	200,000	110,000	27,500,000	C38–42
BERYLLIUM COPPER A.S. 45 A.S. 145 B.S. 2870-CB101	Copper 98% Beryllium 2%	160,000 to 200,000	100,000 to 150,000	16,000,000 to 18,500,000 Subject to Heat-treatment	C35–42
SPRING BRASS A.S. 55 A.S. 155 B.S. 2870 - CZ 106	Copper 64–72% Zinc Remainder	100,000 to 130,000	40,000 to 60,000	15,000,000	B90
PHOSPHOR-BRONZE A.S. 60 A.S. 160 B.S. 2870-PB102/3	Copper 91–93% Tin 7–9% or Copper 94–96% Tin 4–6%	100,000 to 150,000	60,000 to 110,000	15,000,000	B90–100

is to store energy for a period of time and to deliver back the greater part of this energy as and when required, but whilst all bodies possess this ability to a greater or lesser extent, the distinguishing characteristic of a spring is that, normally, the spring is capable of sustaining large deformations without permanent distortion. If a spring does suffer permanent distortion under its designed working load then, to all intents and purposes, that spring has failed in its duty.

1.2. Spiral Springs

One of the earliest and still one of the most commonly used springs is the spiral spring whose purpose when wound as a clock spring is to supply motive power to mechanisms such as clocks, watches, cine-cameras, and toys. In slightly different form it finds use as hair-springs, control springs in switches, and brush springs in electrical motors and generators. When used as a hair-spring (or control spring on an instrument) it is not required to suffer large deformations and the coils do not come into contact. Its use in switchgear is to produce high-speed opening and closing of electrical contacts so as to reduce arcing across them. In order to do this the spring is wound up relatively slowly and then suddenly released. When applied to brush gear its purpose is to exert a constant force on the brushes and the development of the tensator (constant force) spring was a result of this type of requirement.

1.3. Historical

The knowledge that metals possess elastic properties dates back to about the second century B.C. and knowledge of this property in certain types of wood was used in the construction of bows and catapults by our ancestors. The introduction of springs into mechanical devices dates back to about 1400 A.D. but it was not until the enunciation of his well-known law by Hooke in 1678 that any theoretical approach to the design of springs could be attempted.

At the present time knowledge of the elastic behaviour of spring materials is extensive but their behaviour when subjected to plastic deformation is less well known. It is the purpose of this thesis to try to examine, in greater detail than previously, the physical changes experienced by a material when it is formed into a spiral spring and facilitate prediction of the performance of the resulting spring. In order to do this, methods of analyzing the free spiral have been evolved together with means of recording the torque-rotation characteristics of this type of spring.

1.4. Manufacture of a Spiral spring

The work of this thesis is concerned with the analysis of spiral springs manufactured from heat-treated strip material and subjected to no heat treatment after forming.

The manufacturing process for this type of spring is extremely simple and consists, basically, of winding a strip of suitable material onto an arbor or mandrel which is

rotated. Springs can be made on machines which range from small hand operated winders or small power-driven lathes to large power-driven multi-purpose winding machines. In any event the manufacturing process begins by cutting the strip off to a length specified by the designer and including an allowance of about four times the arbor diameter for end fixings. Next the specified end fixings are formed, often requiring heating of the ends of the strip. In the case of thick material it may be necessary to hot-form the inner coil before the start of the coiling operation. The end fixings may necessitate the punching of a shaped hole if the strip is attached to the arbor or drum by means of a peg or in some cases a T-shaped tongue may be required, or perhaps, particularly at the outside end, a loop might be formed for attachement to a pin incorporated in the retaining system (barrel, if one is used).

One of the most common methods of attachment to the arbor and barrel is merely to bend the strip to about 90° and locate in suitable slots in the arbor and barrel. The bends must, of course, necessarily be in opposite directions.

Having formed the end fixings, the inner end of the strip is attached to the winding arbor and the outer end is restrained by hand whilst winding proceeds. If the material is thin, the operator is able to provide sufficient back-tension to wind layer-upon-layer, for very thin material he may even be able to provide a tension in excess of the minimum required and this will affect the depths of the yield surfaces. In the case of thicker materials the operator cannot provide the back-tension necessary to wind layer-upon-layer and the spring is

formed by coiling loosely on the arbor followed by a tightening operation. When springs with a large number of coils are formed in this way, it may happen that the gap in the machine through which the strip has to pass, in order to reach the arbor, may not be sufficiently large to allow the material to feed onto the coils tangentially, in which case reversed bending occurs during the winding process.

The tightening operation referred to above consists of forcibly restraining the outer end of the strip, usually by attaching it, by means of a hooked bar for example, to the frame of the winding machine and rotating the arbor until the coils are tight. At this stage rotation of the arbor is stopped and, whilst the spring is still under load, a spring steel keeper is slipped over the spring, or it is simply bound round with wire, to prevent it unwinding when removed from the machine. The finished spring is then removed from the winding arbor and should be ready for installation in the equipment for which it was designed.

It will be evident that the process described is one in which it is most difficult to ensure reproducible conditions of manufacture.* Results of the analysis of the free form of springs, supposedly from the same type of stock and produced by the same manufacturer, show considerable variation in their spiral form.

The result of subjecting the material to the above

---

* Meyers (R2 p82) claims that helical springs are stress relieved to remove the stresses caused by coiling etc. 'because they are impossible to evaluate'.

process of forming is to induce in it a residual stress pattern which varies along the length of the material and thus determines the radius of curvature attained by the centroidal axis of the strip at any point along its length. The obvious conclusion to be drawn from this statement is that the equation of the spiral is directly related to the manner in which the residual stress pattern changes along the length of the strip.

1.5. Residual stress system

The stress-strain relationship for steel is dependent upon its composition, heat treatment and previous strain history. In the case of a steel which has been previously strained beyond the elastic limit, any further straining in the same sense raises the elastic limit whilst straining in the opposite direction reduces the elastic limit for reverse loading. This phenomenon is described as the Bauschinger effect being named after J. Bauschinger(R3a p413) who drew attention to it in 1881.

It is obvious that the Bauschinger effect should be taken account of in any analysis aimed at determining the final state of stress in material subjected to strain cycles involving plastic deformation. Strain history analysis purports to do just that.

The method involves a step-by-step analysis of the straining of consecutive layers of material and hence determination of the residual stress distribution throughout the material. In order to support this analysis, a routine has been established for a layer removal technique and is reported together with the method of processing the results later in this thesis.

1.6. Idealised material

Tensile tests performed on spring steel stock showed that an idealised elastic-perfectly plastic material should predict a behaviour approximating to that of the materials used in practice. In order to retain simplicity in the theoretical analysis it is assumed that the material behaves in the same way in compression as it does in tension and that there is no Bauschinger effect during unloading and subsequent reverse loading. These assumptions may present an over-simplified picture of the experience to which a particular particle of material is subjected but, at least, enable one to come to terms with the problem.

1.7. Conventional Theory for spiral springs

In his text-book on Mechanical Springs, A. N. Wahl[R1] considers spiral power springs having two types of outer end fixings, pinned-end and clamped-end.

The analyses of the two cases lead to the equation relating the rotation of the arbor to the external (winding or available) torque

$$\phi = a \frac{M_o \ell}{EI} \quad .. \quad .. \quad .. \quad .. \quad .. \quad .. \quad .. \quad (1.1)^*$$

where ϕ = rotation of arbor in radians

a = 1 for clamped outer end

= 1.25 for pinned outer end

M_o = external torque applied to the arbor

ℓ = total (active) length of spiral

E = modulus of elasticity

I = relevant second moment of area.

---

* The derivation of eq. 1.1 is given in Appendix A1.

1.8. Anticlastic behaviour

The term 'anticlastic behaviour' describes the phenomenon whereby a beam, bent about its longitudinal neutral axis, acquires a curvature about its transverse neutral axis due to the Poisson effect. It can be shown (R7 p.44) that, if the relevant slopes are small and the depth of the section is comparable with its breadth, the transverse neutral axis is bent in an approximately circular arc of radius R' given by

$$R' = -\frac{R}{\nu}$$

where R = radius of longitudinal neutral axis and ν = Poisson's ratio. The negative sign indicates that the centres of curvature are on opposite sides of the beam.

Anticlasticity is clearly exhibited in a routine 180° bend test carried out on a testpiece of standard dimensions.

If, however, the strip being bent is wide relative to its thickness, stresses are induced in the transverse direction which tend to suppress the anticlastic behaviour across the middle portion of the strip.

Ashwell(R4) shows that the shape of the deformed cross-section depends upon the quantity b^2/Rt (b = width of strip, t = thickness of strip, R = radius of longitudinal neutral axis) and concludes that for values of b^2/Rt less than unity the simple beam theory is applicable and the transverse neutral axis acquires a radius R/ν. For larger

values of b^2/Rt the cross-section becomes undulating but when b^2/Rt exceeds a value of about 100 the section becomes substantially flat except at the edges where the maximum deflections tend to the value 0.102t.

For very large values of b^2/Rt Ashwell's theory agrees with the conventional theory for the bending of plates. The latter theory involves substituting in equation 1.1 a modified modulus of elasticity (R3a p 77) resulting in the equation:

$$\phi = a(1 - \nu^2) \frac{M_o \ell}{EI} \quad .. \quad .. \quad .. \quad (1.1a)$$

Equation 1.1a indicates a stiffness, defined as M_o/ϕ, 11.0% higher than that predicted by equation 1.1 if $\nu = 0.3$. For reasons explained in Appendix A1.2 the stiffening effect experienced by a clock spring may be considerably less than this and varies along the length of the strip.

Two other factors resulting from the anticlastic curvature produced during the forming process enter into the problem of the spiral spring. One concerns the alteration in the value of the relevant second moment of area due to the curling of the edges of the strip. This results in an increase in the value of I of about 2% (appendix 1.3). The other factor is also associated with the distortion at the edges of the strip. The amount by which the edges rise above the centre of the strip varies along the length of the strip resulting in a lack of fit between adjacent coils and, consequently, a gap. (The theory assumes that the distance between the centrelines of

adjacent coils is equal to the strip thickness). This lack of fit alters the change of curvature suffered by an elementary length of strip in passing from the wound to the unwound conditions and vice versa.

In Appendix A1 the consequences of anticlastic behaviour are explored further. Here we shall discuss the implications so far as the development of the theory, which follows in Chapter 2, is concerned.

Since the value of b^2/Rt varies along the strip forming the spiral spring in both the wound and unwound condition, equation 1.1a should be modified. Should it prove possible to assign a 'mean effective modulus of elasticity' to the material in place of the modified modulus $(E/(1 - \nu^2))$ of the plate theory, then the simple approach of Chapter 2 is easily corrected. Should it not prove possible, or acceptable, to use a 'mean effective modulus' then a correction factor must be found, which is a function of the position on the strip, and applied to the moment equation 1.1 expressed in elemental form.

Figure A1.1 in Appendix A1 has been constructed from data derived from one of Ashwell's curves and indicates that for a strip 0.05 in. thick, 1 in. wide bent to a radius of 2 in. or more, the moment calculated from the theory of Chapter 2 is in error by no more than 5%. For this reason, therefore, the experimental results reported in this thesis are compared with theoretical results derived using the simple beam theory.

1.9. Bending Stresses

The maximum stress due to bending is of importance in designing a spiral spring and occurs at point A (fig. 1.1). The value of the maximum stress may be found using simple beam theory and for a spring of unit width is given by:

$$\bar{\sigma} = 12\,M/t^2 \quad .. \quad .. \quad .. \quad .. \quad .. \quad (1.2)$$

where $\bar{\sigma}$ = maximum bending stress

M = bending moment at point A

t = thickness of spring material.

According to Timoshenko(R3b p369), recourse to curved beam theory is unnecessary provided that the radius of curvature exceeds ten times the thickness of the spring material. Accepted practice is to limit the minimum radius of curvature in a spring to about 10 x thickness, (R1 p149), therefore the simple beam theory suffices since the minimum radius of curvature must occur at the attachment to the arbor.

1.10. Specific Energy

The purpose of a spring is to store energy in the form of strain energy and its capacity for doing this may be expressed as a specific energy

$$u = BM^2\ell/2EIV \quad .. \quad .. \quad .. \quad .. \quad .. \quad (1.3)$$

where u = specific energy in work units/ unit volume

v = volume of material contained by active length.

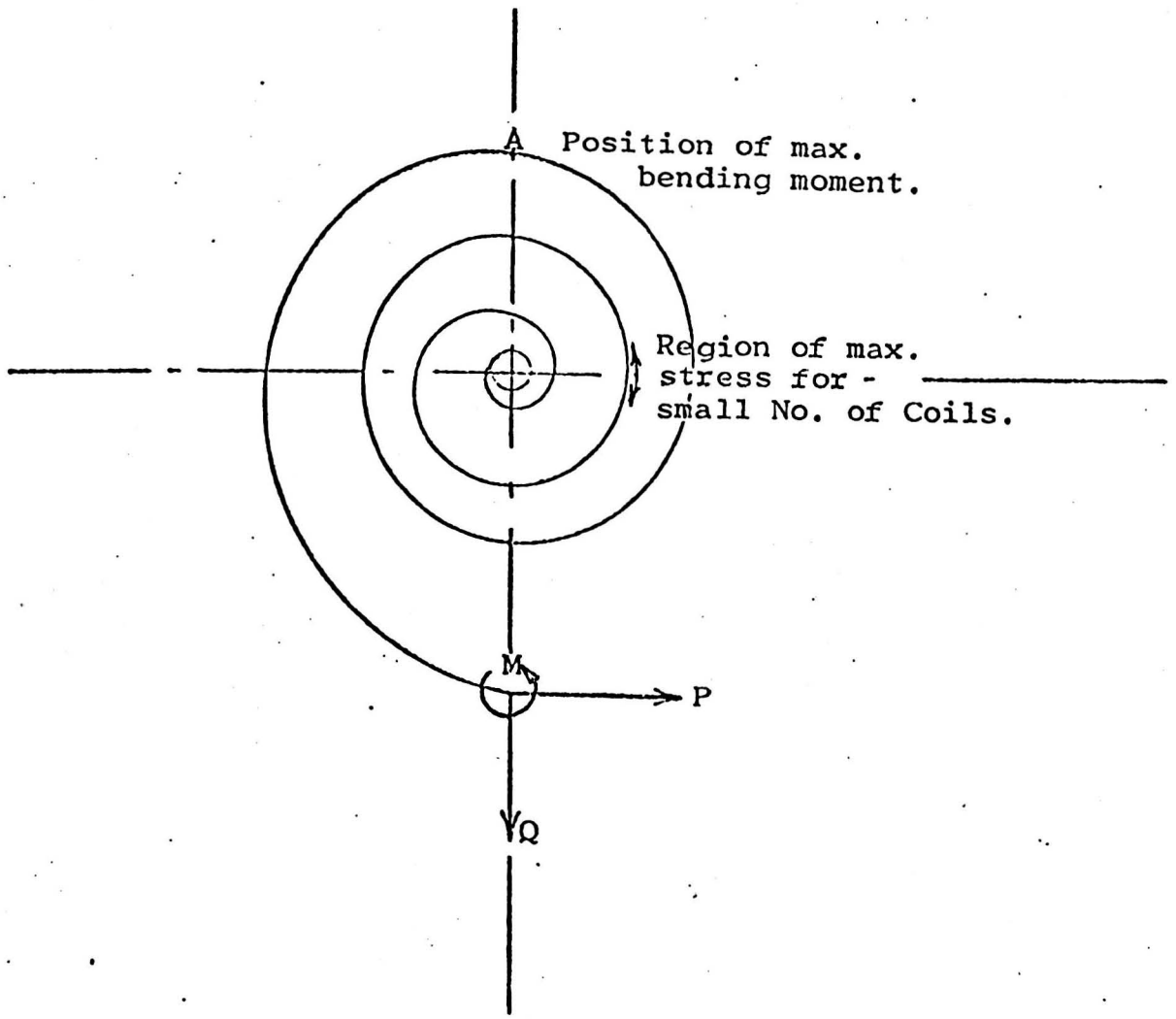

Fig 1.1 Showing the position (A) normally quoted as sustaining the maximum stress (R6 and others) and the region of maximum stress according to Kroon and Davenport (R8 p.184).

B = constant

M, E and I are defined above.

The value of B depends upon the type of loading on the spring. If the spring is subjected to bending moment M^* which is constant throughout the active length then B = 1.0, and substitution in eq. 1.3 of $M^* = \sigma^* t^2/12$ from eq. 1.2 together with the values of I and V for a rectangular cross-section of unit width and thickness t gives

$$u = \sigma^{*2}/24E \quad .. \quad .. \quad .. \quad .. \quad (1.4)$$

If the bending moment is not uniform B has a value less than unity, and if the material were uniformly stressed to a value σ^* the specific energy would be

$$u = \sigma^{*2}/2E \quad .. \quad .. \quad .. \quad .. \quad (1.5)$$

The implication is obvious, if maximum use is to be made of the available material then means must be found of increasing the mean working stress whilst, at the same time, ensuring that the limiting design stresses are not exceeded. It is the aim of pre-stressing techniques to achieve this end.

1.11 Spiral form

In a paper published in 1931, J. A. Van Den Broek[R5] outlined the design of the spring illustrated in its free state in fig. 1.2 (his fig. 12) in which, when tightly wound up, the maximum bending stresses throughout the entire length are equal to the elastic-limit stress for the material. Unfortunately, this spring would be difficult to produce and, therefore, existing facilities for the winding of spiral springs

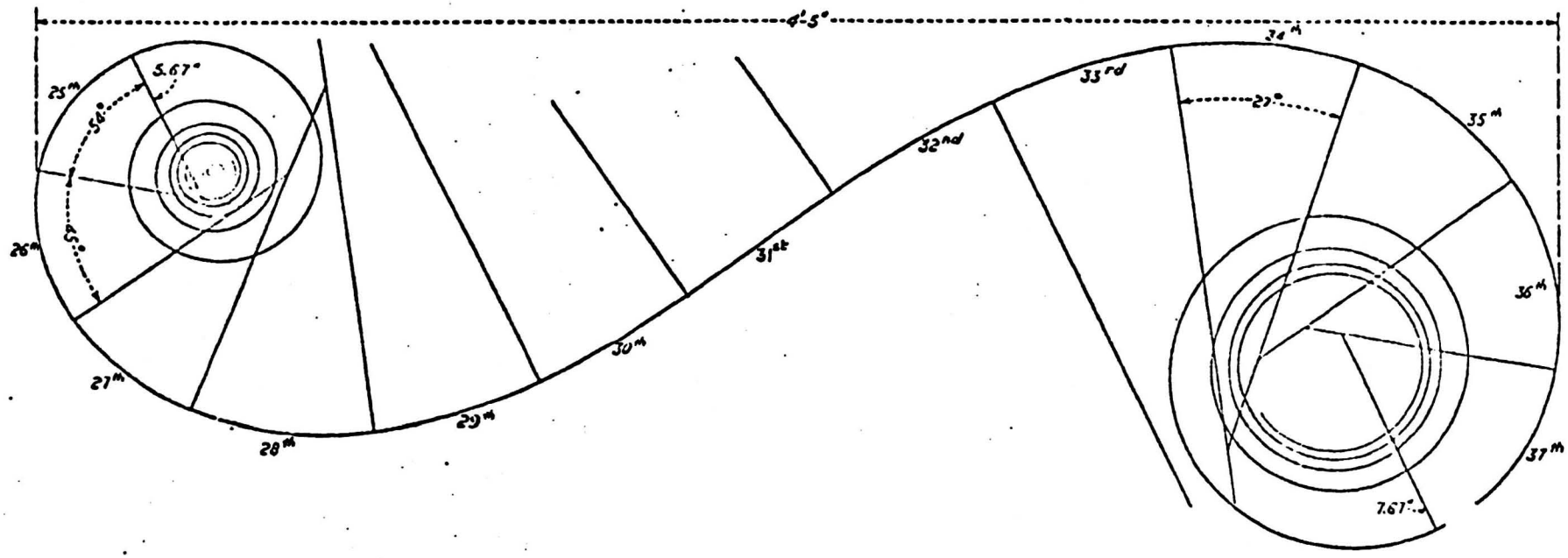

Fig. 1.2 Free form of spiral spring designed by Van Den Broek (R5) to be subjected to a uniform bending stress throughout its length equal to the elastic limit stress when tightly wound on its arbor.

are examined in order to offer more effective utilization of the material.

Dr. S. C. Gross[R6 p6] suggested that a better approach to the design of clock springs might be possible if the equation of the free spiral was known. In the present research, analysis of a large number of springs was carried out with a view to establishing the equations of their spirals. It was found possible to approximate many of them to a logarithmic spiral. The reasons for this logarithmic form were then sought by examing the forming process, recourse being made to elastic-plastic theory.

CHAPTER 2

2.1. THEORY OF THE SPIRAL SPRING (R6)

2.1.1 Definitions and symbols

The following tabulation lists those definitions and symbols which are used repeatedly throughout this thesis. Other symbols and definitions recur less frequently and may be applied in one or two chapters only. Also some of the symbols listed below may be found occasionally to represent meanings other than those defined below. In all such instances the meanings are explained when the symbol is used.

M	-	applied torque or generated torque
E	-	modulus of elasticity
I	-	2nd moment of area for bending
L	-	active length of strip
ϕ	-	radian angle of rotation of arbor
n, N	-	number of coils
s	-	length of spiral from origin to co-ordinates (r, θ)
r, θ	-	polar co-ordinates of point on spiral
K, ΔK	-	curvature and change of curvature
a, b, A, B, C	-	constant defined in text
t	-	thickness of strip
R, R'	-	radius of barrel, arbor

2.1.2. Theory

A spiral spring intended for use as a power spring is usually contained in a barrel. Normally it never attains its free state and spends its working life

alternating between two conditions. In its run-down condition it is coiled layer upon layer on the inside of the barrel and in its fully-wound condition it is coiled layer upon layer on the arbor, fig. 2.1. This type of spring is usually manufactured from hardened and tempered strip by coiling and tightening on a former and, upon completion, some form of retaining clip is fitted which is usually removed only as the spring is pressed into its barrel. In the case of cheap clocks or toys restraint to the uncoiling is usually imposed by the structure of the clock or toy itself and no barrel, as such, is used. However, in these instances also the spring never attains its 'free' form.

If we allow a spiral spring to attain its free state, the length strip, L, is contained by a number of coils, n_o, whereas, if it is in the barrel in the run-down condition, the number of coils in the length L is altered to, say, n_1. In order to achieve the necessary coiling the ends must undergo a relative angular displacement given by

$$\phi_1 = 2\pi(n_1 - n_o)$$

application of the moment equation

$$M = \frac{EI}{L}\phi \quad .. \quad .. \quad .. \quad .. \quad .. \quad (2.1)$$

gives the moment induced in the spring due to the restraining action of the barrel

$$M_1 = 2\pi\frac{EI}{L}(n_1 - n_o)$$

If the spring is now wound up so as to contain n_2 turns then the moment required is changed to

$$M_2 = 2\pi\frac{EI}{L}(n_2 - n_o).$$

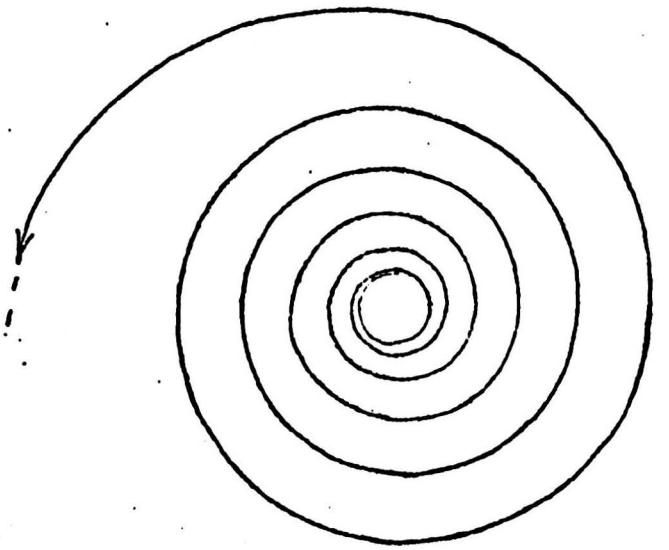

a) Free spiral

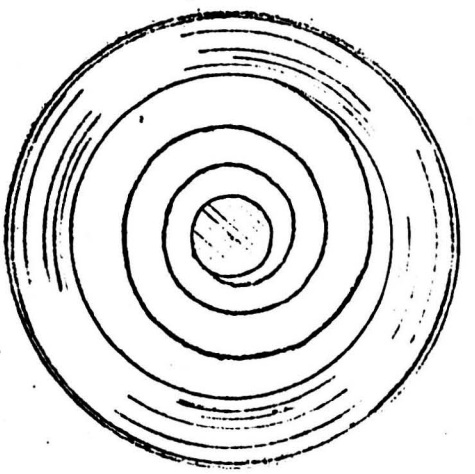

b) Run down in barrel

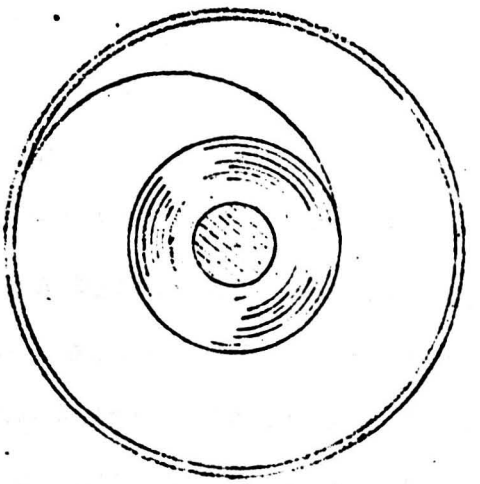

c) Wound on arbor

Fig. 2·1

Thus the useful moment theoretically available between the fully-wound and run-down conditions is

$$M = M_2 - M_1 = 2\pi \frac{EI}{L}(n_2 - n_1)$$

$$= 2\pi \frac{EI}{L} N \quad .. \quad .. \quad .. \quad .. \quad (2.2)$$

Equation 2.2. shows a linear relationship between M and N which is exhibited in practice as the exception rather than the rule. Practical springs of this type often possess non-linear characteristics which give rise to a hysteresis loop when loading is followed by unloading. It is unlikely that any theory could predict the law governing this hysteresis loop but theory should predict the characteristic shape of the curve when hysteresis is negligible.

If we now reconsider equation 2.1, the active length of the spring is assumed to be constant, L. In fact this is not true, the active length varies during both the winding up process and whilst the spring is delivering power. The implication here is that an integration process should be involved.

Let equation 2.1 be written in differential form then,

$$M = EI \frac{d\phi}{ds}$$

or, rearranging,

$$d\phi = \frac{M}{EI} ds \quad .. \quad .. \quad .. \quad .. \quad (2.3)$$

which indicates that the arbor must be rotated by the angle $d\phi$ in order to subject some elementary length, ds, of the strip to a moment M. Resulting from the application of this moment this elementary length experiences a change of curvature given by application

of the simple beam theory:-

$$\Delta K = \frac{M}{EI}$$

which together with equation 2.3 gives

$$\Delta K = \frac{d\phi}{ds}$$

or $$d\phi = \Delta K ds \quad .. \quad .. \quad .. \quad .. \quad .. \quad (2.4)$$

Integrating equation 2.4 we obtain the rotation of the arbor

$$\int_0^{\phi} d\phi = \int_{s_1}^{s_2} \Delta K ds$$

or $$\phi = \int_{s_1}^{s_2} \Delta K ds \quad .. \quad .. \quad .. \quad .. \quad (2.5)$$

2.2. Solution of the integral equation for arbor rotation

Alternative methods of solving equation 2.5 present themselves:

i) the appropriate values can be measured so as to plot the ΔK versus s curve, or,

ii) a mathematical relationship between ΔK and s can be sought so that the right-hand side of equation 2.5 can be integrated.

Both approaches have been applied successfully to practical springs during the course of this research.

In order to relate ΔK and s mathematically it is necessary to establish the equation of the spiral in its free state. The process outlined above is then considered as taking place in two stages. First the spring is imagined to be coiled from the free state to the condition in which it will just fit into the barrel (the run-down condition). It is then imagined to be coiled from the

free state to the condition in which it is tightly wound onto the arbor (the wound-up condition). Thus the right-hand side of equation 2.5 is represented by the area lying between two ΔK - s curves.

2.3. Equation of the free spiral

Detailed examination of a large number of spiral (clock-type) springs followed by the application of much more rapid and simpler but less accurate examination of many more springs of this type leadsto the conclusion that the shape of the free spiral of many of these springs approximates to the logarithmic spiral

$$r = r_o e^{b\theta} \qquad .. \quad .. \quad .. \quad .. \quad (2.6)$$

where b is a constant determined from a plot of log (radius of coil) against rotation, θ, of the radius vector from the position $r = r_o$.

2.4. Curvature of the free spiral

Using the well-known mathematical equation for curvature in its polar form:

$$K = \frac{r^2 + 2\left(\frac{dr}{d\theta}\right)^2 - r\frac{d^2r}{d\theta^2}}{\left[r^2 + \left(\frac{dr}{d\theta}\right)^2\right]^{3/2}}$$

we have, for the logarithmic spiral.+

$$K_o = \frac{1}{r_o e^{b\theta}(1 + b^2)^{\frac{1}{2}}} \qquad .. \quad .. \quad .. \quad .. \quad (2.7)$$

+ For proof see appendix A2.

In order to relate K_o and s, the length of a logarithmic curve is ascertained as being:

$$s = \int_{\theta_1}^{\theta_2} \left[r^2 + \left(\frac{dr}{d\theta} \right)^2 \right]^{\frac{1}{2}} d\theta \quad .. \quad .. \quad .. \quad .. \quad (2.8)$$

and substitution of equation 2.6 into 2.8 and subsequent integration gives:

$$s = \left[\frac{r_o e^{b\theta}}{b} \left(1 + b^2 \right)^{\frac{1}{2}} \right]_{\theta_1}^{\theta_2} ,$$

thus the length of the spiral from the position $(r_o, 0)$ is given by:

$$s = \frac{r_o}{b} \left(1 + b^2 \right)^{\frac{1}{2}} \left(e^{b\theta} - 1 \right) \quad .. \quad .. \quad .. \quad .. \quad (2.9)$$

Equation 2.9 with 2.7 gives the required relationship between K_o and s to be:

$$K_o = \frac{1}{bs + r_o(1 + b^2)^{\frac{1}{2}}} \quad .. \quad .. \quad .. \quad .. \quad (2.10)$$

2.5. Spiral forms in barrel

When the spring is retained in the barrel in the run-down condition it can be considered to be tightly coiled adjacent to the barrel. This assumption neglects the thickness of any film of lubricant which might be present and also ignores a relatively short length of spring stretching across the gap between the bulk of the spring and the arbor. The area of the annulus occupied by these coils is given by the product of the length of spring and its thickness. The curvature at a position

distance s from the inner end of the spring is given by:

$$K_1 = \frac{1}{\sqrt{\left(R - \frac{t}{2}\right)^2 - \frac{t}{\pi}\left(L - s\right)}}$$

and re-arrangement of this equation gives:

$$K_1 = \frac{B}{\sqrt{C_1 + s}} \quad .. \quad .. \quad .. \quad .. \quad .. \quad (2.11)$$

where $B = \sqrt{\frac{\pi}{t}}$

and $C_1 = B^2\left(R - \frac{t}{2}\right)^2 - L$

If we now consider the fully-wound condition and apply similar assumptions the curvature at any distance along the strip is determined in a similar manner, resulting in the equation:

$$K_2 = \frac{B}{\sqrt{C_2 + s}} \quad .. \quad .. \quad .. \quad .. \quad .. \quad (2.12)$$

where $B = \sqrt{\frac{\pi}{t}}$

and $C_2 = B^2\left(R' + \frac{t}{2}\right)^2$

2.6. Change of curvature

Consider the change of curvature occurring at a point in the spring. First the spring suffers a change from its free state to the run-down condition and the point under consideration is subjected to a change of curvature (denoted by ΔK_{10}) which is obtained from equations 2.10 and 2.11

$$\Delta K_{10} = \frac{B}{\sqrt{C_1 + s}} - \frac{1}{bs + A} \quad .. \quad .. \quad .. \quad (2.13)$$

where $A = r_o(1 + b^2)^{\frac{1}{2}} \simeq r_o$

In similar manner when the spring is fully wound, this point in the spring has been subjected to a total change of curvature, from its free state, (denoted by ΔK_{20}) obtained from equations 2.10 and 2.12.

$$\Delta K_{20} = \frac{B}{\sqrt{C_2 + s}} - \frac{1}{bs + A} \quad .. \quad .. \quad (2.14)$$

Application of the above equations for curvature and change of curvature to the integral equation 2.5 will now be examined.

2.7. Significance of the limits of integration

When equation 2.5 was obtained by integrating equation 2.4 it was clear that the left-hand integral represented the rotation of the arbor but the significance of the right-hand integral was not investigated. This situation will now be rectified.

Consider the spring in its fully-wound condition. Only that part of the spring spanning the annulus between the barrel and the wound coils is free to deform and this, therefore, determines the active length at this stage. As the spring runs down this section of the spring goes out of action when it either lies on the barrel or on coils adjacent to the barrel. This process continues until the only remaining portion of spring capable of deforming is that section left spanning the gap between the arbor and the spring coiled against the barrel. Thus the active length of the spring varies and the active section progresses from one end of the spring to the other during both the winding-up process and the running-down process. This, then, indicates the significance of

the limits of integration in equation 2.5: the manner in which the limits are determined and in which the integration is carried out is now explained.

2.8. Evaluation of integral 2.5

Given that it is possible to obtain the curves for K_o K_1 and K_2 (equations 2.10, 2.11, 2.12) then the curves for ΔK_{10} and ΔK_{20} (equations 2.13 and 2.14) can be constructed. The result of carrying out this procedure is presented in figs. 2.2 and 2.3.

In fig. 2.2. the variation of curvature along the strip is shown for the three conditions encountered. The points P and P' indicate the fully run-down condition and the fully wound-up condition and the strip length corresponding to A'P is the length of strip connecting the bundle of coils to the arbor, whilst the length P'B is that portion which never detaches itself from the drum and is never included in the active length. Thus at the commencement of the winding-up process the active length of the spring is s_i.

Each element of strip contained by the coils resting against the inside of the drum is subjected to an initial bending moment due to the change of curvature from that indicated by the K_o curve to that indicated by the K_1 curve. The result of this initial moment is a pressure between coils and a pressure on the inside of the barrel. The value of this initial bending moment at any position is given by

$$M_o = EI(K_1 - K_o) = EI\ \Delta K_{10}$$

and it is not possible for an elementary length

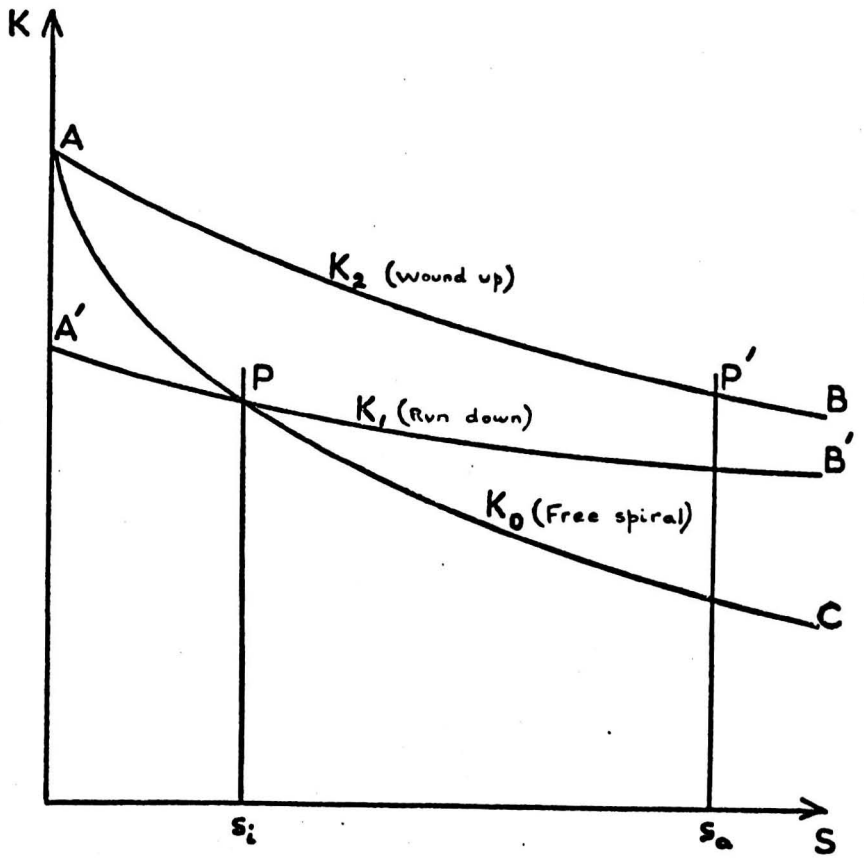

Fig. 2·2 K-S curves

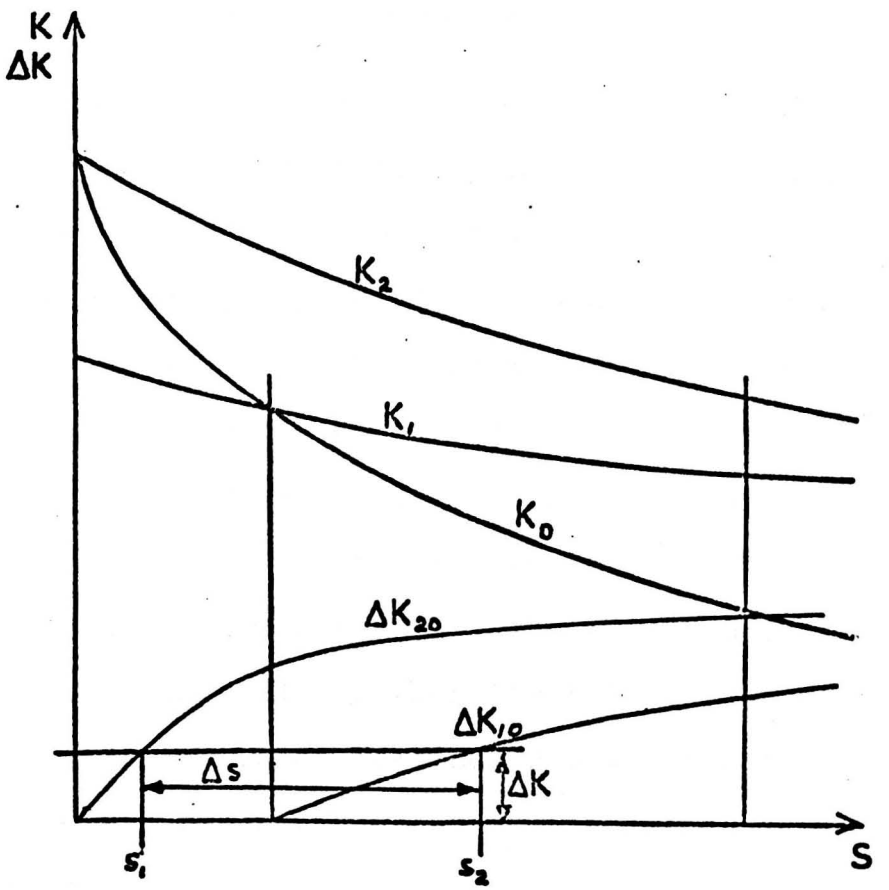

Fig. 2·3 K-S and ΔK-S curves

of strip to detach itself from the remaining coils until this moment is exceeded; its maximum strain energy will be reached when its curvature has a value determined by the K_2 curve.

The length of spring which is active at any given instant is obtained by ascertaining the position of an element being wound onto the arbor and that of an element being detached from the coil inside the barrel when the applied moment has a given value. This condition is indicated by equal ordinates on the ΔK_{10} and ΔK_{20} curves, and is the length Δs indicated in fig. 2.3.

The value of the integral 2.5 is given by the area between the ΔK_{20} and ΔK_{10} curves between the ordinates 0 and s_2. The rotation of the arbor is, therefore,

$$\phi = \int_0^{s_i} \Delta K_{20} ds + \Delta K(s_2 - s_i) - \int_{s_i}^{s_2} \Delta K_{10} ds \quad .. \quad .. \quad 2.15$$

If mathematical relationships between K_o, K_1, K_2 and s are obtainable then the integrals can be evaluated and the M - ϕ characteristic constructed. Alternatively, if the K_o, K_1 and K_2 curves can be drawn, areas between the ΔK_{20} and ΔK_{10} curves can be measured and again the M - ϕ characteristic may be constructed.

Before proceeding further with the theoretical aspects of the M - ϕ characteristic, methods of determining the law for the spiral will be examined followed by examination of M - ϕ characteristics determined from tests on actual springs, particular attention being paid to those springs which produce an s-shaped M - ϕ characteristic.

CHAPTER 3

METHODS OF DETERMINING SPIRAL EQUATION

3.1. Measurements from the spiral spring

A large number of clock-type springs were obtained from various manufacturers. These springs were examined with a view to establishing the equation of their spirals; some of them were tested on the author's testing machine which is described in Chapter 4.

Visits were made to works in order to witness the manufacture of clock-type springs since it was considered early in this work that the spiral equation would depend not only on the physical properties of the strip material, but also on the method of forming. It is in the forming process that events are likely to take place which lead to inconsistencies in the final free spiral form.

Before any start can be made to determine the spiral equation by measuring radii at various angles one must ensure that the spring is in its free state and not distorted due to the frictional effects between the spring and the surface upon which it is resting. Further, it is necessary to locate the origin of the spiral; the accuracy with which this operation must be carried out is discussed later but, regardless of this, measurements must be made from some known reference point.+

The first tests were carried out on fairly stiff springs so that difficulties in eliminating frictional

---

+ Kroon and Davenport (R8 p.184) claim 'That the flexibility of the (spiral) spring is little affected by a change in the shape of the spiral, as long as the length stays the same.'

effects were minimal. The springs were merely placed on a glass plate which was then lightly hammered so that the spring took up its free position. Measurements were made on a Société Genevoise measuring machine which is sited in a metrology laboratory equipped with air conditioning. Under these conditions and with this machine measurements of radius and angle can be made with a high degree of accuracy. It is unlikely that either equipment in this category or similar conditions of working would be available in industry to personnel likely to undertake this particular task; therefore, it was intended that the simplest possible method should be sought which would allow the determination of the spiral equation to an acceptable degree of accuracy.

In the early stages of this work consideration was given to a number of mathematical spirals to which this type of spring might conform. But plotting of the natural logarithm of the radius (measured from an assumed origin) against the radian angle turned through from the initial radius vector position to the current vector position gave some indication of a linear relationship worthy of further study. The plot showed a sinusoidal type variation with decaying amplitude on a straight inclined axis (fig. 3.1). The fact that the amplitude (measured from the sloping axis) decayed with increasing angle and radius, suggested that this feature of the plot might be due to lack of coincidence between the reference point and the origin of the spiral. At first the variations from the linear ($\ln R$ v θ) relationship were disregarded and a mean line constructed to give a law of

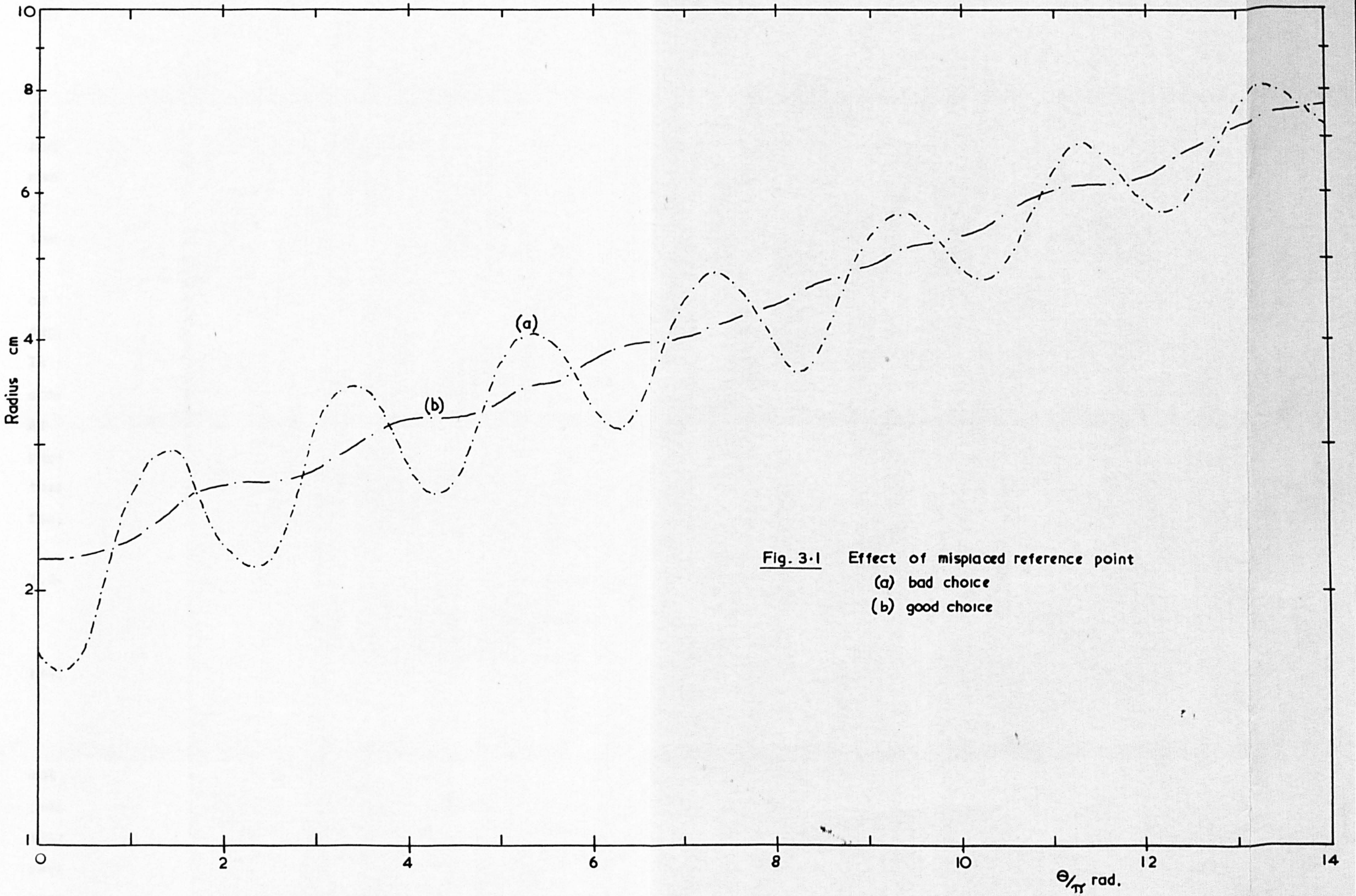

Fig. 3·1 Effect of misplaced reference point
(a) bad choice
(b) good choice

the form

$$r = r_o e^{b\theta}$$

the value of b being ascertained from the slope of the mean line. This procedure was followed for a number of springs and the same effects recorded. The main differences occurred in the positions of the crests of the 'sinusoidal' variations and, as one might anticipate, their amplitudes.

Having now established that at least some springs of this type might possess a logarithmic spiral form, explanation of the sinusoidal claracteristic was sought. It was thought that since location of the origin presented some difficulty, this might be the controlling factor. At the same time it is evident from the Kroon and Davenport paper dealing with spiral springs having a small number of turns[R7], that for the first few turns, at least, other factors might be involved as well.

3.2. Effects due to lack of coincidence of reference point and origin

In order to investigate this effect a spiral having the equation

$$r = 0.7e^{0.03\theta}$$

was constructed. The construction was carried out by plotting values of r for 90^o intervals of θ and joining the points by circular arcs. The resulting spiral is shown in fig. 3.2, O being the origin. The reference point P, from which measurements are taken, is located 0.1 in. in the -x direction and 0.1 in the -y

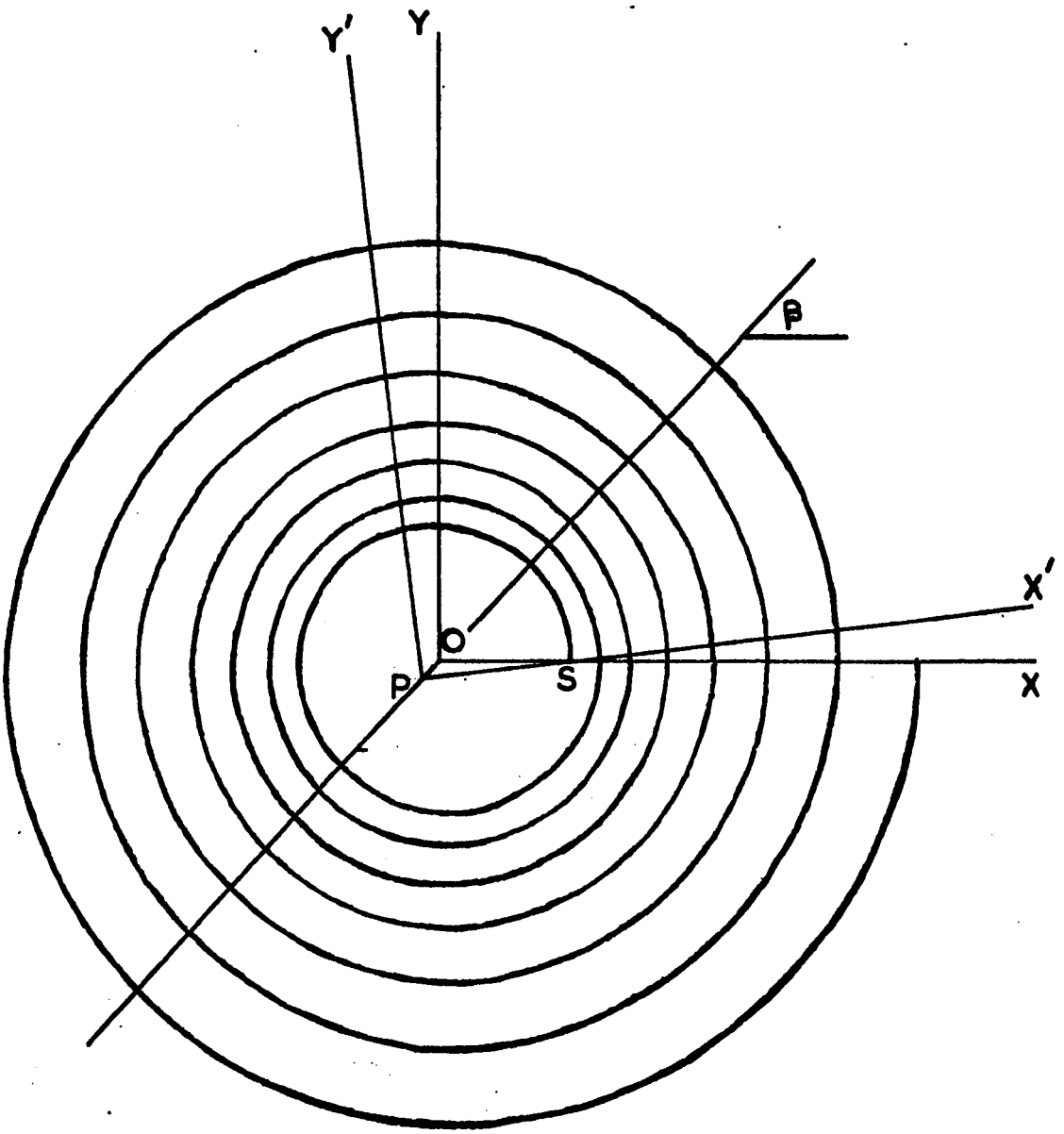

Fig 3·2 Spiral $r = 0{\cdot}7\, e^{0{\cdot}03\theta}$ in.
O is origin of spiral
P is reference point for fig 3·3

direction from O. S is the start of the spiral and axes PX' and PY' are constructed so that S lies on both the OX axis and the PX' axis. The values used for the logarithmic plot of fig. 3.3. are measured with reference to the Y'PX' axes. It is evident that the resulting curve of fig. 3.3. is similar to that obtained from actual springs. The next step is to see if it is possible to determine the value of 'b' without locating the position of the origin.

Examination of the original plot from which fig. 3.3. is traced reveals that the peaks and crests of the curve occur at the angles

$$n\pi + 0.4 \text{ and } m\pi + 0.4 \quad n = 0, 2, 4, \text{ etc.},$$

$$m = 1, 3, 5, \text{ etc.},$$

respectively. We will now investigate this fact further since we note that the line OP (fig. 3.2) is inclined at 45° to the OX axis and 45° is not far removed from 0.4 radian.

If we consider measurements of radius made along OP produced in both directions, we find that values in one direction are increased by the amount OP whilst those in the opposite direction are decreased by the same amount. Measurements in other directions are affected to a smaller extent and therefore the values of radius measured in the direction OP appear at either a crest or trough of the curve at angular positions separated by π radians.

If a line is drawn tangent to the crests then this line will be displaced upwards by the (logarithmic) amount OP from the true lnr v θ curve. Likewise a line drawn tangent to the troughs will be displaced downwards by the same amount. Therefore the true lnr v θ curve

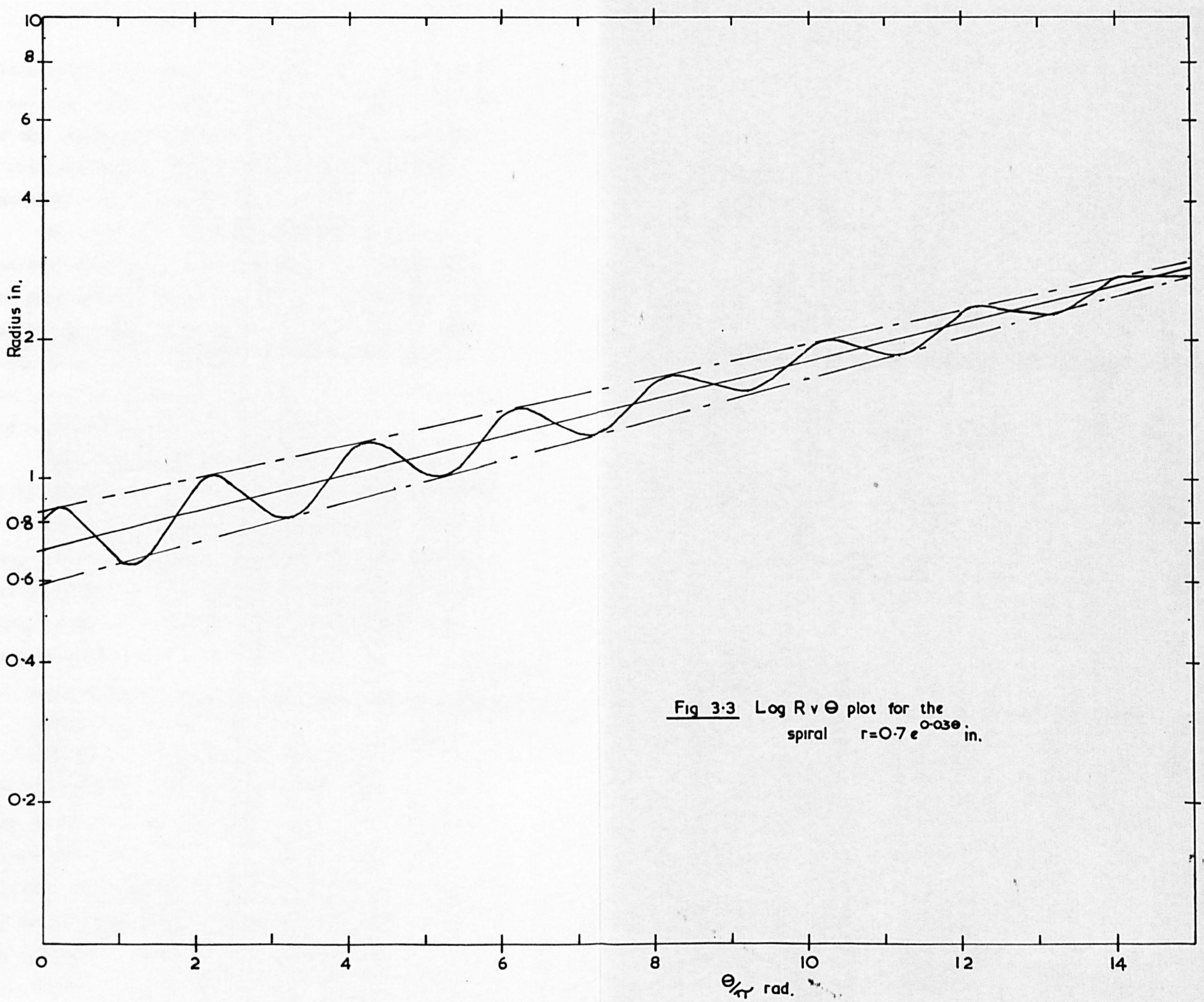

Fig 3·3 Log R v Θ plot for the spiral $r=0{\cdot}7\,e^{0{\cdot}03\theta}$ in.

lies (logarithmically) half way between these two tangent curves and its slope will give the value of 'b'. In the case of the constructed spiral $r = 0.7e^{0.03\theta}$, the value of 'b' obtained was 0.0299, which is sufficient proof that the method is acceptable.

The procedure outlined above will allow not only the determination of the exponent but it will also give the position of the true origin of the spiral. In the case of the constructed spiral the distance OP from the graph agrees almost exactly with the true value 0.1414 in. and the angle ($37\frac{1}{2}^{\circ}$) between OP and PX' agrees with the inclination of OP to OX of 45°.

Thus, a method has been developed which will enable the determination of a logarithmic spiral equation from a reference point close to the origin of the spiral. Obviously one will attempt to place the reference point as close as possible to the origin since a large value of OP will create difficulties in plotting and in the necessary construction.

3.3. Locating the reference point

Ideally the spring being investigated will possess a logarithmic spiral and the reference point will coincide with the origin of the spiral. In practice neither of these conditions is likely to arise, but should it be necessary, non-compliance with the logarithmic law can be overcome by fitting a number (preferably a small number) of straight lines to the plotted curve.

The origin of a logarithmic spiral can be located in a number of ways. If one accepts that the

placing of a tangent to a curve is not an easy task nor is the result likely to be highly accurate, then one may construct tangents to the spiral and make use of the property of a logarithmic spiral that points on the curve with equiangular tangents all lie on the same (straight) line through the origin. Thus if a spring is arranged on squared paper in such a way that the lines are tangent to the coils, then the origin is easily located. The squared paper enables two lines at 90^{o} to each other and passing through the origin to be located. Fig. 3.4 illustrates this method applied to the constructed spiral referred to in section 3.2 above.

Other techniques will be explained but since application of some of these methods is easier if a reproduction of the spiral on paper is available, some of the processes used for producing these replicas will be discussed first.

3.4. Production of replicas of the spiral

A technique which produces acceptable results when used in connection with stiff spiral springs is to place a sheet of graph (or other) paper over the spring and carefully take a pencil rubbing. Fig. 3.5 is a photo-copy of such a rubbing on which construction lines associated with the variation of reference point also appear. Fig. 3.6 is a photo-copy of a record made by tapping round the edge of the spring after placing it on Carbon paper with white paper beneath it.

It will be obvious that neither of these techniques can be applied to weak springs so recourse

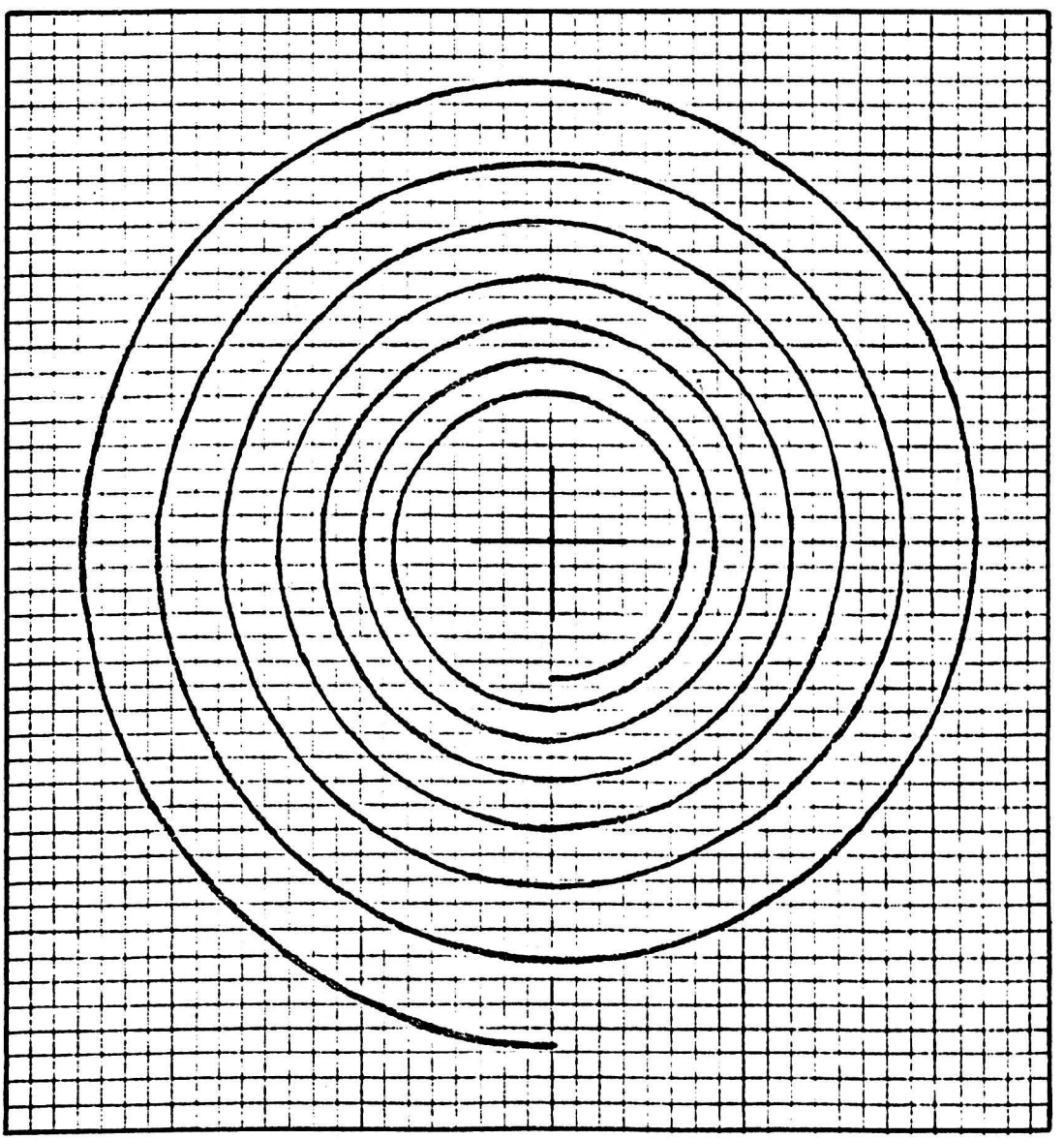

Fig. 3·4 Common normal to tangents passes through origin of spiral $r=0{\cdot}7e^{0{\cdot}03\theta}$

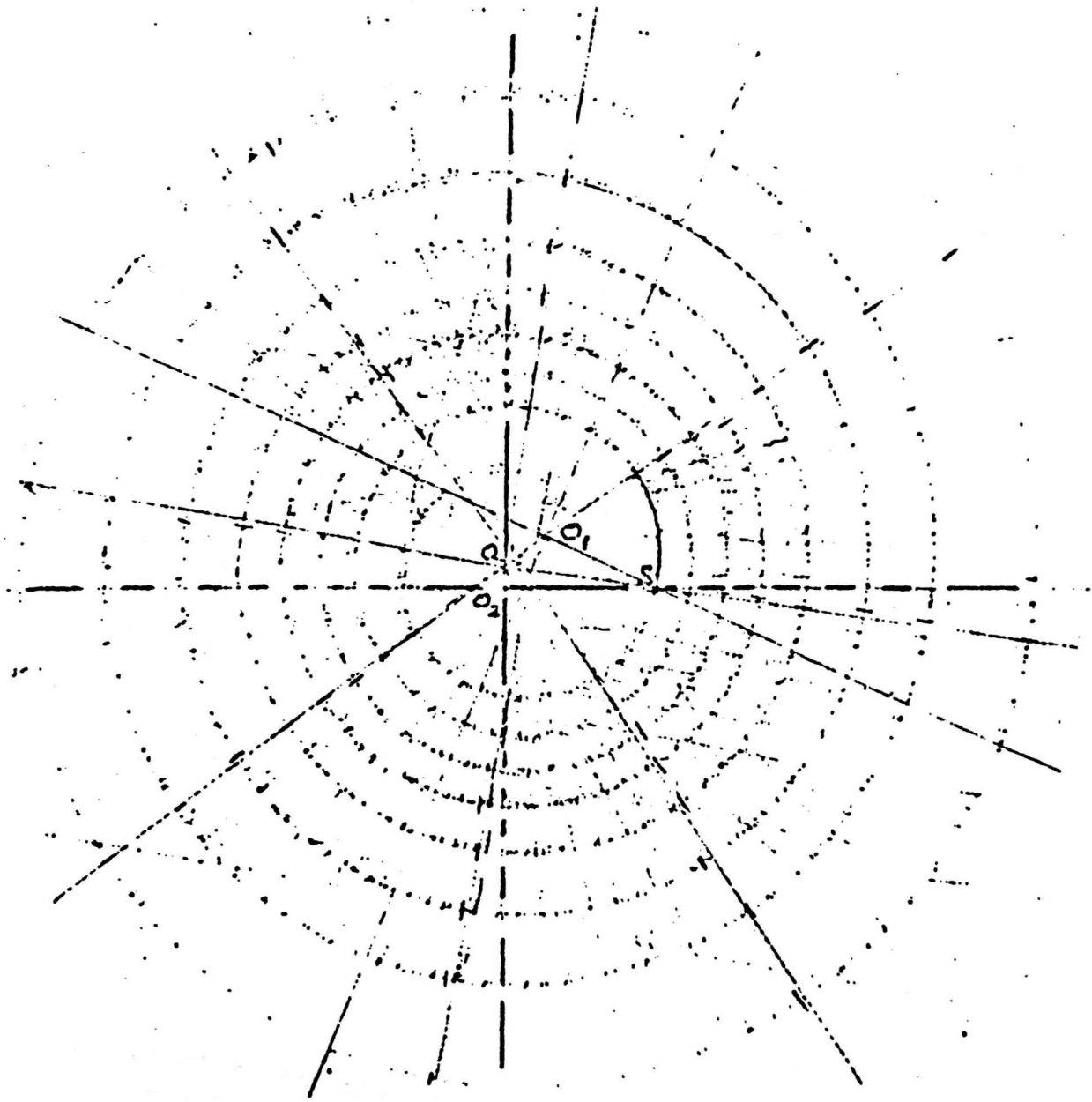

Fig. 3·5 Reproduction of pencil rubbing of spring no.3.

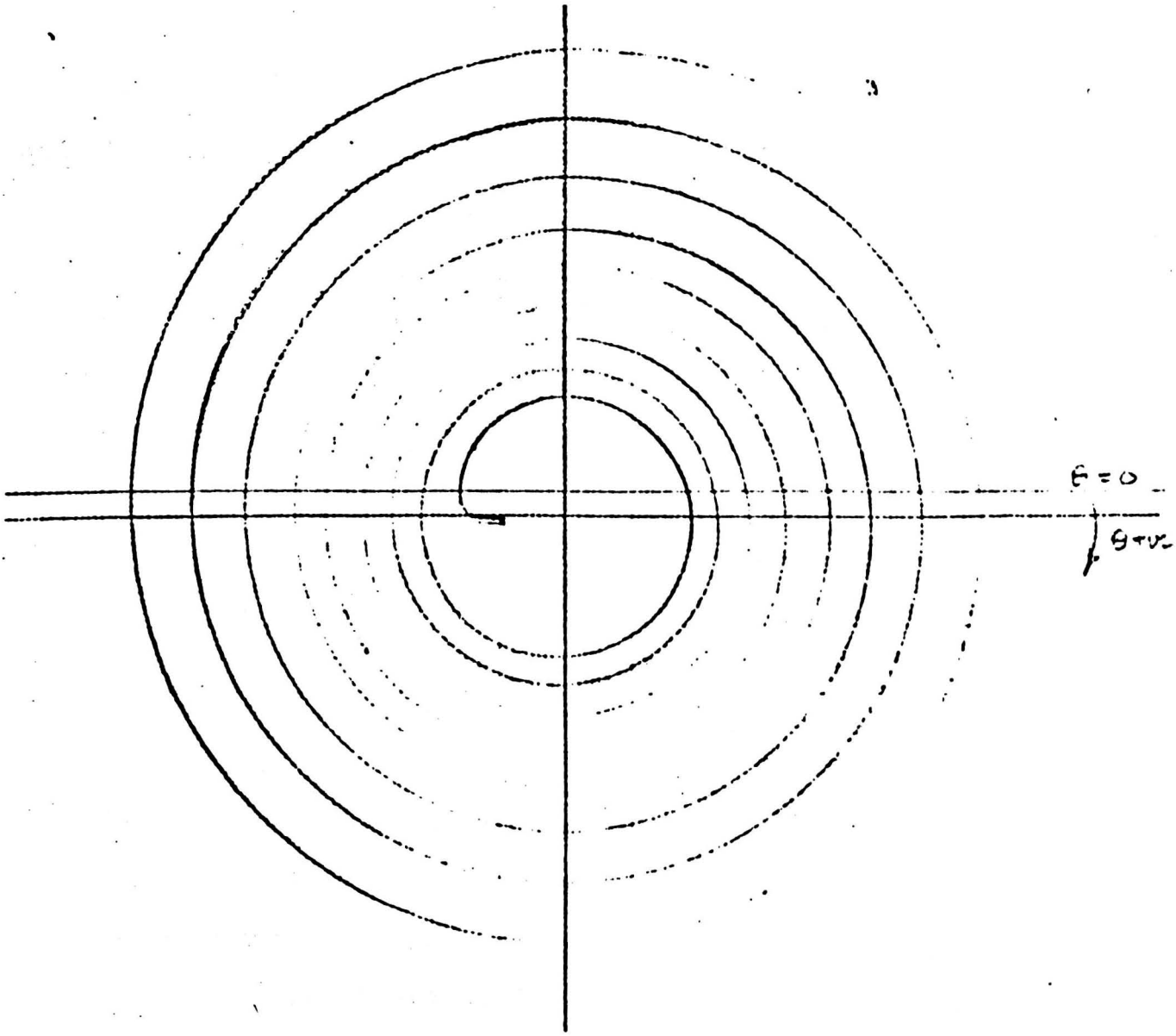

Fig. 3·6 Carbon copy of spiral of spring no.3.
Obtained by tapping round edge of spring

was made to photographic techniques. The springs were placed on the glass plate forming the top of a large light box and photographs taken from above, the top edge of the spring being in focus. Thus a dark line representing the top of the spiral is recorded. Examples of the result of applying this technique appear in figs. 3.7, 3.8 and 3.9. A variation of this method which can be used for springs up to about 8 in. diameter is to place the spring on a flat-bed Xerox copying machine and obtain a copy of the spiral. Some machines introduce a magnification factor but provided that no distortion is introduced, the results are unaffected. When transparencies are required, these can be produced on Fordifax or similar machines used for making overhead projector transparencies.

A photographic technique possesses one great advantage over other methods in that it allows a record to be made of very large springs to a reduced scale. If a spring does have a logarithmic spiral form then the same value for 'b' is obtained regardless of the magnification used in obtaining the print.

3.5. Further techniques of locating the reference point

Fig. 3.10 shows the result of moving a spiral through a distance of $\frac{1}{4}$ in. It is evident that the points of intersection of the two sets of coils lie in a straight line passing midway between the original centre O and the displaced centre O'. Fig. 3.11 shows the effect of moving O' from O a distance of $\frac{1}{4}$ in. in a direction at right angles to that moved in order to

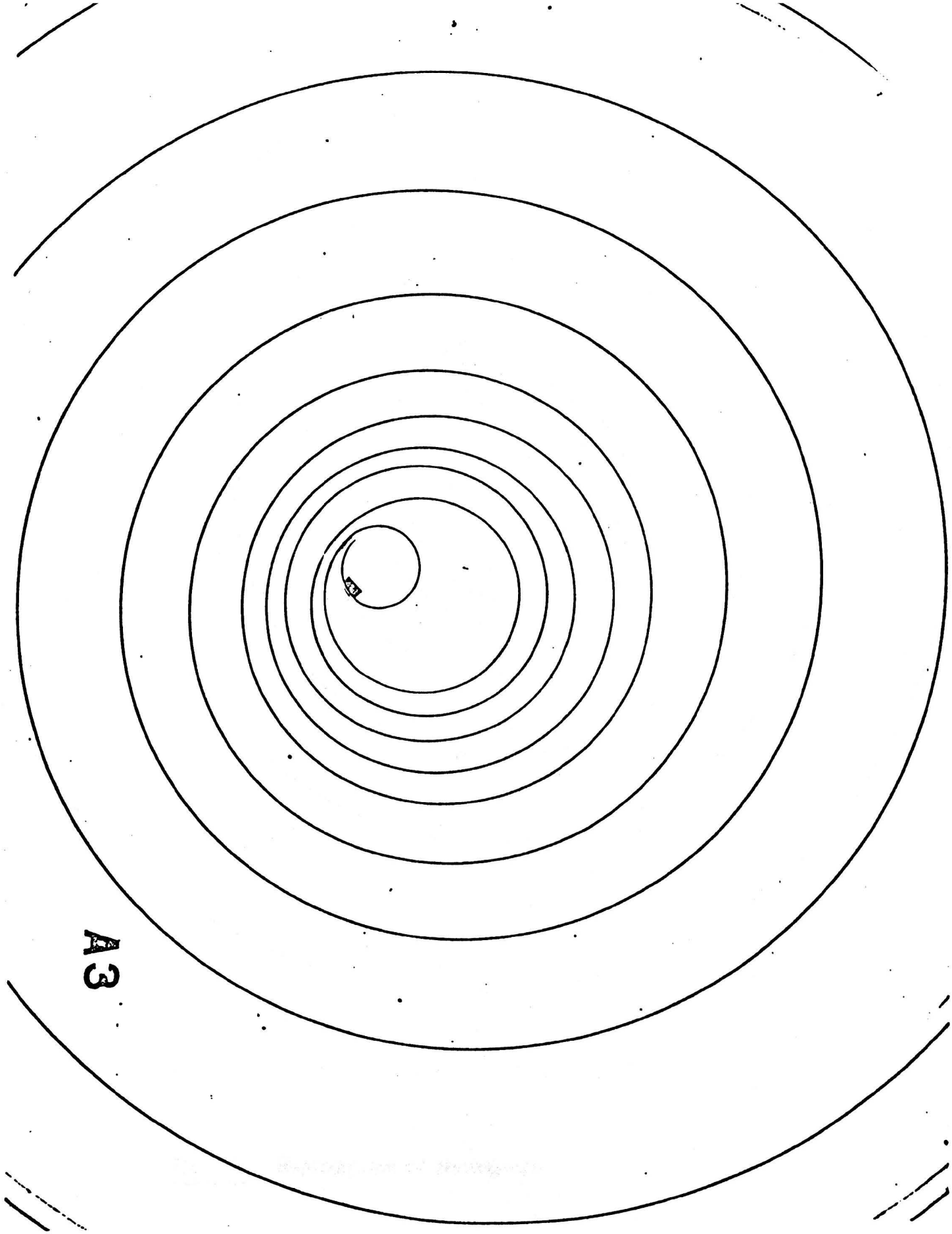

Fig. 3·7 Reproduction of photograph

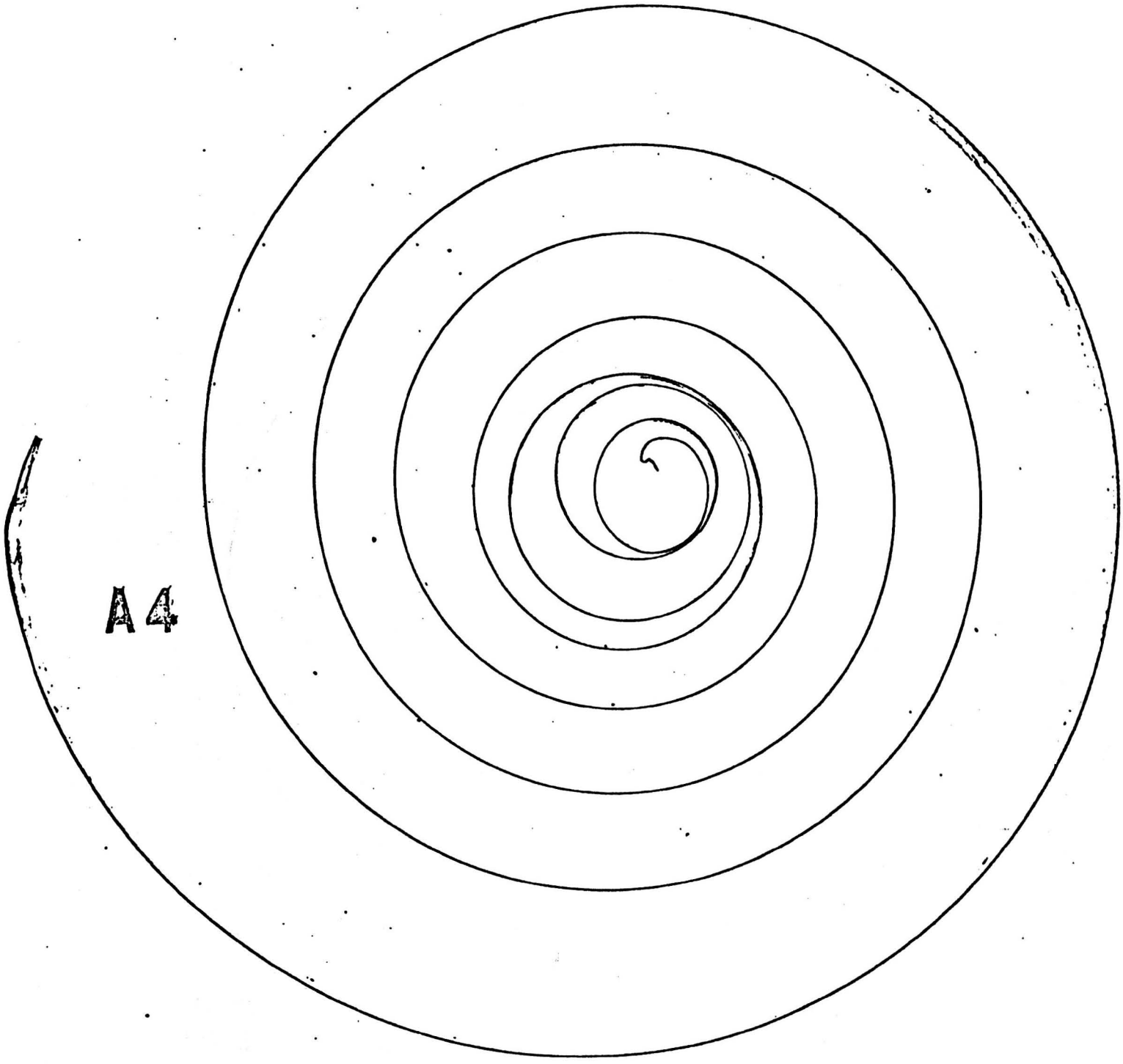

Fig. 3·8 Reproduction of photograph

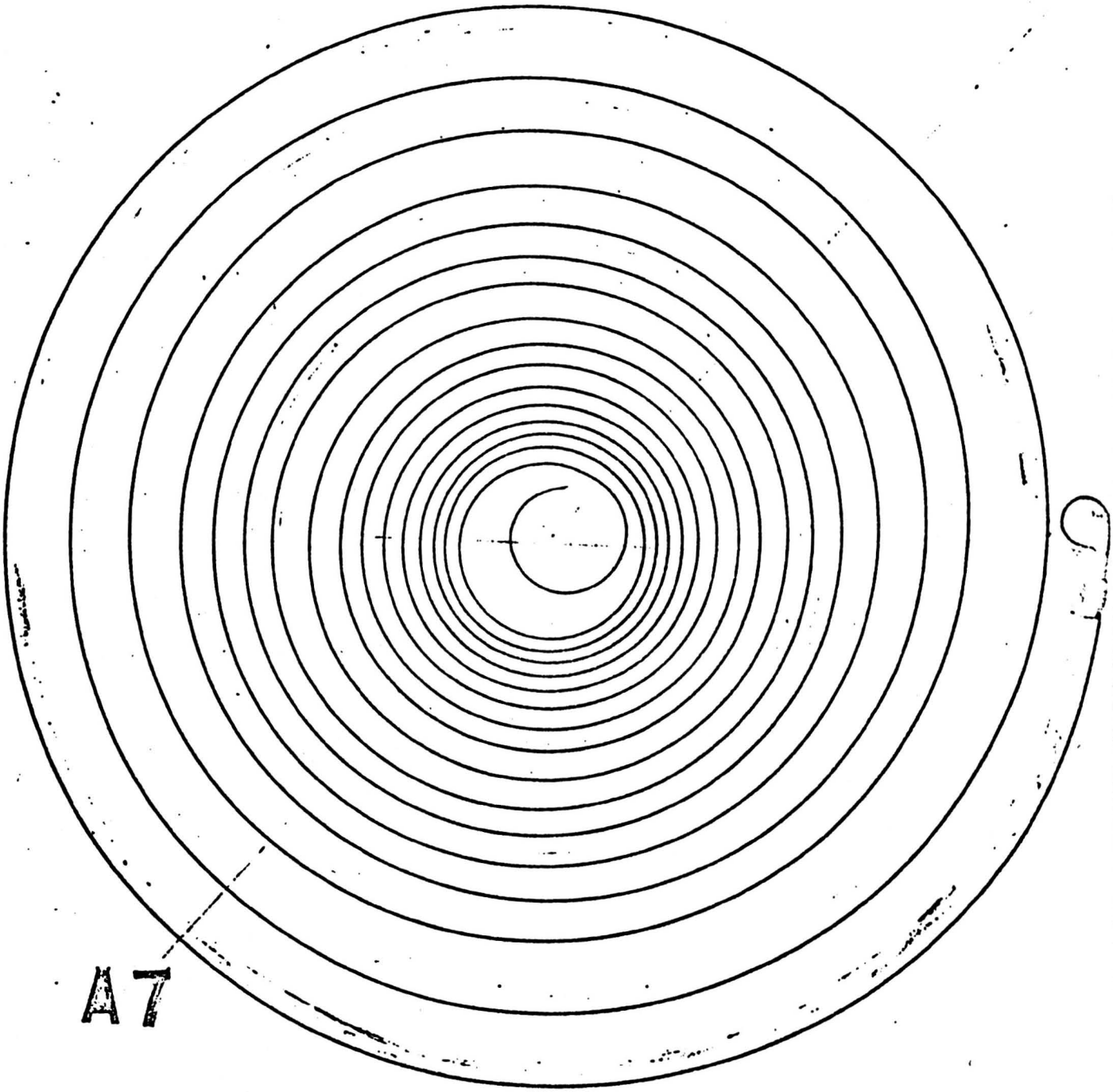

Fig. 3·9 Reproduction of photograph

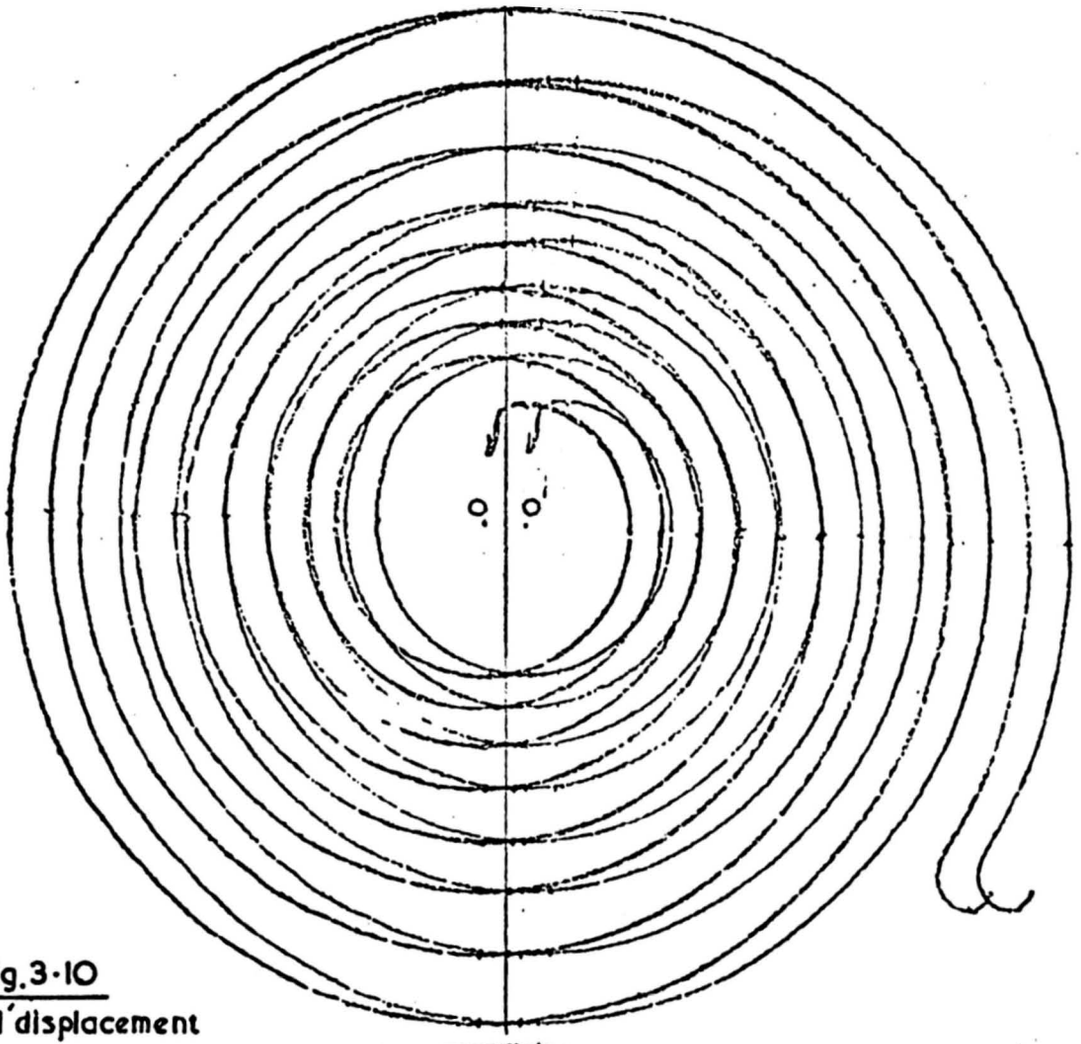

Fig.3·10
'Horizontal' displacement

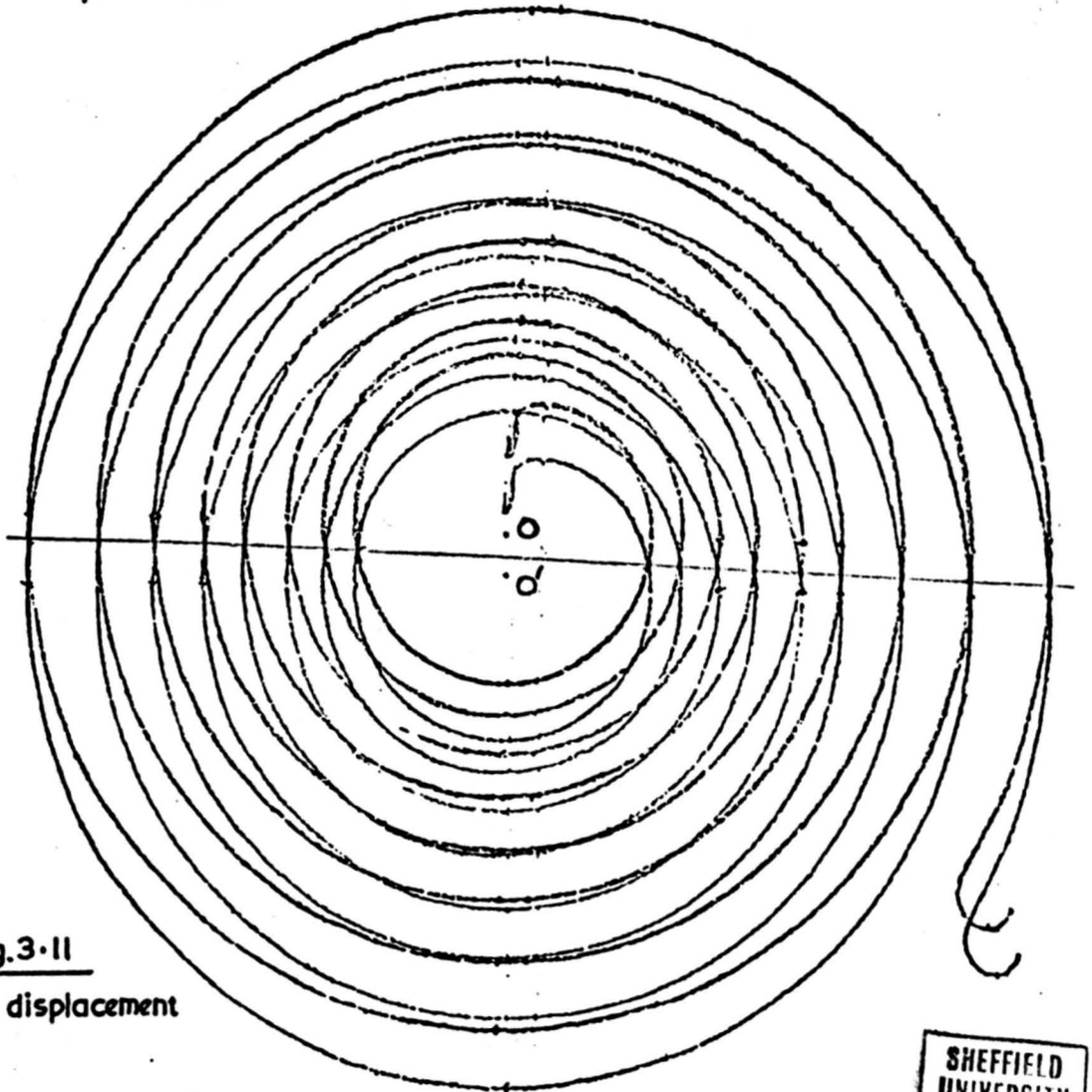

Fig.3·11
'Vertical' displacement

obtain figure 3.10. The result of carrying out these two operations consecutively is that two lines are produced which are displaced $\frac{1}{8}$ in. from parallel lines passing through O.

The method can be applied to a spring resting on a reproduction of its spiral but it is much easier to apply to a reproduction overlaid by a transparency.

One of the simplest ways of locating the reference point is a 'four-point' method illustrated in fig. 3.12 with its overlay. Here two points A and B are marked on the spiral and the coincident points A' and B' on the overlay. The overlay is then rotated through 180° and arranged so that the overlay coils are symmetrically disposed with reference to the spiral below it. The lines joining the points AA' and BB' must pass through the origin of the spiral. It is not too difficult to use the spring itself in conjunction with either the transparency, which is laid on top of the spring, or with the reproduced spiral, which is placed below the spring. In either case, of course, the replica must be full size.

3.6. Inherent difficulties of rapid methods

Two methods of measuring the spirals in order to obtain a value for the exponent and which showed evidence of easy and rapid application are now examined.

i) Returning to the mathematical spiral

$$r = r_0 e^{b\theta},$$

let us examine expressions for the 'coil diameters' given by the sum of the two radii separated

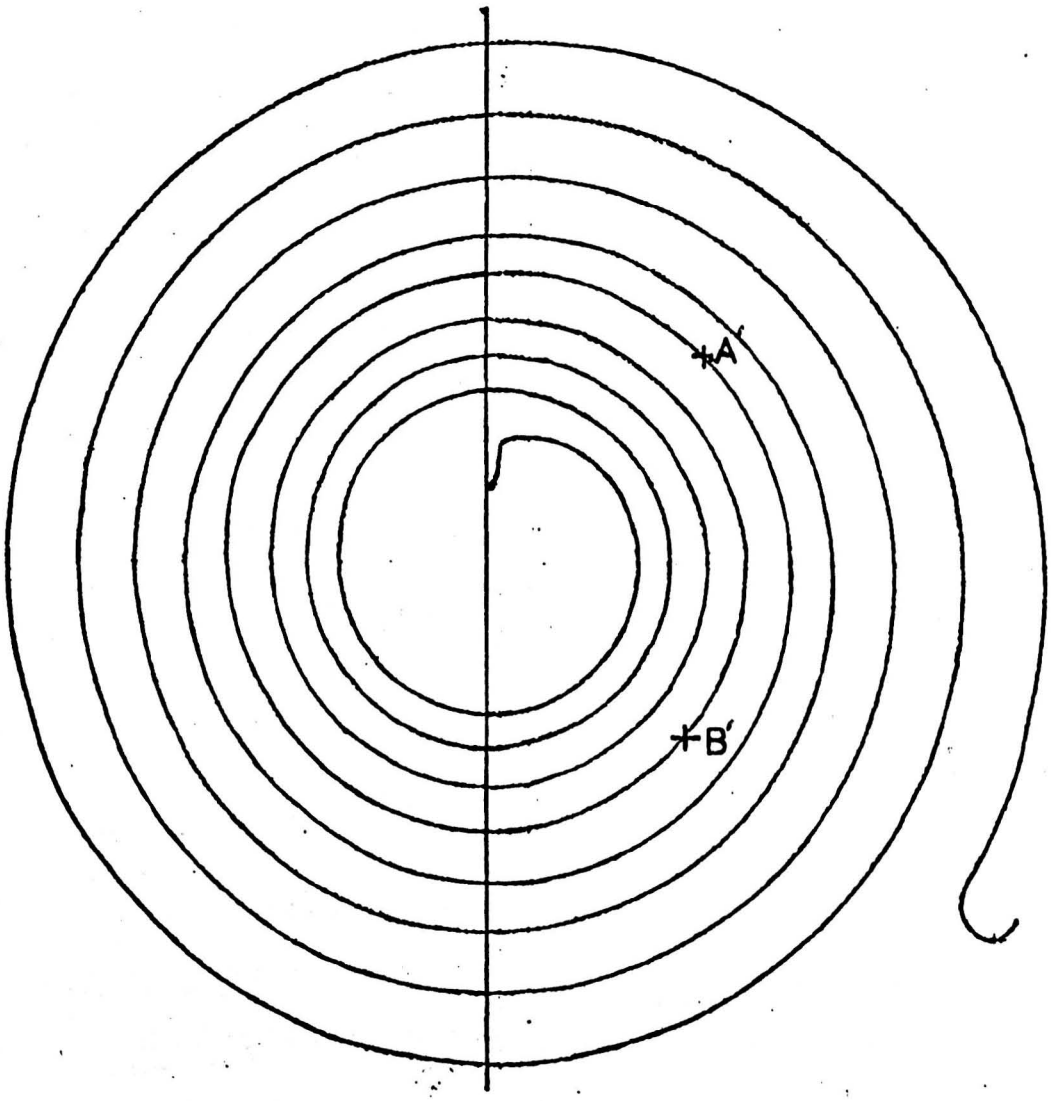

Fig. 3·12 Replica of spiral spring with transparent overlay.

by the angle π radians. The value of radius at $\theta = 0$ is obviously r_0, then let the values of r at π, 2π, 3π, etc., be r_1, r_2, r_3, etc., respectively. The successive coil diameters, D, are obtained as follows:-

$$r_0 = r_0 \; ; \quad r_1 = r_0 e^{\pi b} \; ; \quad D_1 = r_0(e^{\pi b}+1)$$

$$r_2 = r_0 e^{2\pi b} \; ; \quad D_2 = r_0(e^{\pi b}+1)e^{\pi b}$$

$$r_3 = r_0 e^{3\pi b} \; ; \quad D_3 = r_0(e^{\pi b}+1)e^{2\pi b}$$

$$r_n = r_0 e^{n\pi b} \; ; \quad D_n = r_0(e^{\pi b}+1)e^{(n-1)\pi b}$$

$$r_{n+1} = r_0 e^{(n+1)\pi b} \; ; \quad D_{n+1} = r_0(e^{\pi b}+1)e^{n\pi b}$$

from which:-

$$\frac{D_{n+1}}{D_n} = e^{\pi b}$$

Thus, if a ruler is laid across the coils so that the measuring edge passes through the origin of the spiral (the angles between the coils and the ruler, on one side of the origin, are equal) and measurements taken of successive coil diameters, a plot of current diameter versus previous diameter should result in a straight line of gradient $e^{\pi b}$.

Fig. 3.13 shows a typical plot of r against θ obtained during application of this method. (One would not expect this plot to be necessary. It is included only to illustrate the inaccuracies introduced by this method.) Fig. 3.14 shows the plot of raw results for the 'diameter' measurements together with the results when adjusted to the mean r - θ curve. It is interesting and important to note that a change in the slope of

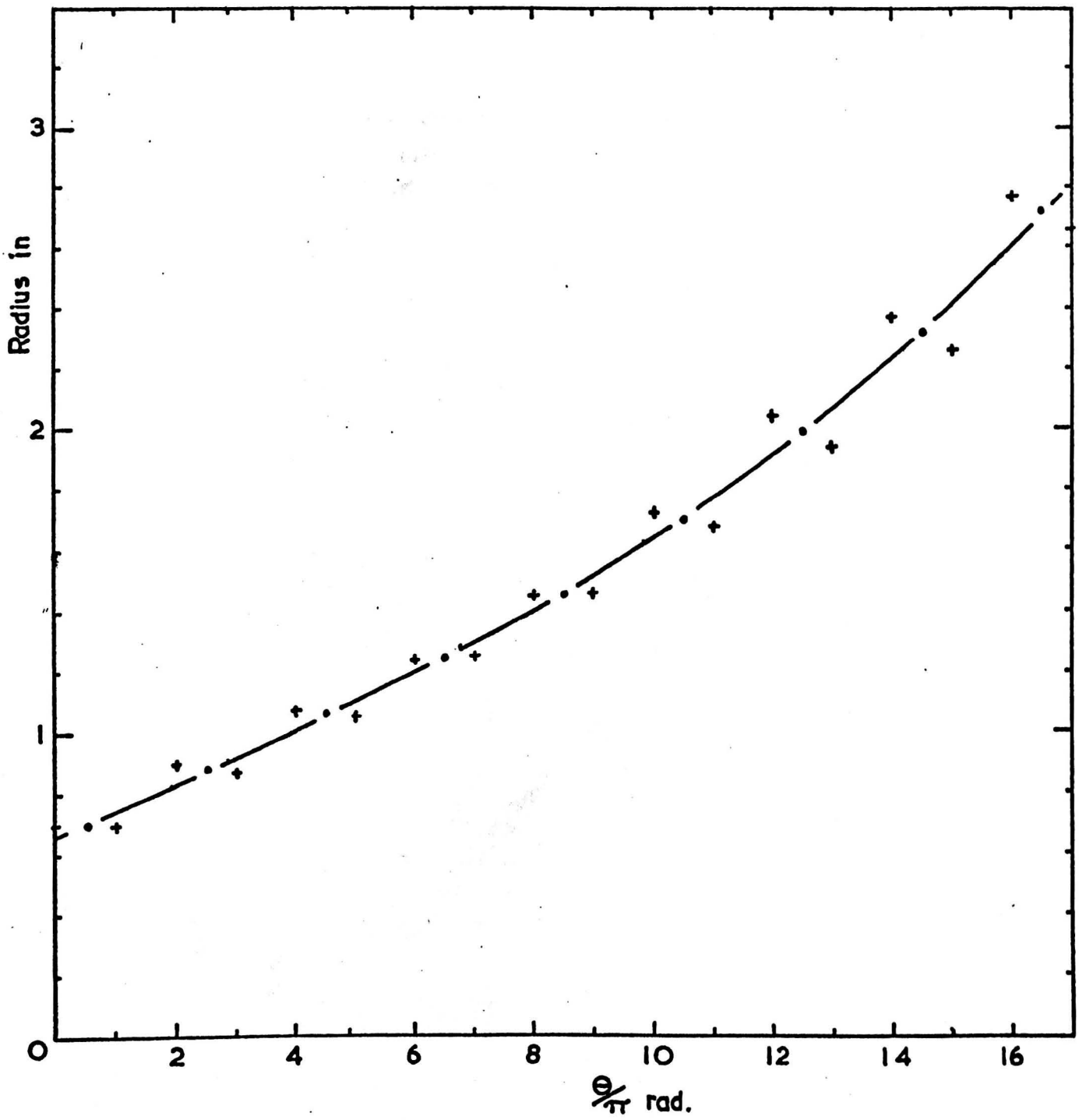

Fig. 3·13 Typical r–Θ plot

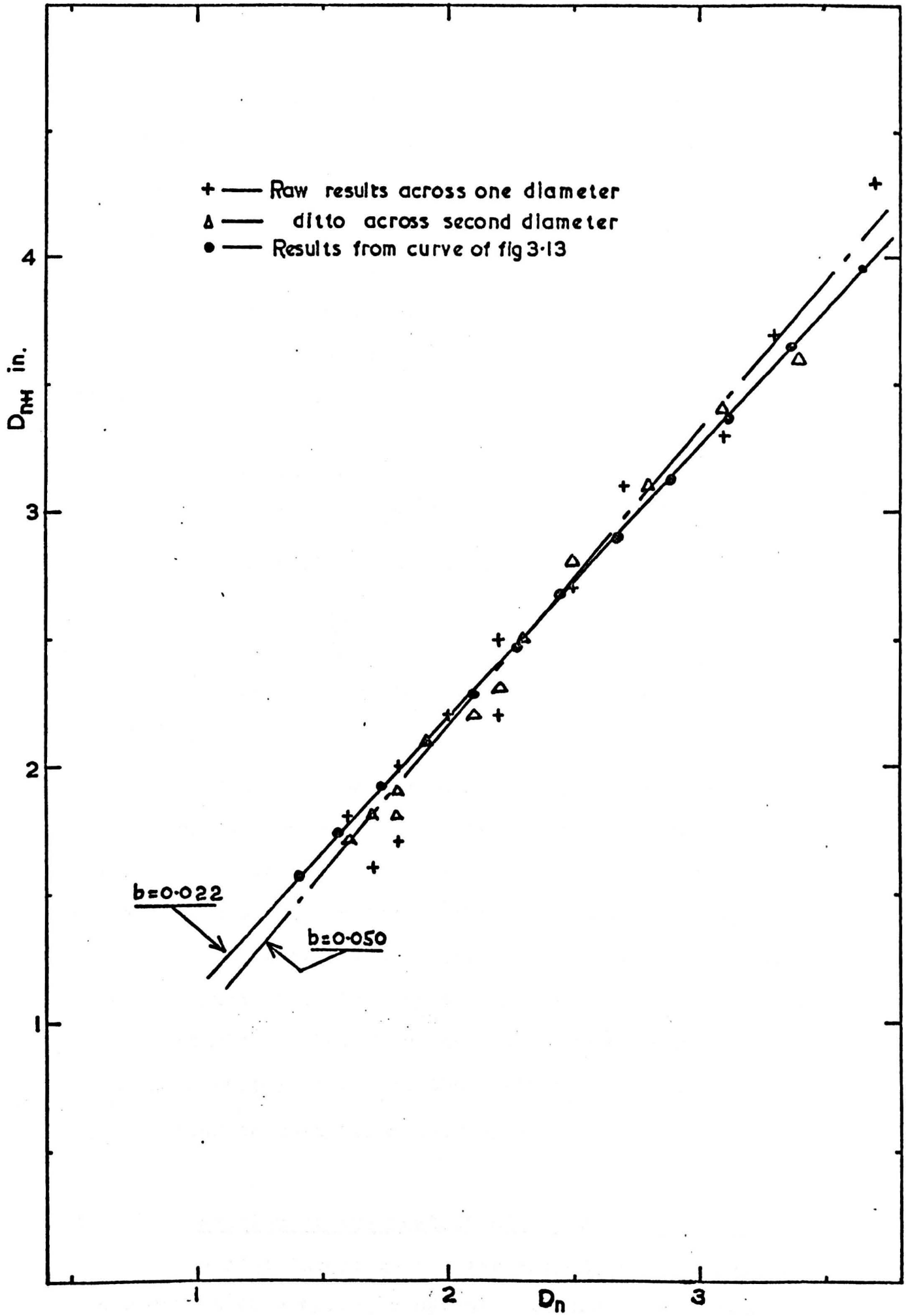

Fig. 3·14 D_{n+1} v D_n in.

D_{n+1} v D_n line of about 10% produces a change in the value of b of approximately 250%, so that whilst this method shows quickly that the spiral approximates to a logarithmic form, (since a straight line results) it is not a good method of determining the constant b.

ii) Let us now examine the coil spacing, S, which is given by the difference between the two values of radius separated by 2π radians. Following the procedure outlined in i) above, we have:-

$$r_o = r_o \quad ; \quad r_2 = r_o e^{2\pi b} \quad ; \quad S_o = r_o(e^{2\pi b}-1)$$

$$r_1 = r_o e^{\pi b} \quad ; \quad r_3 = r_o e^{3\pi b} \quad ; \quad S_1 = r_o(e^{2\pi b}-1)e^{\pi b}$$

from which it is seen that

$$\frac{S_{n+1}}{S_n} = e^{\pi b}$$

which again gives a linear plot of S_{n+1} against S_n.

In this method also, much scatter is obtained if raw results are plotted and even after adjustment of results using an r - θ plot the value of 'b' is extremely sensitive to a small error in the measurement of slope as is evident on examination of fig. 3.15. But, once more, the method will quickly indicate whether or not the spiral is logarithmic. Should the spring conform to an Archimedes spiral, $r = r_o\theta$, then both D_{n+1}/D_n and S_{n+1}/S_n tend to unity as n increases.

3.7. Results of examination of clock-type springs

Whilst investigating the methods of determining the equation of a spring's spiral outlined above, some

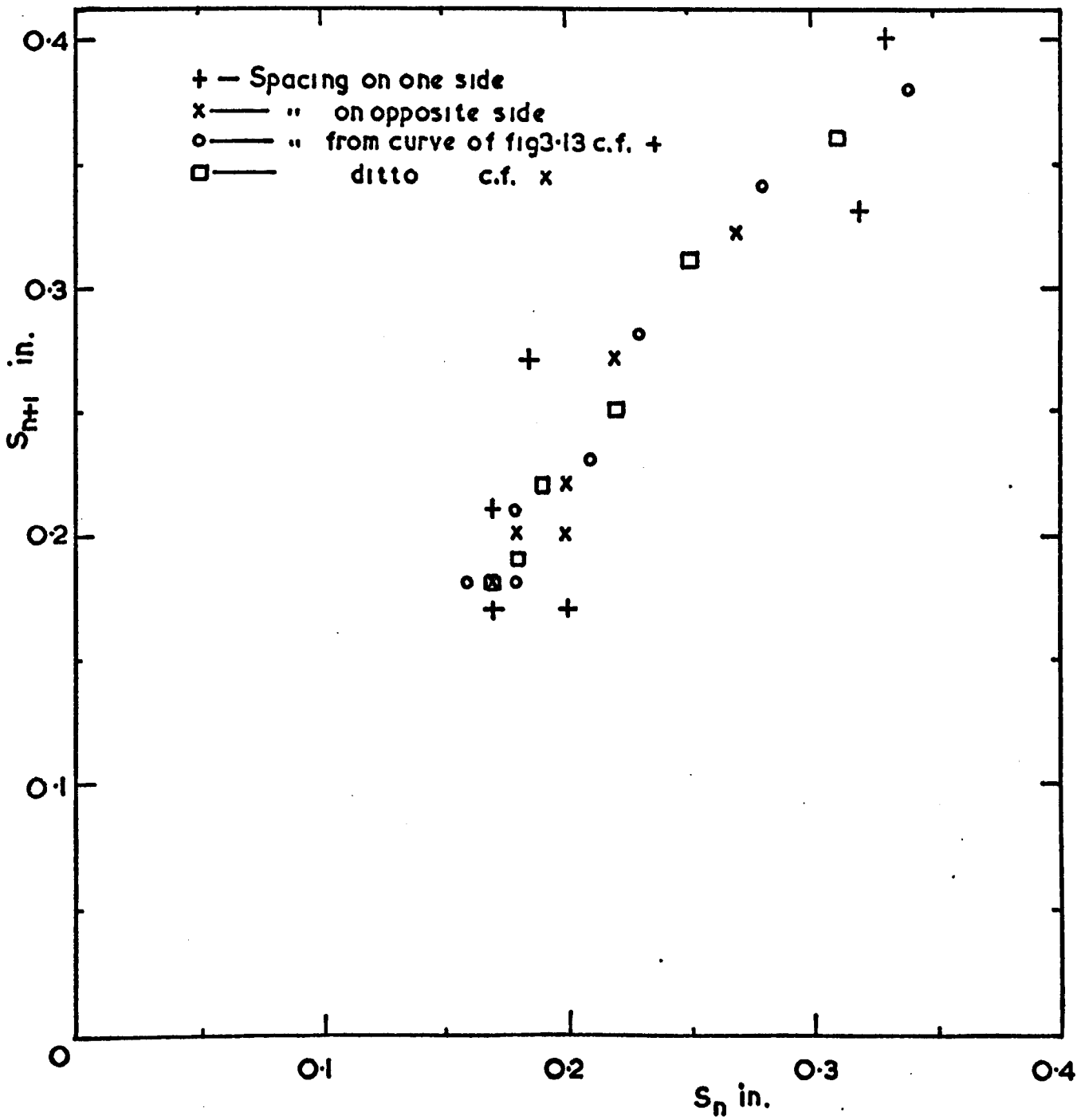

Fig. 3·15 Coil spacing

twenty springs of widely differing sizes were examined. Some of these springs were examined by more than one person using different methods. In these cases acceptable agreement was obtained but all the methods demand some practice before the individual concerned becomes adept.

Table 3.1 summarises the results obtained from the measurements of twenty springs and it is seen that, in the case of sixteen of these, a logarithmic spiral is indicated. In general a straight line could be drawn through the results when carrying out both the 'coil spacing' plot and the 'coil diameter' plot, but the values of 'b' obtained from these plots were seldom in close agreement with the value obtained from the lnr v θ plot for the reason outlined in 3.6 above. Of these twenty springs, one was found to conform to an Archimedes spiral, one to a spiral of the form $r = a\theta^n + C$, and two were found to require two separate logarithmic spiral equations.

It is also evident from the table that there was no obvious relationship existing between the value of 'b' and the physical dimensions of the spring, all of which were made of steel. The most likely parameter to which 'b' might be related is the strip thickness but it might be expected that the arbor diameter also influences the value of 'b'. No firm conclusion can be drawn from the results particularly since the history of the springs was not available. However, it may be of some interest to note that a plot of ln b against thickness, though there is much scatter in the points, gives the impression that a linear relationship might exit between these two variables.

TABLE 3.1

Spring No.	Width of Strip in.	Thickness of Strip in.	Number of Coils	Length of Strip ft. & in.	Value of r_o in.	Value of 'b'
P1	1"	0.059	$7\frac{1}{4}$	6' 11"	0.71	0.0257
P2	1.1875	0.071	$5\frac{1}{8}$	3 2	⁂	
P3	1	0.055	$7\frac{1}{8}$	7 8	0.741	0.0289
P4	1.5	0.049	$6\frac{1}{4}$	11 10	0.704	0.0316
P5	1	0.023	$6\frac{3}{8}$	14	0.726	0.0587
P6	1	0.024	$9\frac{1}{8}$	12 8	0.396	0.040
P7	1	0.023	8	10 11	0.214	0.076
P8	0.8125	0.049	$7\frac{1}{2}$	6 3	0.887	0.0239
P9	1	0.024	7	10	+	
P10	1.5	0.037	$11\frac{3}{4}$	50 11	1. 0.876 2. 0.151	0.0366 0.0630
P11	1.75	0.065	$10\frac{1}{2}$	29 10	1.624	0.0328
P12	1.75	0.058	9	12 2	1.01	0.0309
P13	2	0.049	$7\frac{1}{4}$	13 9	1. 0.748 2. 1.68	0.0632 0.0315
P14	1.75	0.037	$15\frac{1}{2}$	25 4	1.105	0.018
P15	1.75	0.106	$13\frac{1}{2}$	45	2.31	0.0217
P16	0.75	0.027	$11\frac{1}{2}$	8 10	0.267	0.0395
P17	1	0.022	$11\frac{1}{2}$	14 9	0.364	0.0417
P18	0.75	0.023	11	9 3	0.246	0.0433
P19	1	0.023	$10\frac{1}{4}$	13 7	0.31	0.0518
P20	1.25	0.024	8	12 6	0.733	0.0472

⁂ P2 was found to be an Archimedes spiral equation $r = 0.03810$

\+ P9 was found to have the equation $r = 0.00510^{1.91} + 0.22$.

CHAPTER 4

DESIGN OF THE SPRING TESTING MACHINE

4.1. Machine Requirements

The purpose of the machine is to examine the behaviour of clock - type spiral springs during loading, with special emphasis on the confirmation of the foregoing theory for Spiral Springs.

A universal machine was needed in order to test a wide variety of springs, the largest of which was estimated to require a torque of 2000 lbf in.

Due to some evidence produced by a certain spring manufacturer, that different results are obtained depending upon whether a spring is wound by rotating the arbor or the barrel, the machine was originally intended to load the springs by either method. However, it was the author's view that the rotation of a clock type spring was purely dependent on the relative motion of the arbor and the barrel, and that no difference should occur in the results depending upon whether the barrel or the arbor remained stationary.

Consequently, tests were carried out on the spring manufacturer's apparatus and it was discovered that errors due to friction in that particular machine could be of the order of 30%, and that it was almost impossible to obtain reproducible results.

The schematic arrangement of the particular machine in question is shown in fig. 4.1.

The plates (1) and (2), can be interchanged on the machine so that the torque, which is measured by means of a simple arm and weighing machine arrangement, could

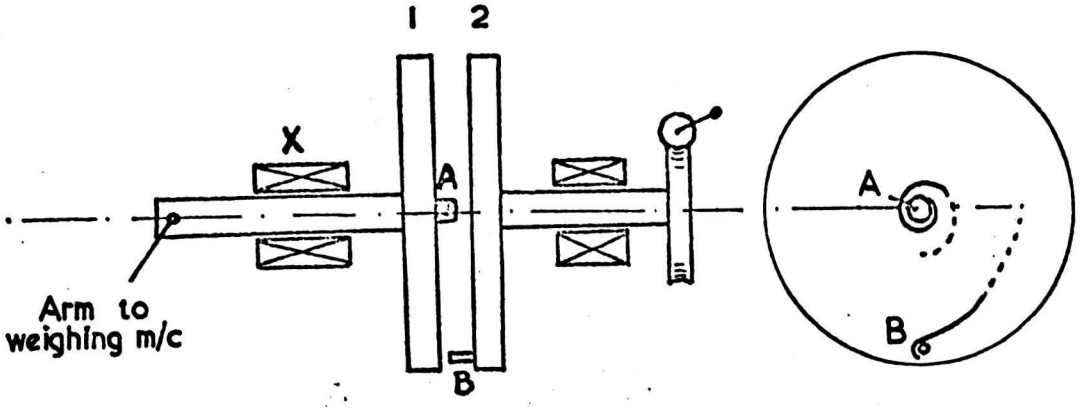

Fig. 4·1. Testing arrangement with high machine friction

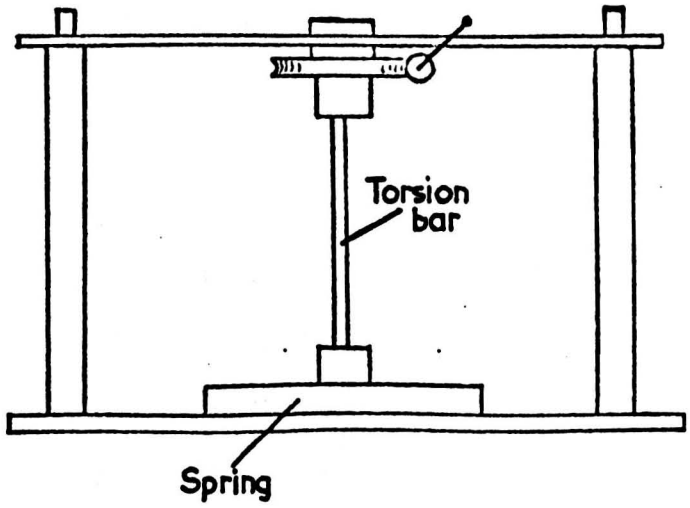

Fig. 4·2. Original concept of testing machine

be measured either from the arbor A, or from the driving peg side B (corresponding to the barrel). The friction due to the journal bearing X depends on its load, and the largest force occurs on plate 1. (Since here the torque is transmitted at a smaller radius.) Clearly, the friction in bearing X will be greater when the plates (1) and (2) are in the positions shown than when reversed. The friction within the machine was large and this explains the difference between the readings obtained on this apparatus for winding by means of the peg and by means of the arbor.

The machine designed for the work described in this thesis was therefore required to load the springs by one method only. To design the machine to wind the springs by both methods would have introduced unnecessary complications.

The springs to be tested were available before a start was made on the design, and so the maximum size of barrel required was known to be about 11 in. diameter.

The basic requirements for the machine were therefore:

(1) Torque range - 0 - 2000 lbf in.

(2) Accommodation for barrel sizes up to 11 in. diameter.

(3) Accommodation for any type of arbor.

(4) Allowance for any type of end fixing for the springs.

(5) Maximum accuracy with special emphasis on the elimination of friction.

4.2. The Design (General)

Many systems were considered but it was finally decided that torque bars would provide the best means for measuring the torque since there should be no inaccuracies incurred due to friction in bearings, etc.

The simplest system considered consisted of a worm gear arrangement suspended on a crossbeam, as shown in fig. 4.2.

The torque was to be transmitted by the torsion bar to the arbor, the barrel being clamped to the base. Measurement of the twist of the torsion bar, it was decided, would be by means of dial gauges actuated by levers attached rigidly at the ends of the torsion bar, the twist being measured by the difference in readings of dial gauges. The torque acting would be determined from a calibration chart or, later, probably strain gauges would be used.

Ultimately, it was decided to incorporate an existing worm and gear into the design. This gear assembly was of a large size, having a 10" diameter drum as an integral part of the gear wheel, and the inconvenience of suspending this, in the proposed plan, led to the final design shown in the photograph, fig. 4.3, and on the assembly drawing, figs. 4.4, 4.5 and 4.6.

Very little calculation was required for the design as only a few components took a sufficiently large load to warrant this. In consequence, the actual dimensions used were arrived at by estimation and availability of materials.

The machine is an experimental one and for this

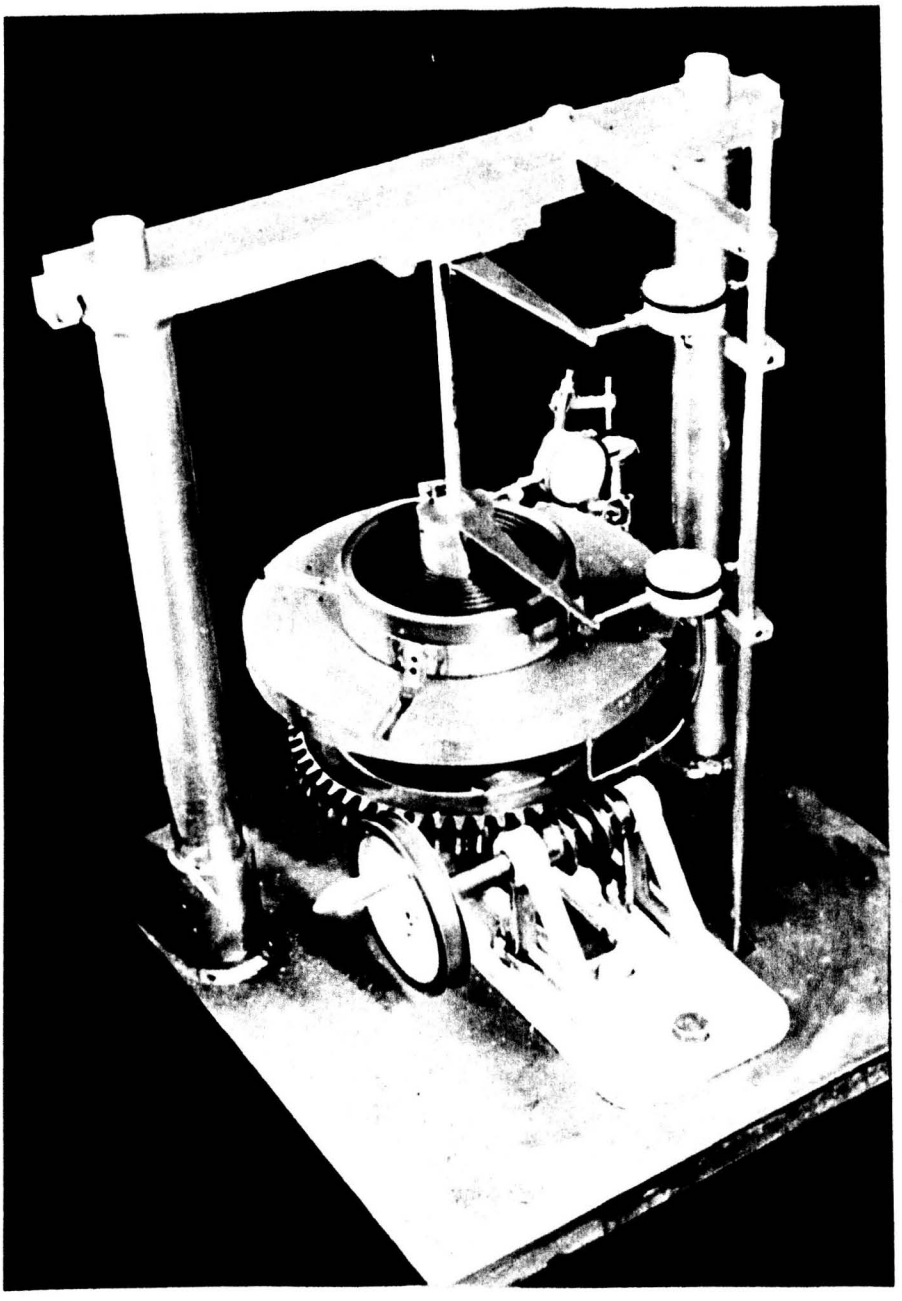

Fig.4.3 Testing machine in its original form

DIMENSIONS IN INCHES AND TO HAVE A TOLERANCE OF ± UNLESS SHOWN OTHERWISE. ALL DIMENSIONS TO BE GIVEN IN

No.	COMPONENT	MATERIAL	No OFF
1	WORM GEAR ASSEMBLY	AS SUPPLIED	1
2	COUPLING PLATE	1¼" M.S. PLATE	1
3	THRUST BEARING	HOFFMANN W1	1
4	GEAR SPINDLE	CARBON STEEL	1
5	¾" WHIT NUT	---	1
6	⅜" WHIT BOLTS ¾" LENGTH	—	8
7	½" WHIT BOLTS ¾" LENGTH	—	2
8	TABLE	1" M.S. PLATE	1
9	BARREL	M.S.	—
10	ANGULAR CONTACT BEARING	HOFFMAN LS12ACD	1
11	ARBOR HOLDER	M.S.	1
12	INDICATOR ARM	⅛" M.S. PLATE	2
13	ADAPTOR	M.S.	1
14	GRUB SCREW ⅜" LENGTH	—	3
15	ARBOR	M.S.	—
16	PLATE	5/16" M.S. PLATE	1
17	CLAMPING PLATE	M.S.	4
18	TORSION BAR	M.S.	-
19	½" WHIT BOLT 1" LENGTH	-	2
20	CARRIER BAR	5/16" M.S. PLATE	1
21	½" WHIT BOLT 1½" LENGTH	-	4
22	ADAPTOR	M.S.	1
23	PILLAR	M.S.	2
24	SLEEVE	M.S.	2
25	BASE PLATE	1" M.S. PLATE	1
26	DIAL GAUGE	-	2
27	GAUGE CARRIER ROD	½" M.S. ROD	1

COMP. No	AMENDMENTS
10.	REPLACE WITH HOFFMAN PLAIN ROLLER BEARING TYPE LS 12.
11.	MANUFACTURE FROM SINGLE PIECE REPLACING 7/8" SQUARE BY ¾" DIA. HOLE OF SAME DEPTH
15.	ALTER ONE END FROM 7/8" SQUARE TO ¾" DIA.

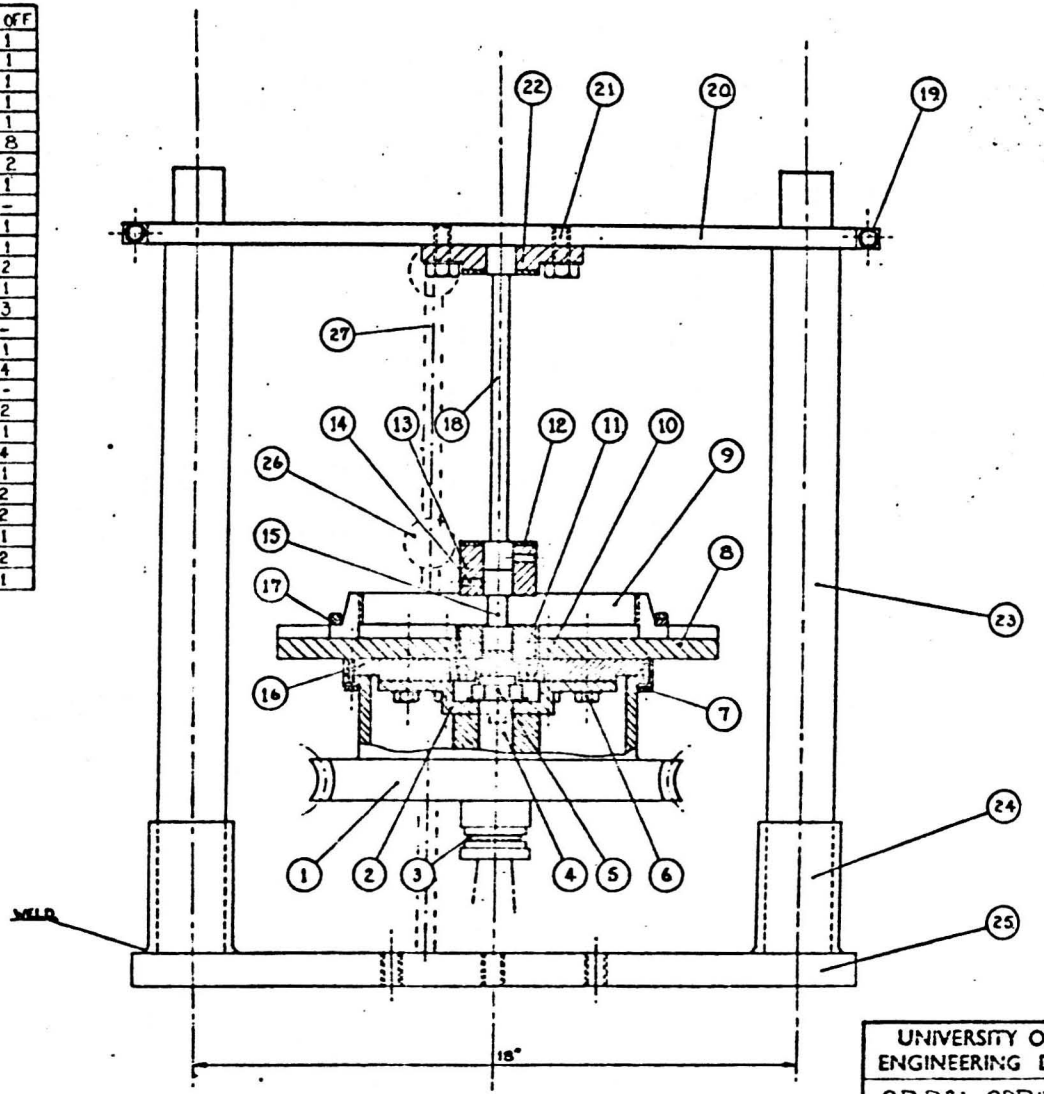

UNIVERSITY OF SHEFFIELD ENGINEERING DEPARTMENTS	Scale	Date
	HALF SIZE	11/11/63
SPIRAL SPRING TORSION TESTING MACHINE	REFERS TO ORIG DRAWING	M 270(1)

Fig. 4·4

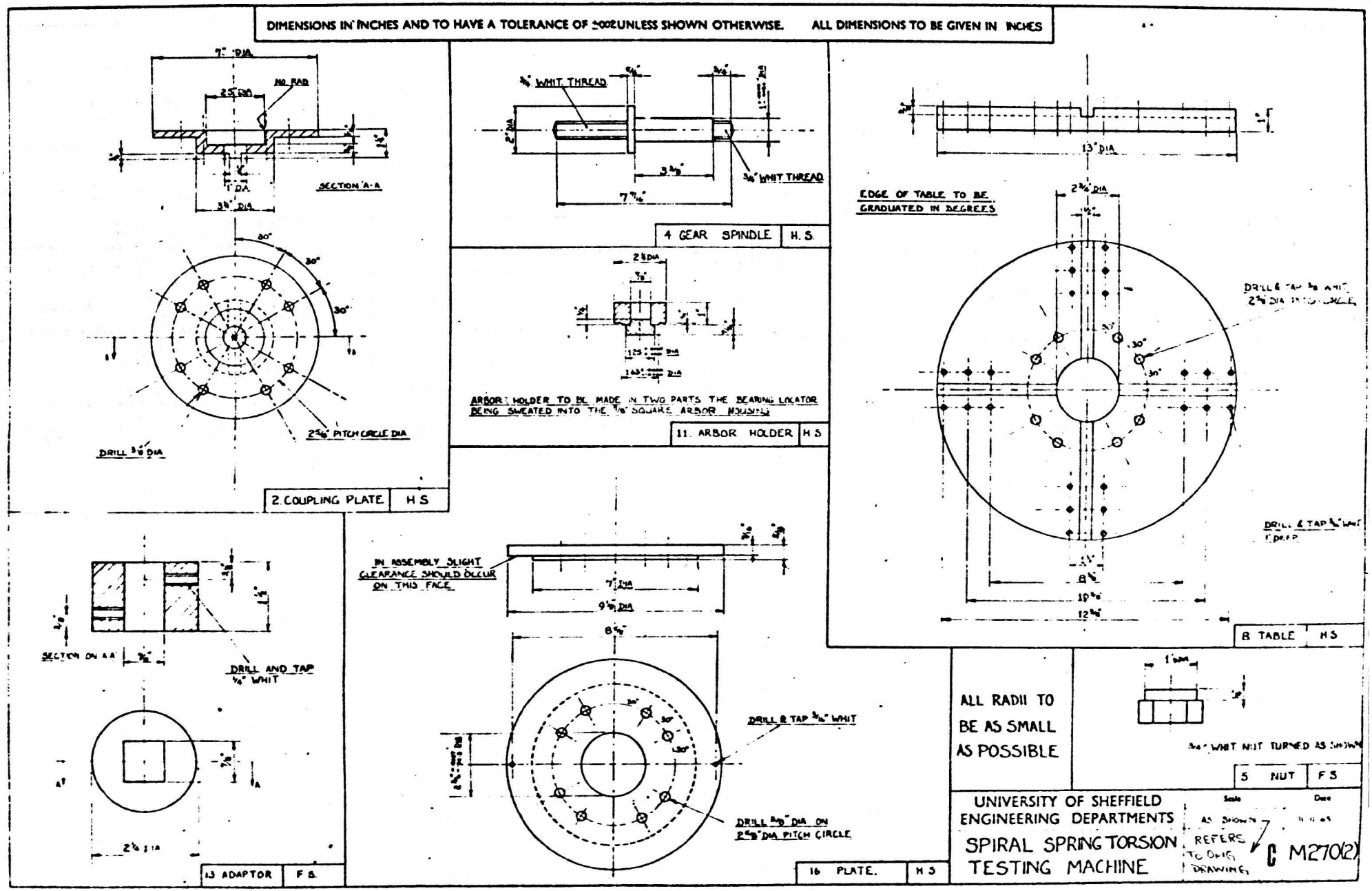
DIMENSIONS IN INCHES AND TO HAVE A TOLERANCE OF .002 UNLESS SHOWN OTHERWISE. ALL DIMENSIONS TO BE GIVEN IN INCHES
7" DIA
NO RAD
2.5" DIA
1" DIA
3.5" DIA
SECTION A-A
30°
DRILL 3/8" DIA
2.5" PITCH CIRCLE DIA
2. COUPLING PLATE H.S
3/8" WHIT. THREAD
3/4" WHIT THREAD
7 7/16"
4 GEAR SPINDLE H.S.
2.5 DIA
ARBOR HOLDER TO BE MADE IN TWO PARTS THE BEARING LOCATOR BEING SWEATED INTO THE 1/8" SQUARE ARBOR HOUSING
11. ARBOR HOLDER H.S
13" DIA
EDGE OF TABLE TO BE GRADUATED IN DEGREES
2.75" DIA
DRILL & TAP 3/8 WHIT 2.5" DIA PITCH CIRCLE
DRILL & TAP 3/8" WHIT 1" DEEP
8 1/2"
10 3/16"
12 3/16"
8. TABLE H.S
SECTION ON A-A
DRILL AND TAP 1/4" WHIT
2.25" DIA
13 ADAPTOR F.S.
IN ASSEMBLY SLIGHT CLEARANCE SHOULD OCCUR ON THIS FACE
7" DIA
9.5/16" DIA
8 3/16"
DRILL & TAP 3/8" WHIT
DRILL 3/8" DIA ON 2.5/8" DIA PITCH CIRCLE
16 PLATE. H.S
ALL RADII TO BE AS SMALL AS POSSIBLE
1" DIA
3/4" WHIT NUT TURNED AS SHOWN
5 NUT F.S
UNIVERSITY OF SHEFFIELD
ENGINEERING DEPARTMENTS
SPIRAL SPRING TORSION TESTING MACHINE
Scale AS SHOWN
Date
REFERS TO DWG
C M270(2)

Fig. 4.5.

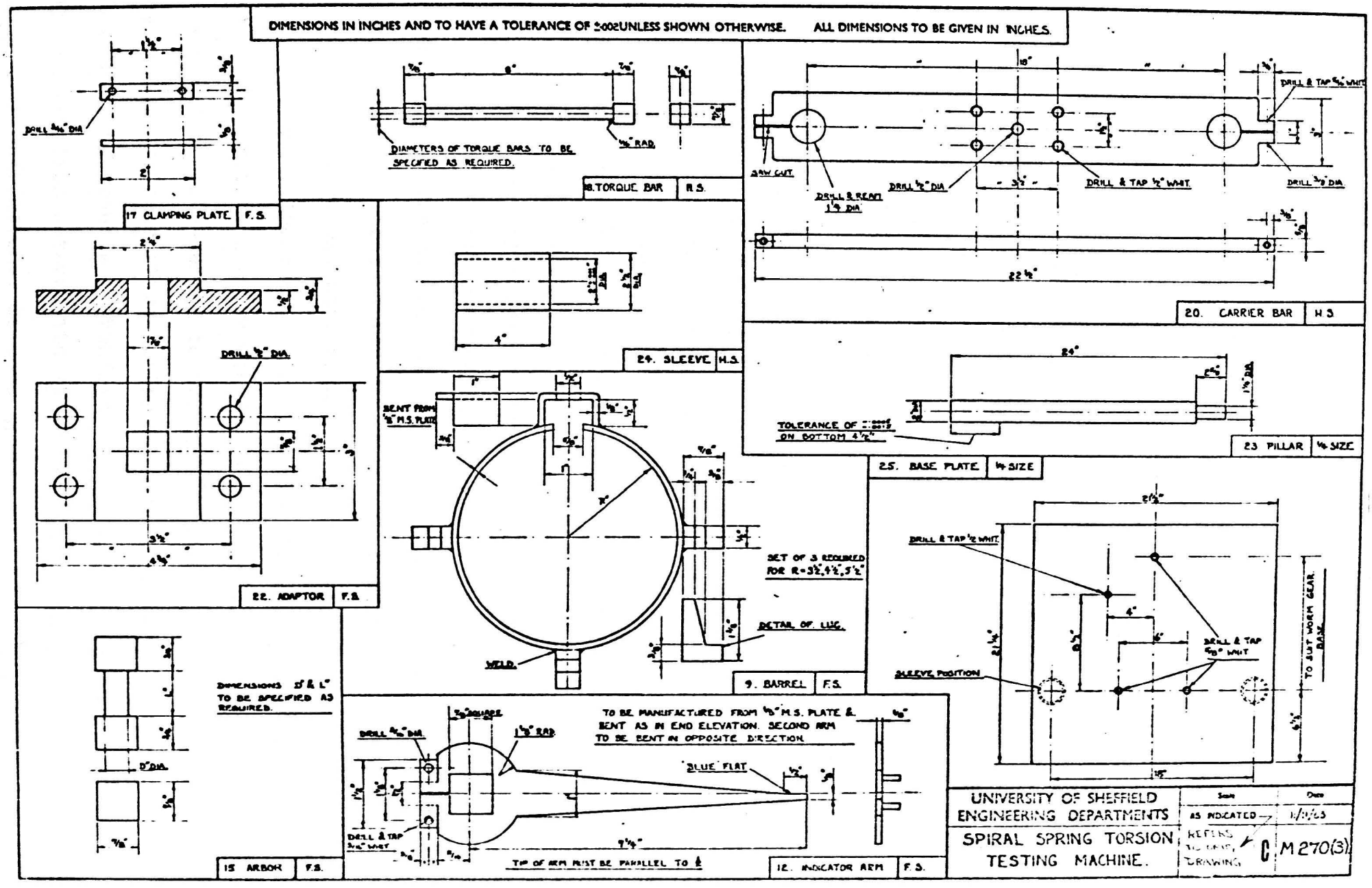
DIMENSIONS IN INCHES AND TO HAVE A TOLERANCE OF ±.002 UNLESS SHOWN OTHERWISE. ALL DIMENSIONS TO BE GIVEN IN INCHES.
17 CLAMPING PLATE F.S.
DRILL 3/16" DIA
DIAMETERS OF TORQUE BARS TO BE SPECIFIED AS REQUIRED.
1/16" RAD
18. TORQUE BAR M.S.
SAW CUT
DRILL & REAM 1" DIA
DRILL 1/2" DIA
DRILL & TAP 1/2" WHIT
DRILL 3/8" DIA
22 1/2
20. CARRIER BAR M.S.
DRILL 1/2" DIA
22. ADAPTOR F.S.
24. SLEEVE M.S.
BENT FROM 1/2" M.S. PLATE
WELD
SET OF 3 REQUIRED FOR R=3 1/2", 4 1/2", 5 1/2"
DETAIL OF LUG
9. BARREL F.S.
TOLERANCE OF ±.005" ON BOTTOM 4 1/2"
23 PILLAR 1/4 SIZE
25. BASE PLATE 1/4 SIZE
DRILL & TAP 1/2" WHIT
DRILL & TAP 5/8" WHIT
SLEEVE POSITION
TO SUIT WORM GEAR BASE
DIMENSIONS 'd' & 'L' TO BE SPECIFIED AS REQUIRED.
15 ARBOR F.S.
TO BE MANUFACTURED FROM 1/2" M.S. PLATE & BENT AS IN END ELEVATION. SECOND ARM TO BE BENT IN OPPOSITE DIRECTION
DRILL 3/16" DIA
1 1/8" RAD
BLUE FLAT
DRILL & TAP 3/16" WHIT
TIP OF ARM MUST BE PARALLEL TO Ø
12. INDICATOR ARM F.S.
UNIVERSITY OF SHEFFIELD ENGINEERING DEPARTMENTS
SPIRAL SPRING TORSION TESTING MACHINE.
Scale AS INDICATED
Date 1/11/63
REFERS TO THIS DRAWING
C M 270(3)

Fig. 4.6.

reason it was not considered important to enter into details of stress calculations in order to make the best use of materials which would be necessary for quantity production.

It will be noticed from the design that the torque acting on the spring is transferred directly to the torque bar, and so there can be no loss of torque by friction within the machine bearings, etc. The friction encountered which can affect the results obtained is that within the spring itself, between the spring and the table, and also slight friction which may occur in the base bearing, component No. 10, fig. 4.4.

The spring centres have a tendency to deflect when the spring is loaded, and for this reason the arbor holder was included in the original design. (Later this arrangement was modified resulting in a simpler design.) This component, No. 11, was purely for location fixing of the arbor and takes no load apart from the deflection force of the spring centre. This force will be small and so friction effects from the bearing will be negligible. Due to the thin section of some of the springs in question, it was necessary to load them in a horizontal position, otherwise the springs would have deformed under their own weight. The effect of this on the torque-rotation curve would probably be small, but the machine was required to examine in detail the behaviour of the springs during winding to ascertain, if possible, the causes of bundling of coils. Thus even though friction between the table and the spring was unavoidable frictional effects should be small enough to be discounted.

One foreseen difficulty with the torsion bar system was the requirement for close tolerances on the torque bar ends and attachments so that the torque bar would be fixed in a rigid vertical position with no side deflection possible. Clearly, any deflection of the ends of the torque bar in a horizontal direction would read directly on the dial gauges thus giving an incorrect torque reading.

Two dial gauges are used so that only relative twist of the ends of the torque bar is measured thus eliminating any error due to end fixings and strain in the machine.

Should it be necessary, correction for any error caused by sideways movement of the lower end of the torsion bar is made by the addition of a further dial gauge to run on the torque-bar-arbor connection, perpendicular to the torque arm, to measure the actual sideways deflection of the lower end of the torsion bar.

Basically then, the machine consists of a worm-gear drive to a horizontal revolving table, to which barrels of various sizes can be attached. The spring is wound onto an arbor which is restrained against lateral movement and rigidly connected to a torsion bar, supported and fixed at the upper end so that the torque transferred to it by the arbor results in a twist. Torque arms and dial gauges at each end of the torque bar are used to measure the twist of the bar and hence, the torque on the arbor. The actual angle turned through by the spiral is measured directly from degree markings on the edge of the table.

4.3. Design (Details)

4.3.1. Worm and Worm Wheel

Very little work was needed to adapt the worm drive for the purpose of the design. The most important alteration was to adapt the table to the gears, and to provide a positive drive between the two.

The rim on the gear wheel drum was not wide enough to use for the purpose of loading the springs and difficulties would have been met due to the cast iron construction so the final solution was to provide means of transmission by a tongue and groove arrangement in the gear wheel hub.

4.3.2. Table Design

In order to position the barrels on the table, two mutually perpendicular slots were machined in the table top as shown in fig. 4.5. When the barrel is positioned clamping plates, (component No. 17) are used to secure the barrel.

4.3.3. Barrel Design

Three main types of end fixing are commonly used for springs of spiral form. The end may be bent over at right angles forming a small tongue (which may be shaped) or a hole or slot may be cut in the strip near to its extremity, or the end may be bent in the form of a loop suitable for locating on a circular bar or stub. The end of the loop may then be rivetted or spot welded onto the strip to prevent the loop from opening out.

The design of barrel adopted (fig. 4.6) will

allow any type of end fixing to be accommodated.

Originally, a set of three barrels of diameters 7", 9" and 11", was provided but further barrels may be added as required.

From the detail, fig. 4.6, it will be seen that the barrels are not continuous. The gap enclosed by the welded bracket enables various adaptors to be used in conjunction with the barrels for end fixing the springs. In this way any adaptor is interchangeable with the barrels. The actual design of the adaptors (or fixing pins) must necessarily depend on the spring to be tested. In the case of fixing pins, the pins are placed in the gap provided so that they do not interfere with the uncoiled bundles of the spring.

4.3.4. Spring Arbor Design

It is impossible to cater for all sizes of springs and it was an accepted part of the design that an individual arbor must be designed for each spring tested. The design was planned to include a simple and cheap arbor.

4.3.5. Torsion Bar Design

A range of torsion bars for use with torques of between 0 and 2000 lbf in., and producing a twist of approximately 3° at the maximum design torque, were required. It was decided to use a set of five bars with maximum torques of 200, 300, 500, 1000 and 2000 lbf in. A convenient length was chosen for the torsion bars and the well known formula:

$$\frac{T}{J} = \frac{G\theta}{L} = \frac{\sigma}{R}$$

was used to determine the necessary diameters.

4.3.6. Gauge arm design

Little is required in the way of design for the gauge arms, the requirements are simple. The arms must be attached rigidly at the ends of the gauge length and must operate the dial gauges at a predetermined radius. In fact, the arms attach to the square ends of the torsion bars and the gauges are attached to a pillar and arranged so that their plungers rest on the torque arms at the 7" length mark on the arms. The whole arrangement is then calibrated by applying known torques as described in appendix A4. The error introduced due to obliquity as the torsion bar rotates is also dealt with in appendix A4.

4.4. Operation of machine (Refer to fig. 4.4.)

The operation of the machine is quite simple. The carrier bar, 20, is raised after slackening the clamp, 19. The required barrel is then located centrally on the table, 8, and clamped into position with the clamping plates, 17. The torsion bar to suit the designed torque of the spring is then selected and one end inserted into the adapter, 22, on the carrier bar. It is found that part of the square end of the torsion bar stands proud and to this is fixed one of the gauge arms. The second gauge arm is fitted to the lower end of the torsion bar followed by the arbor. Next the spring is attached to the arbor and the table rotated so that the outer end

may be fixed in the 'cut-out' of the barrel. The carrier is now lowered so that the arbor is located in its holder, 11, and the spring is fed into the barrel.

The dial gauges are now fixed into position on the rod, 27, and positioned to the 7 in. mark on the gauge arm. A third dial gauge is positioned to measure the lateral movement (at right angles to the gauge arm) of the lower end of the torsion bar. The table (barrel) is then rotated by operating the handwheel and readings taken of angle turned through by the table and the difference in dial gauge readings. These latter readings are then converted to torque and the torque-rotation characteristic is plotted for both loading and unloading.

CHAPTER 5

COMPARISON OF THEORETICAL AND EXPERIMENTAL RESULTS

5.1. Introduction

The theory and techniques discussed in the previous chapters have been successfully applied to a number of springs. Little purpose would be served in referring to each test here but the validity of the theory will be demonstrated by reference to one cr two special examples.

5.2. Testing of spring T.S.1

Fig. 5.1 is a reproduction of the spiral of this particular spring and figs. 5.2 and 5.3 show the $r - \theta$ and the $\ln r - \theta$ plots for this spring. From these plots the spiral equation is found to be

$$r = 0.81\, e^{0.0253\,\theta} \quad .. \quad .. \quad .. \quad (5.1)$$

The total angle of the spiral is 16π if a short length at the start of the spiral is ignored. The measured length of the spiral, obtained by marking off one foot lengths of the spring making use of thin paper tape wrapped tightly round the spring, is 82.5 in. and the length excluded from the ensuing calculation is approximately $1\frac{3}{4}$ in.

Integrating the spiral equation 5.1 over the total angle of the spiral gives

$$L = \int_0^L \sqrt{r^2 + \left(\frac{dr}{d\theta}\right)^2}\, d\theta = \left[\frac{0.8197e^{0.0253\theta}}{0.0253}\right]_0^{16\pi}$$

$$= 82.2 \text{ in.}$$

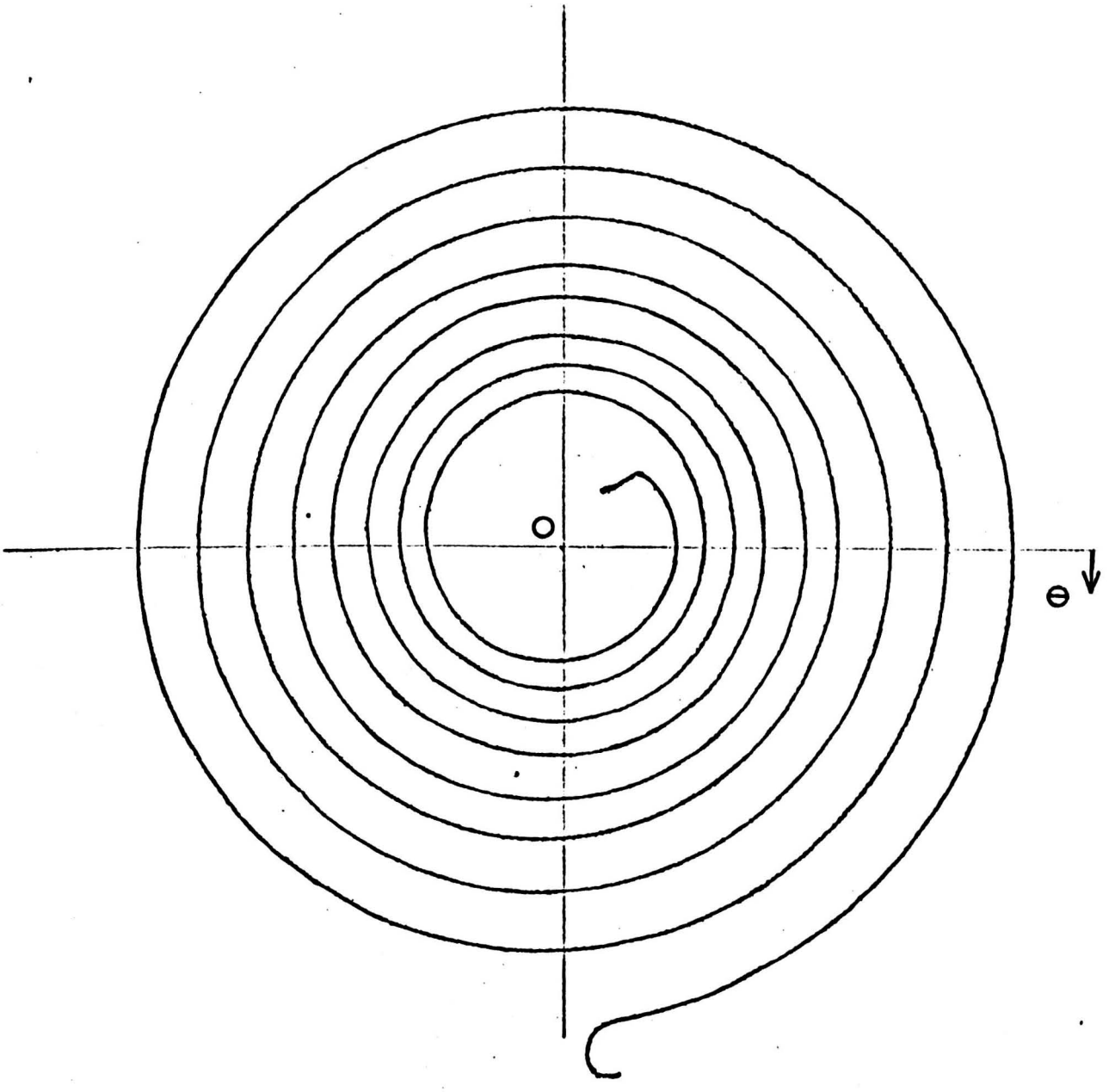

Fig. 5·1 Free spiral of spring TS 1
see figs. 5·2, 5·3 for R-θ & LnR-θ plots.
Reference point located by 4-point method.

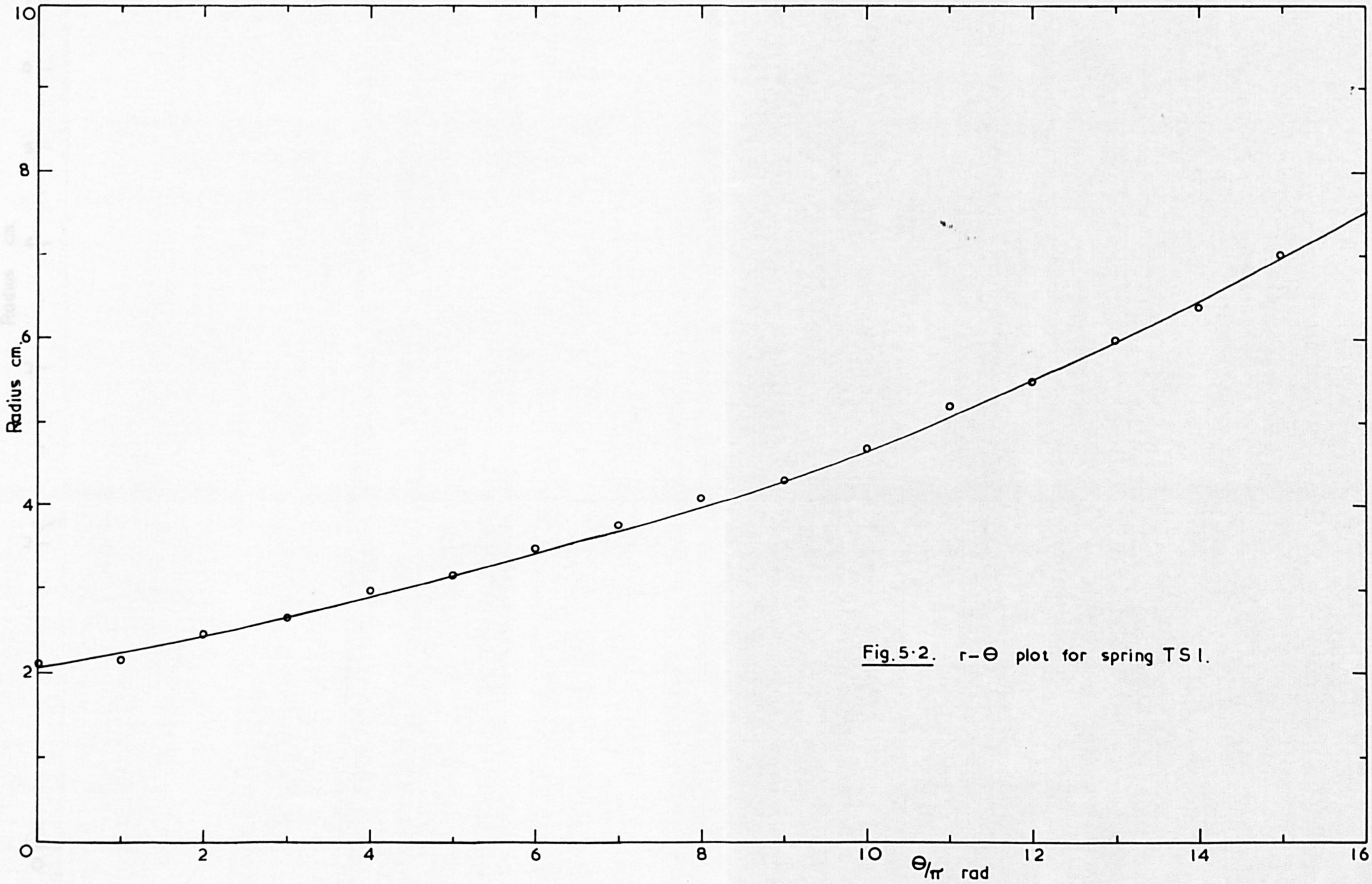

Fig. 5·2. r–Θ plot for spring T S 1.

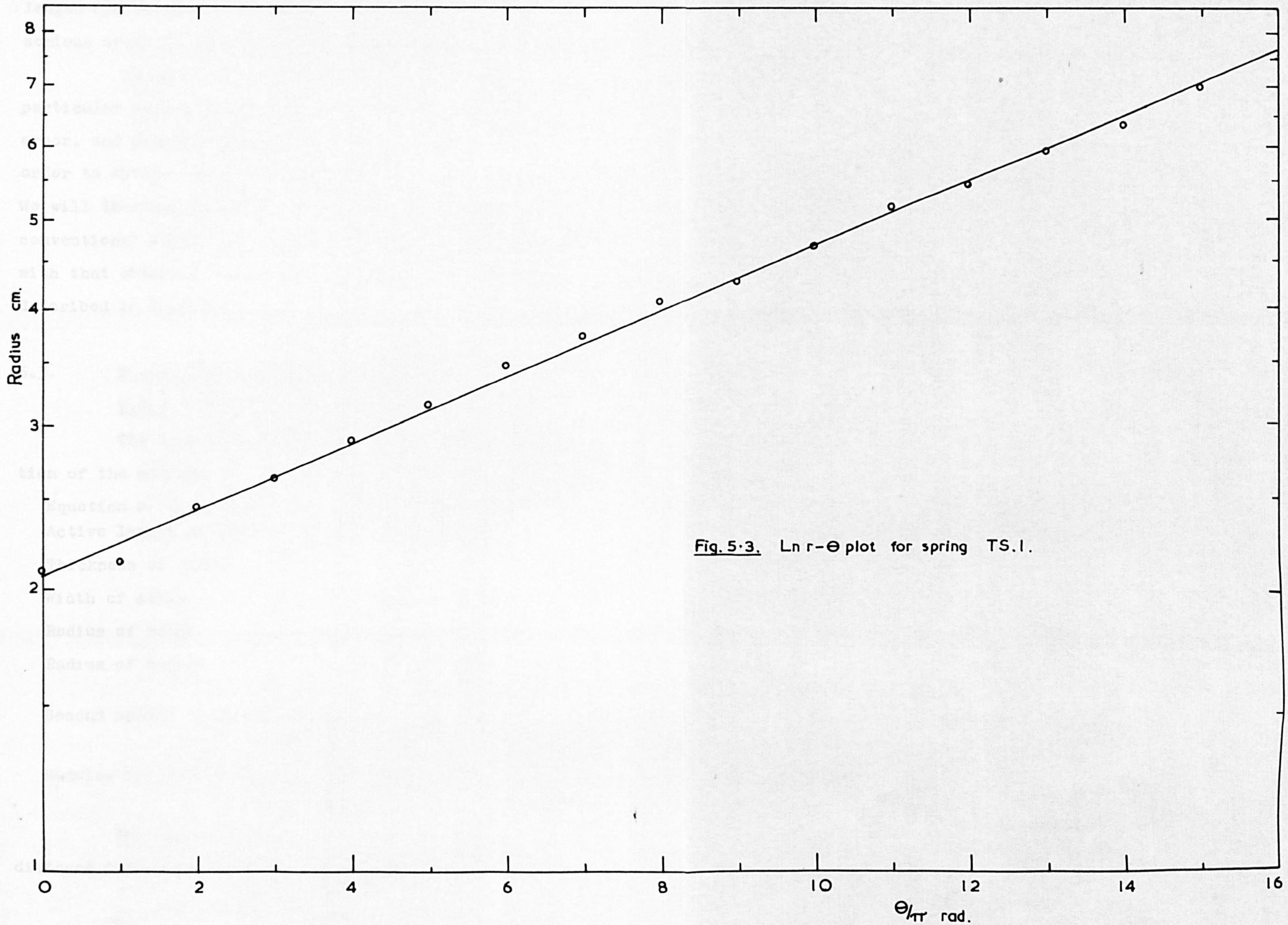

Fig. 5·3. Ln r–Θ plot for spring TS.1.

which is in close agreement with the measured length (80.75 in.). This suggests that there is no serious error in the equation for the spiral (eq. 5.1).

We will now consider the case when this particular spring is inserted into a barrel with its arbor, and progress through the method of Chapter 2 in order to obtain the M - ϕ characteristic for the spring. We will then obtain the M - ϕ characteristic in the conventional manner and compare these two characteristics with that obtained by testing the spring in the machine described in Chapter 4.

5.3. M - ϕ characteristic for spring

T.S.1 (Case 1)

The following data apply to the first illustration of the method:-

Equation of free spiral	:	$r = 0.81\ e^{0.0253\ \theta}$
Active length of strip	:	$L = 81.5$ in.
Thickness of strip	:	$t = 0.056$ in.
Width of strip	:	$w = 1.000$ in.
Radius of arbor	:	$R = 0.625$ in.
Radius of barrel	:	$R' = 1.875$ in.
Second moment of area of strip	:	$I = \frac{wt^3}{12} = 14.62 \cdot 10^{-6}$ in.^{4}
Modulus of elasticity	:	$E = 30 \cdot 10^6$ lb/in.^{2} (assumed)

The curvature at any point on the spiral distance S from the start is given by eq. 2.10

$$K_o = \frac{1}{bs + r_o(1 + b^2)^{\frac{1}{2}}} \simeq \frac{1}{bs + r_o} \quad .. \quad (2.10)$$

i.e. $$K_o = \frac{1}{0.0253\ S + 0.81} \quad .. \quad .. \quad .. \quad .. \quad (5.2)$$

Equations 2.11 and 2.12 respectively, give the curvature at the same point when the spring is run-down and wound up in its barrel:-

$$K_1 = \frac{B}{\sqrt{C_1 + S}} \quad .. \quad .. \quad .. \quad .. \quad .. \quad (2.11)$$

where $B = \sqrt{\frac{\pi}{t}}$

$$C_1 = B^2(R - \tfrac{t}{2})^2 - L$$

$$K_2 = \frac{B}{\sqrt{C_2 + S}} \quad .. \quad .. \quad .. \quad .. \quad .. \quad (2.12)$$

where $B = \sqrt{\frac{\pi}{t}}$

$$C_2 = B^2(R' + \tfrac{t}{2})^2$$

For the present case the values of the constants are

$$B = 7.4900$$

$$C_1 = 109.8794$$

$$C_2 = 23.9215$$

and the plotted values of K_o, K_1 and K_2 are shown in fig. 5.4 together with the ΔK_{10} and ΔK_{20} curves.

Now it was shown in Chapter 2 that the rotation of the arbor is given by the area lying between the ΔK_{10} and ΔK_{20} curves and the abscissa corresponding to M. (It must be noted that ΔK_{10} is zero for the first 30 inches of the spring.) The torque required at the arbor is given by

$$M = EI\Delta K$$

$$= 30 \cdot 10^6 \cdot 14.62 \cdot 10^{-6} \Delta K$$

i.e. $$M = 438.6\ \Delta K \text{ lbf.in.} \quad .. \quad .. \quad (5.3)$$

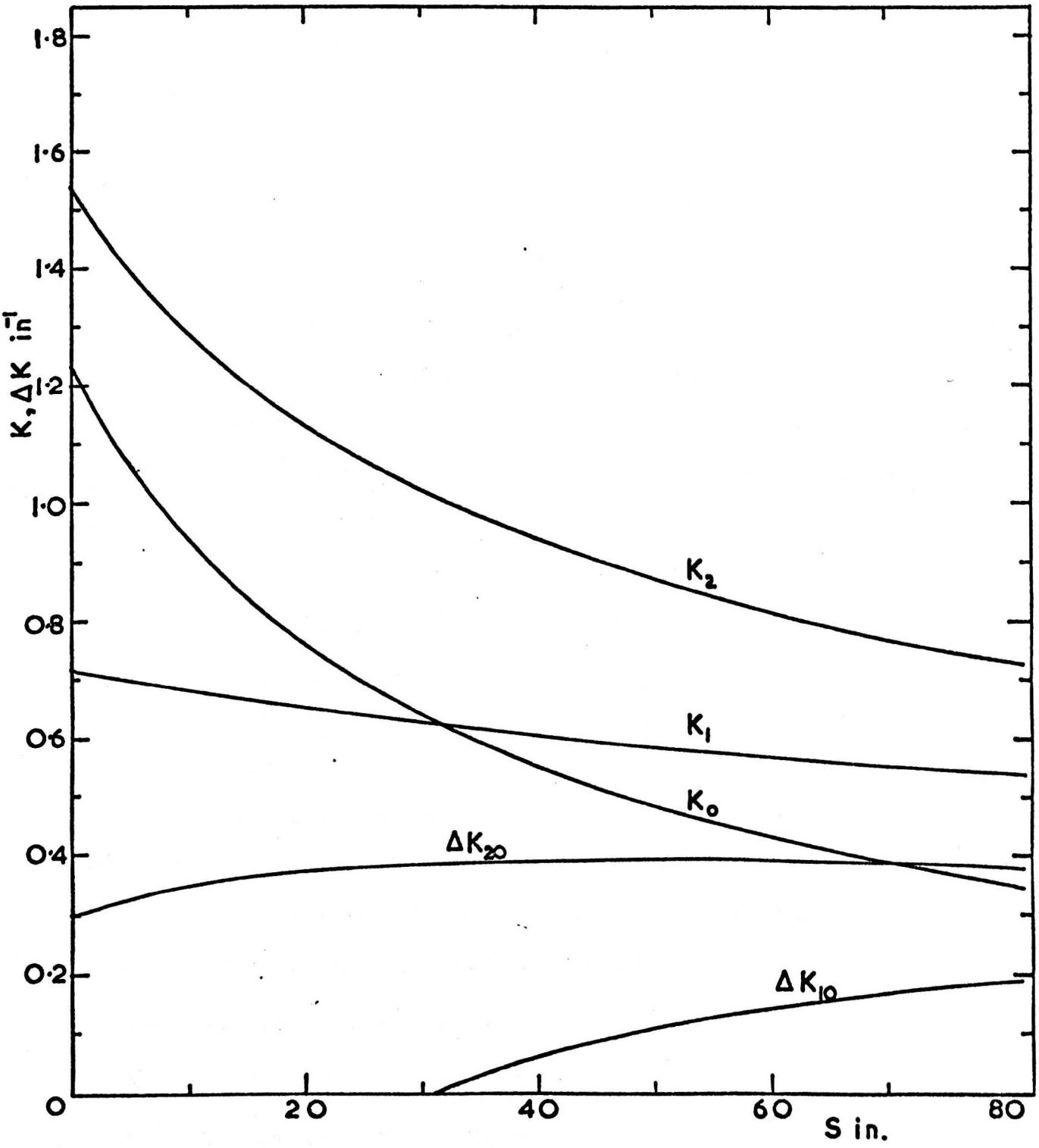

Fig 5·4. K–S & ΔK–S curves for spring of fig 5·1 when used with arbor 1¼in dia and barrel 3¾ in dia.

If measurements of area are made from the graph, fig. 5.4, in order to compute the twist ϕ, then, since the graphs are plotted to scales of 10 mm. = 0.2 in^{-1} for curvature and 10 mm. = 10 in. for strip length, rotation of the arbor in radians is given by

$$\frac{\text{area measured } (mm^2)}{50}$$

A table of results for this spring is included in appendix A5 together with the practical test results, both of which are plotted in fig. 5.5. along with the results obtained in applying the conventional theory. We will now consider the conventional theory applied to this spring.

5.4. Conventional theory applied to the present case

The theory was examined in Chapter 2 but will be reiterated here.

It is based on the relationship $M = \frac{EI\phi}{L}$ and if n_o is the number of coils in the free state, n_1 the number when run down in the barrel and n_2 the number when fully wound on the arbor, we showed that:

Initial torque (applied to spring): $M_1 = \frac{2\pi EI}{L}(n_1 - n_o)$

Maximum torque: $M_2 = \frac{2\pi EI}{L}(n_2 - n_o)$

Useful torque: $M = M_2 - M_1$

$$= \frac{2\pi EI}{L}(n_2 - n_1) \quad .. \quad .. \quad (2.2)$$

If we now visualise the spring coiled against the barrel, the area of the annulus (neglecting the thickness of any lubricant film) is:-

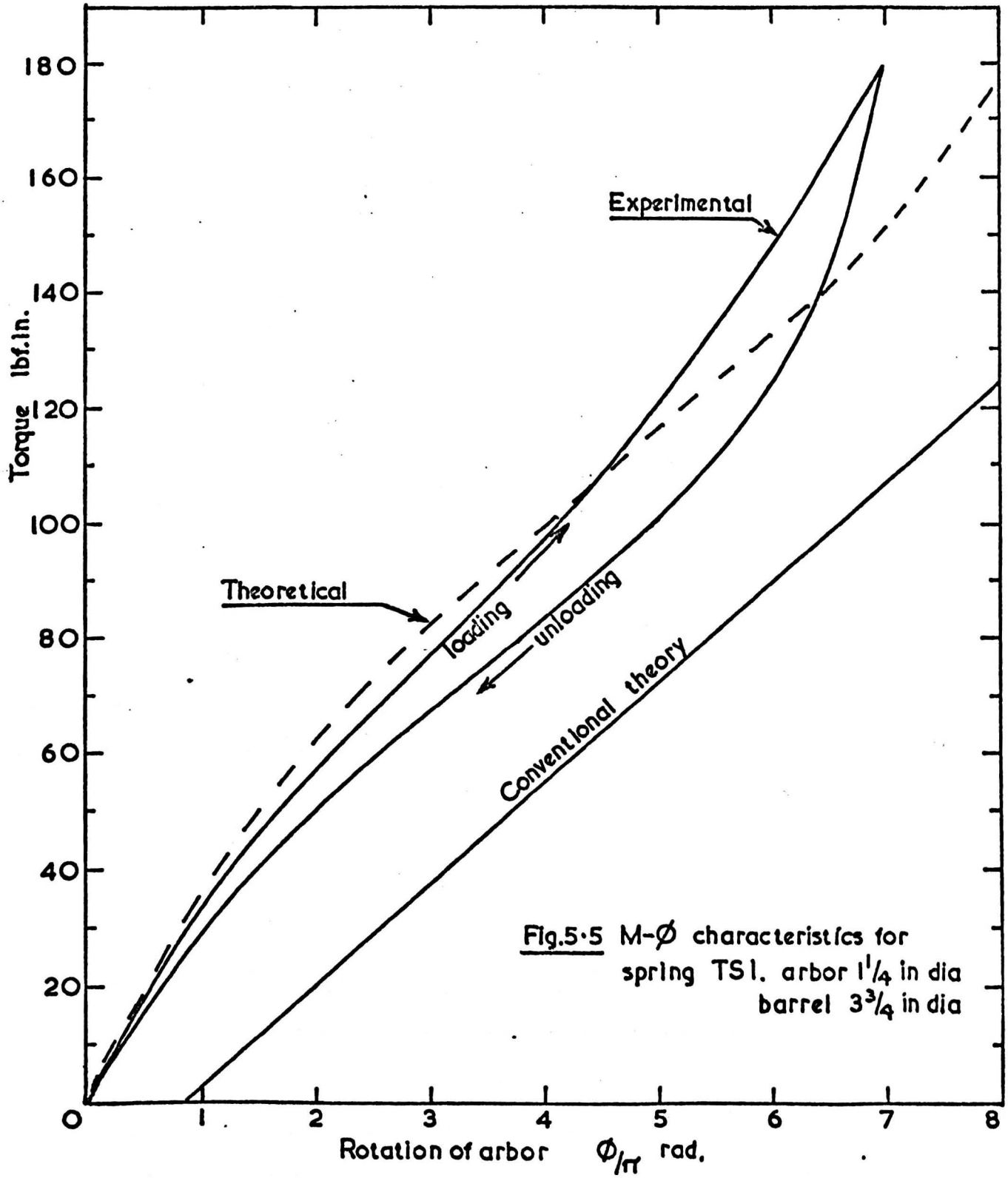

Fig.5·5 M-Ø characteristics for spring TS1. arbor $1\frac{1}{4}$ in dia barrel $3\frac{3}{4}$ in dia

$$Lt = \frac{\pi}{4}(D_2^2 - D_1^2) \quad .. \quad .. \quad .. \quad (5.4)$$

where L = strip length

D_2 = inside diameter of barrel

D_1 = inside diameter of coils

$$\text{Also } n_1 t = (D_2 - D_1)/2 \quad .. \quad .. \quad .. \quad (5.5)$$

From equation 5.4 it is seen that

$$D_1 = \sqrt{D_2^2 - \frac{4Lt}{\pi}}$$ and substitution

in equation 5.5 gives:-

$$n_1 = \frac{D_2 - \sqrt{D_2^2 - \frac{4Lt}{\pi}}}{2t} \quad .. \quad .. \quad (5.6)$$

Similarly $$n_2 = \frac{\sqrt{\frac{4Lt}{\pi} + D_1^2} - D_1}{2t} \quad .. \quad (5.7)$$

In the present case these equations give

n_1 = 7.95 and

n_2 = 13.17

n_o = 8.375

M_1 = -14.3 lbf.in.

M_2 = 161 lbf.in.

ϕ = $2\pi(n_2 - n_1)$ = 10.44 radians.

5.5. Some comments on the results

Although the practical and theoretical torque-rotation curves differ slightly in shape, the proximity of the theoretical to practical results is quite good, especially over the working range. The conventional theory is clearly in error in this particular case. In the conventional theory the spring is assumed to be

totally coiled against the barrel when unwound, and a negative initial torque is given by the theory. If the spring were housed in a smaller barrel then the conventional theory would provide a closer approximation to the actual behaviour of the spring.

In a retest of the spring all the machine readings were repeated with very great accuracy, indicating that the results themselves were valid. Only very slight differences were obtained with the spring liberally oiled which suggests that frictional effects between the spring and table were negligible.

The failure of the conventional theory in this instance is obvious. The whole of the strip length is not resting against the barrel or the coils adjacent to the barrel in the unwound state, and the length of strip involved is not L. There are, in fact, only $2\frac{1}{3}$ coils, in the free state, lying outside the barrel diameter.

In Chapter 6, the effects of altering the arbor size and the barrel size will be investigated.

CHAPTER 6

FURTHER TESTS

6.1. Purpose of the investigation and its execution

The primary object of the tests now described was to provide further evidence in support of the theory of Chapter 2 and to examine the effects of the variables barrel diameter and arbor diameter. It was intended also to explore the possibility of applying the theory to open-coiled springs. The spring to be tested, therefore, was chosen so that it could be fitted into a number of barrels, at least one of these producing open-coil conditions during testing. Also, it had to be capable of accommodating arbors sufficiently different in diameter to produce discernible changes in the M - ϕ characteristic.

The spring selected was one of those supplied by the Airedale Spring Company and referred to as spring No. A7. Details of the spring itself appear later in the text.

Three tests are reported here in which the following barrel and arbor diameters were employed:

Test	Barrel	Arbor
a	7 in.	1.375 in.
b	11 in.	1.375 in.
c	7 in.	2.06 in.

It was anticipated that an arbor diameter of 2.06 in. might cause some distortion of the innermost coils and so tests a and b were to be carried out before attempting to fit the spring to this arbor. It will, of course, be appreciated that the arbor radius is given,

theoretically, by the value of r_o in the spiral equation $r = r_o e^{b\theta}$ so that initially ΔK_{20} is zero. Expanding the inner coils onto an over-large arbor will induce stresses in the inner coils different from the residual stresses existing in the spring in its free state. As a further precaution, it was decided that care must be taken in carrying out tests a and b since overtightening in either of these tests might affect subsequent results.

In each test the coils were to be manually disturbed before taking readings from the testing machine; this precaution being taken to eliminate as far as possible any frictional effects.

6.2. Constants for spring A7.

The equation of the free spiral of the spring, as reported above, is given by equation 6.1. This, together with the relevant constants is quoted here for convenient reference.

Equation of free spiral: $r = 1.03e^{0.01834\theta}$ in.

Strip thickness : $t = 0.038$ in.

Strip width : $w = 1.757$ in.

Strip length : $L = 300$ in.

Modulus of Elasticity : $E = 30.10^6$ lbf/in^2 (assumed)

6.3. Calculations for the curvature curves

From eq. 2.10 $K_o = \dfrac{1}{0.01834s + 1.03}$

From test (a):-

From eq. 2.11 $K_1 = \dfrac{9.09}{\sqrt{702 + s}}$

From eq. 2.12 $K_2 = \dfrac{9.09}{\sqrt{41.3 + s}}$

For test (b):-

$$K_1 = \frac{9.09}{\sqrt{2180 + s}}$$

$$K_2 = \frac{9.09}{\sqrt{41.3 + s}} \quad \text{as for test (a)}$$

For test (c):-

$$K_1 = \frac{9.09}{\sqrt{702 + s}}$$

$$K_2 = \frac{9.09}{\sqrt{90.9 + s}}$$

6.4. Results of tests on spring A7

The curvature and change-of-curvature curves for the three cases examined are shown in figs. 6.1, 6.3 and 6.5. The influence of arbor size on the ΔK_{20} curve is clearly seen on comparing figs. 6.1 and 6.3 with fig. 6.5. It will be noted that the ΔK_{20} curve of fig. 6.5 falls short of the origin. This is the result of forcing the spring onto an arbor which is too large. The effect of the over-sized arbor is clearly seen in fig. 6.7 on comparing curves a and c, the stiffness is increased and the total rotation of the arbor restricted.

Comparison of the theoretical torque-rotation characteristic, predicted using the theory of Chapter 2, with that predicted using the conventional approach and with the experimentally determined characteristic is presented in figs. 6.2, 6.4 and 6.6.

The three theoretical curves may be compared by referring to fig. 6.7.

6.5. Conclusions to be drawn from the tests

The figures referred to in article 6.4 show clearly the degree of agreement obtained between the experimental and theoretical curves. The conventional theory predicts torques considerably lower than those measured and it must be clearly understood that the conventional theory will give good agreement only in cases in which no coils find themselves in their free form in either the wound or the unwound condition.

It will be observed on referring to figure 6.2, that the experimental and theoretical curves are parallel to the curve for the conventional theory over a considerable part of the working range. This is not generally the case as the slope of the conventional theory curve is constant and is given by

$$\left(\frac{dM}{d\phi}\right)_{conv.} = \frac{EI}{L}$$

in which L is the total length of strip, whereas the slope of the theoretical curve will be given by

$$\left(\frac{dM}{d\phi}\right)_{th} = \frac{EI}{S}$$

where S is the active length of strip. Therefore it will be in only those

cases where almost the whole of the strip is active that the curves will be parallel. Fig. 6.1 shows that in test (a) the ΔK_{20} curve has an initial value and it shows also that the active length of strip is initially about 110 inches increasing rapidly to almost the full length of strip, and this condition persists until the spring is fully wound. In test (c) (figs. 6.5 and 6.6) the active length is less to start with and is never either constant or equal to the total length of strip, consequently the curves of fig. 6.6 are not parallel.

It is significant, therefore, that the conventional theory will give an incorrect value of spring rate unless either the design of the spring is such that its active length rapidly approaches the full length of strip and remains so, or unless some correction is applied to L when using equation 2.2. Fig. 6.5 suggests (make area below ΔK_{20} rectangular) that L should be reduced by about 10% in the case of test (c). This increases the slope of the conventional theory curve by approximately 10% (shown dashed on fig. 6.6) and it is seen that the three curves are now almost parallel.

In test (b) very few coils were bundled against the barrel and the spring was effectively without a barrel after a few turns of the arbor. In this configuration it resembles an open-coiled spiral spring and is worthy of note that the theory of Chapter 2 gives close agreement with practical results. It is also to be noted that the $M - \phi$ characteristic for this case is almost linear.

The most marked effects of altering the barrel

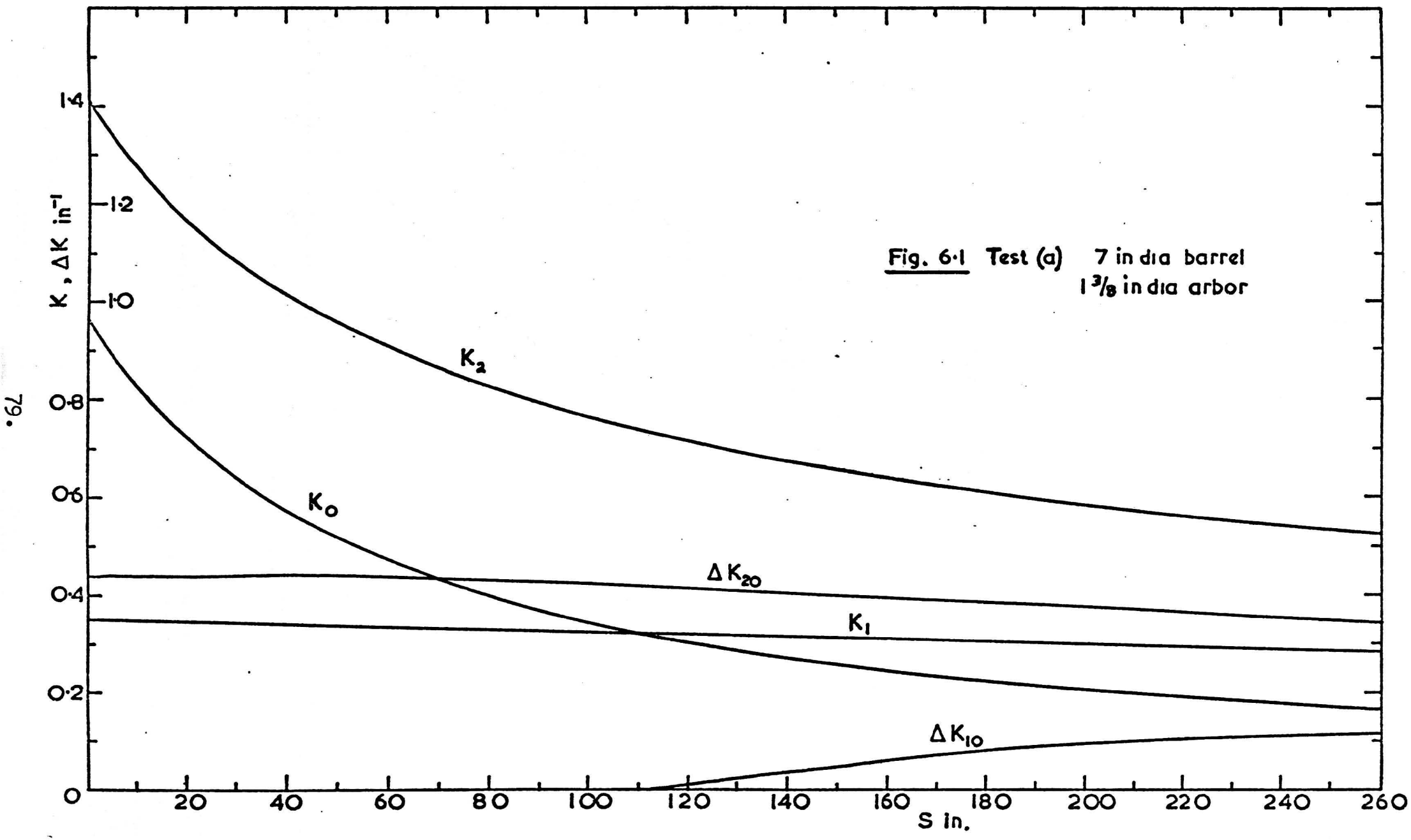

Fig. 6·1 Test (a) 7 in dia barrel
1 3/8 in dia arbor

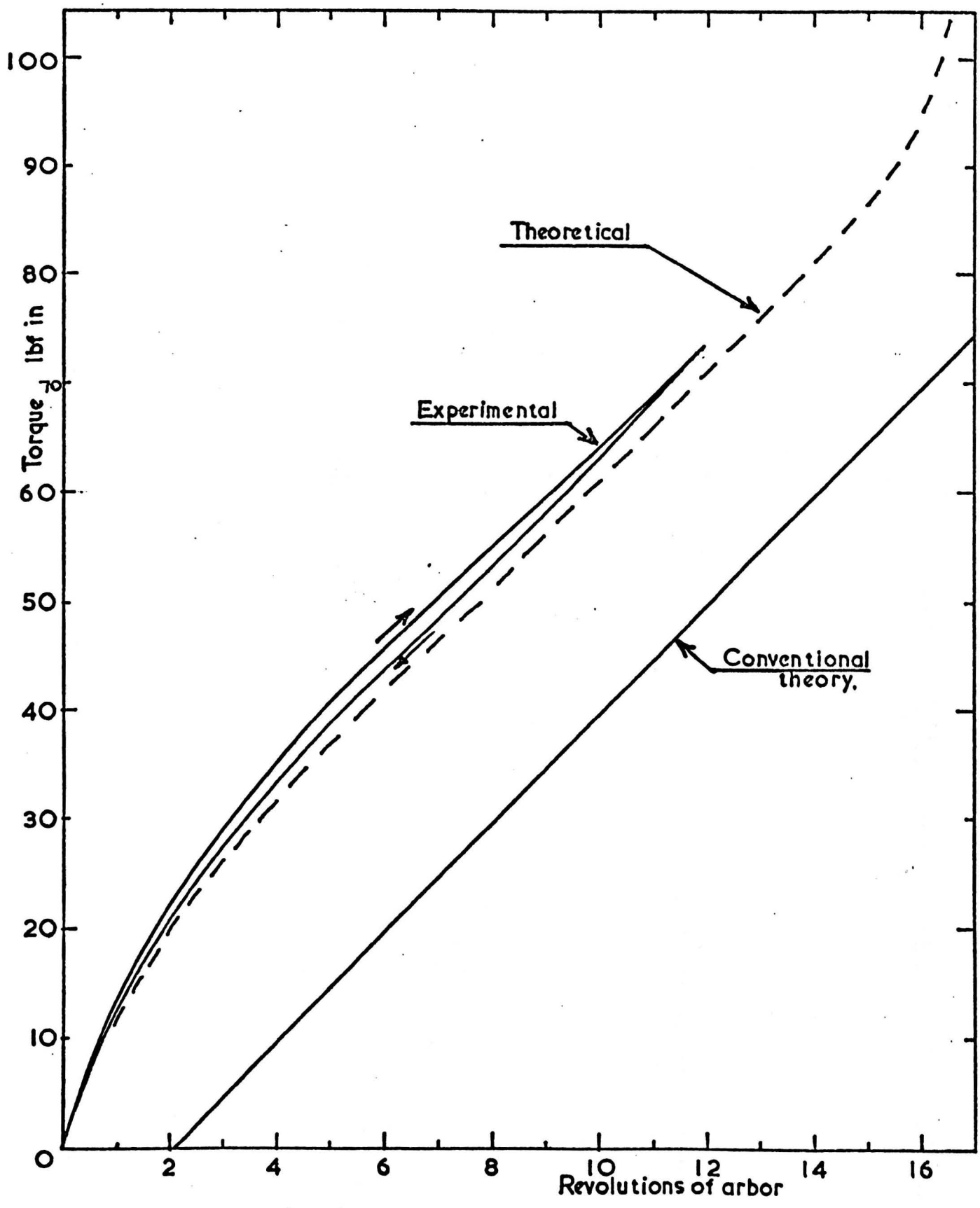

Fig. 6:2. Test (a) 7in dia barrel
$1\frac{3}{8}$ dia arbor

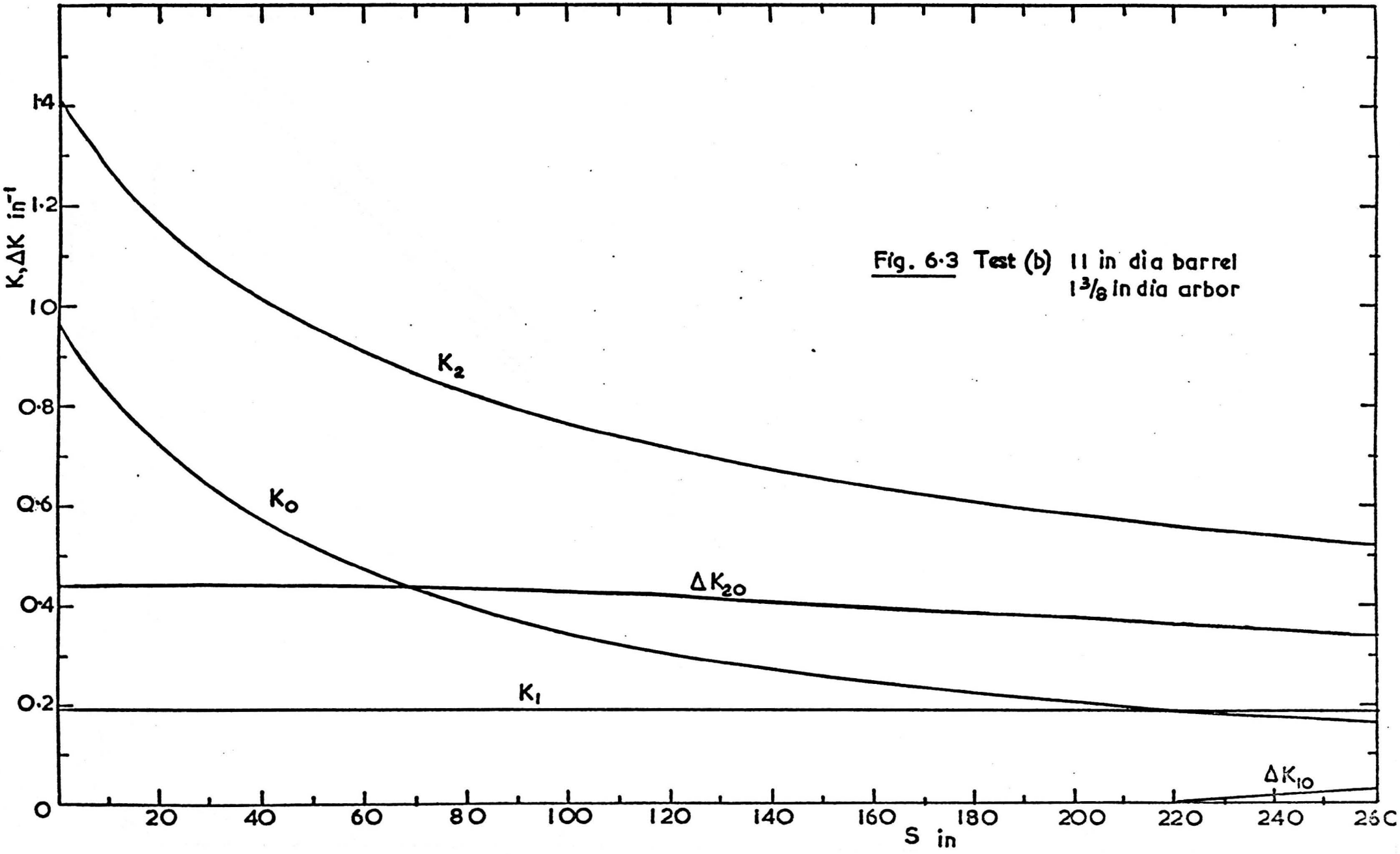

Fig. 6·3 Test (b) 11 in dia barrel
1 3/8 in dia arbor

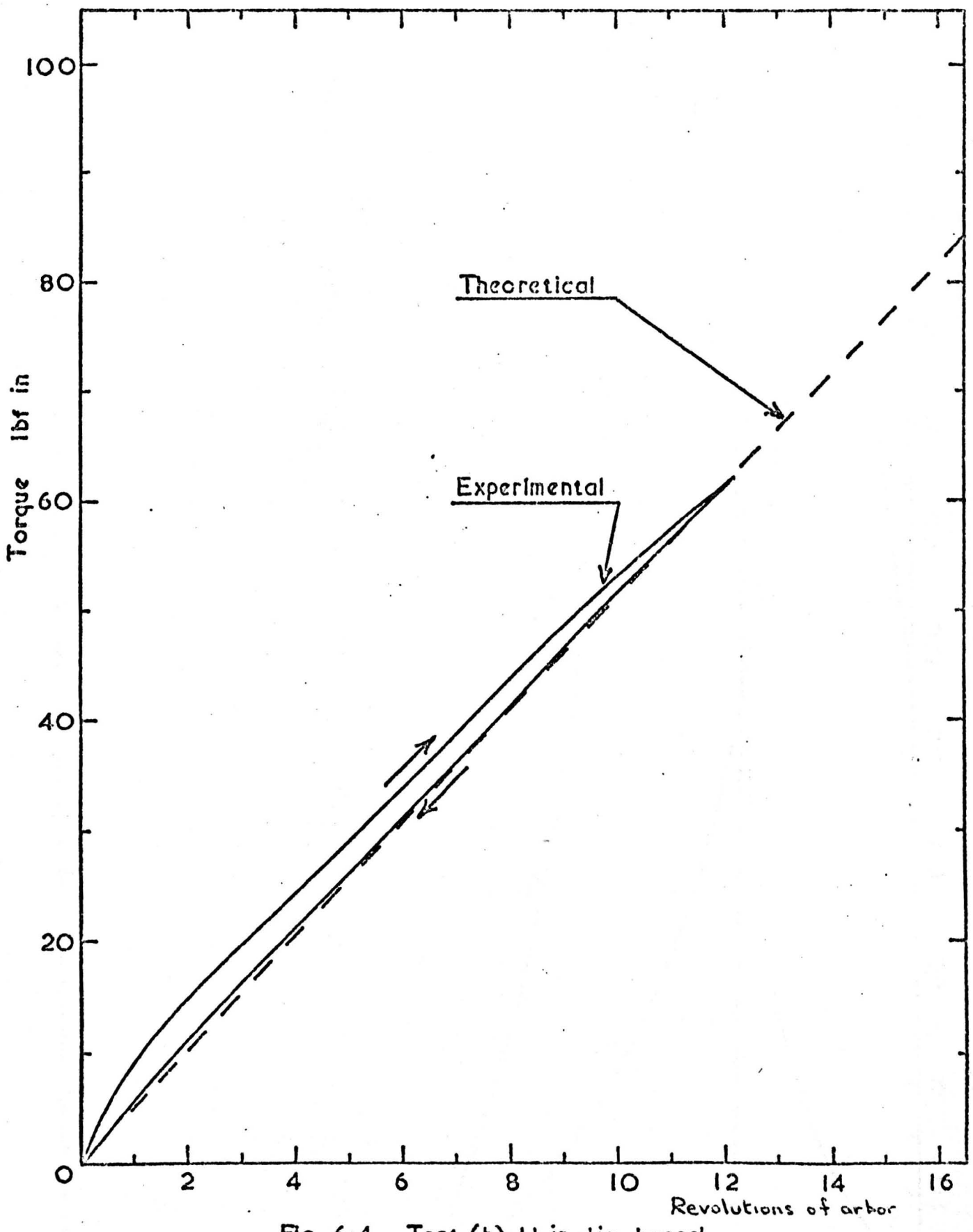

Fig. 6·4. Test (b) 11 in dia barrel
$1^{3}/_{8}$ in dia arbor

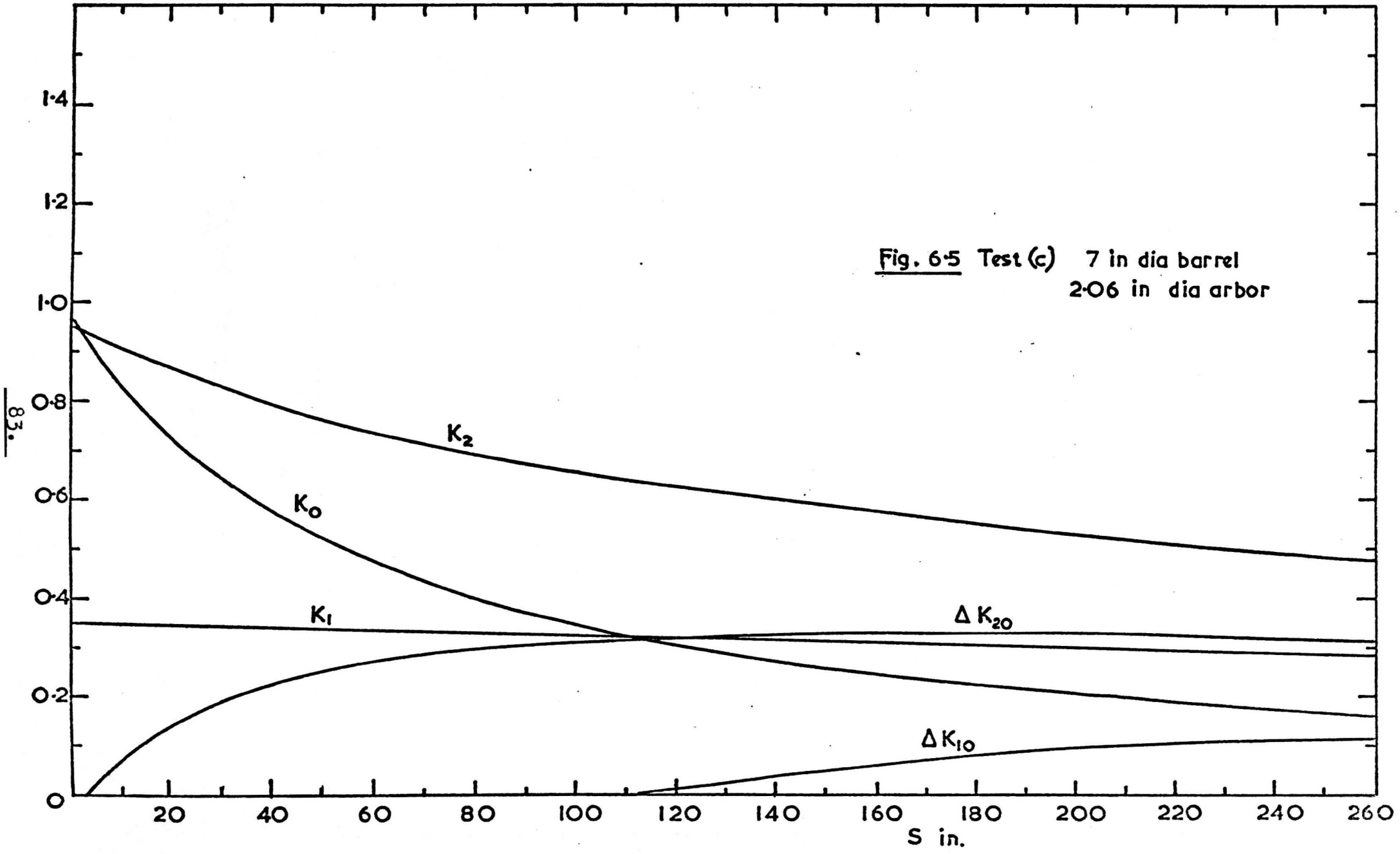

Fig. 6·5 Test (c) 7 in dia barrel
2·06 in dia arbor

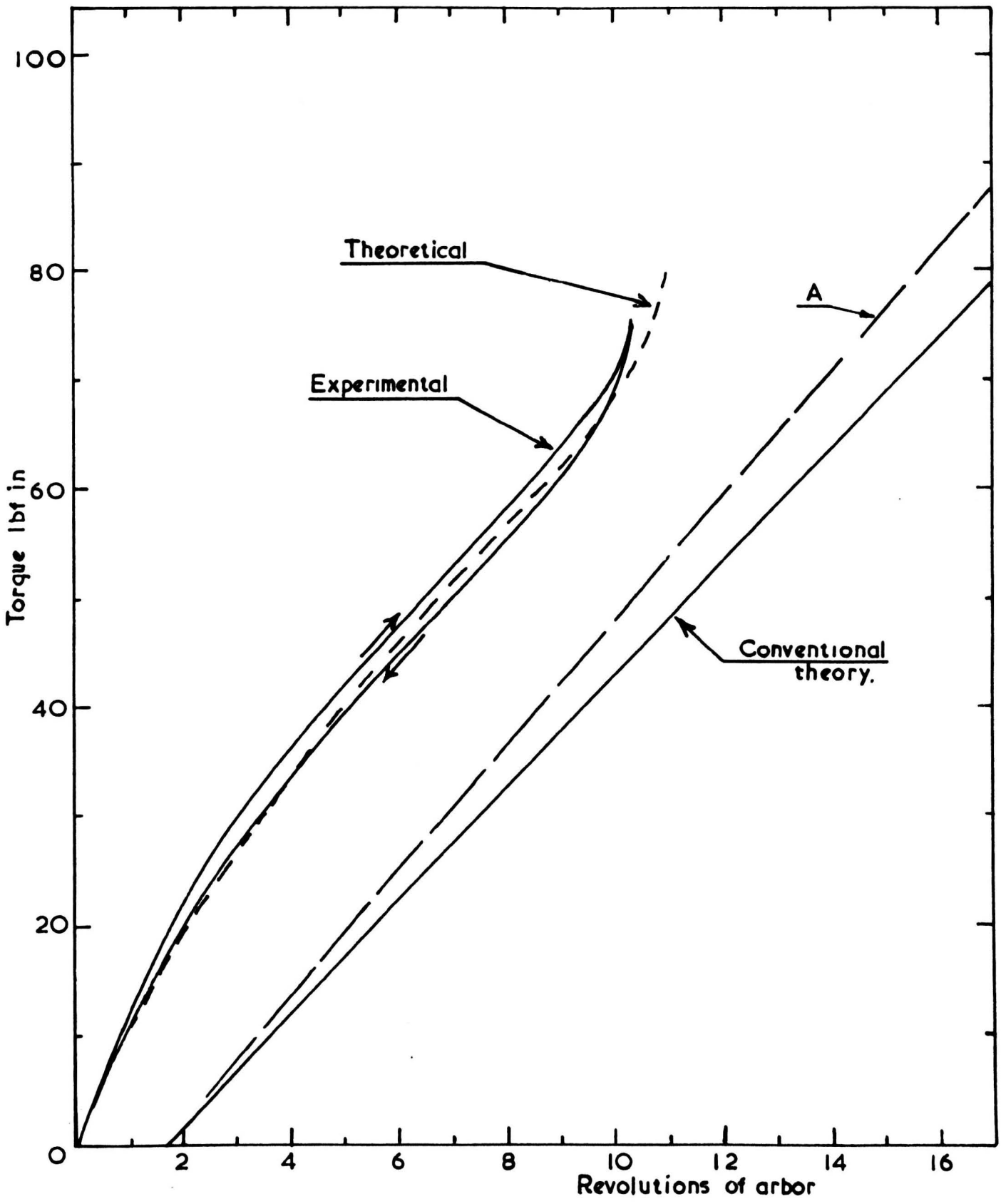

Fig. 6·6 Test (c) 7 in dia barrel
2·06 in dia arbor

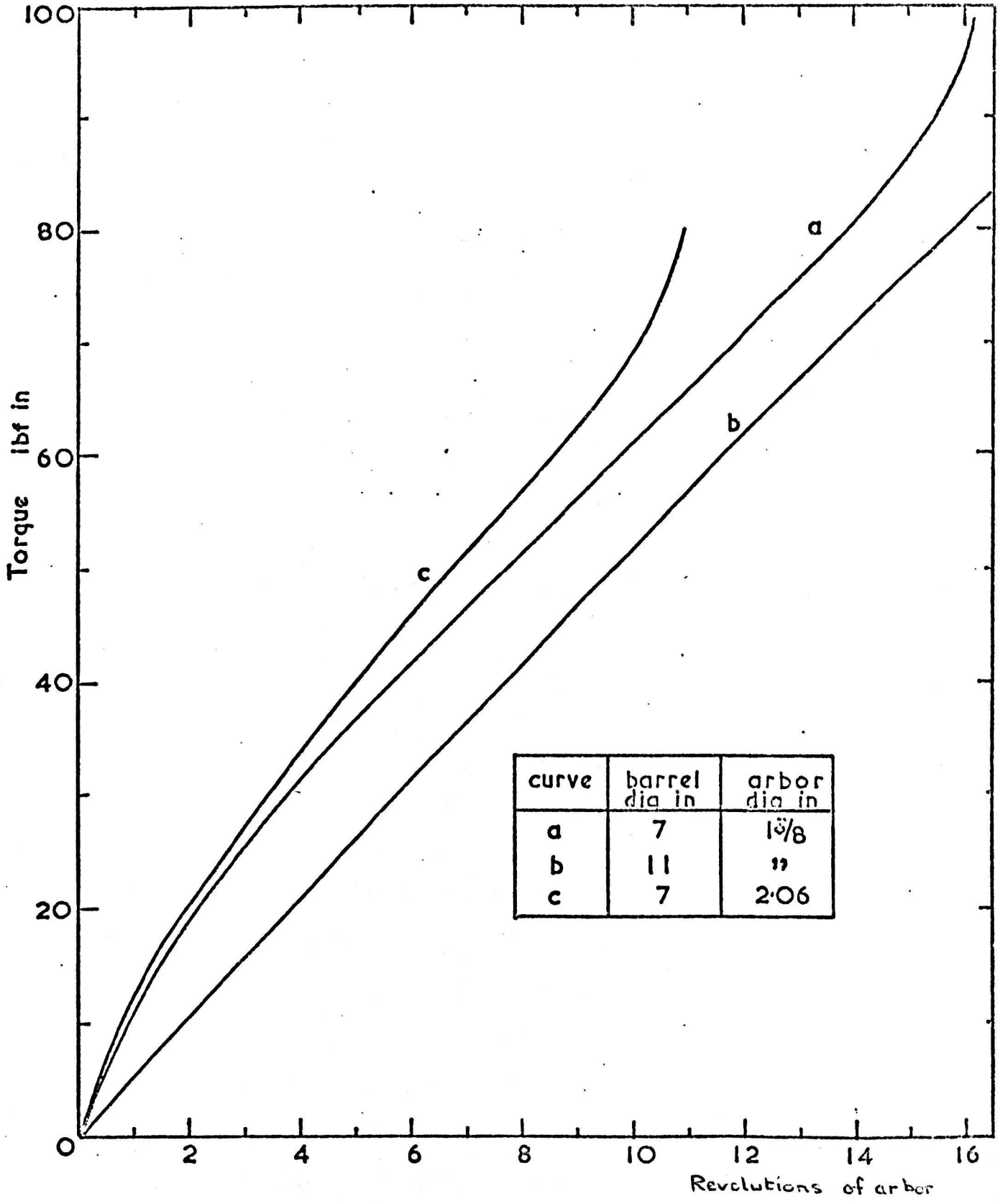

Fig 6·7 Influence of barrel and arbor size on M–Ø characteristic

and arbor diameters are, evidently, as follows:-

1) An increase in arbor diameter decreased the number of useful turns of the arbor. (In this instance by about 30%) But the spring rate, represented by the slope of the M - ϕ characteristic increased only slightly.

2) A decrease in barrel size increased the torque for a given rotation without altering the stiffness over most of the working range of the spring.

It is unwise to attempt to generalise with the evidence of only three tests and many more tests must be performed if the effects noted are to be thoroughly understood.

6.6. Analytical procedure applied to test (c)

The spring A7 was photographed, a transparency made, and the origin of spiral found using the 'four-point method' referred to in article 3.5. If the transparency of fig. 6.8 is superimposed on the photograph in the 180° position it will be seen that there is some distortion of the inner coils. Superimposing in the position where A and A' and B and B' coincide indicates the manner in which the position of the reference point O was arrived at. Fig. 6.9 shows the r - θ plot.

The logarithmic plot of radius against angular position on the spiral is shown in Fig. 6.10. The values of radius were taken from the photograph of the spring, not from the spring itself. The equation of the mean line in Fig. 6.10 is:-

$$r = 1.40e^{0.018340} \text{ in.}$$

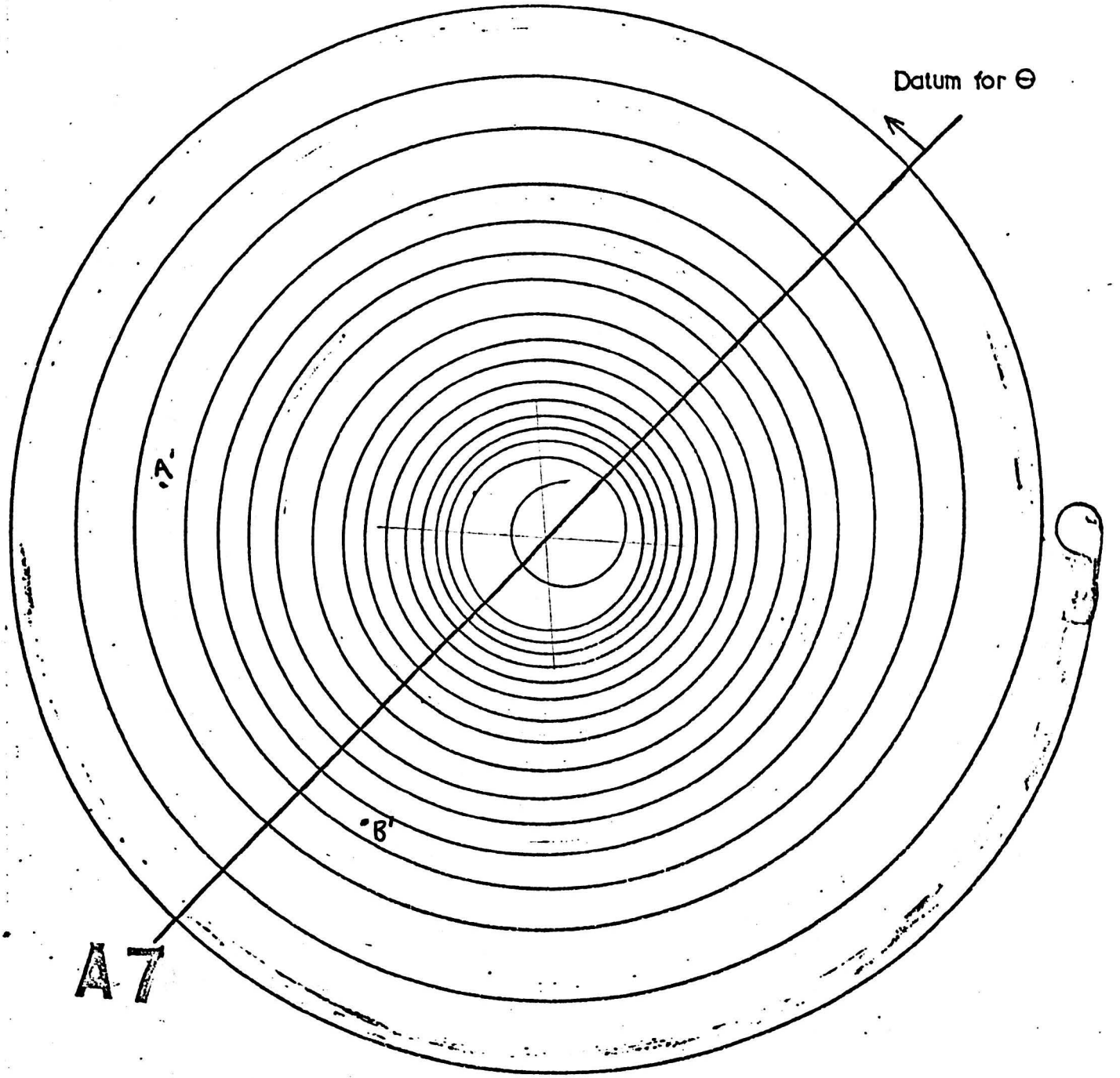

Fig.6·8. Spiral of spring for which figs. 6·9 and 6·10 are constructed. Measurements were taken from a photograph of which the above is a Xerox copy. (×1|1·87)

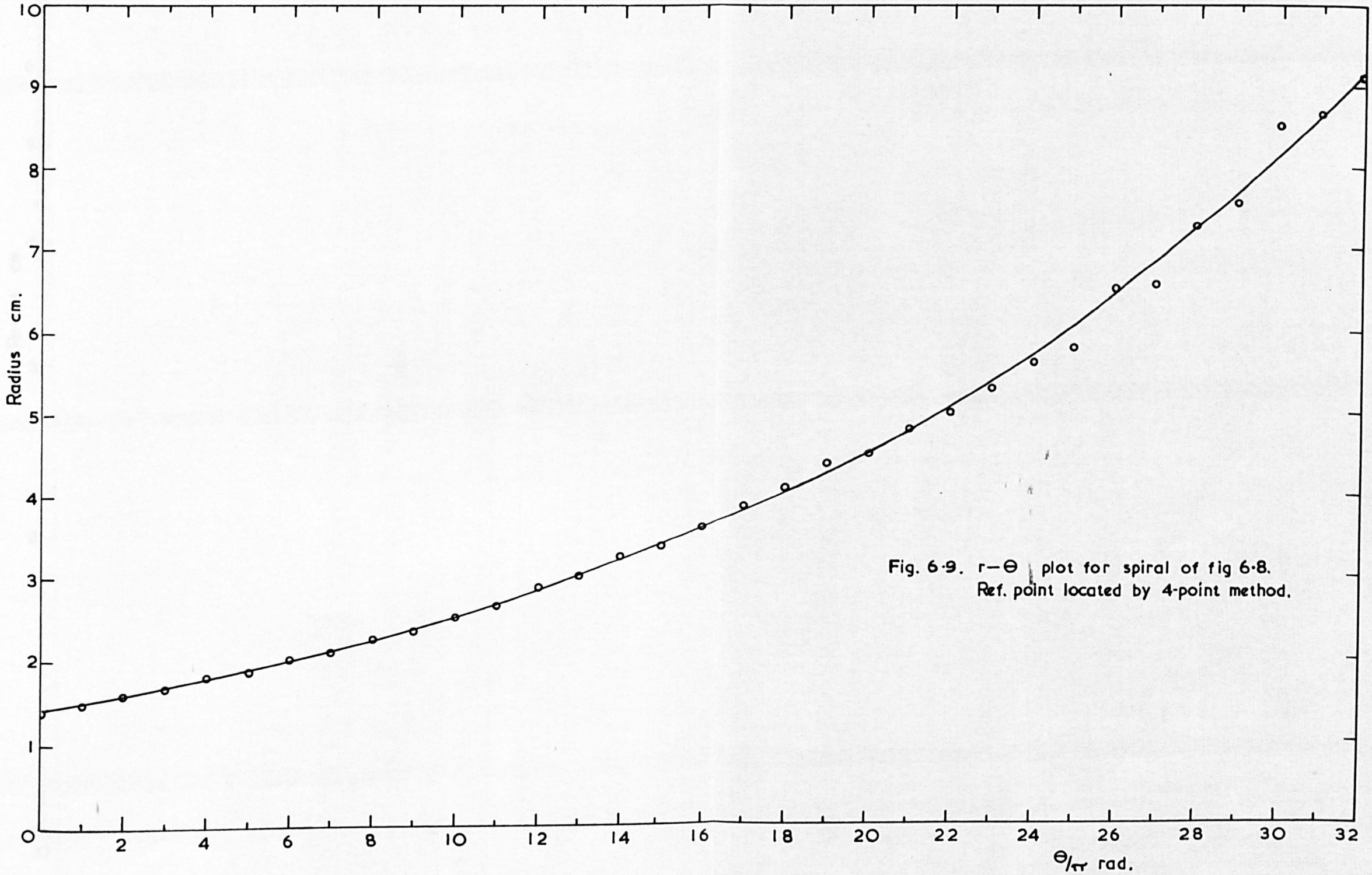

Fig. 6·9. r—Θ plot for spiral of fig 6·8.
Ref. point located by 4-point method.

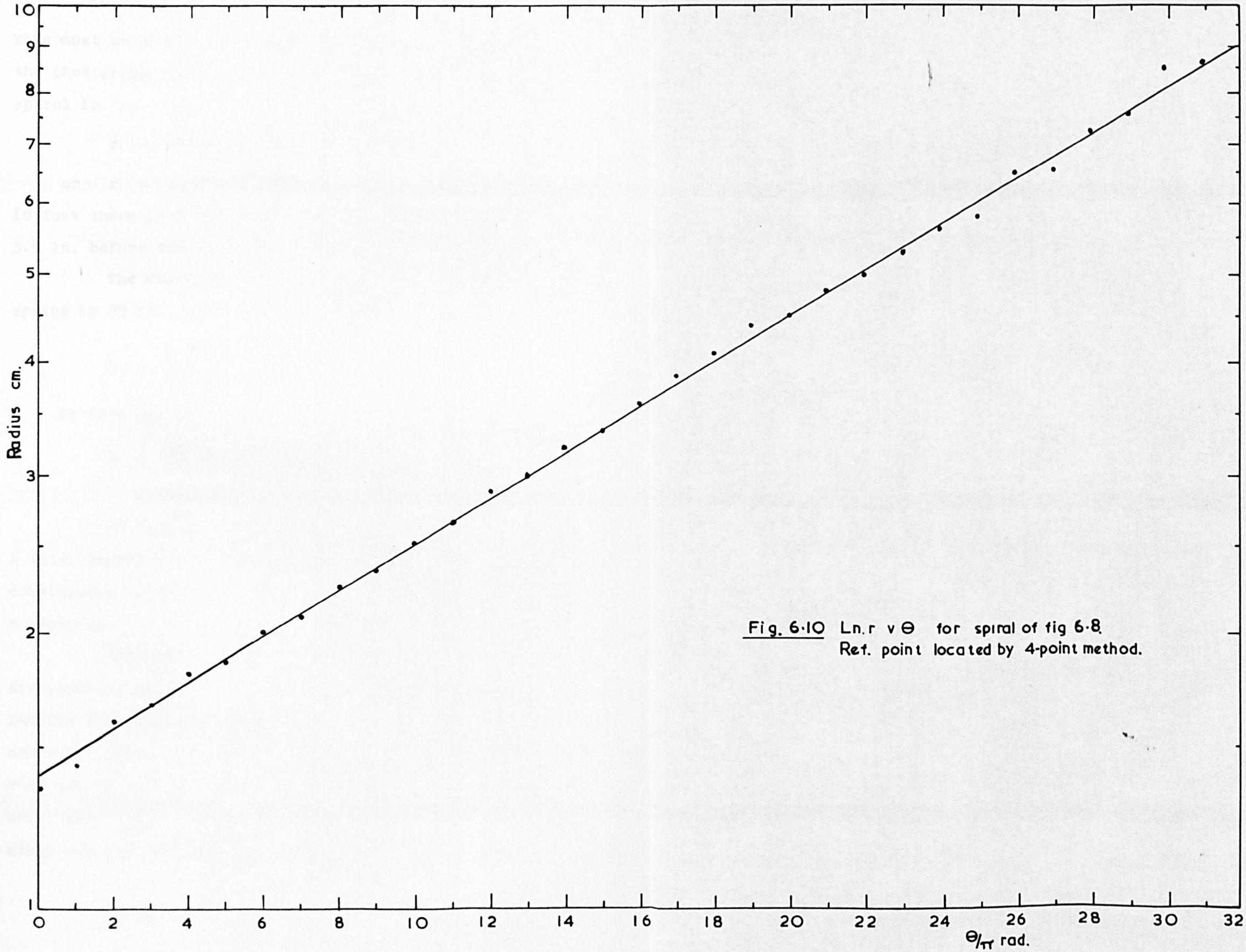

Fig. 6·10 Ln.r v Θ for spiral of fig 6·8.
Ref. point located by 4-point method.

This must be corrected to take into account the scale of the photograph which is 1/1.87. Thus the equation of the spiral is

$$r = \frac{1.4 \cdot 1.87}{2.54} e^{0.018340} \text{ in.}$$

$$\text{or} \quad r = 1.03\, e^{0.018340} \text{ in.} \qquad .. \quad .. \quad .. \quad (6.1)$$

In fact there is a length of strip measuring approximately 3.9 in. before the position at which r = 1.03 in.

The measured length of strip comprising the spring is 25 ft., the calculated length is given by

$$L = \frac{r_o\sqrt{1 + b^2}}{b} \left[e^{b\theta} \right]_o^{\theta}$$

or from fig. 6.9

$$L \simeq \frac{(89.5 - 14.0) \cdot 1.87}{0.01834 \cdot 25.4 \cdot 12}$$

$$= 25.2 \text{ ft.}$$

or including the length prior to the r_o position a total length of 25.5 ft. giving an error of + 2.0% which, considering the distortion of the spiral, is deemed to be acceptable.

Measurement of strip thickness can present difficulties due to lubricant or plating which must be removed before measuring and also due to the curvature and anti-clastic curvature of the strip. These can be overcome by using either a thread micrometer or standard balls with a flat-ended micrometer. The thickness of strip for the spring A7 was

$$t = 0.038 \text{ in.}$$

and the mean width

$$w = 1.757 \text{ in.}$$

which gives a relevant second moment of area

$$I = \frac{wt^3}{12} = 8.04 \cdot 10^{-6} \text{ in}^4$$

ignoring the rounded edge of the strip.

The constants involved in the calculation and defined by equations 2.10, 2.11 and 2.12 are:-

$$B = 9.09$$

$$C_1 = 702$$

$$C_2 = 90.9$$

and the curvature equations are as follows:

$$K_o = \frac{1}{1.03 + 0.01834\ s}$$

$$K_1 = \frac{9.09}{\sqrt{702 + s}}$$

$$K_2 = \frac{9.09}{\sqrt{90.9 + s}}.$$

whence

$$\Delta K_{10} = \frac{9.09}{\sqrt{702 + s}} - \frac{1}{1.03 + 0.1834\ s} \quad .. \quad .. \quad (6.2)$$

$$\Delta K_{20} = \frac{9.09}{\sqrt{90.9 + s}} - \frac{1}{1.03 + 0.1834\ s} \quad .. \quad .. \quad (6.3)$$

Let ΔK_{10} be represented by X and

ΔK_{20} be represented by Y

now let x_o be value of s when X = 0 and

y_o be value of s when Y = 0

Then solving equation 6.2 for X = 0 $s = x_o$ gives

$$0.0278\ x_o^2 + 2.12\ x_o - 614.4 = 0$$

and taking the positive root

$$x_o = 115 \text{ in.}$$

Similarly, solving equation 6.3 for Y = 0 $s = y_o$ gives

$$y_o = 1.97 \text{ in.}$$

Now consider a specimen calculation for $\Delta K = 0.1$.

The torque exerted is given by

$$M = EI\Delta K$$
$$= 30 \cdot 10^{6} \cdot 8.04 \cdot 10^{-6} \cdot 0.1$$
$$= 24.12 \text{ lbf.in.}$$

The positions on the X and Y (ΔK_{10} and ΔK_{20}) curves corresponding to this torque are given by substituting X = Y = 0.1 in equations 6.2 and 6.3 in which case equation 6.2 reduces to

$$3.361 \cdot 10^{-6} s^{3} - 21.3 \cdot 10^{-3} s^{2} + 0.94s + 768.5 = 0 \quad .. \quad .. \quad .. \quad (6.4)$$

whence $x_{0.1} \simeq 214$ in. if the cube term is ignored. This may be corrected later if it is found necessary to do so.

Likewise, equation 6.3 reduces to an equation similar to equation 6.4, viz.

$$3.361 \cdot 10^{-6} s^{3} - 23.4 \cdot 10^{-3} s^{2} - 1.562s + 22.5 = 0 \quad .. \quad .. \quad .. \quad (6.5)$$

whence $y_{0.1} \simeq 12.1$ in.

Thus equation 2.5 for the rotation of the arbor required to produce this torque may be re-written (for proof see Appendix A6)

$$\phi = \Delta K \, [s]_{y_1}^{x_1} + \left[2B\sqrt{c_2 + s} - \frac{1}{b} \ln \left(s + \frac{r_o(1+b^2)^{\frac{1}{2}}}{b} \right) \right]_{y_o}^{y_1} - \left[2B\sqrt{c_1 + s} - \frac{1}{b} \ln \left(s + \frac{r_o(1+b^2)^{\frac{1}{2}}}{b} \right) \right]_{x_o}^{x_1}$$

Let $\phi = (A) + (B) - (C) - (D) + (E)$

where $(A) = \Delta K \, [s]_{y_1}^{x_1} = 0.1 \, (214 - 12.1) \doteq 20.19$

$(B) = \left[2 \cdot 9.09\sqrt{90.9 + s} \right]_{1.97}^{12.1} = 9.26$

$$(C) = \left[\frac{1}{0.01834} \ln \left(s + \frac{1.03}{0.01834} \right) \right]_{1.97}^{12.1} = 8.80$$

$$(D) = \left[2 \cdot 9.09 \sqrt{702 + s} \right]_{115}^{214} = 30.7$$

$$(E) = \left[\frac{1}{0.01834} \ln \left(s + \frac{1.03}{0.01834} \right) \right]_{115}^{214} = 24.9$$

whence $\phi = 14.85$ rad.

This process may now be repeated for increments in ΔK and the $M - \phi$ characteristic constructed.

6.7. Discussion on the use of the analytical solution

It is evident from article 6.6 that the analytical solution involves much arithmetic calculation. Consequently, the probability of errors occurring is high. Further, should two intercepts of ΔK_{10} or ΔK_{20} arise for a given torque (see Chapter 7) the solution is more involved. However, agreement between the results just calculated, that from the graphical solution and the measured value, is very good.

There is some difficulty in obtaining the limits of integration when constructing the $M - \phi$ characteristic in this way, but if the main interest lies in determining the maximum rotation of the arbor and the corresponding torque, the method is much less cumbersome and is illustrated below:-

Maximum rotation available $= \phi_{max.}$

$\phi_{max.}$ = Area below ΔK_{20} curve -

Area below ΔK_{10} curve.

$$\therefore \quad \phi_{max.} = \left[2B\sqrt{c_2 + s} - \frac{1}{b} \ln \left(s + \frac{r_o(1+b^2)^{\frac{1}{2}}}{b} \right) \right]_{y_o}^{L}$$

$$- \left[2B\sqrt{c_1 + s} + \frac{1}{b} \ln \left(s + \frac{r_o(1+b^2)^{\frac{1}{2}}}{b} \right) \right]_{x_o}^{L}$$

$$= \left[18.18\sqrt{90.9 + s} - \frac{1}{0.01834} \ln (s + 56.1) \right]_{1.97}^{300}$$

$$- \left[18.18\sqrt{702 + s} - \frac{1}{0.01834} \ln (s + 56.1) \right]_{115}^{300}$$

whence $\phi_{max.}$ = 69.9 radians (11.1 revolutions)

The difference between this value and that obtained by measuring the enclosed area is about 1.4%. In proceeding through 'the area method' increments in area are measured and added to the previous total, a process in which errors tend to accumulate. The example with which the present calculation is compared will, therefore, contain one of the largest errors encountered. The conclusion to be drawn from this is that 'the area method' is sufficiently accurate and, moreover, is simpler to apply than is the purely analytical approach. However, as stated above, the analytical approach quickly gives the maximum available rotation. Should it prove possible to predict the spring form, then we have here a useful tool for the spring designer.

6.8. Comments on the shape of the ΔK curves

Doubtless it will have been observed that the ΔK_{10} and ΔK_{20} may pass through maximum values in which case for certain values of torque there are two corresponding values of ΔK. We will consider cases for which the curves have the shapes shown in Fig. 6.11. Case 1 is perfectly straightforward and is dealt with in the manner already described.

In Case 2 on Fig. 6.11 two intercepts occur on the X-curve. This may be interpreted as meaning that the end part of the spring has unwound from the barrel housing but the central part of the spring has remained unchanged. This is, of course, impossible as the central part of the spring cannot be tightly coiled against the barrel whilst the end part is free. This may however explain the 'bundling behaviour' of this type of spring in which a number of coils remain in contact and separate from the remainder of the bundle.

In a like manner, as in Case 4, two intercepts may occur on the Y-curve giving rise to similar reasoning. The implication is that it is possible for one part of the spring to be wound tightly on the arbor whilst some previous part of the spring remains free, again an impossible situation.

No mathematical correction has been discovered which can be applied to the theory so that these incongruities may be overcome, and so it has been assumed that there is, in fact, a rotation equal to the area A on the diagram because springs often do separate unevenly.

In the event that the spring concerned has the

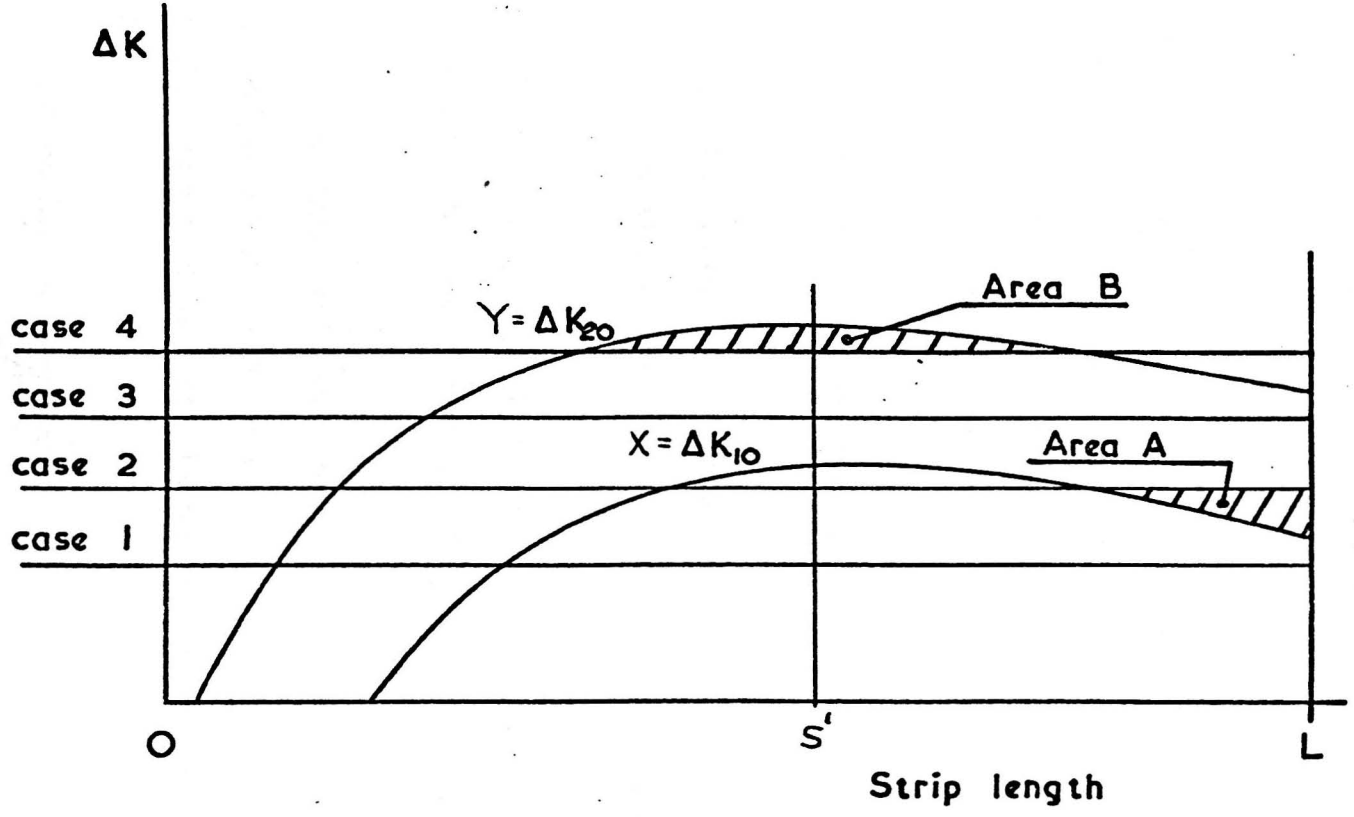

Fig. 6·11 case 1—1 value of ΔK_{10}, 1 value of ΔK_{20} for given torque.
case 2—2 values of ΔK_{10}, 1 value of ΔK_{20}
case 3—no intercept on ΔK_{10}, 1 on ΔK_{20}
case 4—— ditto , 2 on ΔK_{20}

inherent property that the central region of the spring prevents part of the outer region from unwinding (coils remain in contact) then the area A must be ignored.

Similarly, no allowance appears possible when two intercepts appear on the Y-curve in which case any part of area B encountered in the calculation is excluded.

From the nature of the K curves, it is evident that the maximum turning point of the ΔK_{20} curve occurs before that of the ΔK_{10} curve, and hence if the spring length were s' instead of L, the above conditions which cause the bundling would not apply.

Had the spring used been of length s' instead of L, the same torque range would occur but the angle of rotation would have been reduced by some 40 - 50%.

Note

If the spring is designed so that no bundling occurs, then in the winding and unwinding of the spring no friction can occur between coils. The result therefore would be a smoothly running spring, and a torque-rotation curve obtained from the above theory should be very accurate.

A maximum will not occur however between 0 - L if the modulus of the gradient of the K_2 curve is not greater than the modulus of the gradient of the K_o curve for s = L.

So as $K_2 = \dfrac{B}{\sqrt{c_2 + s}}$

and $K_o = \dfrac{1}{r_o + bs}$

then $\frac{dK_2}{ds} = \frac{-B}{2(c_2 + s)^{3/2}}$ and $\frac{dK_o}{ds} = \frac{1}{(r_o + bs)^2}$

Hence, for no bundling

$$\frac{1}{(r_o + bs)^2} \geqslant \frac{B}{2(c_2 + s)^{3/2}}$$

so $$\frac{1}{\left(bL + r_o\sqrt{1 + b^2}\right)^2} \geqslant \frac{1}{2}\sqrt{\frac{\pi}{t}} \quad \frac{1}{\left((R' + \frac{t}{2})^2 + L\right)^{3/2}} \quad .. (a)$$

This equation gives the turning point of K_{20} curve when the equals sign applies, this being the maximum value of L for no bundling.

The variables involved in a spring system are seven in number, namely:

b and r_o - the constants of the spring free form equation

$$r = r_o e^{b\theta}$$

R and R' - the radii of the barrel and arbor

L, t and w - the length, thickness and width of the spring strip.

The width of the strip affects only the torque given by a particular rotation, hence the spring should first be designed for rotation. The required torque may then be attained by correct choice of the strip width.

Investigations are reported later in this thesis on an analysis designed to predict the constant b of the spring spiral form before manufacture. Failing this 'b' must be assessed from previous experience.

The arbor diameter cannot be significantly altered and its effect on condition (a) above, can be considered unimportant.

The two governing parameters of this condition (for no bundling) may therefore be assumed to be t and L. For no bundling it is necessary to decrease t in order to extend the range of the spring, i.e. in order to satisfy the condition given, a maximum value of t will exist for a given spring length L. The maximum torque required also imposes a limit on t, this being a minimum limit given in spring design tables(R9 p.61).

If a suitable strip thickness t cannot be determined to satisfy the condition, then the length L, already assumed, will have to be altered.

It may happen that using a minimum value of t and a maximum value of L, the rotation given by the system will be too small, in which case it appears that bundling would be unavoidable.

The suggested procedure in design is to select the smallest strip thickness allowable for the torque required and use this to determine the approximate value of L to provide the rotation required. Then using the condition (a), determine if possible, a greater and more satisfactory strip thickness. The change in t will have little affect on the rotation available.

The condition given for non-bundling of the coils depends on the outer end of the spring being fixed rigidly to the barrel.

In designing a spring system for non-bundling therefore, it will be necessary to clamp a short length of the spring to the side of the barrel.

This should, in fact, improve the working of any spiral spring system whether open or close coiled, by reducing friction.

CHAPTER 7

WINDING OF SPIRAL SPRINGS

7.1. Introduction

The purpose of the preceding chapters has been to establish the form of spiral exhibited by this type of spring when allowed to attain its free form. It has been shown that, in general, a logarithmic spiral equation can be found which will approximate to the free form of a particular spring. Reasons are now sought to explain why the free spring should exhibit a logarithmic spiral form.

7.2. Examination of the winding process

On observing the winding of spiral springs it becomes evident that there may be considerable lack of consistency on the part of the operator. Summarising the process described in art.1.4, the operator attaches the 'hook' end of the strip to the arbor and applies sufficient tension to the free end of the strip to gain some control over the manner in which the strip approaches the arbor. Especially in the case of the larger sizes of strip used in the cold forming of this type of spring, it seldom occurs that this back-tension has any significant effect on the residual stress distribution. Thus the strip winds onto the arbor with practically no back-tension, forming a loose coil the size of which is controlled only by the available 'gap' in the machine through which the material has to pass on its way to the arbor. If the loose coils have a large outer diameter, it may well be that some of the strip is subjected to reverse bending

on passing through the gap.

When the end of the material reaches the gap in the machine it may be restrained by jamming it against the machine frame using some form of hooked bar, whilst the arbor is rotated. This part of the process induces tensile stresses in the coil and, at the same time, increases the bending stresses. The absence of control during this final stage causes unpredictable variations in the free spiral form of springs supposedly to identical specifications.

7.3. Experimental winding rig

It was decided that one aspect of this research would be to examine the history of the strip during the winding process. Consequently, the testing machine described in Chapter 4 was modified slightly, by creating a gap through which strip could be fed. Arrangements were then made by which the strip could be subjected to tension whilst being wound onto the arbor. Strain gauges were attached to the strip and a photographic method devised to enable the passage of a point on the strip to be followed from the gap to its final position on the arbor. Figs. 7.1, 7.2 and 7.3 are almost self-explanatory. The equation of the path was derived (Appendix A7) but is not considered of great significance. Good agreement was obtained when comparing the recorded path with the theoretical prediction. What is more important is the strain history of an elementary length of strip during the winding process.

Strain gauges were stuck onto opposite faces of the strip. Obviously there are serious criticisms of

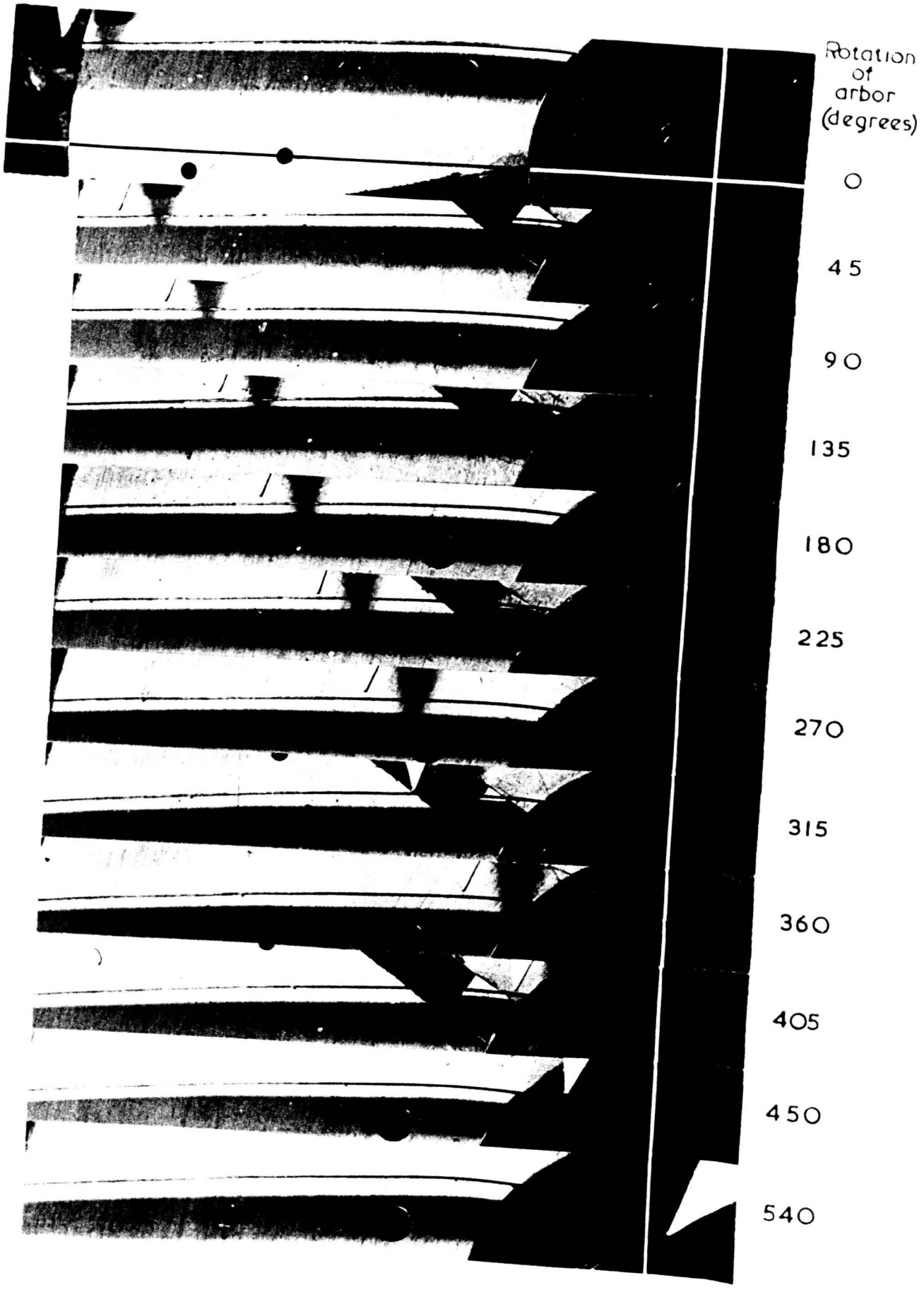

Fig 7·1 Path of point on 0·02 in thick strip during winding. Arbor dia. 1·375 in. Direct stress 1,000 lbf/in²

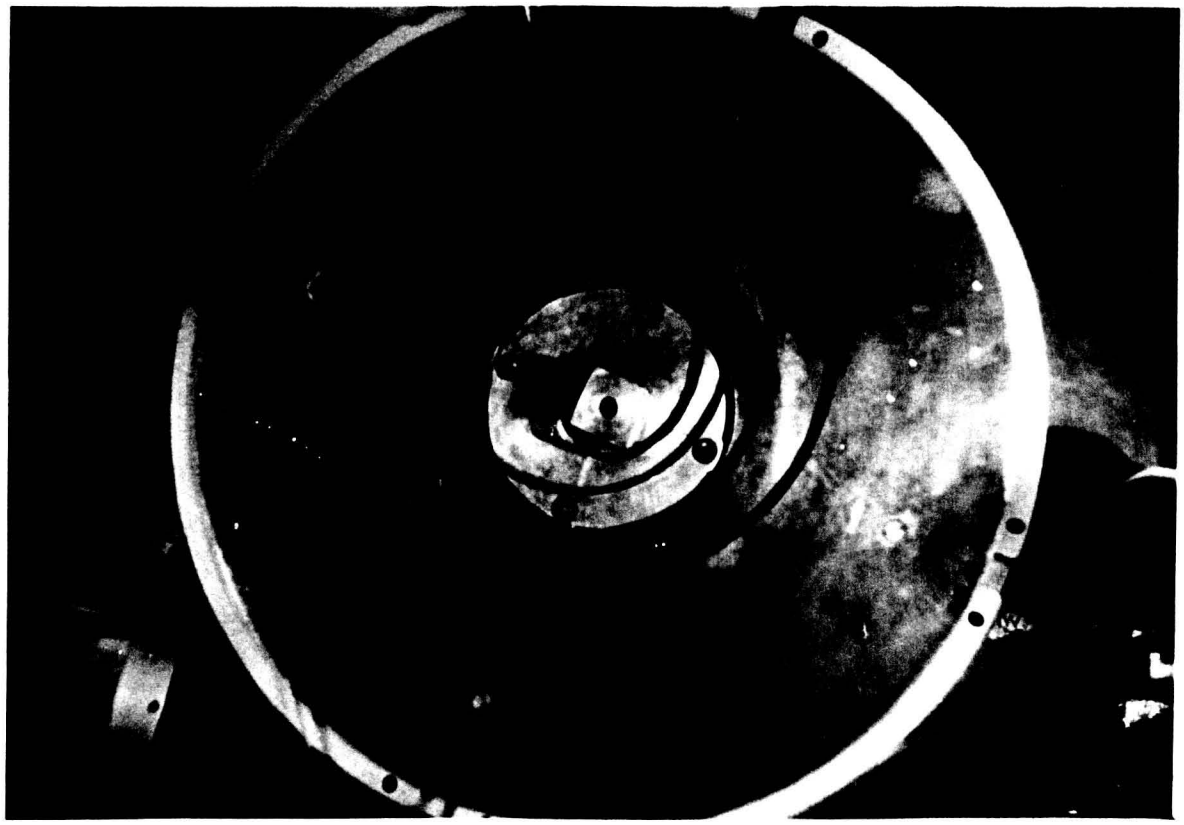

Fig.7.2 Photograph of strip after winding under tension. (x1/5.5)

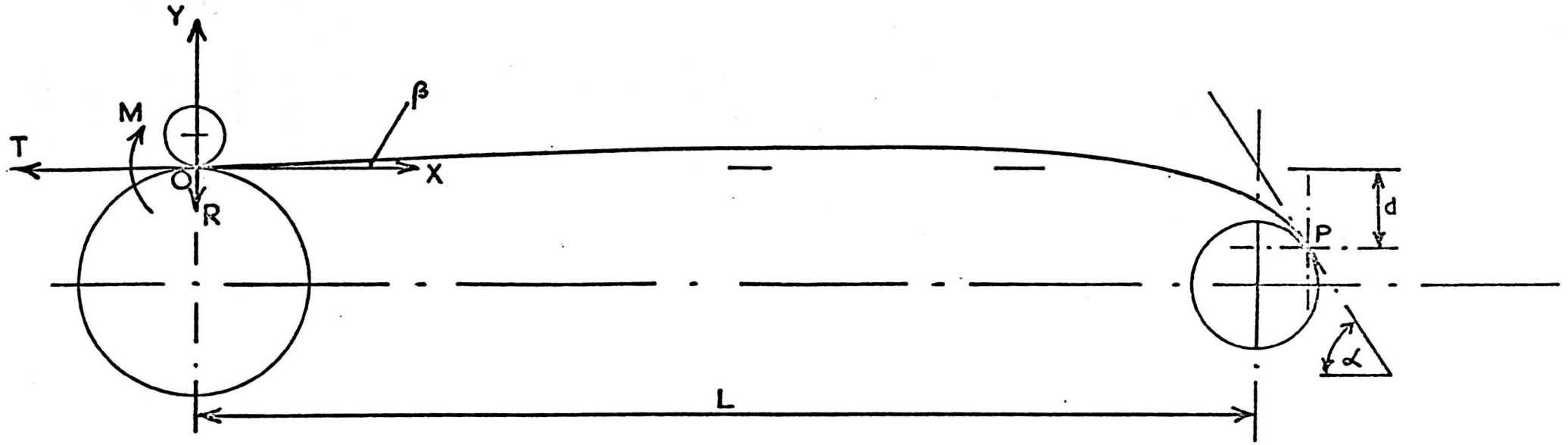

Fig. 7·3. Path of an element during winding.

applying gauges to thin material; the gauges with their backing and glue-line form a sandwich of a thickness approaching the half-thickness of the material in some cases. Also there must be some local stiffening of the strip in the vicinity of the gauges and they prevent the coils from coming into contact at the arbor. Further to this there are electrical difficulties on reaching the arbor and the fact that the gauges are useless when strains approach those encountered at the onset of plastic deformation.

The stress induced in the material during its passage from the gap to the arbor was calculated from the equation of the path and compared with that calculated from the measured strain. The results of this comparison are to be seen in Figs. 7.4 and 7.5. These indicate that the material does suffer reverse bending within the elastic limit. They also show that the stresses induced in the outer fibres are almost equal, i.e. the back-tension employed had little influence on the stress distribution.

The results just described taken in conjunction with the basic idea leading to the theory of Chapter 2 prompted an investigation into the 'spring-back' behaviour of spring steel strip. A previous investigation carried out under the author's supervision[R.10] had examined the behaviour of torsion bars when subjected to overstrain in torsion in which a strain-history analysis had been employed. Consequently, it was known that Gardiner[R.11] and Woo and Marshall[R.12] had studied the spring-back properties of sheet materials. It was decided, therefore, that information was required regarding

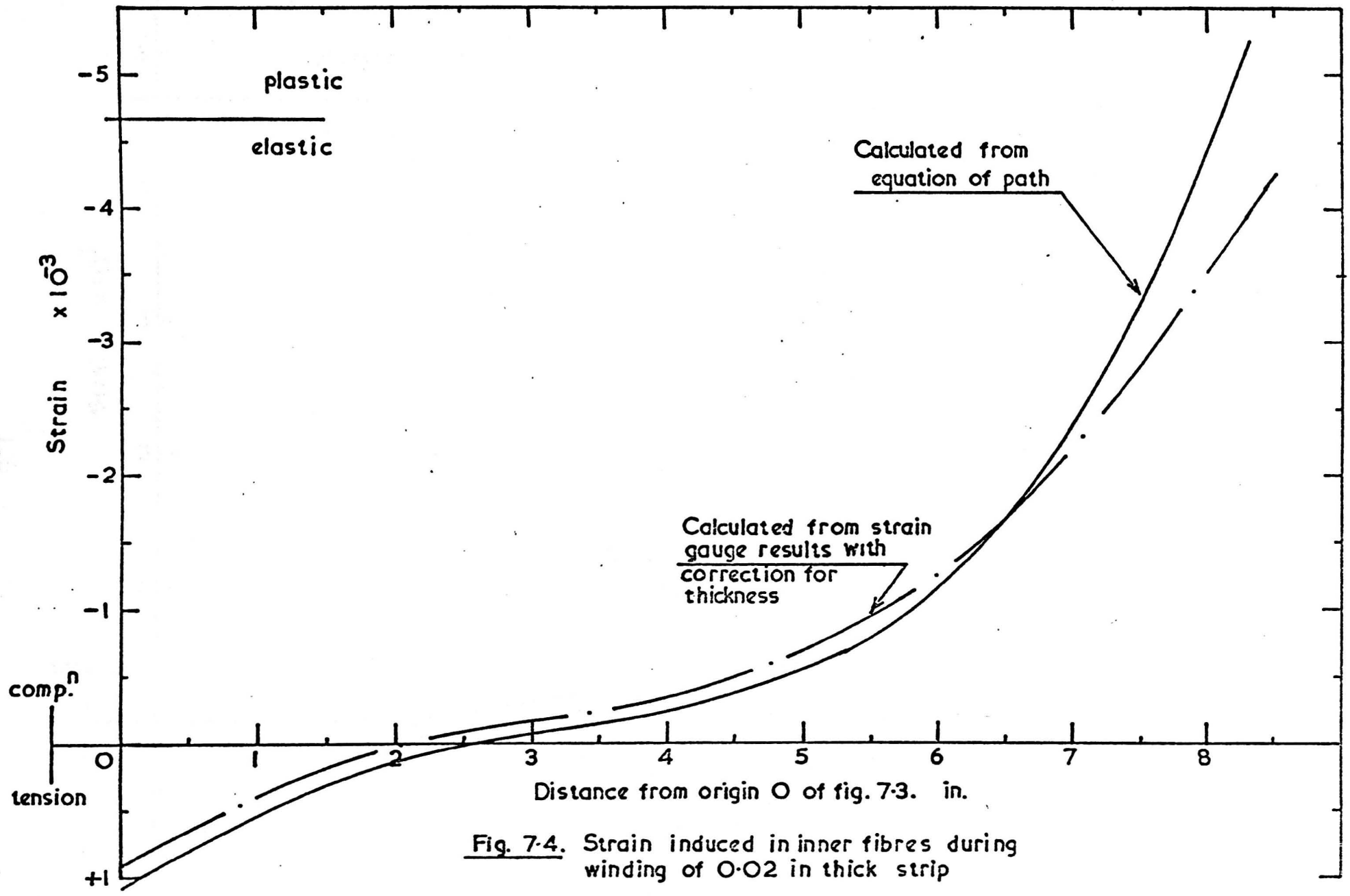

Fig. 7-4. Strain induced in inner fibres during winding of 0·02 in thick strip

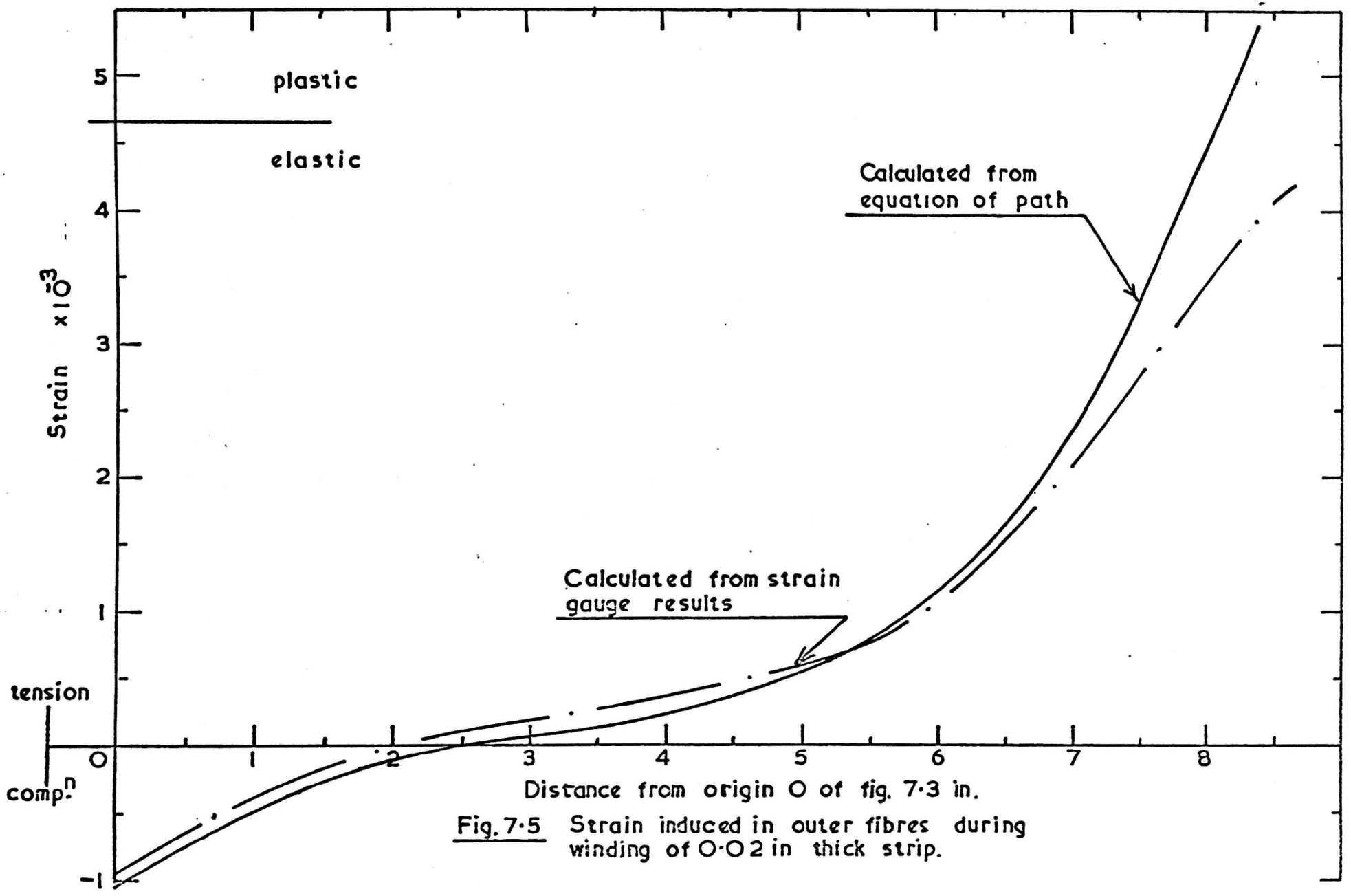

Fig. 7·5 Strain induced in outer fibres during winding of 0·02 in thick strip.

i) spring strip deformed in bending (Gardiner).

ii) spring strip deformed by bending under tension (Marshall and Woo).

iii) spring strip deformed by bending followed by tension (strain-history analysis).

It was realised that practical data on spring back were essential and that the material properties must be investigated and idealised if any successful theory was to be evolved. It was also evident that a thorough investigation of (iii) above is necessary and should form an investigation supplementary to the present research. In this thesis, therefore, the treatment of bending followed by tension is limited to outlining the procedure to be adopted in further research.

7.4. Testing of spring strip

7.4.1. Material used in tests

The material chosen for the investigation was spring steel strip in thicknesses varying between 0.010 and 0.030 in. The tensile test data were obtained using a Hounsfield tensometer, the extensions being measured on a Hounsfield extensometer having a 2.0 gauge length. Table 7.1. summarises the results obtained. Materials A, B and C were used in their 'as-received' condition but material D was tempered to reduce the hardness from 600 VPN. to 388 VPN. The tensile specimens were cut from the strip and shaped to the conventional 'plate tensile specimen' shape the parallel portion being about 2.5 in. long. The final shaping was carried out by carefully draw-filing by hand.

TABLE 7.1

Material	Thickness in.	Width in.	Hardness V.P.N.	Yield Stress ton/in^2	E ÷ 10^2 ton/in^2
A	0.012	1.1/16	360	80.5	12.8
B	0.020	7/8	400	89.3	14.1
C	0.021	1.1/4	446	79.0	13.7
D*	0.031	0.788	388	68.3	13.1

* Material D was supplied with a hardness of the order of 600 V.P.N. Re-tempering resulted in the values given in the Table.

Tensile tests were carried out into the plastic region with unloading and reloading cycles performed during the test. The stress-strain curves (figs. 7.6, 7.7, 7.8, 7.9) indicated that each of the materials approximated to an ideal elastic-perfectly plastic material having an elastic recovery line parallel to the original elastic loading line. It was assumed that the behaviour in compression would be similar.

7.4.2. Pure bending tests

One of the difficulties encountered during the bending of strip materials is due to the Poisson effect which manifests itself in the production of anti-clastic curvature, the presence of which affects the spring-back properties of the strip. Whilst it is accepted that anti-clastic curvature will be present in manufactured springs and affect their performance, it is considered that its presence should modify a simple theory evolved neglecting its presence, rather than attempt a complex theory taking account of anti-clastic curvature, always assuming that this is possible. (See Appendix A1.2.)

It was considered, therefore, that if strip material is pressed into a semi-circular die, the conditions can be assumed to be almost identical to those obtained in pure bending. To this end a semi-circular die was made to accommodate a strip of the thinnest material. After tests on this thickness of strip had been carried out the die was machined to accommodate progressively thicker strips, next a new press-tool of larger radius was made and the process repeated.

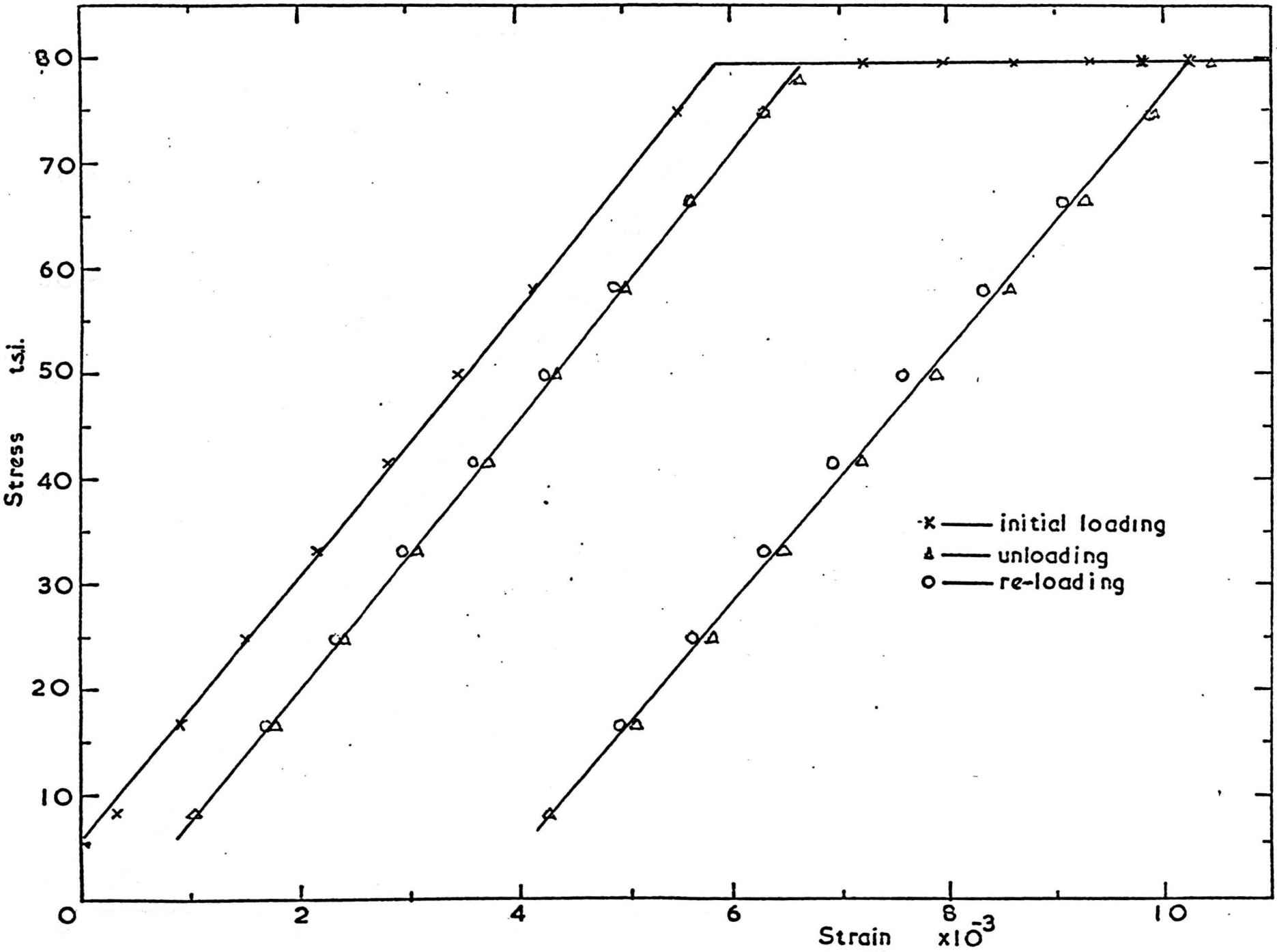

Fig. 7·6 Stress-strain curve for material 'A' of table 7·1

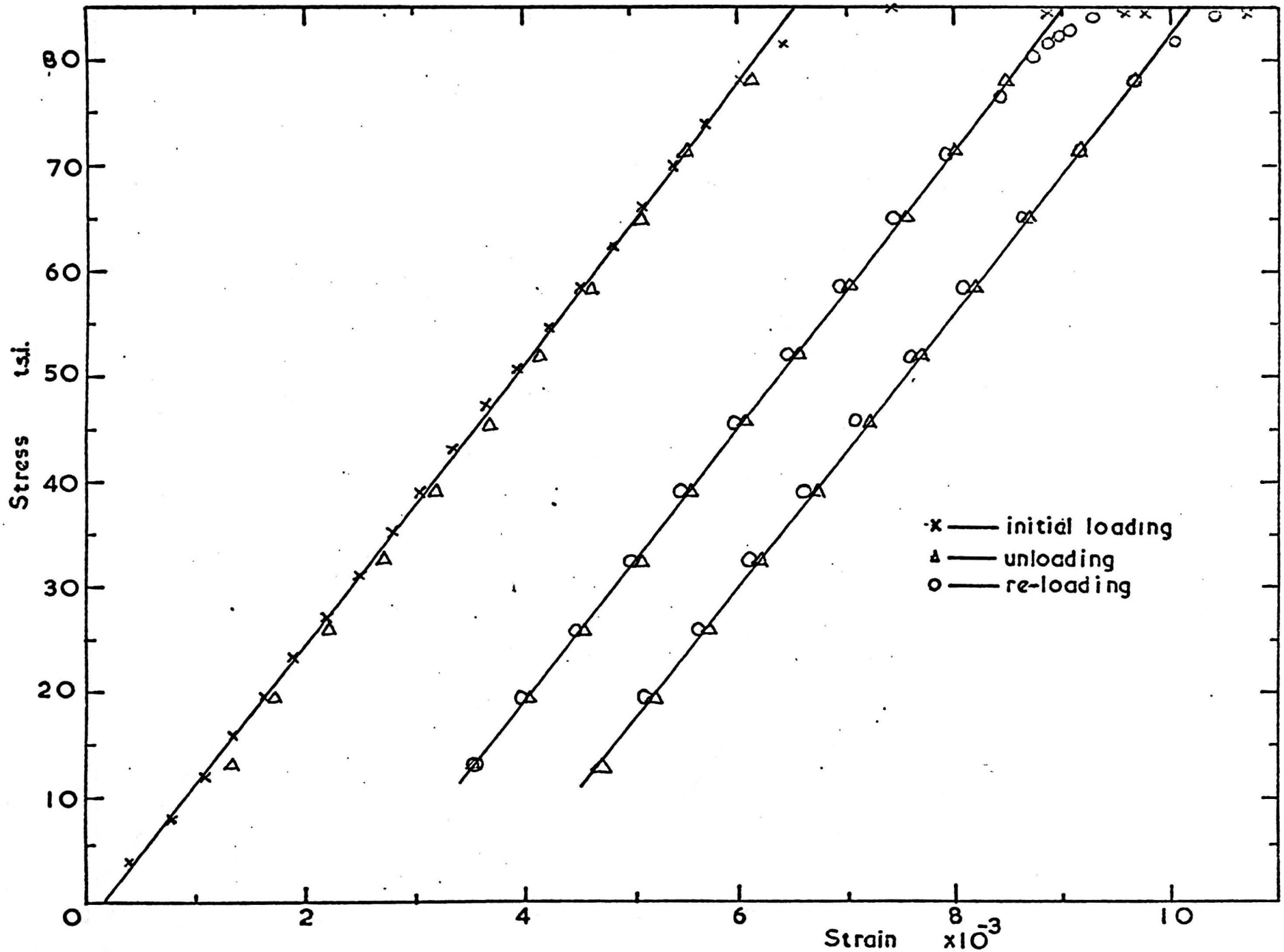

Fig. 7·7 Stress-strain curve for material 'B' of table 7·1

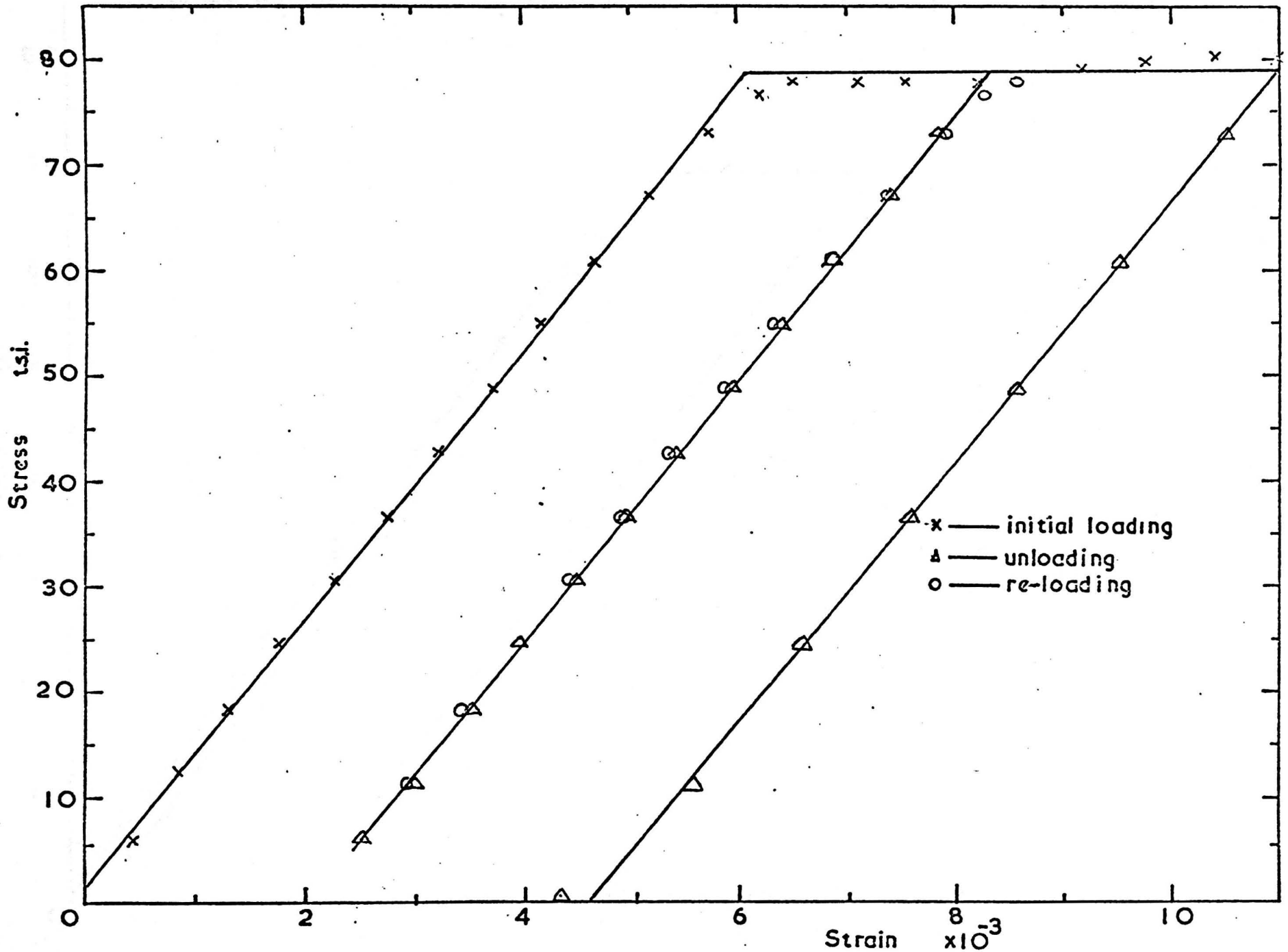

Fig. 7·8 Stress-strain curve for material 'C' of table 7·1

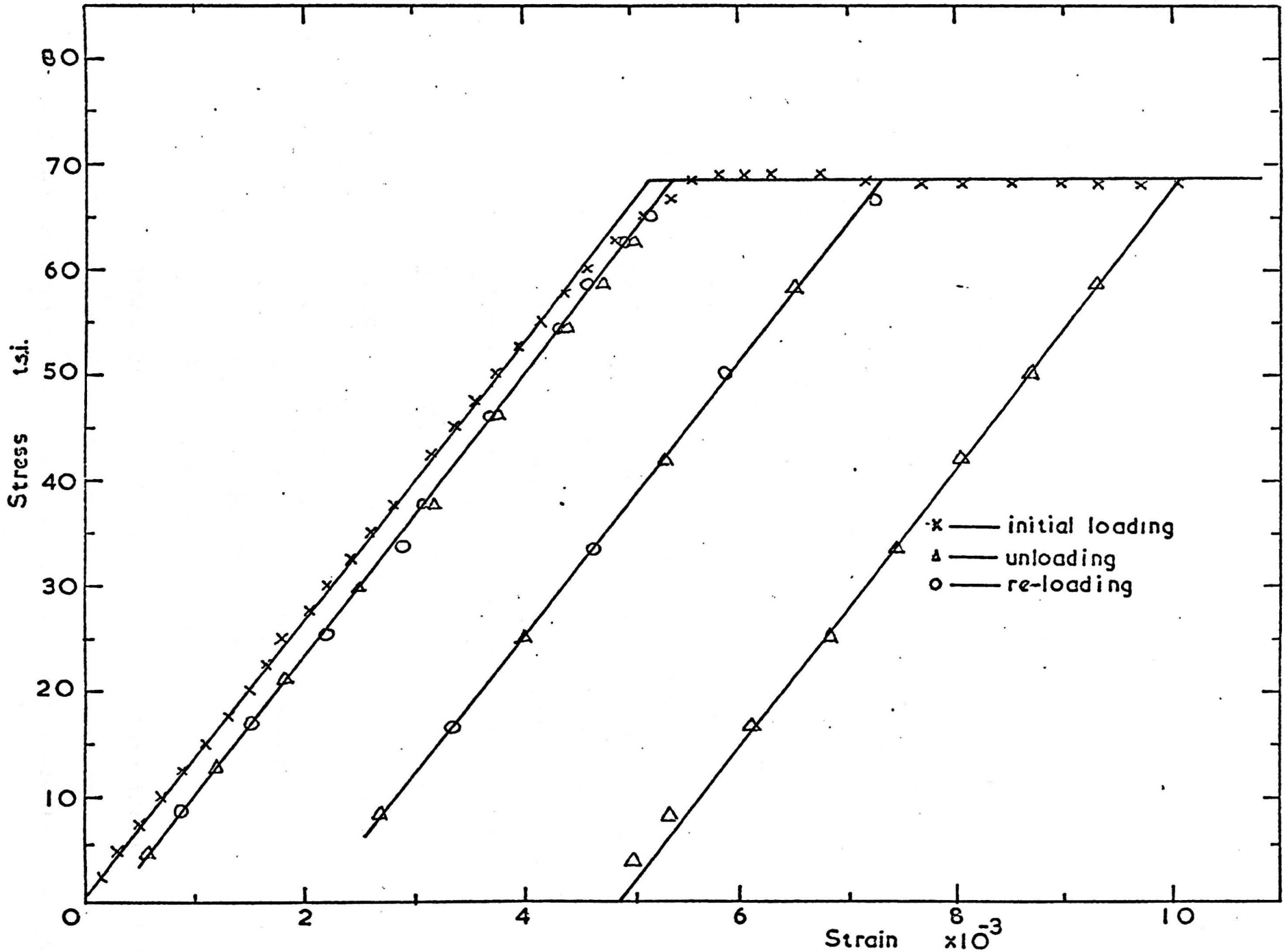

Fig. 7·9 Stress-strain curve for material 'D' of table 7·1

Several tests were performed with each thickness of material.

The radius of the bent strip after removal from the die was determined by measuring the chord and sagitta. The measurements were made accurately using a travelling microscope and less accurately (but much more speedily) by placing on millimeter squared paper. If one accepts that the behaviour of this type of material when subjected to elastic-plastic deformation is not entirely consistent, then little purpose is served in ensuring highly accurate measurements. Of far greater value is the acquisition of a large number of results of a lower, but acceptable, standard of accuracy.

Thus, the strips were considered to have been subjected to pure bending to an inside radius equal to the radius of the press tool. If this radius is sufficiently small to produce plastic deformation then spring-back will occur to a circular arc of radius greater than that of the press-tool. Gardiner showed that this effect can be measured in terms of the spring-back ratio.

$$\frac{R}{r} = 1 - 3\frac{RY}{Et} + 4\left(\frac{RY}{Et}\right)^3 \quad .. \quad .. \quad .. \quad (7.1)$$

where R = initial radius of neutral axis

r = final radius of neutral axis

Y = yield stress for material

E = modulus of elasticity

t = thickness of strip.

Since the strip retains some curvature there must be present within the strip residual stresses. These residual stresses may be determined from simple

theory and expressed in terms of the yield stress. Referring to fig. 7.10, the residual stress distribution across the strip is given by

$$\frac{\sigma_{res}}{Y} = \frac{E}{Y} \cdot \frac{x}{r} \quad \text{if } 0 < x < h \quad .. \quad .. \quad (7.2)$$

or $$\frac{\sigma_{res}}{Y} = 1 - \frac{E}{Y} h \left(\frac{1}{r} - \frac{1}{R}\right) \text{ if } h < x < \frac{t}{2} \quad .. \quad (7.3)$$

where σ_{res} is the residual stress and h is the distance from the neutral axis to the yielding layer which is given by

$$\frac{h}{t} = \frac{RY}{Et} \quad .. \quad .. \quad .. \quad .. \quad (7.4)$$

Since the residual stress distribution (eq. 7.2 or eq. 7.3) is linear and must be zero at the neutral axis, only two values (at $x = h$ and $x = \frac{t}{2}$) need be calculated.

7.5. Results of the bending tests

The test strip lengths were calculated before inserting in the die, so that fouling of the ends would not occur on closure of the die. After removal from the die the strip was placed on millimeter graph paper and viewed through an illuminating magnifier. Measurements were made on the inside edge of the specimen which admittedly is not accurate but the error incurred is only of the order of one or two per cent (1.1% for material B at 0.5 in. radius). Readings were taken for both edges of the strip in case the strip had not been inserted squarely in the bending rig. The extreme ends of the test strip were not included in the measurements.

From simple geometry the radius of the inside of the strip (fig. 7.11) is given by:-

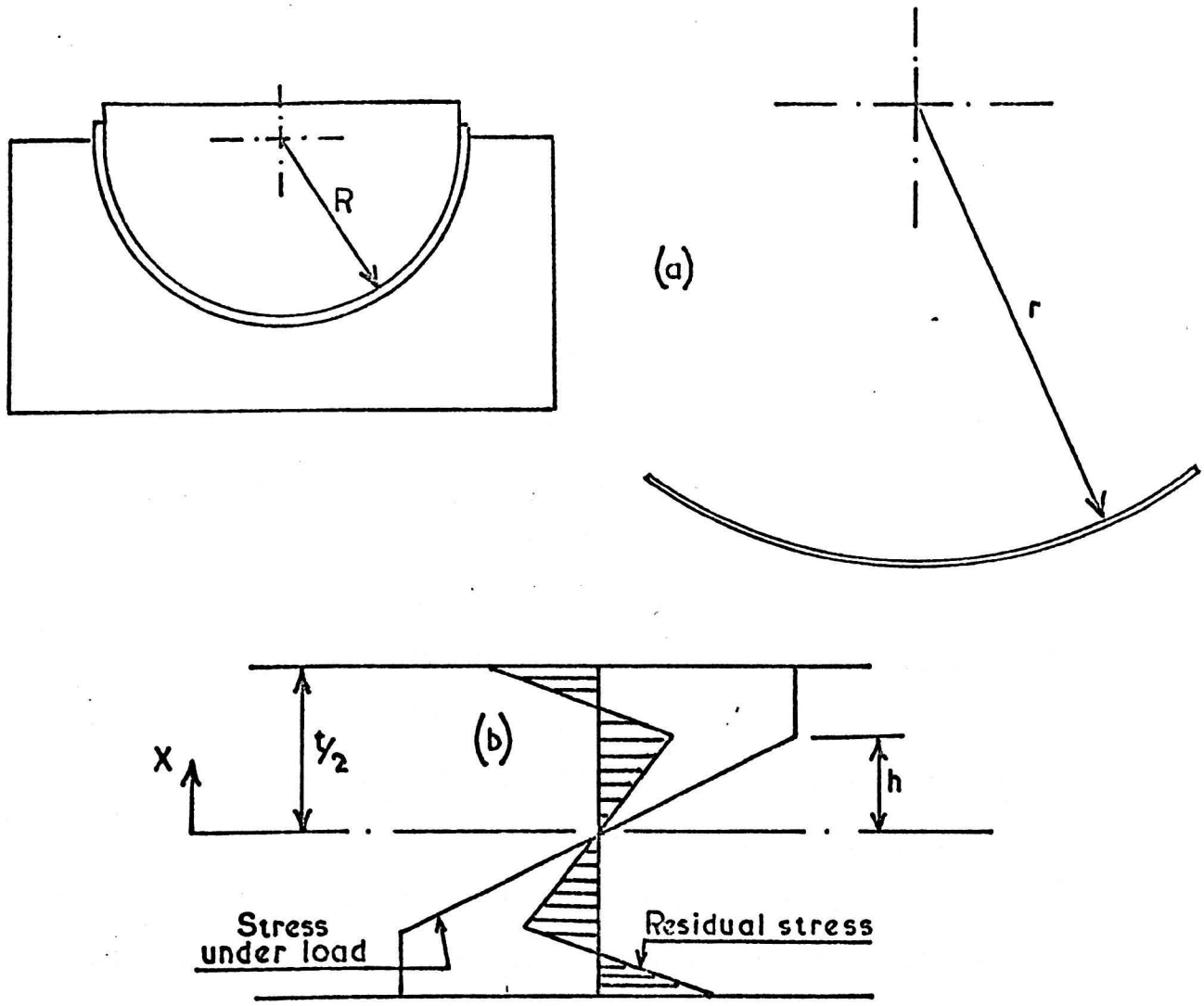

Fig. 7·10 (a) Spring-back ratio R/r
(b) Residual stress after bending

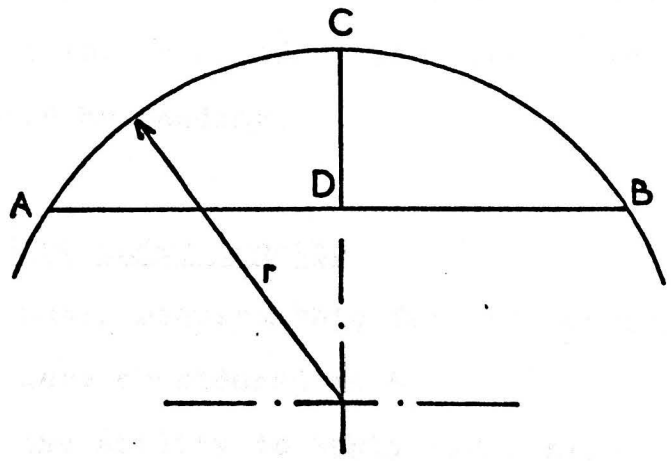

Fig 7·11. Sagitta CD of chord AB

$$r = \frac{BD^2 + CD^2}{2CD} \quad .. \quad .. \quad .. \quad .. \quad .. \quad (7.5)$$

Results of the tests are presented in Table 7.2 which also shows the percentage variation of the theoretical results (r_t) from the experimental results (r_e). The basis of this comparison is to be found in Appendix A7. The theoretical spring-back curves are shown in fig. 7.12 and the experimental results are indicated.

The theoretical residual stress distribution was determined from equations 7.2, 7.3 and 7.4 using both the experimental value of radius and the theoretical value. These results are depicted in figs. 7.13 - 7.16.

The experimental determination of the residual stress distribution is best carried out by etching successive layers from the specimen and measuring the resulting change in radius. This technique will be discussed in greater detail later in this thesis.

The next step in the investigation is to examine the influence of back-tension on the spring-back characteristics. In order that some control might be gained over all of the parameters involved, it was decided at this stage that the order of application of load must be tension followed by bending.

7.6. Bending under tension

The basic requirements for the bending under tension tests were considered to be

i) the ability to apply and control a measured back-tension whilst winding the strip round the arbor.

ii) the ability to carry out a number of

TABLE 7.2

Material	R in.	r_e in.	r_t in.	% Variation
A	0.506	1.85	1.81	2.2
A	1.00(6)	inf.	303	-
B	0.510	0.937	0.963	2.84
C	1.01	4.19	3.84	8.47
D	0.515	0.696	0.687	1.37
D	1.01(5)	1.99	1.90	4.56

Comparison of theoretical and experimental values of radius of curvature after press-forming.

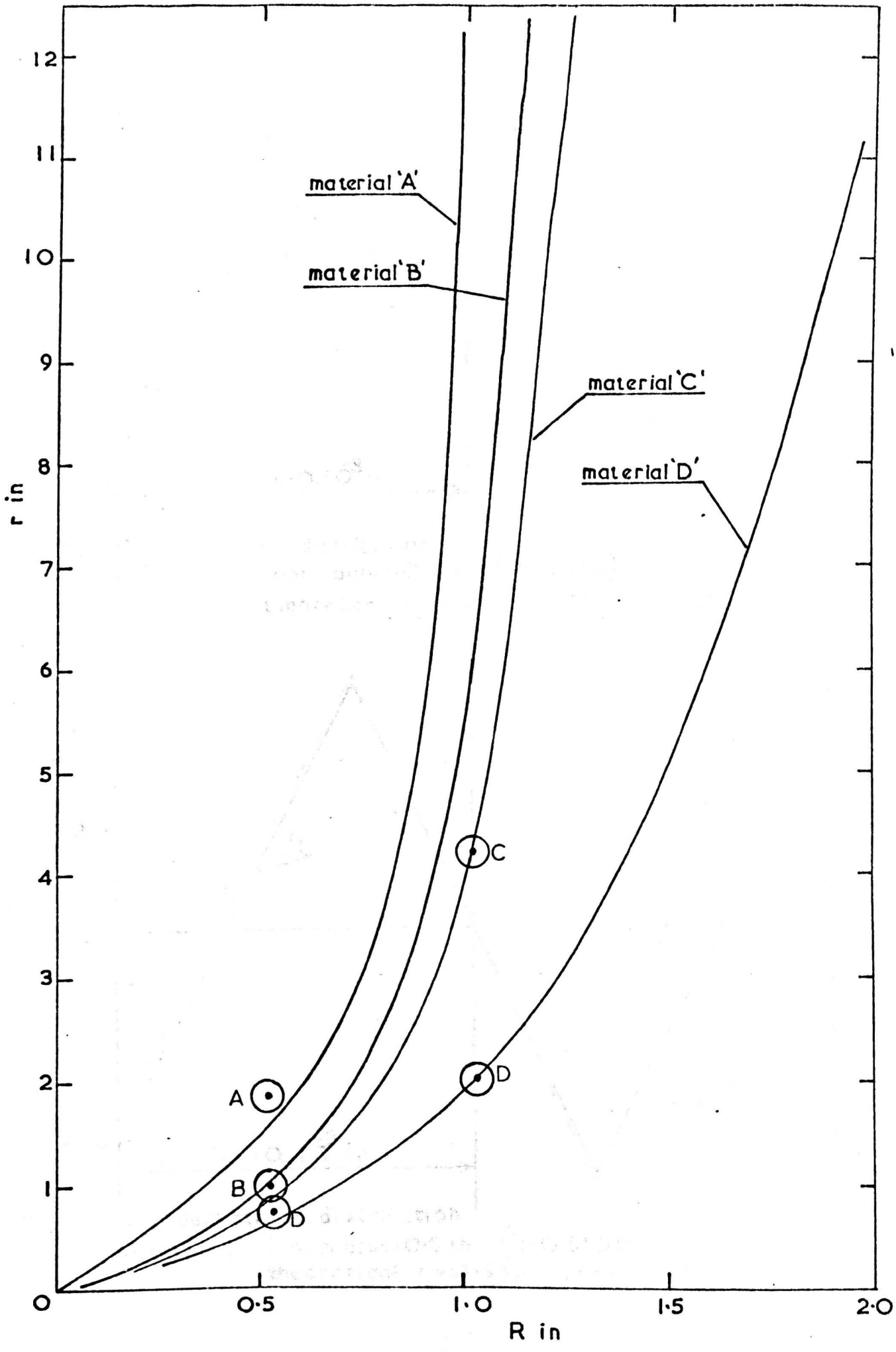

Fig. 7·12 Spring back in pure bending.

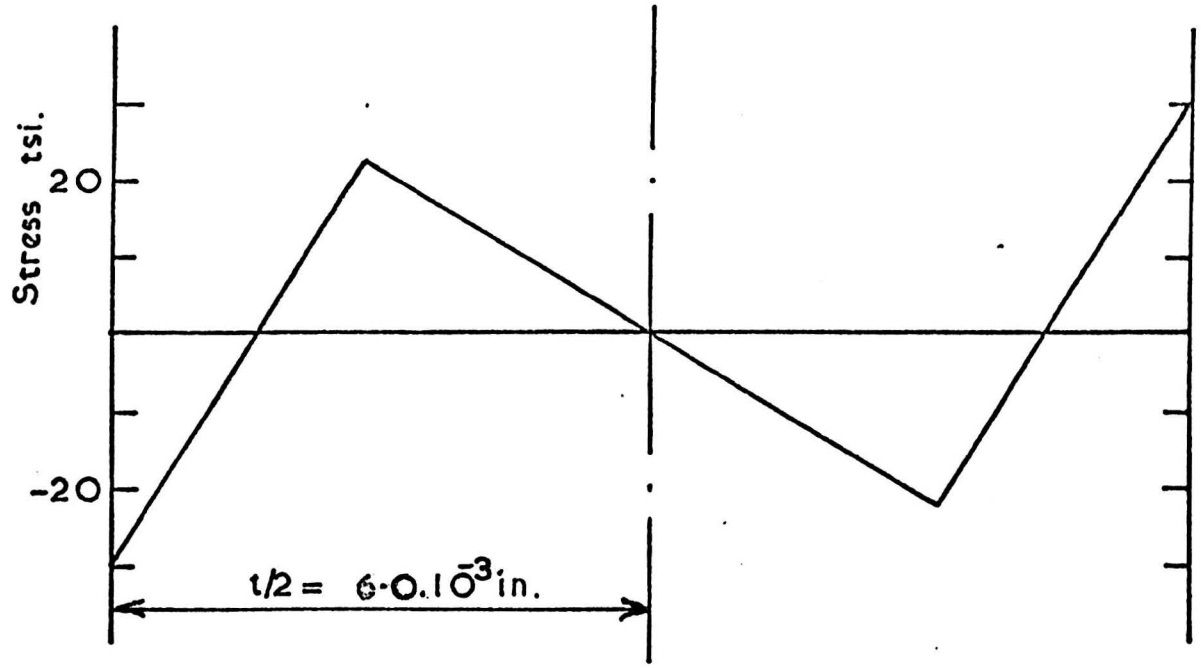

Fig. 7·13 Residual stress distribution
Material 'A' Tool radius=0·5 in (R=0·056 in)
theoretical r_t=1·81 in., experimental r_e=1·85 in.

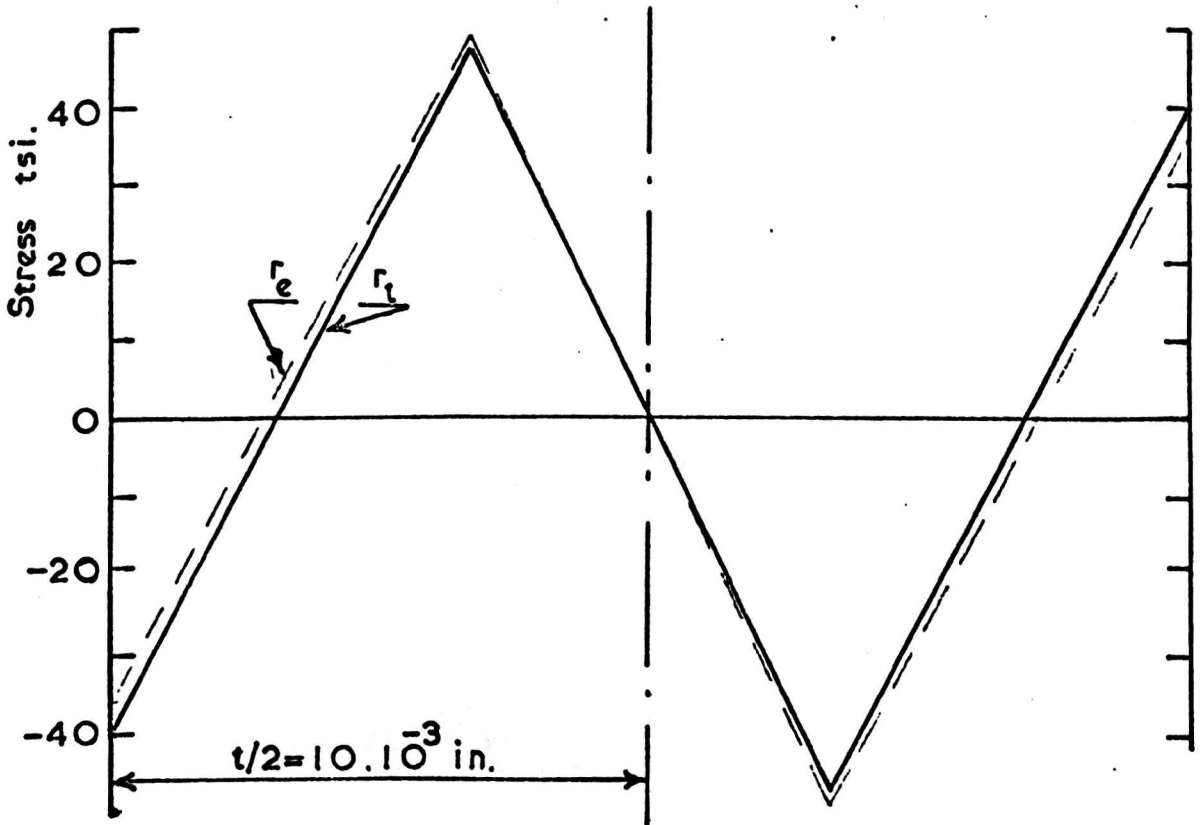

Fig 7·14 Residual stress distribution
Material 'B' Tool radius=0·5 in (R=0·510 in)
theoretical r_t=0·963 in., experimental r_e=0·937 in.

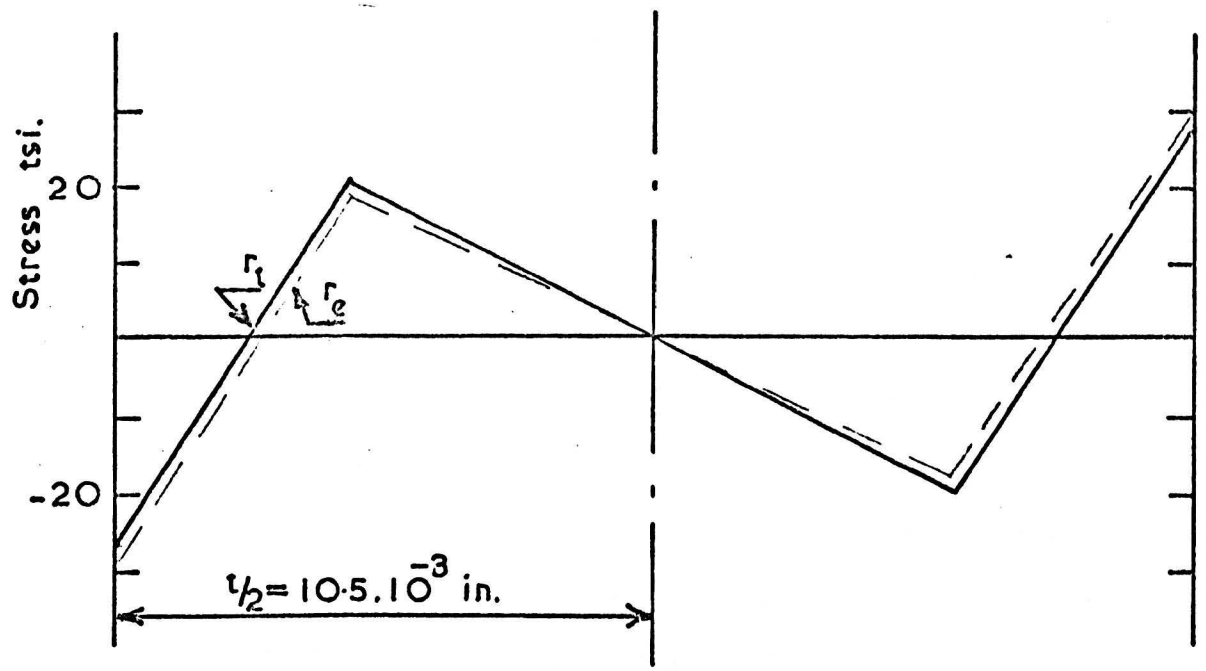

Fig. 7·15 Residual stress distribution
Material 'C' Tool radius=1·0 in (R=1·01 in)
theoretical r_t=3·98 in., experimental r_e=4·19 in.

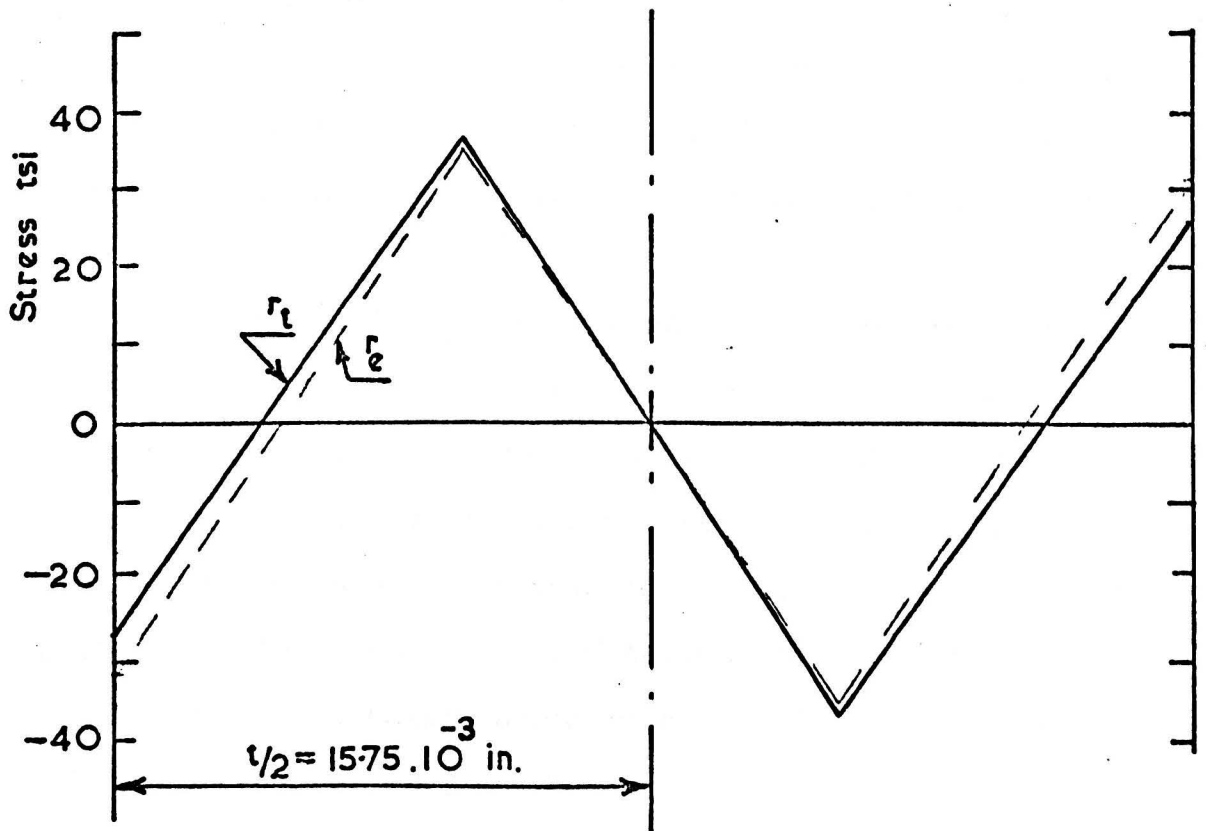

Fig. 7·16 Residual stress distribution
Material 'D' Tool radius=1 0in (R=1·015 in.)
theoretical r_t=1·90 in , experimental r_e=1·99 in.

revolutions of the arbor whilst maintaining the required back-tension.

These requirements were met by designing an attachment for the Hounsfield tensometer which was capable of accommodating different sizes of arbor. The torque was applied to the arbor by hand. This imposed limitations which might be overcome in later experiments. The design of the arbor housing was such that the strip winding onto it lay along the axis of the testing machine, the other end being held in the normal plate grip of the machine. Fig. 7.17. The machine itself was clamped to the bench.

The materials listed in Table 7.1 were used and the direct stress (due to back-tension) was calculated from the maximum torque available at the arbor, which was about 246 lbf.in., and the width of the strip. In this way it was possible to attain direct stresses up to about 35 ton/in^2.

The radius of curvature of the specimens was determined in the manner already described in article 7.5. It was assumed that the shape of the portion of strip being measured would not differ greatly from a circular arc. The spring-back ratios thus obtained are compared with the theoretical values obtained in accordance with the theory for bending under tension which forms the subject matter of Chapter 8.

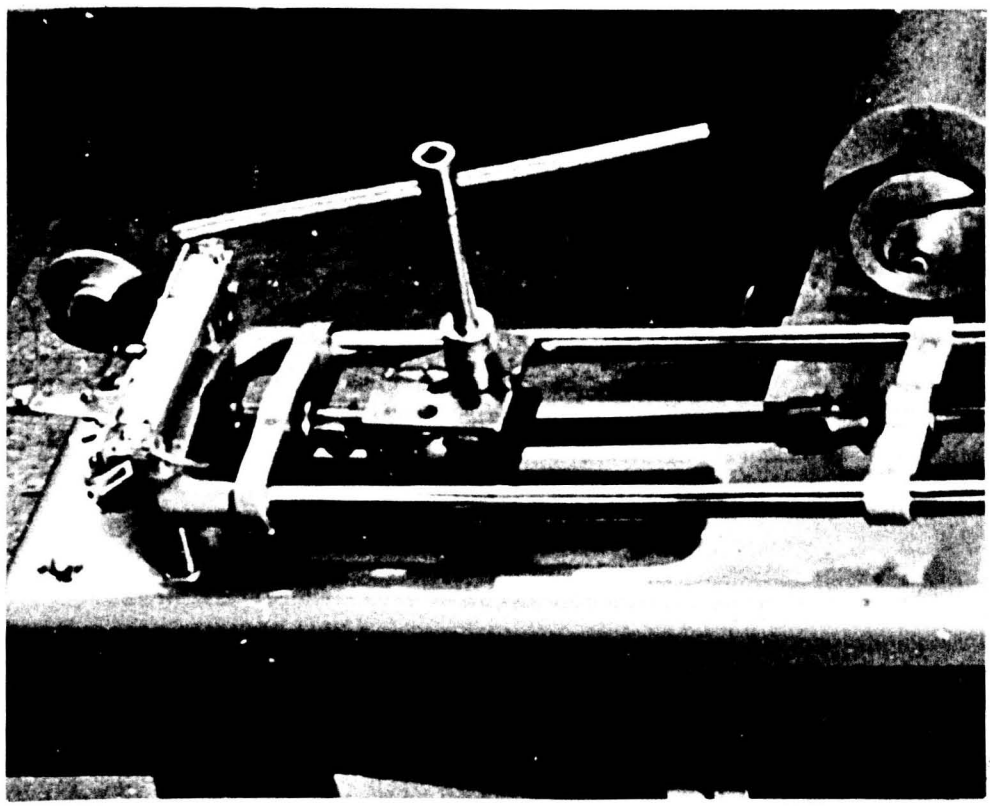

FIG. 7.17. RIG FOR WINDING UNDER TENSION

CHAPTER 8

THEORY FOR BENDING UNDER TENSION

8.1 Introduction

The variation of curvature along the length of a strip wound into a spiral form is a direct consequence of the dependence of the amount of plastic deformation suffered by an element upon its position in the strip. Since all elements of the cross-section of the strip are not subjected to the same plastic deformation during the forming process, residual stresses are induced and, when subsequently unloaded, the strip possesses curvature. The plastic deformation also varies along the length of the strip with consequent variation in the residual stress pattern. The equation of the spiral is, therefore, dependent upon this variation of the residual stress pattern which manifests itself in the amount of springback from the fully deformed position and can be measured in terms of a 'springback ratio'.

In this chapter Woo and Marshall's[R12] theory for stretch forming is modified to non-dimensional form so that curves and tables can be produced for spring-strip materials giving springback ratios and residual stress distribution for a wide range of arbor diameters and back-tensions, with a view to predicting the free-spiral equation. The present investigation has been restricted to consideration of an ideal elastic - perfectly plastic material since the materials tested exhibited no significant work hardening and conformed closely to this model material. The Bauschinger effect is ignored* together with two systems of loading which call for a different analytical approach. In one of these systems it

---

* Sidebottom and Chan[R13 p.631] showed that errors of 30% can result from ignoring the Bauschinger effect.

CHART No. 1

CLASSIFICATION OF STRESSES

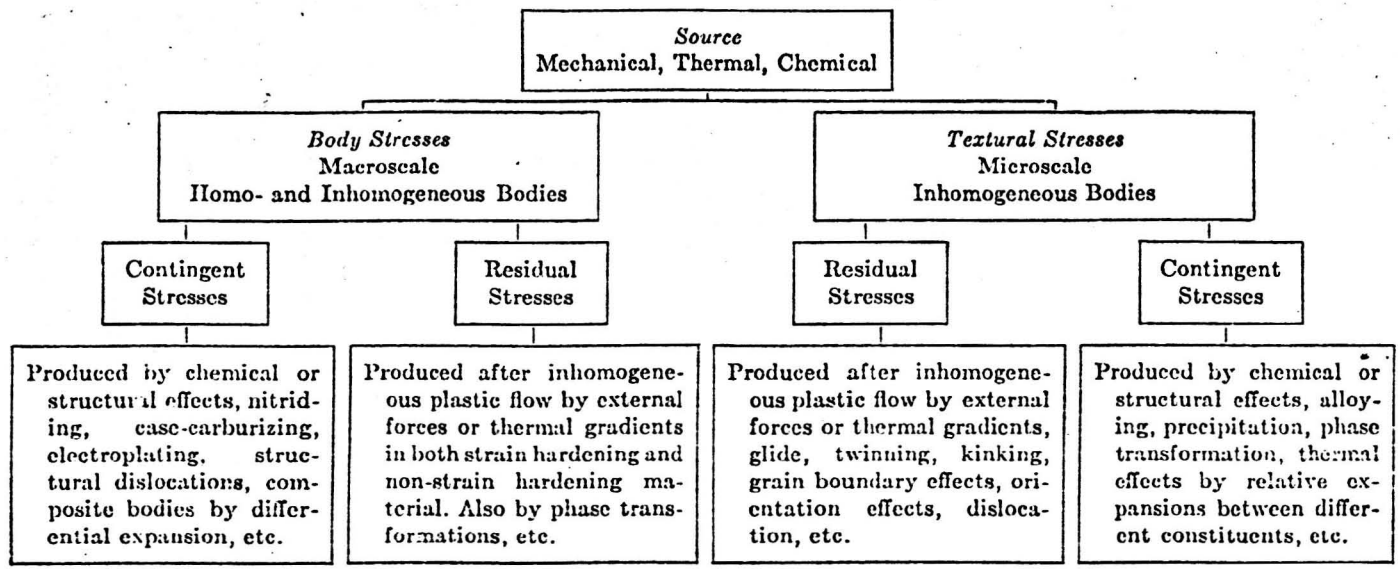

Note: *Contingent stresses* are those stresses which are contingent upon the co-existence of the source from which they are derived. They also include elastic stresses produced by external loads while the loads remain on the body. Except for the latter they can be called *contingent residual stresses.*

Residual stresses may be present without, and are not contingent upon, the co-existence of the source from which they are derived, such as the external loads causing plastic flow, etc.

FIG. 8.01 Classification of residual stresses ex Residual stresses in metals and metal construction - Osgood(R14)

is possible for yielding in compression to occur before applying the back-tension and in the other it is possible for yielding to occur during the springback after forming.

It is considered that strain history analysis supported by experimental determination of the residual stress distribution in actual springs wound under controlled conditions should be used in a further investigation aimed at modifying the theory presented later in this chapter. This should then facilitate prediction of the free spiral equation resulting from any of the current processes of cold forming spiral springs.

8.2. Experimental determination of residual stresses

Stresses can be classified in different ways depending on the objective in mind. The chart constructed by C.W. MacGregor (R14 p105) and reproduced in fig. 8.01 presents a classification well suited to our present purposes.

Assuming that the strip from which a spiral spring is formed is initially stress-free, the type of residual stresses we are interested in are the macroscale body stresses due to non-uniform plastic flow.

Residual stresses may be measured by physical or mechanical methods. Of the former X-ray methods, which measure crystal lattice strains have found wide acceptance. Other properties which are affected by residual stress are electrical resistivity, magnetic permeability, density, internal friction and stress-wave propagation. So far (R16) methods based on these properties have been limited to qualitative observations, but they can yield information about sub-surface stresses and are non-destructive.

Mechanical methods are destructive, or at least partially so, whilst X-ray techniques are limited to the determination of surface stresses and the accuracy with which these stresses can be determined leaves much to be desired[R17-21].

One of the earliest recorded attempts to measure residual stress was that by Kalakoutzky[R22] in 1887. Some time later, Howard[R23] reported longitudinal compressive stresses calculated from the increase in length of a bar after boring out, but did not appreciate that the stress distribution was not uniform. Heyn and Bauer[R24] used a layer removal technique which consisted of measuring changes of length of tubes and rods when successive layers were turned off the outside. The method, and attendant calculations, omits to take account of the presence of tangential and radial stresses and can be seriously in error. An exact method of determining the longitudinal, tangential and radial residual stresses in bars and tubes was proposed by Mesnager[R25] and modified by Sachs[R26] to his well-known boring-out technique. This method is limited to cylindrical bodies in which the residual stresses may vary in the radial direction but are constant in the tangential and longitudinal directions. The Sachs boring method also precludes determination of the residual stress at the outside of the tube or bar which information is often of greatest importance. Fuchs and Matson[R27] determined residual shear stresses in tension bars by grinding concentric layers from the outside of the bars and measuring the resultant deformation. Whiteside[R10] carried out a similar procedure using etching techniques.

Heyn and Bauer's method of calculation can be applied to plate material where there is a symmetrical stress

distribution and this is the method outlined in Chapter 9. Treuting and Read[R28] extended the Heyn and Bauer method to determine the biaxial residual-stress on the surface of a thin sheet. Their method of metal removal was to cement the sheet to a flat block and carefully polish and etch. The sample was then released and the principal curvatures measured. The theory represents an advancement on that due to Heyn and Bauer and is recommended for use in the future work on spiral springs.

The etching technique is discussed further in Chapter 9 and it is sufficient to say here that it is accepted that etching of steels with nitric acid diluted with water or alcohol is one of the least offensive methods of metal removal as far as introduction of stress by the layer removal itself is concerned. Loxley[R29], Hill[R30], Taira and Yoshioka[R31], Jackson[R32], Botros[R33] and Whiteside all report favourably on this method of metal removal. The author has used etching techniques on torsion bars and sections of clock springs using an apparatus described in the next chapter.

One of the foreseeable problems associated with the layer removal technique as applied to the spiral spring concerns the induction of inelastic strains in the remaining material. The residual stress distribution in the specimen cannot be related to the measured deformations (during etching) unless the stress-strain relationship is known for all parts of the specimen remaining at any particular stage in the layer-removal process. In order to ensure that no inelastic strains occur during etching, it is suggested that a jig be designed in which the

geometry of the specimen remains constant and the necessary restraining forces are measured by strain gauges attached to the jig.

8.3. Woo and Marshall theory for stretch-forming

As stated in article 8.1, it is considered sufficient at this stage to develop the theory in non-dimensional form (Appendix A8) for an ideal elastic-perfectly plastic material. Examination of the figures 7.6, 7.7, 7.8, 7.9 reveals that the actual materials tested exhibited almost ideal stress-strain curves. The assumptions regarding homogeneity of the material, absence of warping of the cross-section during bending and shift of the neutral axis which are usually made in simple bending theory, are taken to apply here. The fibres are taken to unload elastically along a line on the stress strain curve parallel to the elastic loading line, i.e. the Bauschinger effect is ignored at this stage.

The theory is considered in two distinct phases. First the conditions under which compressive yielding of the inside fibres takes place are considered and then the treatment is adjusted to consider what happens if there is no compressive yielding of these inside fibres. From the equations derived computer programmes were written which will give values of the spring-back ratio for, what is believed to be, the working ranges of materials, thickness of strip, radius of arbor, and back-tension likely to be encountered. Programmes were also written to give the residual stress distribution. Tables compiled from

these programmes accompany this thesis.

8.3.1. Compressive yielding at the inside fibre

It is evident that the amount of spring-back (measured by the spring-back ratio) exhibited by a particular strip depends upon two factors:

1) Plastic deformation must take place; the greater the depth of the plastic layer, the smaller is the spring-back ratio. In pure bending the depth of yielded material is approximately the same on either side of the strip.

2) The presence of a back-tension causes an unbalance in the depth of the yielded material on either side of the strip, increasing that on the tensile side and, perhaps eliminating, but certainly reducing that on the compressive side. Obviously this affects the spring-back ratio and exposes one of the facets of the problem to be explored.

It is shown in the Appendix A8 that for the above idealised material subjected to bending under tension of such a magnitude that yielding in compression occurs at the inside fibres, the spring-back ratio is given by:-

$$\frac{R}{r} = \frac{(1 + \varepsilon_a) + 6 \frac{RY}{Et} \left(\frac{P}{Y} - \frac{E}{Y} \cdot A\right)}{D_A} \quad .. \quad (8.1)$$

in which the symbols are in accordance with

the following notation:-

R	radius to which the centroidal axis of a particular element is bent initially.
r	radius of that element after removal of all external forces and moments.
ε_a	maximum strain at the inside fibres.
Y	yield stress of material.
E	modulus of elasticity.
t	thickness of strip.
P	tensile stress applied.
A	constant defined below.
D_A, D_B	also defined in text.

The corresponding equation of R/r with no yielding at the inner fibres is similar but with different expressions for ε_a, A and D_A.

The present conditions give rise to the expressions

$$\varepsilon_a = \varepsilon'/(1 - \varepsilon') \quad .. \quad .. \quad .. \quad (8.2)$$

where $\varepsilon' = (1 - \frac{P}{Y})/2 \frac{RY}{Et} \cdot \frac{E}{Y}$

(NOTE: The terms are not cancelled because the term RY/Et is used as a parameter.)

$$A = \frac{Y}{E} - 2(\frac{RY}{Et}/(1 + \varepsilon_a))^2 (\frac{Y}{3E} + \varepsilon_a^2 \cdot \frac{Y}{E}) \quad .. \quad (8.3)$$

and $$D_A = 1 + \varepsilon_a - 4 \frac{P}{Y}/\frac{E}{Y} + 3A \quad .. \quad .. \quad .. \quad (8.4)$$

The depths of the two yield surfaces are of interest and expressed in terms of the strip thickness are given by

$$\frac{d_t}{t} = \frac{1 - \frac{E}{Y} \cdot \varepsilon_a) \frac{RY}{Et}}{1 + \varepsilon_a} \quad .. \quad .. \quad .. \quad .. \quad (8.5)$$

and $$\frac{d_c}{t} = \frac{-(1 + \frac{E}{Y} \varepsilon_a) \frac{RY}{Et}}{1 + \varepsilon_a} \quad .. \quad .. \quad .. \quad .. \quad (8.6)$$

where d_t and d_c are measured from the tension and compression faces respectively.

The residual stress distribution is determined from the equations:-

$$\frac{\sigma_{res}}{Y} = \frac{S}{Y} - \frac{P}{Y} + (1 - R/r)/2 \frac{RY}{Et} - \frac{d}{t}(1 - \frac{R}{r})/\frac{RY}{Et} \quad .. \quad (8.7)$$

in which σ_{res} is the residual stress at layer distance d from the compression face and S is the stress at this layer in the fully bent condition. It is shown (Appendix A8) that if $S \neq \pm Y$ then

$$\frac{S}{Y} = \frac{E}{Y} \cdot \varepsilon_a + \frac{d}{t}(1 + \varepsilon_a)/\frac{RY}{Et} \quad .. \quad .. \quad .. \quad (8.8)$$

8.3.2. <u>No compressive yielding at the inside fibre</u>

This will be the case for higher values of back-tension. The analysis (Appendix A8) is seen to follow the same lines as that for compressive yielding and gives rise to the same form of equation for spring-back ratio:-

$$\frac{R}{r} = \frac{(1 + \varepsilon_a) + 6 \frac{RY}{Et}(\frac{P}{Y} - \frac{E}{Y}B)}{D_B} \quad .. \quad .. \quad .. \quad (8.9)$$

in this case

$$\varepsilon_a = \varepsilon'/1 - \varepsilon' \quad .. \quad .. \quad .. \quad .. \quad (8.10)$$

as before but

$$\varepsilon' = \frac{1 - \sqrt{(2 - 2\,P/Y)/\frac{RY}{Et}}}{E/Y}$$

and

$$B = \frac{Y}{E} - (\frac{Y}{E} - \varepsilon_a)(\frac{d_t}{t})^2 + 2(\frac{d_t}{t})^3(1 + \varepsilon_a)/3\,\frac{RY}{Et} \cdot \frac{E}{Y} \qquad (8.11)$$

$$D_B = 1 + \varepsilon_a - 4\,\frac{P}{Y} \cdot \frac{Y}{E} + 3B \qquad (8.12)$$

It should be noted that if ε_a is regarded as a small quantity, the value of the spring-back ratio becomes independent of the material, depicted by the value of E/Y, and therefore the same curve, relating R/r to RY/Et, applies to all materials.

The equations for residual stress are equations 8.5, 8.7 and 8.8. Under these present conditions equation 8.6 does not apply since d_c is zero.

In the computer programme the change over from the compressive yield equations to those for no compressive yielding is brought about by evaluating the strain on the compressive face and, when this equals the yield value, the computer is directed to a second part of the programme.

8.4. Output of results

For the materials tested the value of E/Y was 168.6. Sets of tables were printed for various values of RY/Et and P/Y giving the spring-back ratio, the strain at the inside fibre, the depths of the tensile and compressive yield surfaces and the magnitude of the residual stress throughout the strip. In certain cases the

residual stress is listed as exceeding the yield stress which is obviously incorrect. For these conditions the theory does not hold because, theoretically at least, the material is strained plastically on release of the load. Clearly, such cases call for a strain history analysis. These results could be excluded from the tables by evaluating the final strain at the inside fibre and rejecting the results if this strain exceeds the yield strain of the material. However, it is considered useful to leave the results in the tables in order that attention may be drawn to conditions which might produce plastic deformation on recovery.

The chart (fig. 8.1) shows the spring-back ratio for variations of initial radius (represented by RY/Et) and back-tension (expressed as P/Y). In the region of the chart to the left of the S-shaped boundary curve yielding in compression takes place at the inside fibres whilst in that to the right the conditions for no compressive yielding pertain.

The distribution of residual stress is shown in fig. 8.2 for various values of back-tension and initial radius. Also displayed is the stress distribution in the bent position which should approximate to that existing when a spring is in the fully wound up condition. The spring-back curve is drawn for each value of back-tension and can be seen to approximate to two straight lines.

8.5. Wound spiral

If we assume that the radius of curvature of

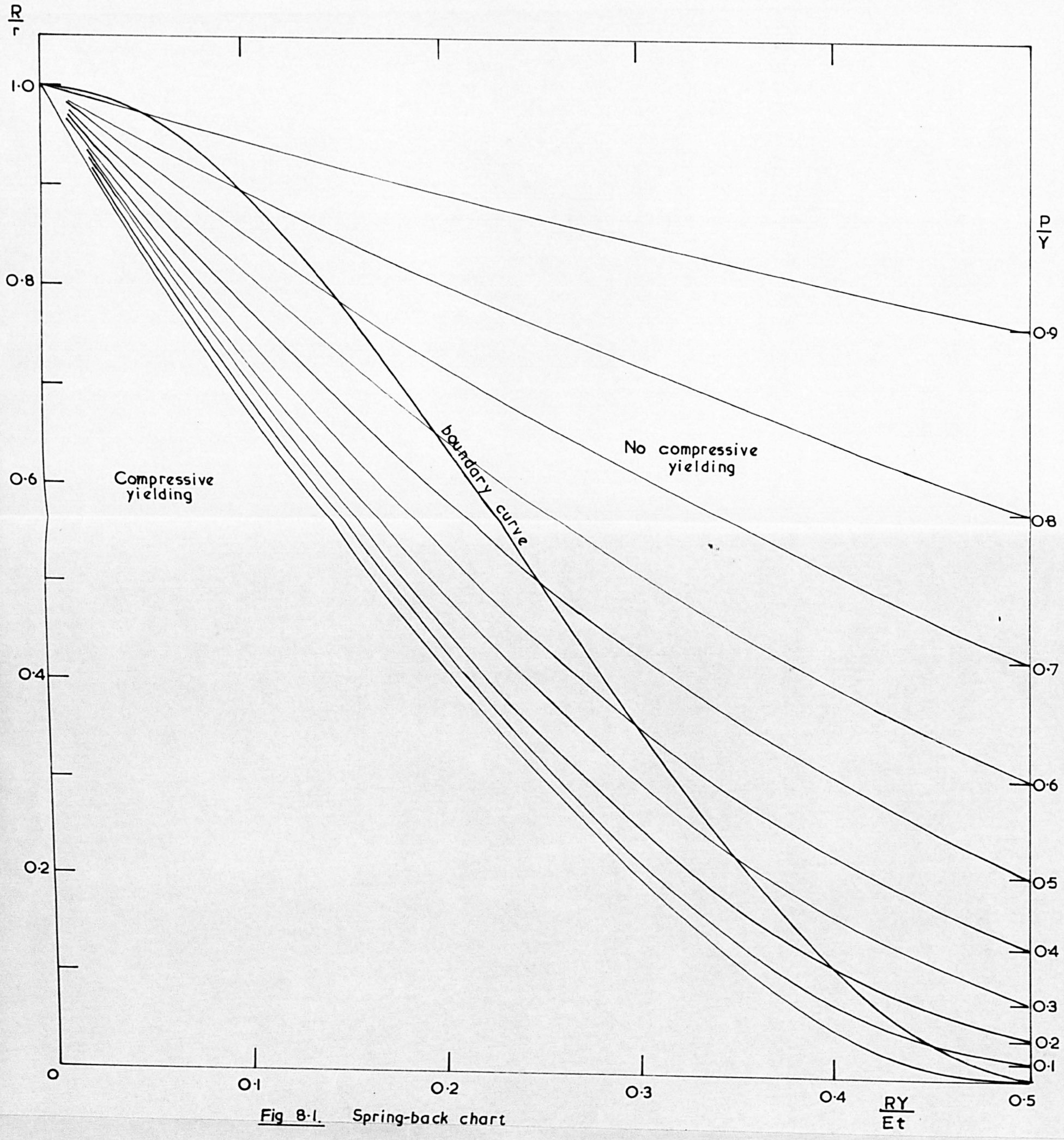

Fig 8·1. Spring-back chart

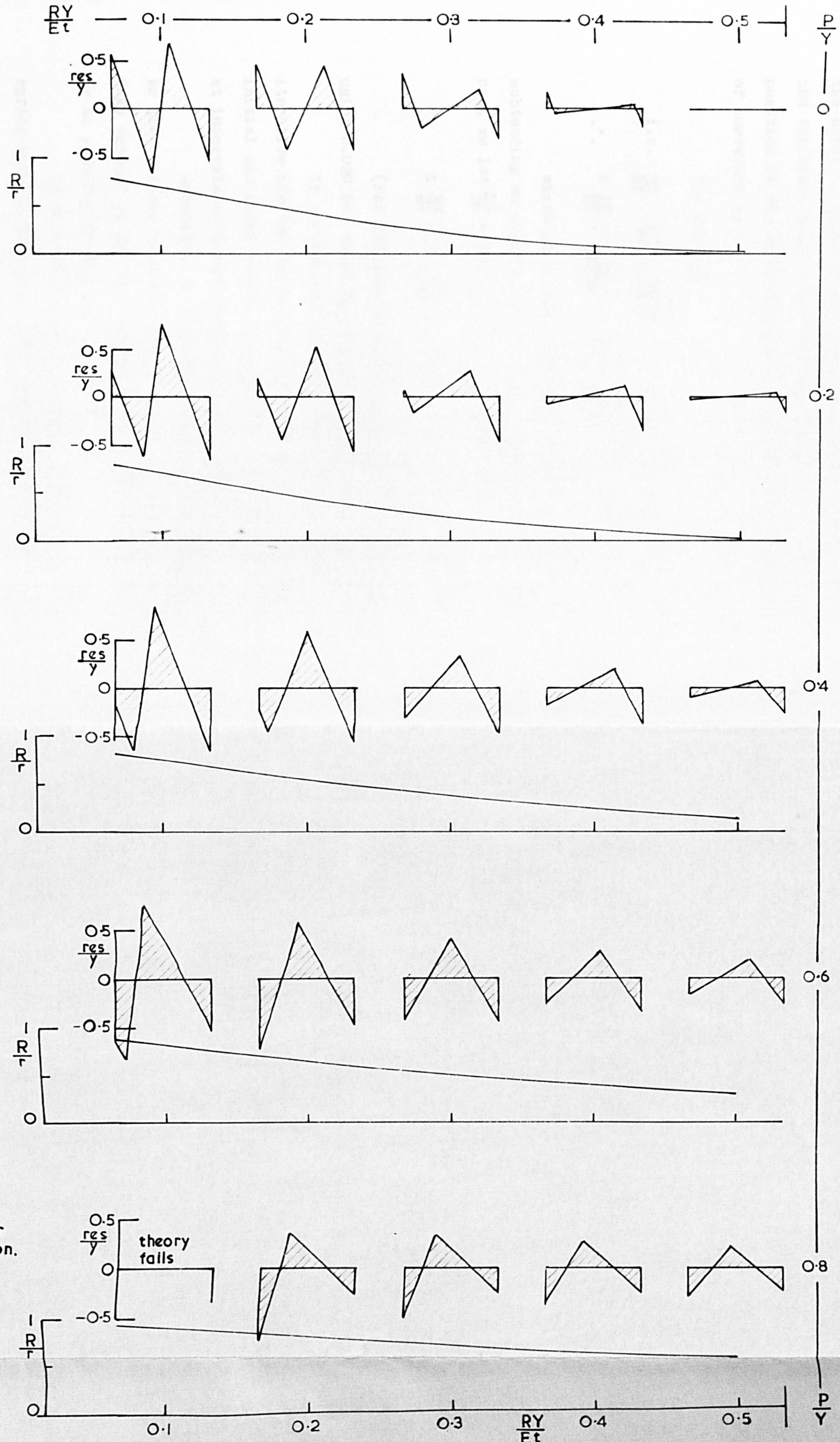

Fig. 8·2

Residual stress and spring back ratio for bending under tension.

the strip is equal to the radius to centre of the arbor and thickness small compared with radius, then, for any position on the wound spiral, we can express the radius of curvature as:-

$$R = R' + \frac{\theta}{2\pi} t$$

i.e. $$\frac{RY}{Et} = \frac{R'Y}{Et} + \frac{\theta/2\pi}{E/Y}$$

$$\therefore \quad \Delta \frac{RY}{Et} = \frac{\Delta\theta}{2\pi E/Y} \simeq \frac{\Delta x}{2\pi} \quad \frac{1}{RE/Y}$$

where Δx is the elementary length of strip subtending an angle $\Delta\theta$ at the centre of the arbor. If now, we let $\frac{\Delta x}{2\pi} = ct$, c being a constant then:

$$\Delta \frac{RY}{Et} = c \cdot \frac{Et}{RY} / (E/Y)^2$$

(For incremental lengths of, say, $\frac{1}{2}$ inch (Δx) using 0.020 in. thick spring steel strip, then $c \simeq 4.0$.)

If an initial value of RY/Et is chosen then an iterative process can be started in which are evaluated initial and final (after spring-back) radii of curvature at intervals of $\frac{1}{2}$ inch along the strip length.

Actually, a computer programme was designed to give a finer interval than this and was written to take account of the two conditions of either yielding or no yielding of the inside fibres.

If we assume that the radius of curvature after spring-back is the same as the radius given by the spiral equation

$$r = r_o e^{b\theta}$$

i.e. that b is small, then we can work out the angular position on the spiral of an element after spring-back

since, approximately,

$$\Delta x = r\Delta\theta$$

or $$\Delta\theta = \Delta x/r.$$

The computer programme was designed to carry out the iterative process for θ. From these results (Appendix A8) the R - θ curve can be plotted and analysed to determine its mathematical form.

8.6. Examination of theoretical results

From the computed values ln r vθ curves were constructed for values of P/Y ranging from zero to 0.8 (fig. 8.3). It is seen that the resulting curves for values of P/Y up to 0.4 can be approximated to two straight lines. The final parts of the curves will naturally have infinite slope (no plastic deformation) and consequently this part of the curve is disregarded.

Fig. 8.4 shows a plot of the values of b with respect to P/Y and it is seen that a linear relationship exists for the first part of the ln r vθ curves and a curvilinear relationship for the second part. If a logarithmic plot is made (fig. 8.5) it is found that b is related to the back-tension by the law

$$b = -\frac{\ln P/Y}{4\cdot4}.$$

8.7. Experimental determination of the spring-back ratio due to bending under tension

8.7.1. Description of apparatus and method

Basically the apparatus used for these tests comprised a simple winding rig which could be fitted to

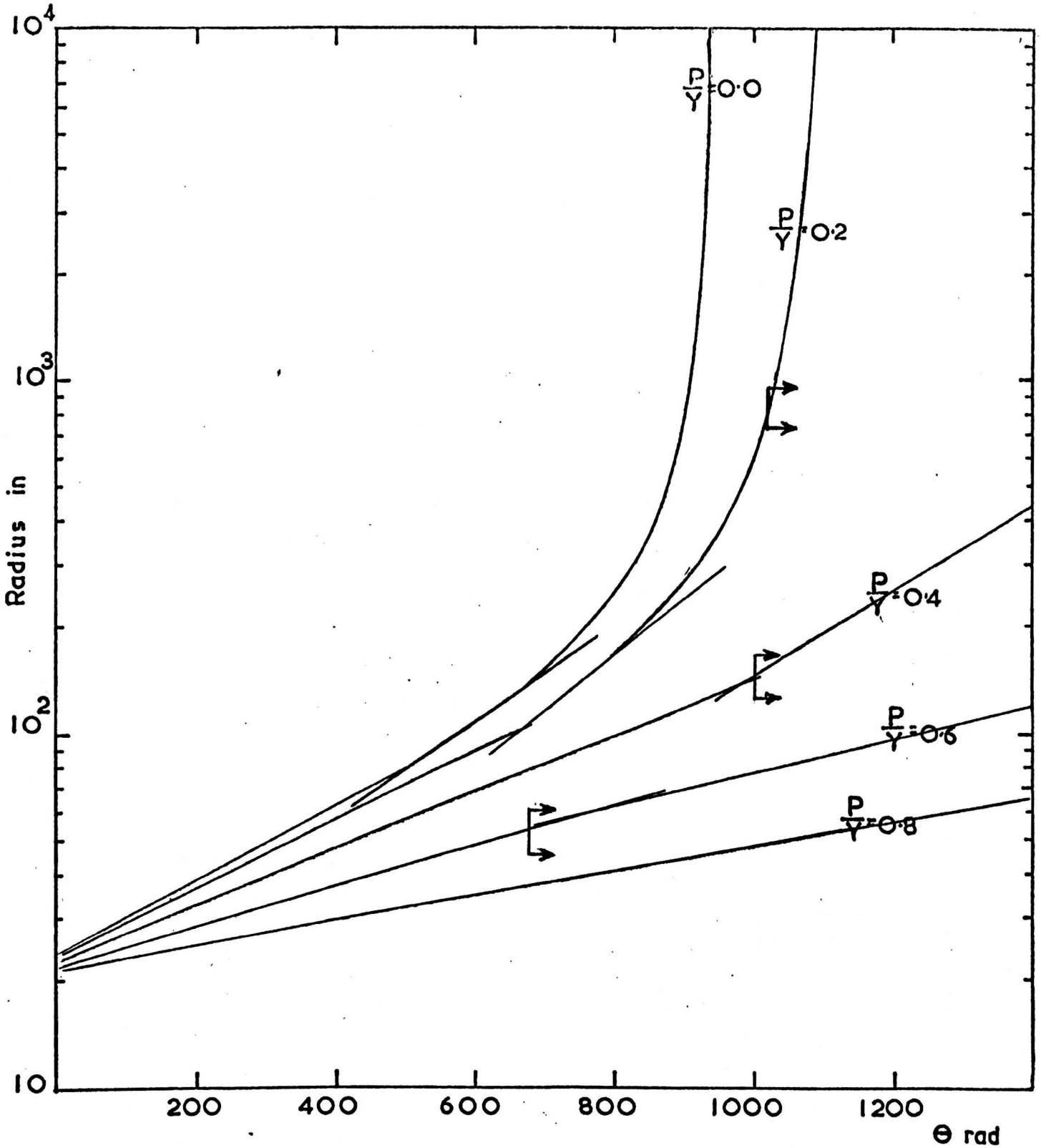

Fig. 8·3 lnR-Θ Plot. Computed values for bending under tension.

↱↳ — Indicates limit of compressive yielding.

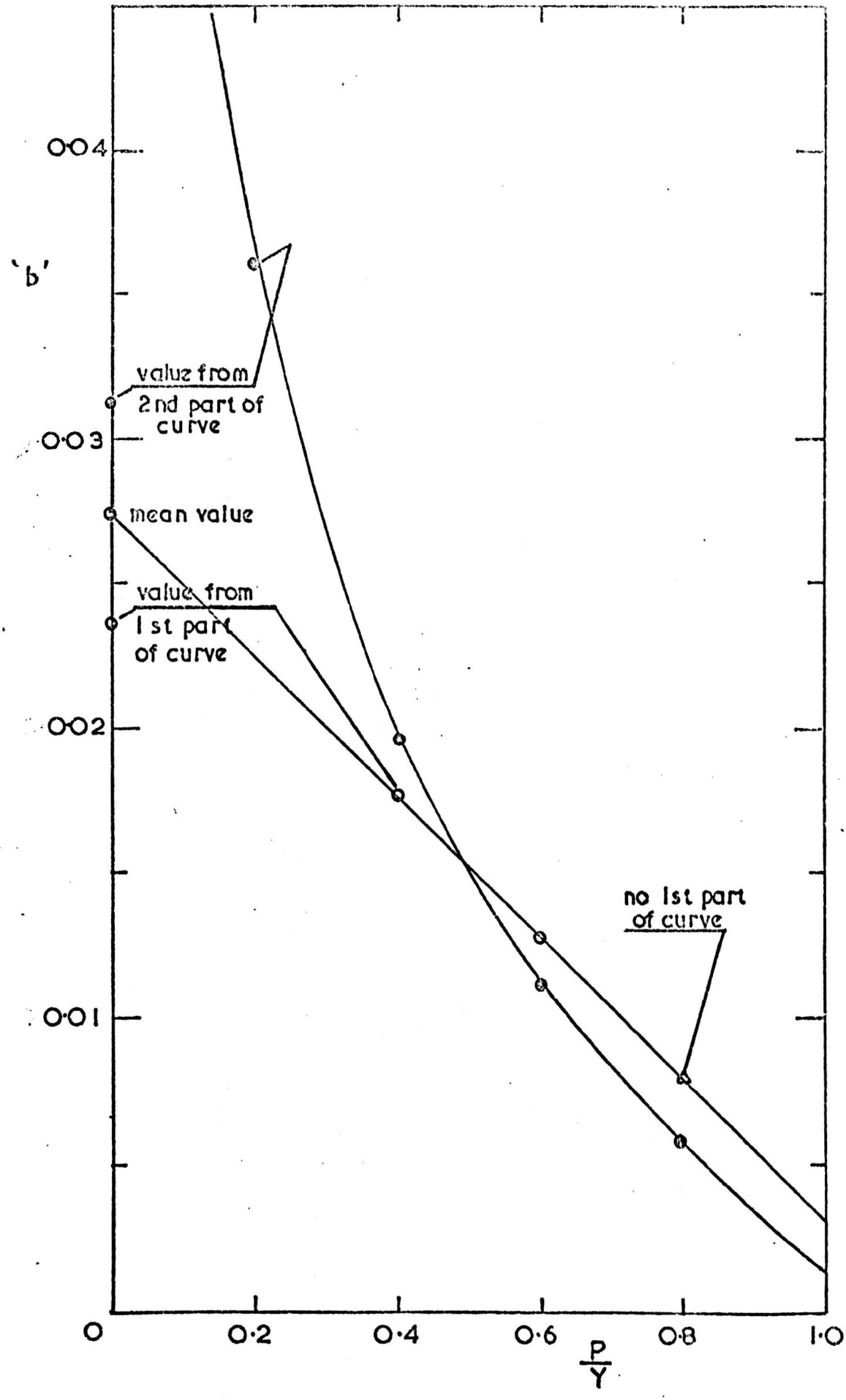

Fig 8·4. Dependence of 'b' on back tension. values from fig. 8·3.

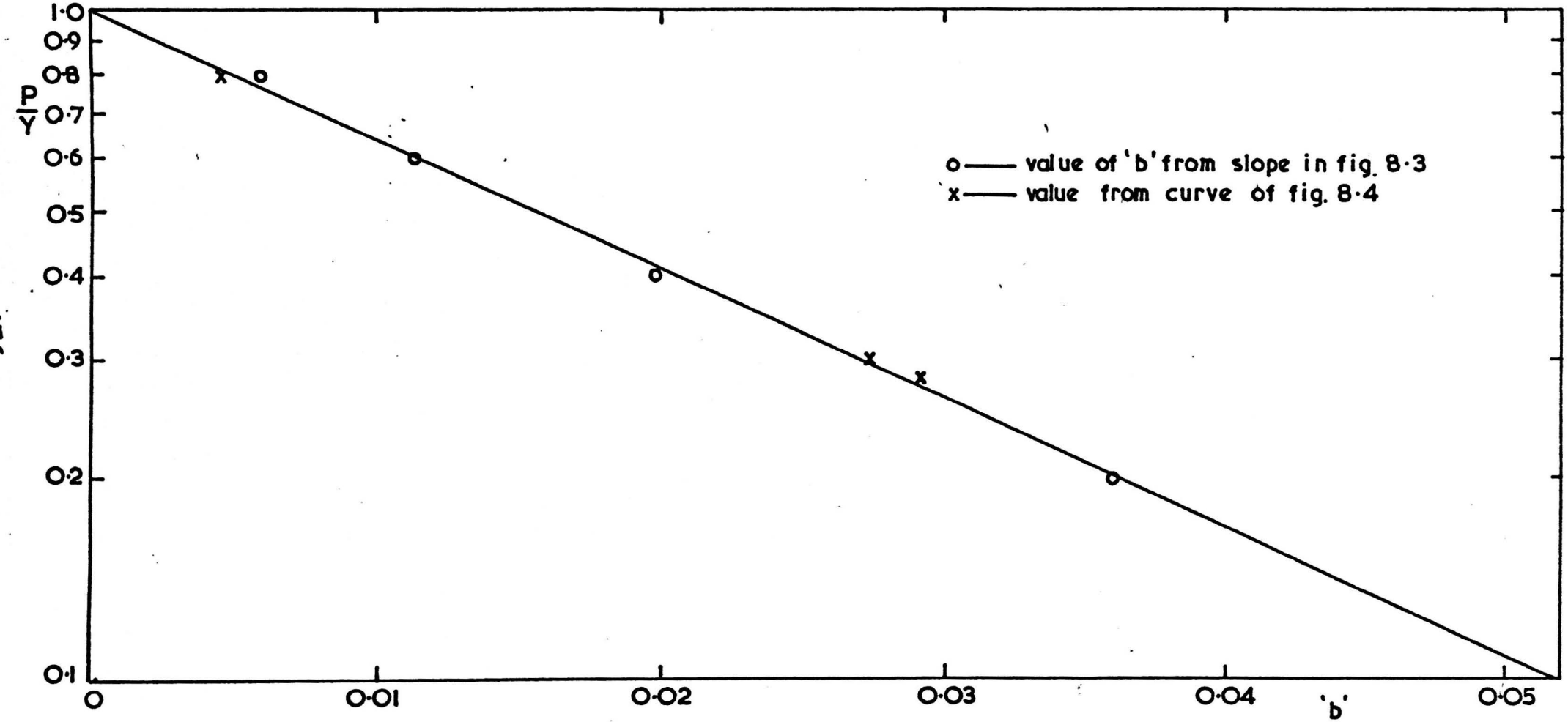

Fig. 8·5. $\text{Ln}\frac{P}{Y}$ v 'b'

a Hounsfield tensometer, the idea being to wind the strip round an arbor in this rig whilst tensioning in the tensometer. The winding rig is shown at A in fig. 8.6 and merely consisted of an arbor mounted in an adapter for fitting to the tensometer so that the strip winding onto the arbor lay along the tension axis of the tensometer. The winding torque was provided by hand as is evident from the photograph. When the technique had been mastered, it was reasonably easy to operate the tensometer lead screw by means of the motor B (fig. 8.6) so as to maintain an almost constant back-tension (as indicated by the mercury column, C) whilst winding the strip.

8.7.2. Preparation of test pieces

The materials used were those decribed in Chapter 7 for the pure bending tests. Samples were prepared for use with arbor diameters of 1 in., 2 in. and 3 in. The maximum torque which could comfortably be applied by hand was found to be about 250 lbf.in. This value was used to determine the width of specimen which could be wound under tensile stresses up to about 40% of the yield stress. Thus samples were marked out and prepared by bending over at one end and forming a short length to the arbor radius and drilling the other end for use with the Hounsfield tensometer plate grip (see the specimen marked S, fig. 8.7, for details of shape). The edges of the strip were finally prepared by draw filing after guillotining approximately to width. The tolerance on width is approximately 0.015 in in $\frac{1}{2}$ in. if the variation in stress is to be maintained within

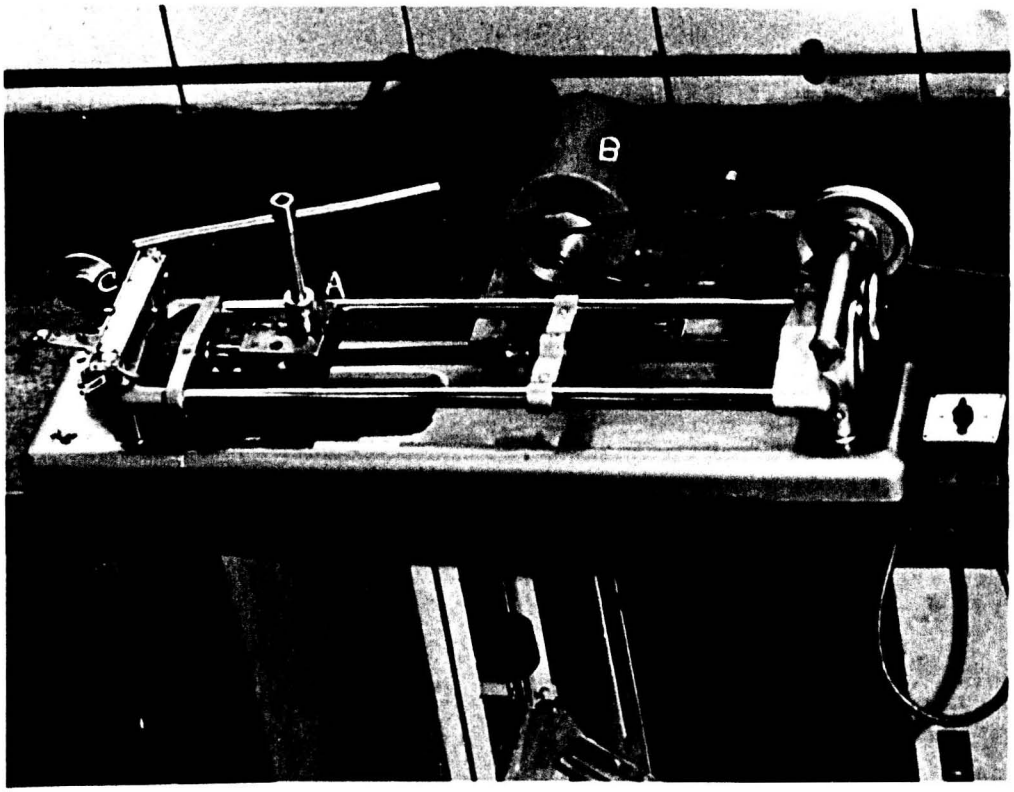

Fig.8.6 Winding under tension.
A -- winding rig, B -- motor, C -- mercury column.

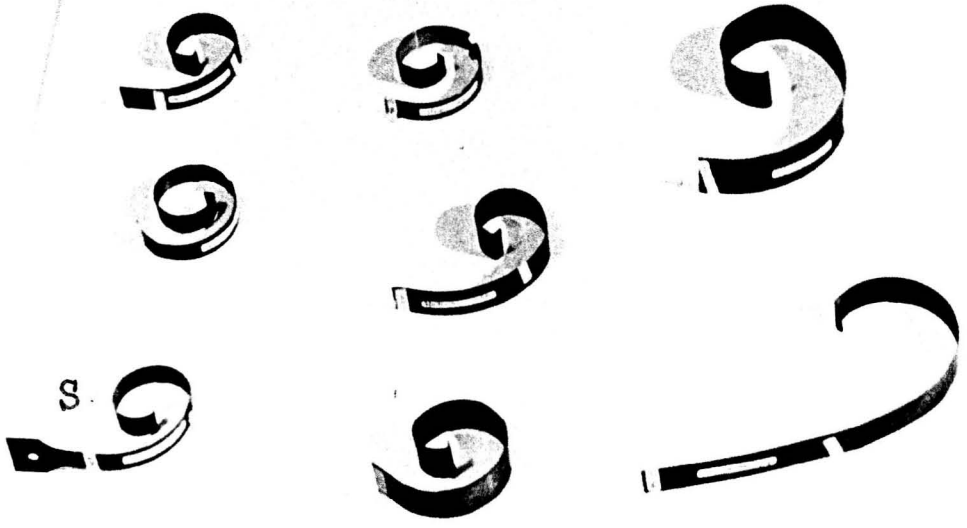

Fig.8.7 Specimens after winding under tension.

about 2½% of the mean value. This degree of accuracy is easily attained.

8.7.3. Observations and results

After forming, the specimen was removed from the rig, the gripped end cut off and the radius of curvature of the formed part of the strip was determined by the graph-paper method. It is significant that quite large variations in final radius were noticed in samples which had received practically the same treatment. This indicates some randomness in the process which is difficult to explain other than to attribute it to non-uniform behaviour of the material itself when subjected to plastic deformation. Never-the-less, the measure of agreement between the theoretical and experimental behaviour (if not the actual values expressed as percentage variance) of the material under these conditions of deformation is encouraging and leads one to believe that the results of winding strip in this manner may be predictable. Similar occurrences were noticed by Woo and Marshall working with other materials. It is possible that tests on high-purity material might throw some light on this problem. The results obtained are presented in graphical form in fig. 8.8 and show the same sort of agreement between experimental and theoretical values as were obtained by Woo and Marshall.

It is interesting to note that neither the experimental nor theoretical values of spring-back ratio show any marked alteration from the value for pure bending for direct stresses up to about 15 tsi.

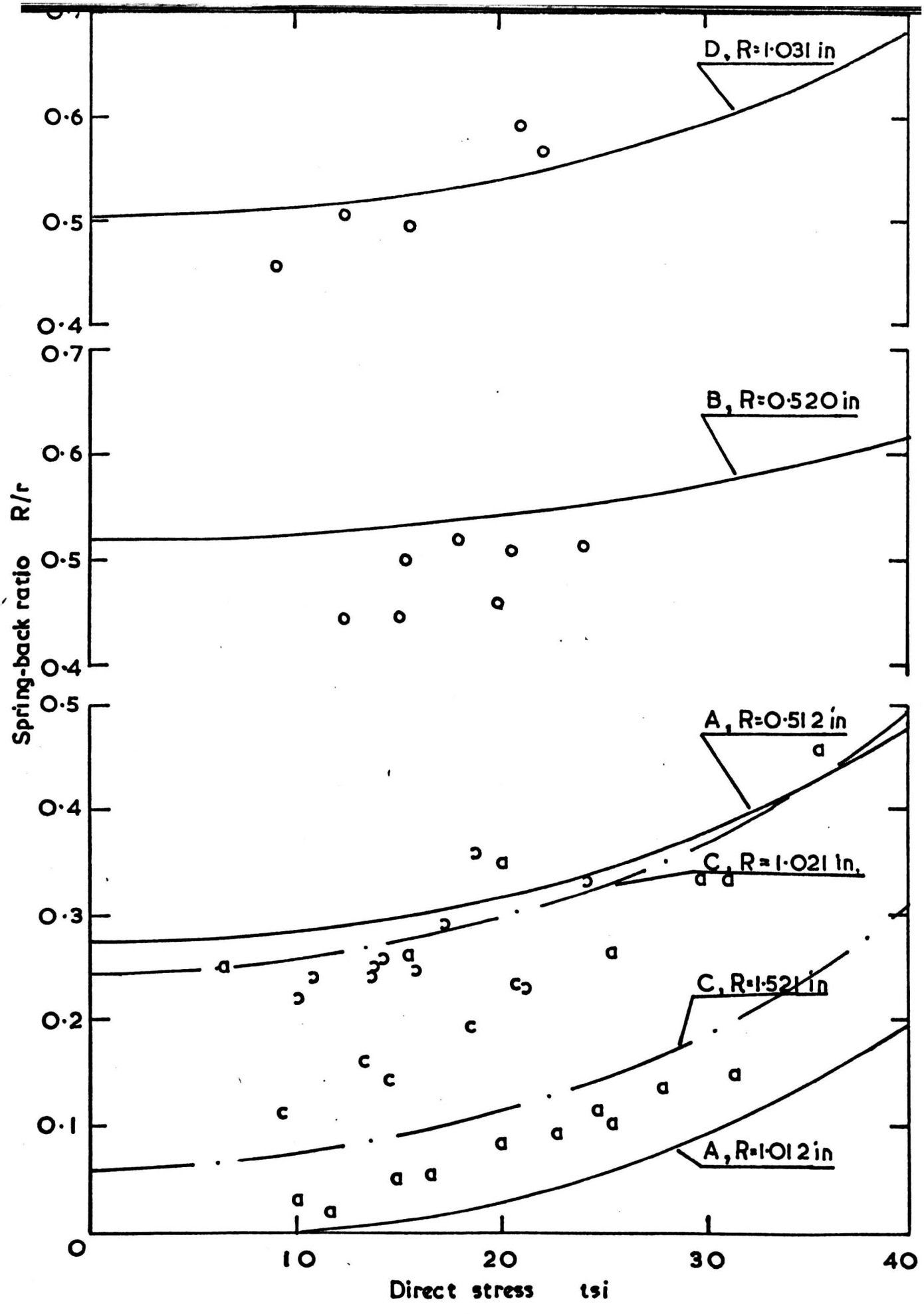

Fig. 8·8 Spring back ratios for materials listed in table 7·1 p.108 subjected to bending under tension.
c-exp results mat: C, R=1·521 in
ɔ—ditto ——— 1·021 in
a—ditto ——— A

8.8. Possible extension of the stretch-forming theory

The argument from this stage develops along the lines that if the winding is such that yielding in compression takes place before the tensile force is applied, a process requiring a quite different theoretical approach, then for the limiting case, at least, where compressive yielding just occurs, both methods of treatment should give results which agree. This would lead one to expect that the results of a strain history analysis might be used to modify the foregoing theory to take account of the different process. If the conditions are not widely different from those specified for the stretch-forming theory, in other words, if the depth of yielding in bending is not great, then a modification of this theory into a three-stage theory in place of the present two-stage theory by empirical means should be sufficiently accurate.

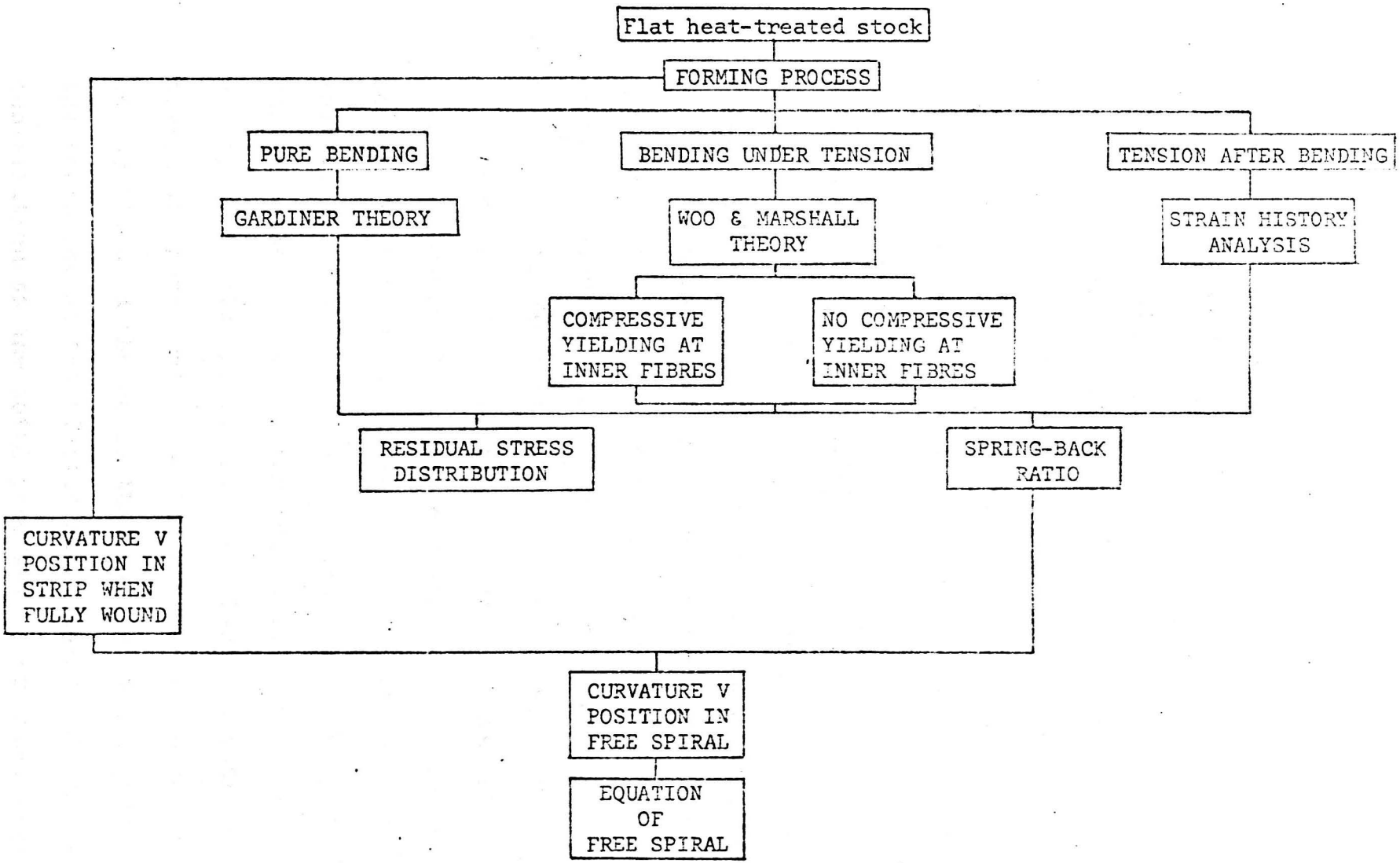

FIG. 8.9 SCHEMATIC DIAGRAM OF THE ANALYSIS OF THE FORMING OF SPIRAL SPRINGS

CHAPTER 9

STRAIN-HISTORY ANALYSIS AND LAYER REMOVAL TECHNIQUE

9.1. Strain-History analysis

9.1.1. Introduction

In this Chapter is offered an outline of procedures which are considered suitable for the examination of spring material deformed plastically and then subjected to reverse loading. Details of similar techniques applied to overstrained torsion bars are to be found in J. B. Whiteside's thesis(R.10).

The stress-strain relationship for a steel depends primarily upon its composition and heat-treatment but is markedly affected by any previous straining in the plastic region. For further straining in the direction of the original strain the elastic limit stress is raised, the extent to which it is raised depending on the degree of overstraining and whether or not the material work-hardens. Obviously, these effects have an important bearing on the manner in which the results of forming springs by bending followed by tension can be predicted. One important factor is the magnitude of the overstrain at any particular position. For large overstrains a bi-linear approximation to the stress-strain curve can be justified on the basis that the 'parabolic' portion at the beginning of the plastic stage makes only a small contribution to the total process. For small degrees of overstrain, however, the situation is quite the reverse and other methods of approximating the shape of

the stress-strain curve must be resorted to.

The method used to study the elastic-plastic process of bending a strip so that it attains a permanent set is a step-by-step analysis of the deformations of successive layers of fibres. The behaviour of any layer during recovery from the (over-) strained state, possibly followed by subsequent reversed loading is predicted from the results of separate tension and compression tests carried out for various degrees of overstrain.(R13)

9.1.2. Theoretical determination of residual stress after bending

When cold forming a spiral spring an elementary length of the strip is bent to a curvature depending upon the arbor diameter and the position of the element in the coiled strip. On relaxation of the bending forces there is some elastic recovery to the final curvature of the element in the free spiral.

Although in the final state the average stress in the strip must be zero and the first moment of the stresses about the neutral axis must be zero, there are stresses in each fibre. Those fibres which have not been subjected to plastic yielding have stresses corresponding to their final strain whilst those which were plastically deformed undergo a reduction in stress during the unloading process. Those fibres near the surface are, in fact, subjected to reverse loading and consequently suffer a reversal of stress.

If the Bauschinger effect is to be taken into account it is essential that the strain history of each

layer be ascertained. If an ideal bi-linear material is considered, the residual stress distribution can be calculated from the geometry of the stress-distribution across the strip when loaded, together with the strain distribution when loaded and unloaded. The analysis can, therefore, follow similar lines to the stretch-forming analysis.

In order to demonstrate strain-history analysis, consider a material possessing the ideal stress-strain curve shown in fig. 9.1. If a strip of this material is bent so as to suffer plastic deformation, the magnitude of the strain at any fibre can be represented by the straight line OS fig. 9.2 and the stress distribution by OPT. Let OR represent the final strain distribution across the half-thickness of the strip, i.e. AR represents the strain in the outside fibres corresponding to the final curvature of the strip. This is, in fact, the quantity we require. The distance SR on fig. 9.2. can be calculated as follows.

AT represents the yield stress Y and, to this scale, the reduction in stress due to unloading is given by the (vertical) distance between the lines OS and OR. (Thus, the residual stress at the outside fibre is given by AT - SR.)

Now, the applied bending moment at maximum curvature is given by the first moment of area OPTA about O together with the corresponding moment for the other half of the strip thickness. The change of stress on relaxation must be such as to balance the applied bending moment. Hence, the moment of area OSR about O together

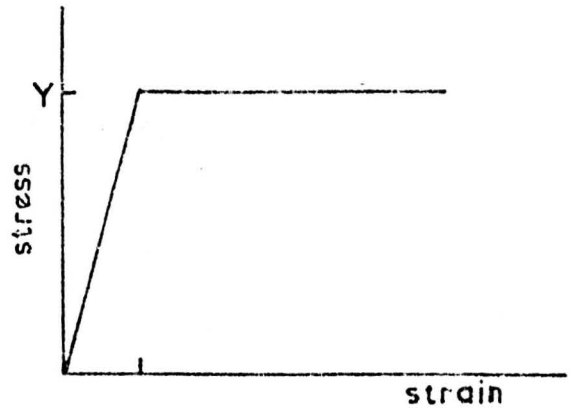

Fig. 9·1 Ideal elastic–perfectly plastic material

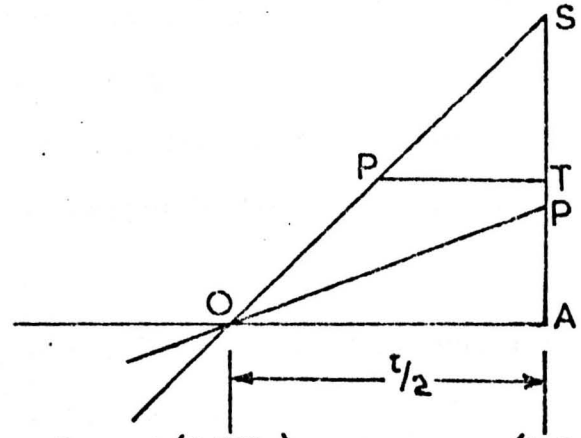

Fig. 9·2 Stress (OPTA) and strain (OSA) distributions across semi-thickness for pure bending of ideal material

Fig. 9·3

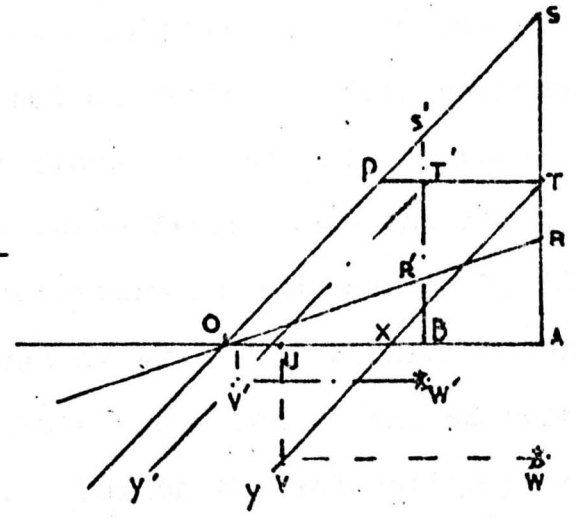

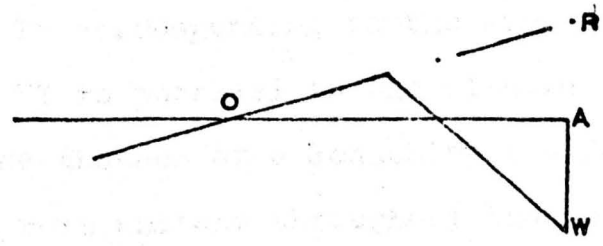

Fig. 9·4 Residual stress distribution for pure bending.

with the corresponding moment for the other half of the strip must also equal the applied bending moment. This condition leads to the equation

$$\frac{SR}{3} \cdot OA^2 = AT \cdot AQ \cdot QO + \frac{AT}{2} \cdot AQ^2 + \frac{AT}{3} \cdot OQ^2$$

whence $$SR = \frac{3}{2} AT - \frac{1}{2} AT \left(\frac{OQ}{OA}\right)^2 \quad .. \quad .. \quad .. \quad .. \quad (9.1)$$

Therefore since the diagram OSTA can be drawn, the line OR can be constructed.

The final strain at the surface fibres is represented by AR and corresponds to a calculated strain

$$e_A = t/2R$$

where R is the final radius of curvature of the strip and t is the strip thickness.

Referring now to fig. 9.3 we can follow the strain-history of fibres when unloading occurs. The procedure for a material exhibiting a Bauschinger effect will follow a similar but slightly modified procedure.

Consider the fibres at the outside edge of the strip. The strain in these fibres when the strip is subjected to maximum curvature is represented by AS and the corresponding stress by AT. The strain in the subsequent relaxed position is given by AR, RS being given by equation 9.1. During the relaxation process the stress at A decreases, the value being given by a position on the line TY corresponding to the strain at any given instant. TY is parallel to the elastic loading line OP in the absence of a Bauschinger effect. If the overstraining were uniform throughout the section then the stress at A would reduce to zero (position x)

and the final strain would be represented by OX. The value would be given, by considering the geometry of fig. 9.3, as

$$e_{AR} = AS \cdot \frac{OX}{OA} \quad .. \quad .. \quad .. \quad .. \quad (9.2)$$

e_{AR} signifying the remaining strain for point A.

Since the strain across the section is not uniform the stress reduces to zero only at certain points. In the case of point A, the stress must correspond to the final strain AR so that the final strain is represented by OU on the stress-strain diagram OPTA where

$$\frac{OU}{OA} = \frac{AR}{AS}$$

that is, the point V on TY. If V is now projected to point W on SA produced then AW (= UV) is, to the scale AT = yield stress, the residual stress at A. Similarly for a fibre at position B, the initial strain is BS' the final strain BR', the unloading line is T'Y'. The final strain is represented on axis OA by OU' where

$$\frac{OU'}{OB} = \frac{BR'}{BS'}$$

and the corresponding point on T'Y' is V' which projected onto S'B produced gives point W'. Again the residual stress at position B is represented by BW'.

In this way the residual stress distribution across the thickness of the strip can be plotted with the result shown in fig. 9.4.

If material which has yielded in compression is subjected to tension, then the unloading and possible subsequent reverse loading of the fibres must be studied in the above manner.

9.2. Experimental determination of residual stress distribution

9.2.1. Method adopted

Of all the methods available for the determination of the residual stress distribution, by far the cheapest and simplest is the layer removal technique. Research has been carried out by Sachs[R26 & 34] and others using various methods of removing layers and measuring the resulting strains. This technique is easily applied but one must be aware of the fact that it is quite easy to introduce stresses into a material whilst carrying out metal removal processes. Disturbances do not penetrate deeply but in the case of thin strip even this might represent a high proportion of the material remaining.

Where the material under investigation possesses an awkward shape, normal machining processes present difficulties. Whilst a spiral itself is not too difficult a shape to deal with in short lengths which can be fixed to a circular adapter for maching purposes, the presence of anti-clastic curvature does present problems. In cases such as this electro-chemical machining or acid etching appear to offer greater potentialities than other techniques. Of these two processes acid etching is the simpler, the main difficulties being the restriction of etching to the surface under investigation and control of the depth of layer removed.

The method adopted by the author is to 'stop off' with special lacquer the surfaces where etching is not required and to mount the section of the spiral

(usually half a coil which approximates to a semicircle) under investigation in the etching rig shown in fig. 9.5. The bath contains 25% nitric acid/water etchant and the specimen is rotated in this etchant for a set time. It has been found that the time required to remove a layer of material 4/1000 in. thick is approximately 10 minutes.

The thickness of layer removed is determined by careful measurement using a micrometer. The radius of curvature before and after layer removal is determined by measuring a chord and its sagitta. The calculation of the stress in the removed layer is then carried out as outlined below.

9.2.2. Calculation of Residual stress

It is assumed that the radius of curvature is at all times much greater than the thickness of the strip and consequently curved-beam theory is an unnecessary complication. Referring to fig. 9.6, if a layer of material of thickness Δ, is removed from a strip of material containing a residual stress system, then two processes are set in motion:

i) since removal of the layer represents removal of an axial internal force, there must result a change in the axial internal stress system in the remaining material. Removal of subsequent layers results in further changes in the internal stress system.

ii) since the layer is situated (and always will be situated) to one side of the centroidal axis of the strip, then a bending moment is associated with the internal force contributed by the layer and removal of

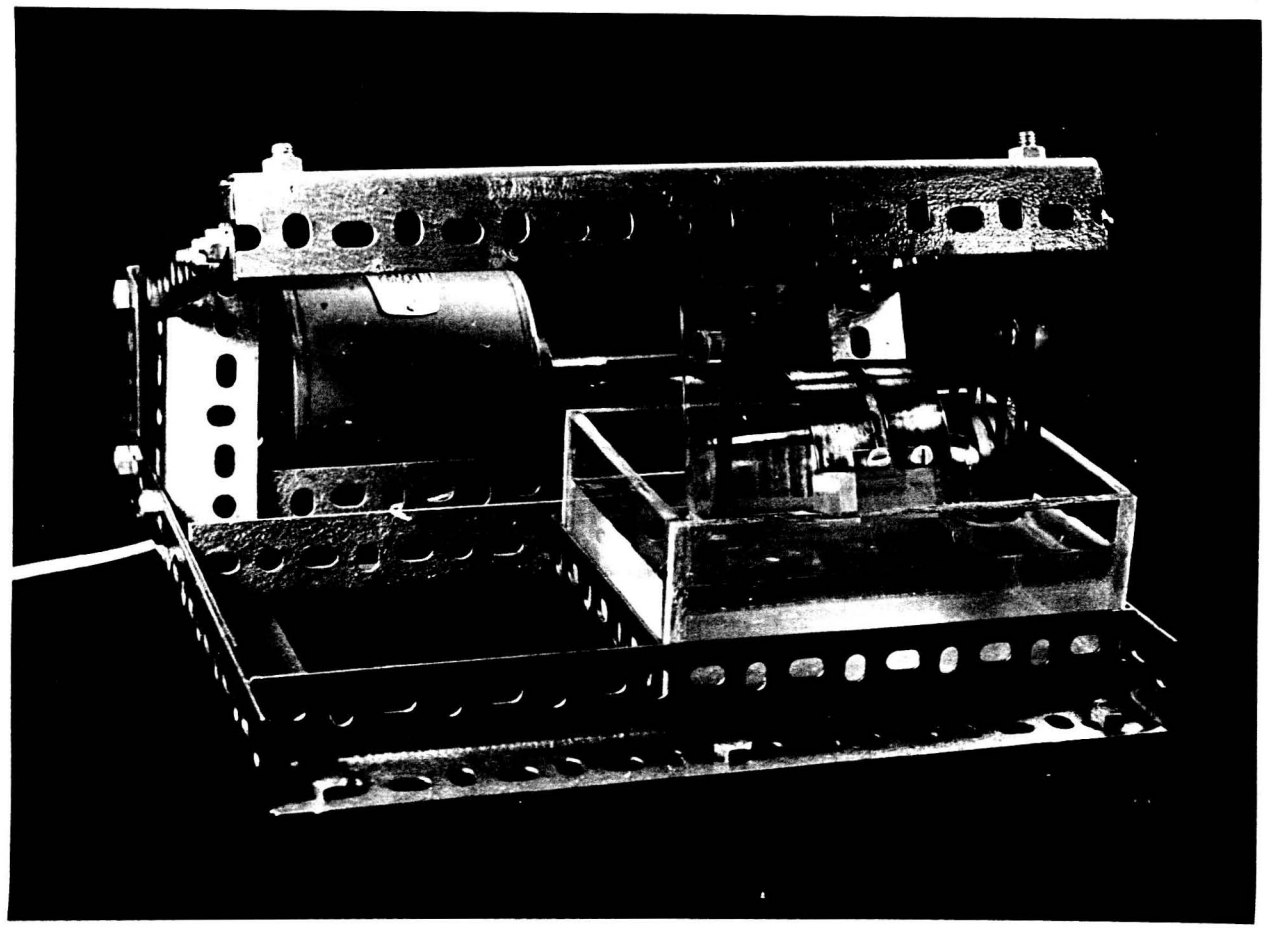

FIG. 9.5. ETCHING RIG FOR LAYER REMOVAL TECHNIQUE

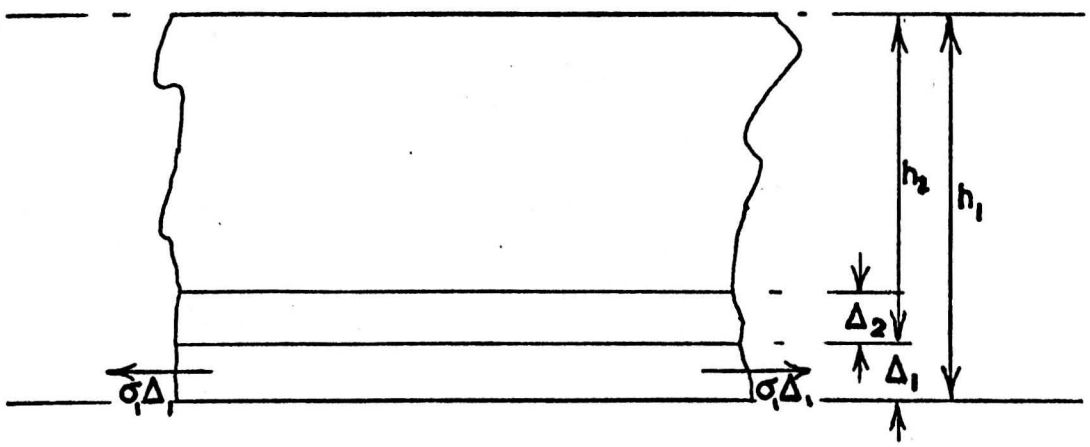

FIG. 9.6. LAYER REMOVAL TECHNIQUE

this moment must result in a change of curvature and consequently a further change in the internal stress system. Clearly, an iterative process is indicated for removal of successive layers in which the apparent mean stress in the layer is calculated from the measured change in curvature. This apparent mean stress is then corrected to allow for the effect of the removal of previous layers. Obviously, no correction is required for the first layer. The procedure is outlined below.

9.2.3. Calculation of stress in removed layer

Let the strip be of unit width.

For first layer let original thickness be t_1, the thickness of layer removed be Δ_1 and the mean stress σ_1. The arrows on fig. 9.6 indicate the direction of a force applied to the remaining material which would produce the same effects as removal of the layer.

The elongation of the strip is given by

$$d(\varepsilon)_1 = \frac{\sigma_1 \Delta_1}{E h_1}$$

and the change of curvature from simple beam theory is:

$$d\left(\frac{1}{r}\right)_1 = \frac{\sigma_1 \Delta_1 (h_1 - \Delta_1) \cdot 12}{2E(h_1 - \Delta_1)^3}$$

$$= \frac{6 \sigma_1 \Delta_1}{E(h_1 - \Delta_1)^2} \quad .. \quad .. \quad .. \quad (9.1)$$

or approximately:

$$d\left(\frac{1}{r}\right)_1 = \frac{\sigma_1 \Delta_1 h_1}{2EI}$$

where I = 2nd moment of area about the neutral axis for the material remaining.

Rearranging eq. 1. the mean stress in the layer removed is given by

$$\sigma_1 = \frac{d(\frac{1}{r})_1 (h_1 - \Delta_1)^2 \cdot E}{6 \Delta_1} \quad .. \quad .. \quad .. \quad (9.2)$$

Now consider the removal of a second layer. Equation 9.2 will give us the apparent stress as:

$$\sigma_2' = \frac{d(\frac{1}{r})_2 (h_2 - \Delta_2)^2 \cdot E}{6 \Delta_2}$$

where $h_2 = h_1 - \Delta_1$.

This is now corrected to allow for changes in the direct and bending stresses caused by removal of layer 1.

Direct stress due to removal of first layer is:

$$\sigma_{d_1} = \frac{\sigma_1 \Delta_1}{h_1} \quad .. \quad .. \quad .. \quad .. \quad (9.3)$$

Bending stress due to removal of first layer is:

$$\sigma_{b_1} = \frac{\sigma_1 \Delta_1}{h_1^3} \cdot \frac{h_1}{2} \cdot \frac{h_1}{2} \cdot 12$$

$$= 3 \frac{\sigma_1 \Delta_1}{h_1} \quad .. \quad .. \quad .. \quad .. \quad (9.4)$$

The true mean stress in the second layer is now given by:

$$\sigma_2 = \sigma_2' - \sigma_{d_1} - \sigma_{b_1} \quad .. \quad .. \quad .. \quad (9.5)$$

For the third layer the apparent stress is given by application of equation 9.1 using the appropriate values for the change of curvature, the thickness of material and the depth of layer removed. This is then corrected for changes in stress due to removal of layers 1 and 2.

Direct stress correction due to removal of previous layers is:

$$\sigma_{d_2} = \frac{\sigma_1 \Delta_1}{h_1} + \frac{\sigma_2 \Delta_2}{h_2} = \sigma_{d_1} + \frac{\sigma_2 \Delta_2}{h_2}$$

and the bending stress correction is:

$$\sigma_{b_2} = 3\frac{\sigma_1 \Delta_1}{h_1} + 3\frac{\sigma_2 \Delta_2}{h_2} = \sigma_{b_1} + 3\frac{\sigma_2 \Delta_2}{h_2}$$

and, then

$$\sigma_3 = \sigma_3' - \sigma_{d_2} - \sigma_{b_2}$$

It will be obvious how succeeding layers are dealt with.

9.2.4. Results of layer removal tests

In spite of the lack of knowledge of the true history of the springs supplied for investigation, it was decided to select some of these for layer removal tests.

The results now reported refer to spring T.S.1 for which results of other tests have been reported earlier in this thesis. In these tests half-coils were cut and etched from one side only. (It is suggested that in the full scale tests the half-coils are carefully slit along the length of the strip and then one half subjected to removal of layers from the outside whilst the other is subjected to removal of layers from the inside.) The mean radius of curvature of the remaining material is shown plotted against the depth of material

removed in figs. 9.7 and 9.8 in which samples 'A' and 'B' are successive half-coils subjected to layer removal from the outside and samples 'C' and 'D' are different successive half-coils subjected to layer removal from the inside. The curvature curves are also plotted in these figures.

The stresses in the removed layers were calculated in accordance with the procedure established in article 9.2.3 and are presented in fig. 9.9.

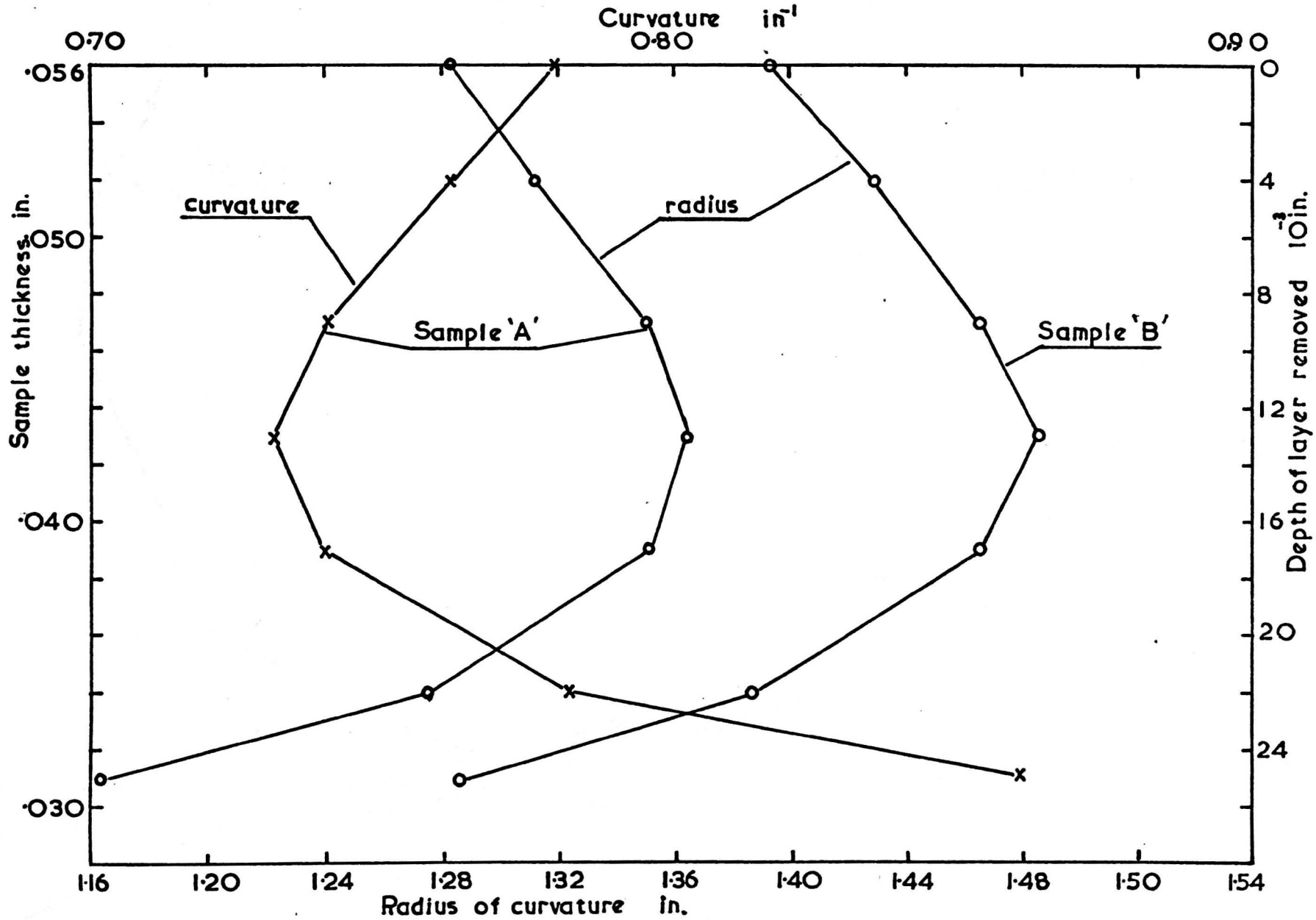

Fig. 9·7 Layer removal from convex surface.

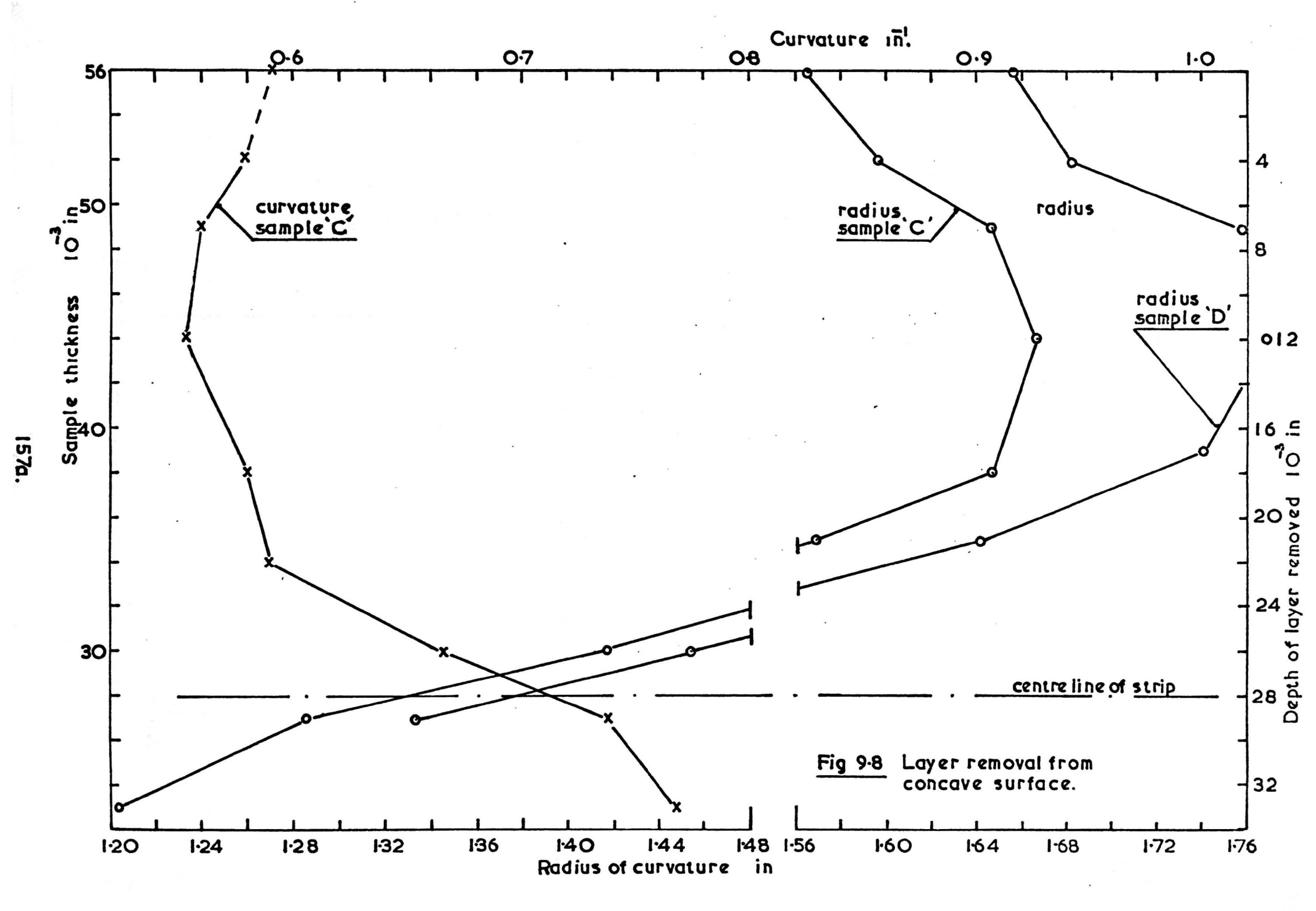

Fig 9·8 Layer removal from concave surface.

157a.

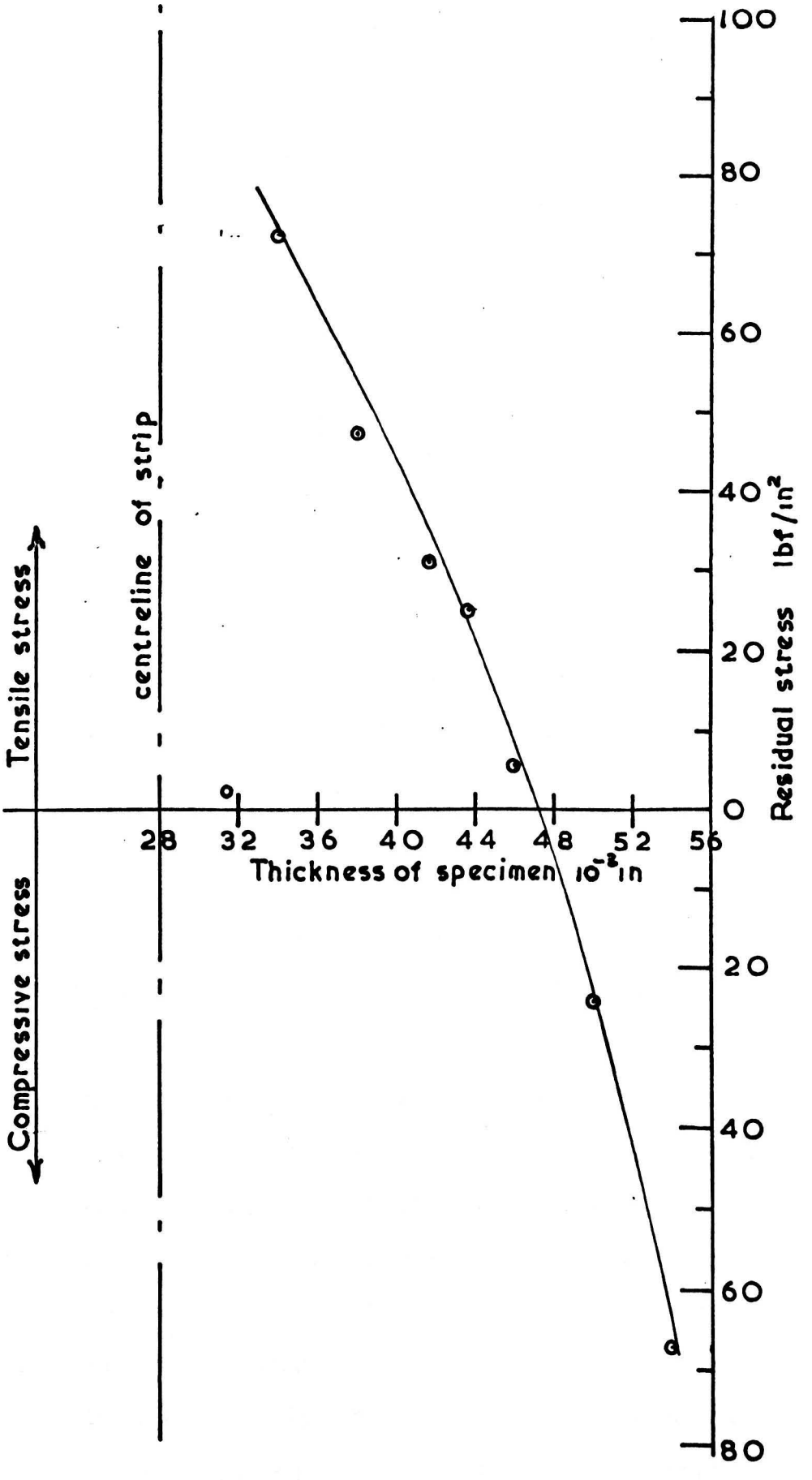

Fig. 9.9 Residual stress distribution sample 'A'

CHAPTER 10

REVIEW OF TECHNIQUES AND RESULTS

10.1. Introduction

The investigation reported in this thesis has fallen into a number of quite separate but supplementary phases. These, it will be remembered, arose out of the suggestion that the conventional theory applied to the spiral (clock-type) spring has certain undesirable limitations particularly when the spring possesses a non-linear M - ϕ characteristic.

The theory presented requires a knowledge of the mathematical form of the spring when it is allowed to attain its free state. As a result of this, techniques of examining spiral forms were evolved resulting in, finally, a simple technique which will allow the equation of the (assumed logarithmic) spiral to be determined in a matter of minutes. This technique will be described in detail later in this chapter. Thus far then, two phases have been described, the call for and the presentation of a new look at the basic theory, and evolution of a method of examining existing springs.

The third phase embodies the work necessary to validate the first two phases and this involves testing the theory and techniques against measured results. In order to carry out these tests a reliable testing machine has been designed. This machine has spent much of its life being used by an industrial concern for routine testing of this type of spring. The machine described in Chapter 4 has now been modified so that autographic recording may be used.

In phase four of the work reasons for the mathematical form were sought and, in particular, methods of predicting the spiral equation were examined. The scope of this phase has been reduced to a manageable task by restricting the analysis to a simple idealised material. This has led to the drawing up of charts to be described later from which it is possible to predict the value of 'b' in the spiral equation $r = r_o e^{b\theta}$. In this phase, also, the residual stresses induced in the material were examined theoretically by the use of a computer programme, and experimentally by applying a layer removal technique.

Finally, suggestions are put forward for supplementing the present work by examining in detail the mechanics of the formation of springs of this type by plastic bending followed by tension.

10.2. Use of the theory

10.2.1. Method

The theory of Chapter 2 has been fully supported in the tests reported in this thesis, and has given a far better prediction of the $M - \phi$ characteristics than has the conventional theory. But it must be added in support of the conventional theory that the cases chosen for examination were selected for this reason. There are many instances in which the conventional theory gives good results. Furthermore, it is simple in its application.

The theory advanced in this thesis is most easily applied by measuring the required areas. Recapitulating, it will be recalled that the technique in applying

the theory is to obtain curvature curves plotted against strip length for the wound, un-wound and free spiral conditions. From these curves are plotted the curvature-change curves and the area required is determined from these last mentioned curves. If the method is to be adopted it is a simple matter to draw up standard curves for the fully-wound and run-down conditions. It will be possible also to accumulate data so that standard curves for the free spiral are available for springs manufactured by a particular firm, i.e. the values of 'b' associated with an established technique of forming.

10.3. Determination of spiral form

10.3.1. Rapid determination of 'b'

If the free spiral is free from gross distortions then the outside and inside 'diameters' may be used to ascertain the value of 'b'. The inner and outer 'diameters' should be measured through the origin of the spiral, but if it is remembered that when the ruler is laid across the centre, the coils 'spring' from the ruler measuring edge at equal angles, no serious error should be incurred. The only restriction in the theory below is that there must be the same number of coils on either side of the origin. This may necessitate discounting the outside coil on one side.

For n coils on either side we can write

$$r_n = r_o e^{2n\pi b}$$

$$r_m = r_o' e^{2n\pi b}$$

$$r_n + r_m \text{ (= outer 'diameter')} = (r_o + r_o')e^{2n\pi b}$$

$$\therefore \quad \frac{\text{outer 'diameter'}}{\text{inner 'diameter'}} = \frac{r_n + r_m}{r_o + r_o'} = e^{2n\pi b}$$

$$\text{and} \quad \frac{\ln \dfrac{r_n + r_m}{r_o + r_o'}}{2n\pi} = b$$

in which n = no. of coils

r_o = radius at $\theta = 0$

r_o' = radius at $\theta = \pi$

r_n = radius of n^{th} coil on side of r_o

r_m = radius of n^{th} coil on side of r_o'

10.3.2. <u>K_o - s chart (fig. 10.1)</u>

It has been shown that the curvature of the free spiral is given by

$$K_o = \frac{1}{bs + r_o}$$

$$\text{whence} \quad r_o K_o = \frac{1}{bs/r_o + 1} \qquad .. \quad .. \quad .. \quad .. \quad (10.1)$$

and approximately $K_o = 1/r$, the radius on the free spiral at distance s from the start of the spiral. Further r_o is approximately equal to the arbor radius. Equation 10.1 can be re-written as

$$\frac{r}{r_o} = b\frac{s}{r_o} + 1 \qquad .. \quad .. \quad .. \quad (10.2)$$

CURVATURE—POSITION CHART

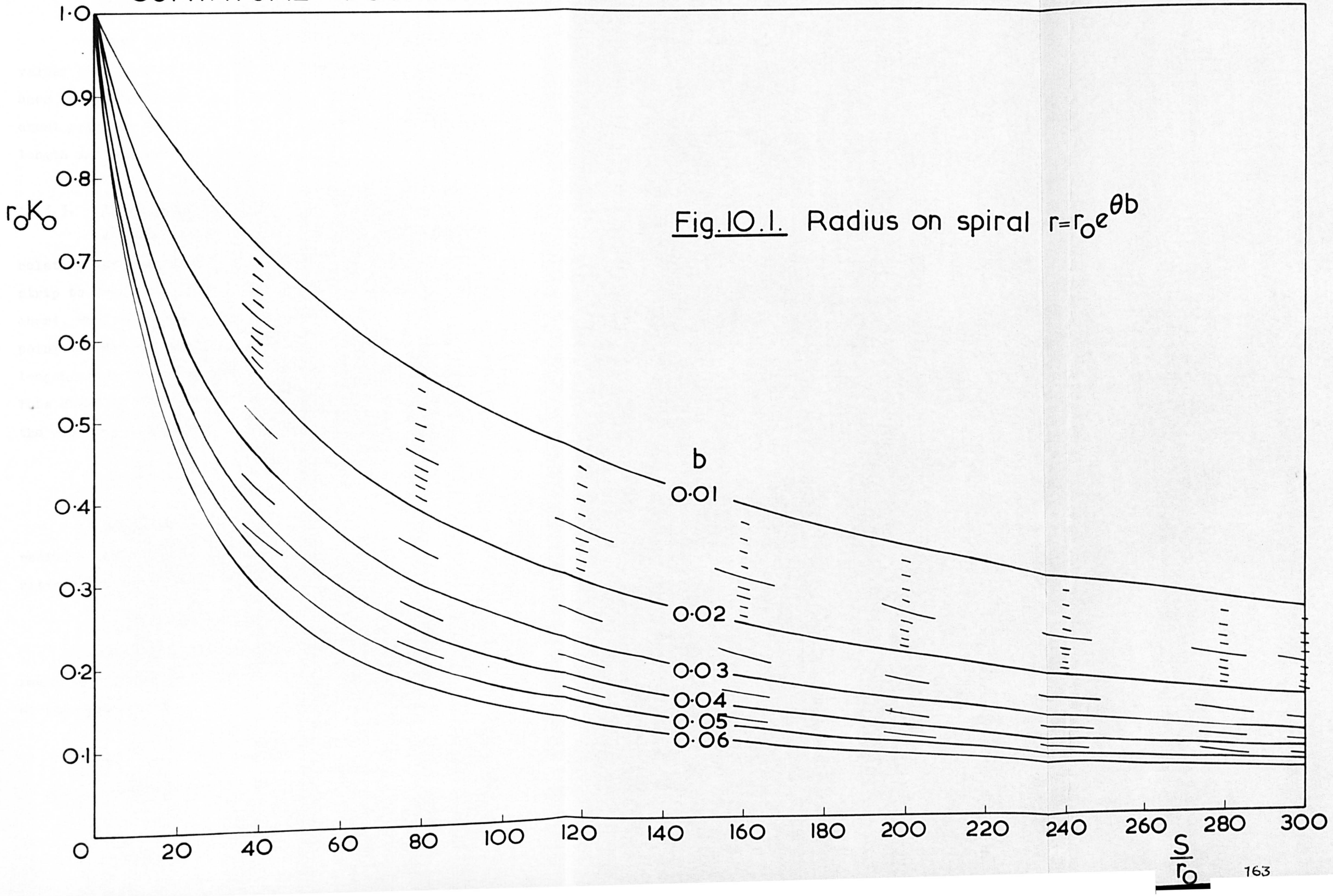

Fig.10.1. Radius on spiral $r=r_oe^{\theta b}$

This relationship has been plotted for various values of b in fig. 10.1 and the resulting chart may be used to construct the K_o - s curve. Alternatively, the chart provides for the determination of b from the strip length and the arbor diameter.

10.3.3. Fully wound condition

A chart similar to fig. 10.1 has been prepared relating the radius of a point on the centreline of the strip to its distance from the start of the strip. This chart, fig. 10.2, shows the ratio of the radius at the point to that of the arbor plotted against the strip length/arbor ratio for various thickness ratios (t/r_o). This chart is based on the relationship for curvature in the wound-up condition; equation 2.12.

$$K_2 = \frac{1}{\sqrt{(r_o + t/2)^2 + st/\pi}}$$

But $\frac{1}{K_2}$ is approximately equal to the minimum radius R (this is the same as the 'R' in the spring back ratio R/r), therefore,

$$R^2 = (r_o + t/2)^2 + st/\pi$$

and either approximately if r_o is the arbor radius or exactly if r_o is the radius of the centre-line of the strip at the start of the spring:

$$R^2 = r_o^2 + st/\pi$$

whence $$(R/r_o)^2 = 1 + s/r_o \cdot t/r_o \cdot 1/\pi \quad .. \quad (10.3)$$

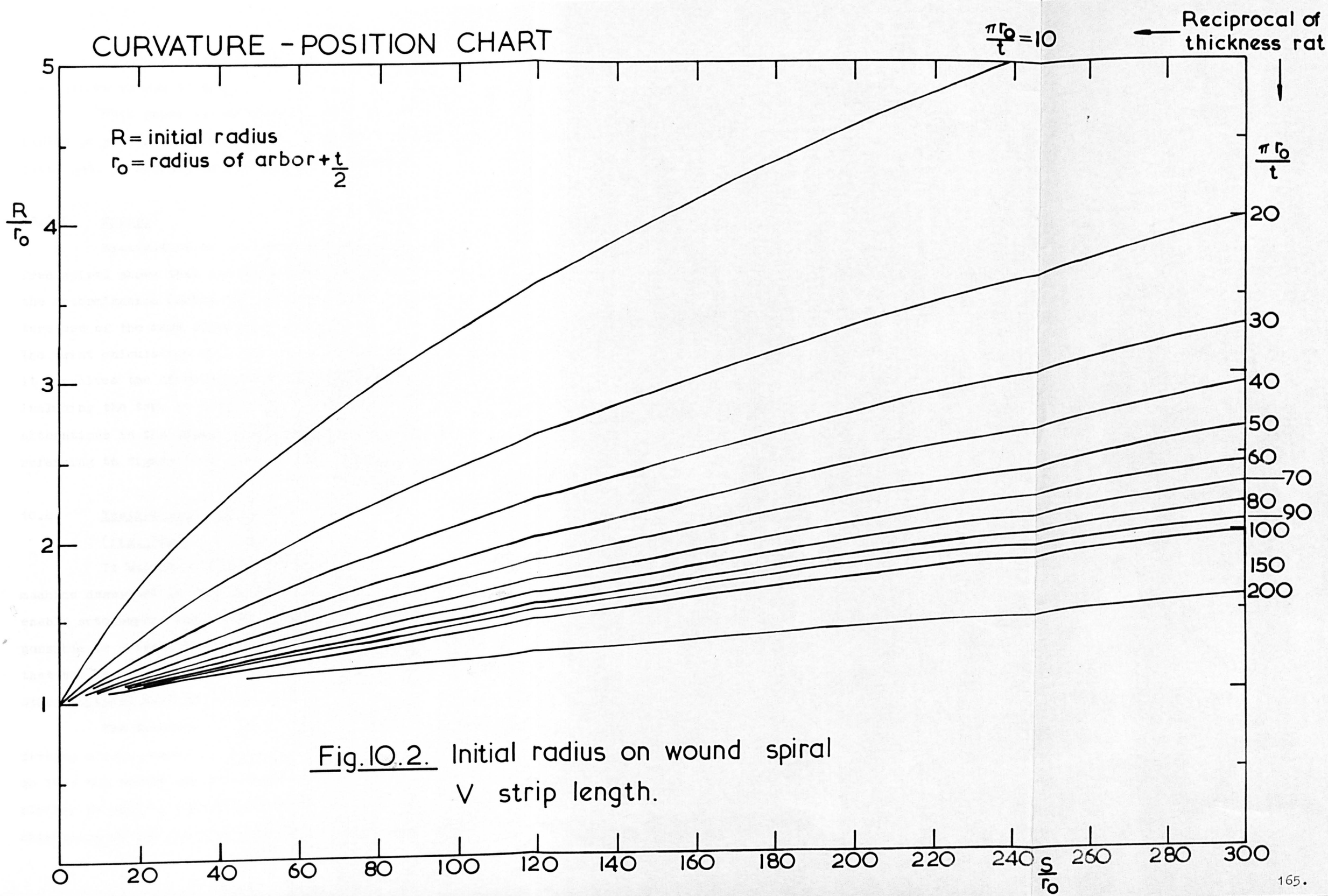

Fig.10.2. Initial radius on wound spiral V strip length.

Equation 10.3 has been used to plot figure 10.2 for various values of t/r_o.

This chart may be used to determine the initial radius of points along the strip in the fully wound condition, and, of course, to plot the K_2 - s curve.

10.3.4. Errors

Examination of the equations concerned with the free spiral shows that the percentage error incurred in the determination (using 'b') of strip length, and curvature are of the same order as the percentage error in 'b'. The twist calculation will tend to minimise errors because it involves the difference between two quantities each including the term in error ($+K_o$). The effect on K_o for alterations in the value of 'b' are best visualised by referring to figure 10.1.

10.4. Testing using autographic recording (fig. 10.3)

It was mentioned earlier that the testing machine described in Chapter 4 has now been modified to enable autographic recordings to be made. It is also possible to drive the turntable by an electric motor so that the testing operation is now comparable with most other physical testing techniques.

The autographic recording has been achieved by fitting strain gauges to the torsion bar and re-calibrating so that the torque can be plotted directly. An X - Y plotter is used to record the results and makes use of an attenuator on the input to each axis so that the torque

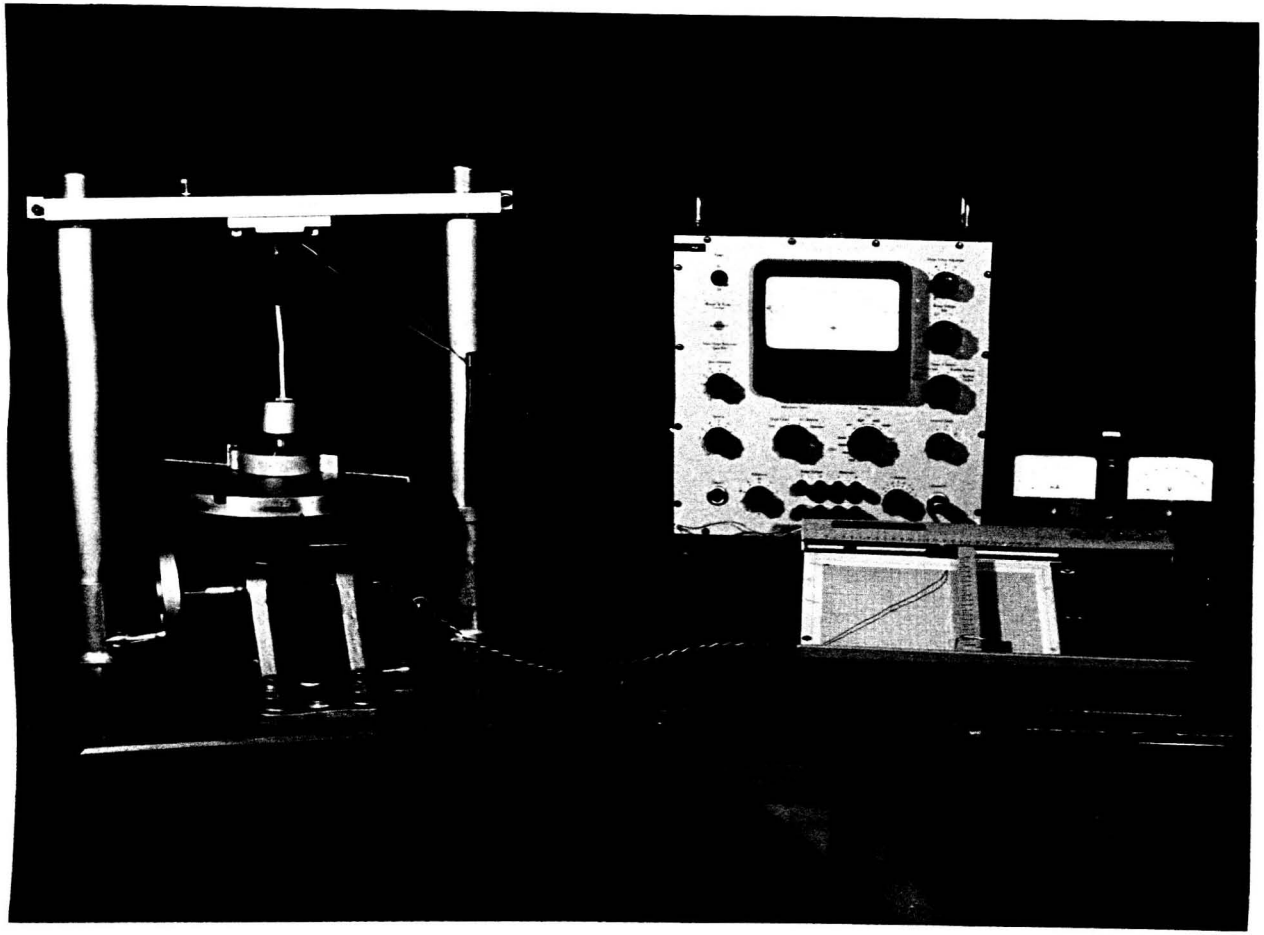

FIG. 10.3. TESTING MACHINE WITH AUTOGRAPHIC RECORDING

and rotation scales can be adjusted to suit the spring in use. The rotation is monitored by driving a 10-turn helipot through reduction gearing. The potentiometer has a linear resistance characteristic so that its output is directly related to the relative rotation of the barrel and arbor.

This recording arrangement is quite sensitive; so much so that it is able to monitor the effect of coil bundling and instability of the coils.

The machine is now being copied by an industrial concern for their own use and should be capable of being modified for use in a project designed to examine tensioning of a strip after bending.

Figs. 10.4, 10.5 and 10.6 are copies of autographic recordings for the springs whose details are noted on the recordings.

10.5. Use of charts and tables

10.5.1. 'b' charts

In fig. 10.1 we see plotted, for various values of 'b', the dimensionless term r_oK_o (arbor radius x curvature at a point on the free spiral) against the dimensionless term s/r_o (s = distance of the point from the start of the spiral). This information is presented in a slightly different manner in fig. 10.7.

Basically the chart is for the spiral equation

$$r = r_o e^{b\theta}$$

If θ is made to correspond to a whole number of turns then

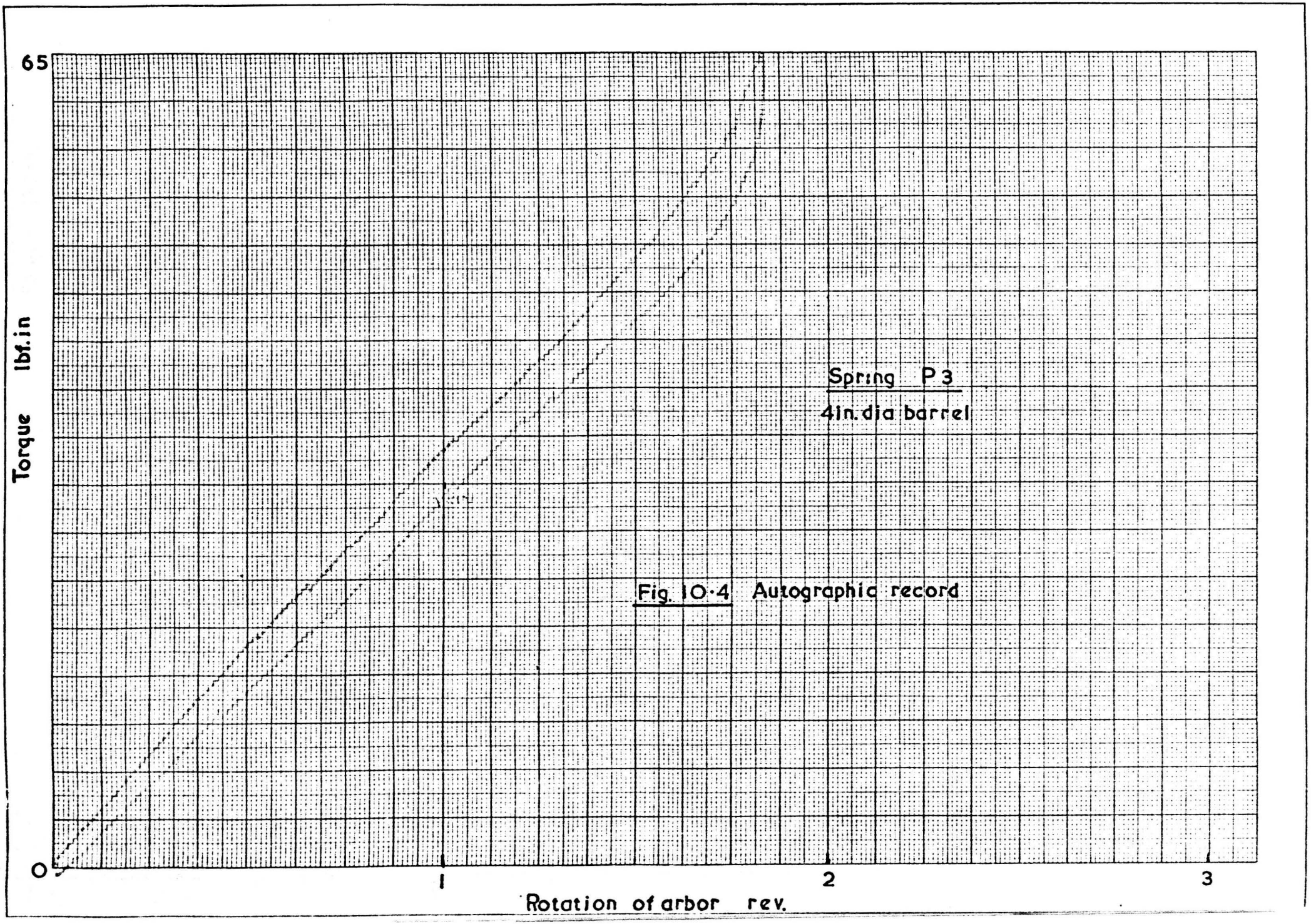

Fig. 10·4 Autographic record

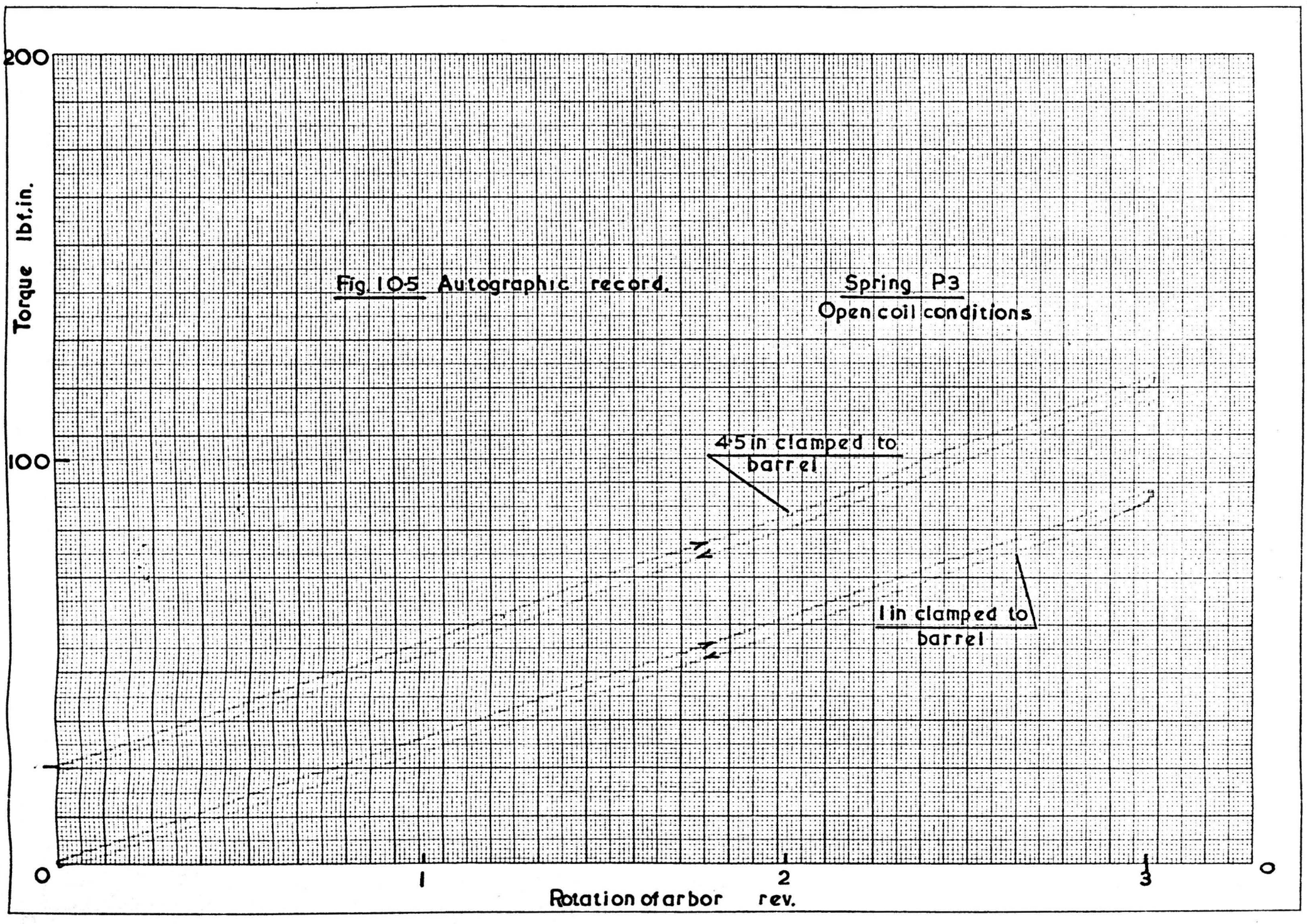
200
100
0
Torque lbf.in.
Fig. 105 Autographic record.
Spring P3
Open coil conditions
4·5 in clamped to barrel
1 in clamped to barrel
0
1
2
3
Rotation of arbor rev.

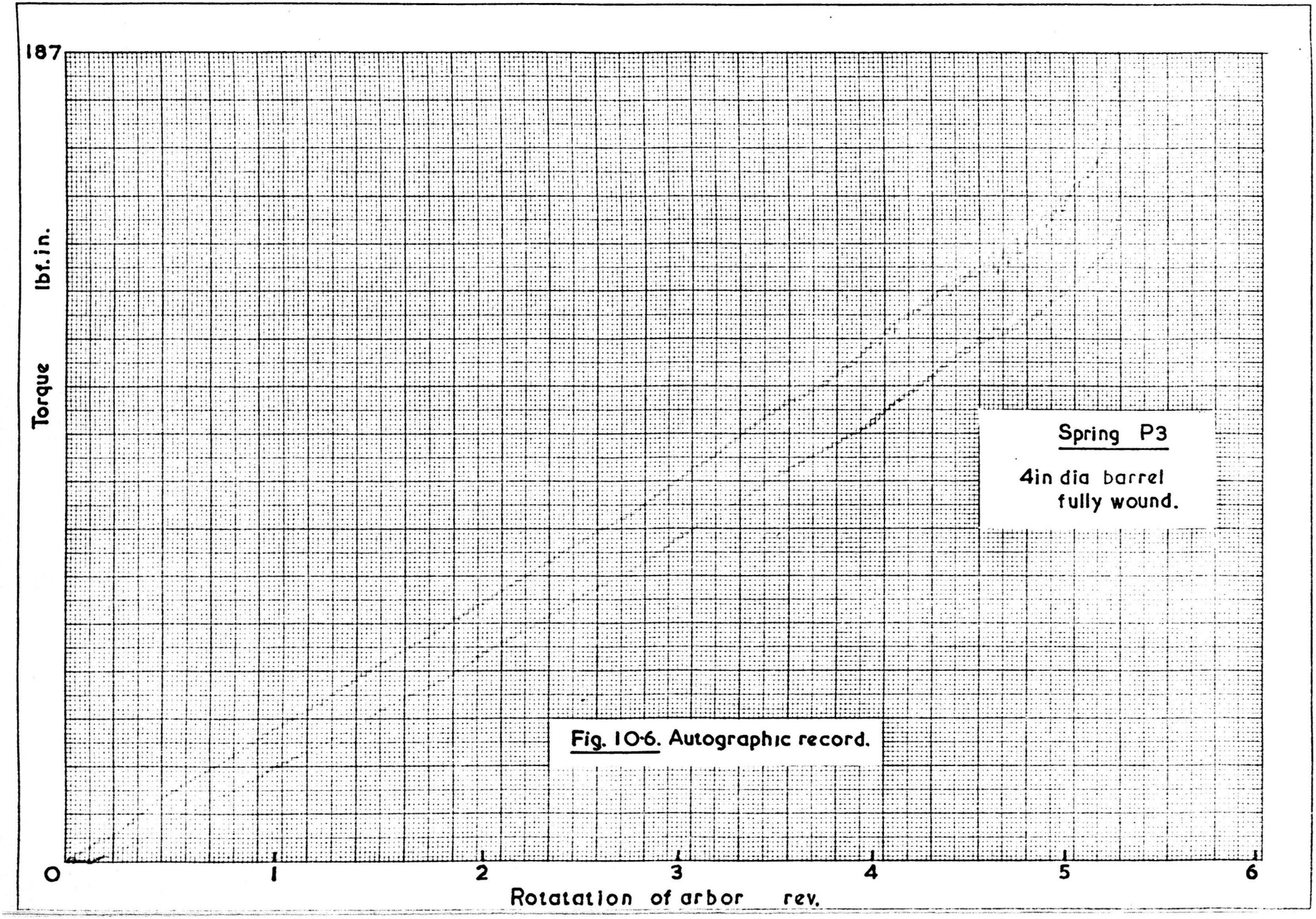

Fig. 10-6. Autographic record.

RADIUS CHART

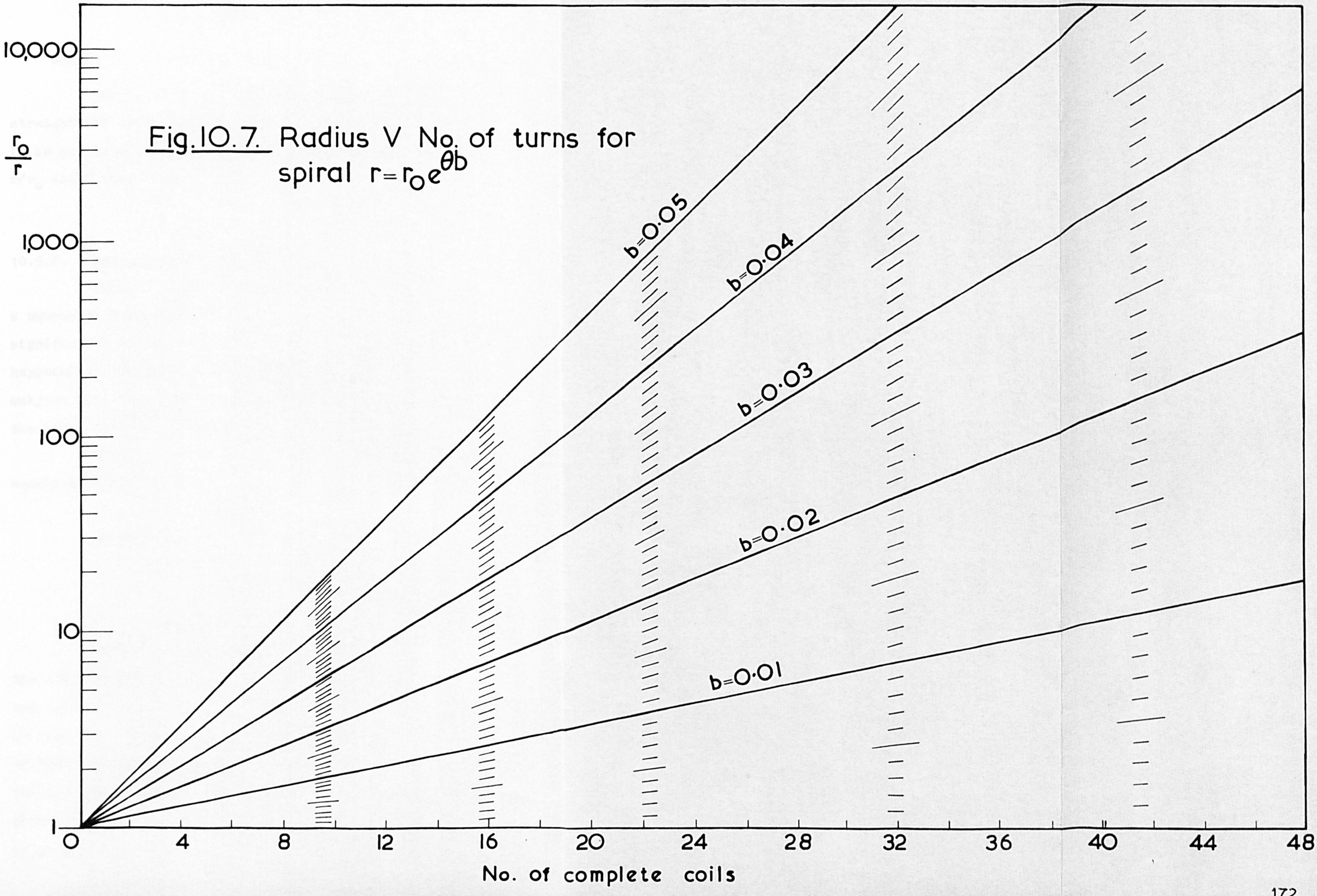

Fig. 10.7. Radius V No. of turns for spiral $r = r_o e^{\theta b}$

$$r = r_o e^{2\pi N b}$$

whence $\ln r/r_o = 2\pi N b$

and this is the expression which gives the straight 'b' lines when $\ln(r/r_o)$ is plotted against N. It is possible to affix scales for $r_o K_o$ and s/r_o to the r/r_o and N axes respectively.

10.5.2. Example on spring T.S.1

This is a spring which has been the subject of a number of tests reported in this thesis. There is no significance to be attached to this fact, it merely happened by chance that this particular spring was a subject of nearly every exercise carried out, including the layer removal technique.

Referring back, it will be seen that the equation of the spiral was:

$$r = 0.81e^{0.02539}$$

and the data for the spring were:

thickness t : 0.056 in.

arbor radius : 0.625 in.

length of strip : 82.5 in.

We will now use this data in conjunction with the charts, figs. 10.2, 10.7 and 8.1. By determining the initial radius (wound-up) of a point (given value of s) from fig. 10.7 (or 10.1) we can determine the value of RY/Et and look up the spring-back ratio R/r on fig. 8.1 for any given back tension (P/Y). Then using a step-by-step method we could construct the free-spiral form and, if we saw fit, analyse it.

Let us consider a point at the outside end of the strip then, noting that

$$t/r_o = \pi/35 \quad \text{and} \quad L/r_o = 132$$

then from fig. 10.2

$$R/r_o = 2.35$$

The value of RY/Et is for E/Y = 168.6:

$$RY/Et = \frac{2.35 \cdot 0.625}{0.056 \cdot 168.6} = 0.156.$$

From fig. 8.1 the spring-back ratio is

$$R/r = 0.55$$

$$\frac{r_o}{r} = \frac{R}{r} \Big/ \frac{R}{r_o} = 0.218$$

Now referring back to fig. 10.7 for

$r_o K_o = 0.218$ and $s/r_o = L/r_o = 132$

we find that

$$b = 0.027.$$

This value is within 10% of that obtained by experiment.

10.5.3. Investigation of spring A7

(refer to article 6.2)

The data for this spring were:

strip thickness : $t = 0.038$ in.

strip length : $L = 300$ in.

arbor radius : $r_o = 1.375$ in.

spiral constant : $b = 0.0183$

Measuring the photograph for 15 coils on either side of the origin, the inner and outer 'diameters' are, at one position, 1.05 in. and 6.75 in. respectively. Then applying equation 10.4, the value of 'b' is given by:-

$$b = \frac{\ln 6.43}{30\pi} = 0.0197$$

This operation takes five minutes at the most and gives a result within 10% of the value obtained as a result of careful measurement.

The values required for use with the charts are:

$$\frac{t}{r_o} = \frac{\pi}{86.8} \quad \text{and} \quad \frac{s}{r_o} = 140 \quad \text{for convenience.}$$

From the chart fig. 10.2

$$\frac{R}{r_o} = 1.62$$

giving $\frac{RY}{Et} = 0.349.$

From the spring-back chart fig. 8.1 for low values of P/Y which will give compressive yielding

$$\frac{R}{r} \simeq 0.2$$

and $$\frac{r_o}{r} = \frac{R}{r} \Big/ \frac{R}{r_o} = 0.124$$

which value on chart fig. 10.1 gives

$$b = 0.506.$$

Obviously, the spring has been formed under quite different conditions.

The value of b = 0.0183 requires that the value of

$$\frac{r}{r_o} = 0.3 \quad \text{be given and consequently that}$$

$$\frac{R}{r} = 0.486$$

which could be obtained (fig. 8.1) if the strip is bent under a back tension producing approximately 63% of the yield stress. It is quite possible that a similar residual stress pattern might be produced by tensioning after bending.

Had we known that this spring had been formed under tension, we could now examine the theoretical residual stress distribution throughout the length, the pattern would be in accordance with fig. 8.2.

CHAPTER 11

CONCLUSIONS AND RECOMMENDATIONS

11.1. Regarding application of the theory

The theory of chapter 2 has been substantiated and the various techniques tested and compared in those instances when more than one technique is available.

Whilst the theory is easily applied to a known design, i.e. when the choice of arbor and barrel sizes is restricted and the strip thickness is known, it is not an easy task to apply the method of analysis described in this thesis to the design of a spring. A trial and error method could be established using plots on transparent paper of the three curvature curves (K_1, K_2 and K_o) which would allow rapid plotting of the two change-of-curvature curves and from these the Moment twist curves. Obviously, this ultimately reduces the design operation to a process of selection rather than a process of calculation.

The theory examined has been shown to produce a far better approximation to the actual $M - \phi$ characteristic than does the conventional (linear) theory, particularly for those cases in which the $M - \phi$ characteristic is inherently non-linear.

Fig. 6.2 is reproduced in Fig. 11.1 with superimposed on it the design curve proposed by the Associated Spring Corporation (R35) applied to the spring A7 using the arbor and barrel sizes recorded. Clearly in this instance the theory examined in this thesis gives closer agreement with the experimental results than does the A.S.C. curve.

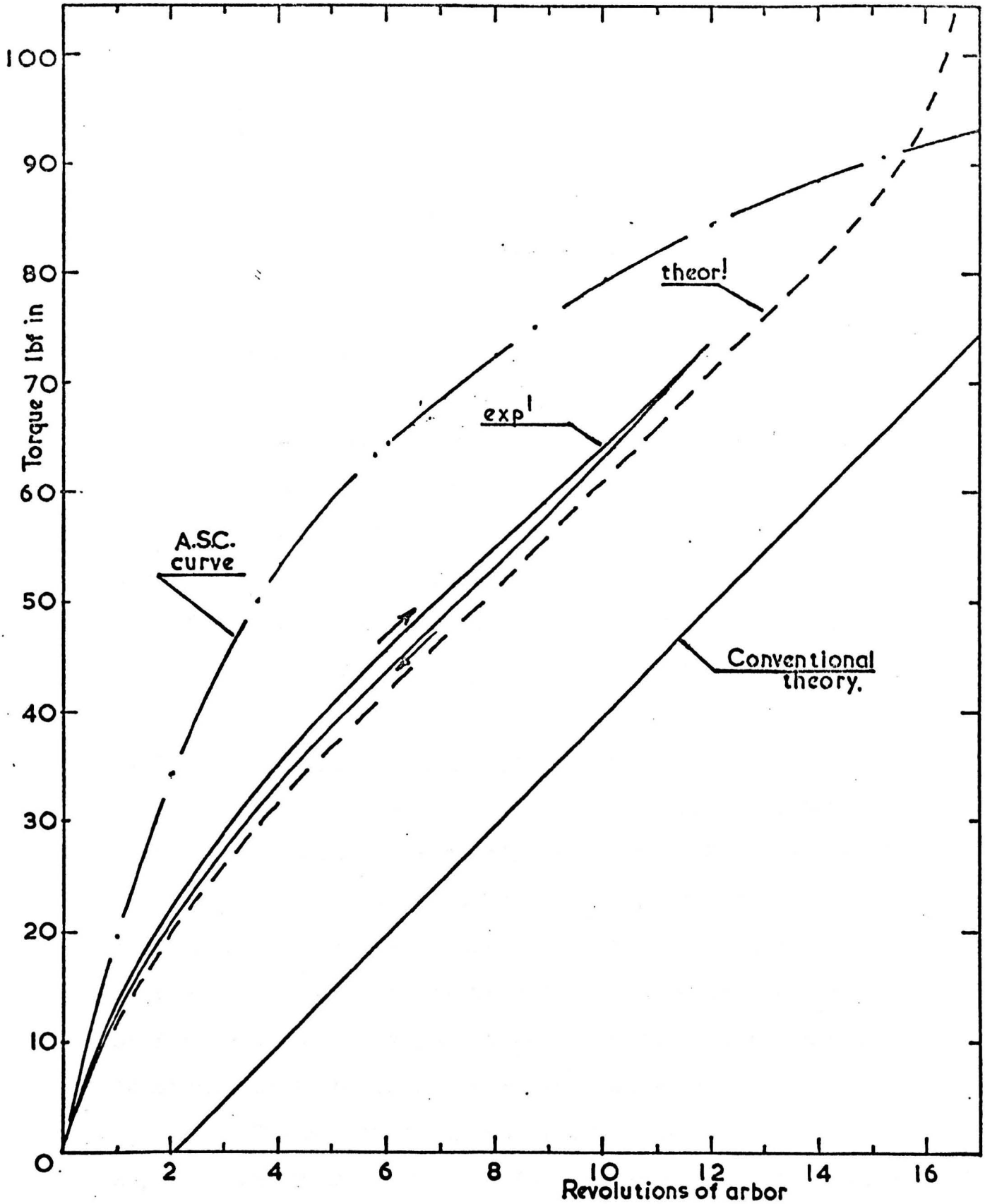

Fig.11·1. Spring A4. 7in dia barrel
$1\frac{2}{8}$ dia arbor

It appears that the proposals in this thesis could serve most usefully in predicting the $M - \phi$ characteristic after the spring dimensions have been decided. This could save the time and expense involved in winding a prototype spring and then testing it.

11.2. Regarding testing techniques

The autographic recording and manual testing techniques using the author's testing machine have been well tried and found to be satisfactory. The method of testing used by some industrial concerns leaves much to be desired; in particular it has been demonstrated that friction in the machine can easily be excluded from the torque measured at the arbor (or barrel).

11.3. Regarding supplementary work

At the outset it was thought that the clock-spring problem could be neatly wound up. However, as in most research projects, more work is involved in this task than is apparent in the early stages. It was necessary to restrict the investigation to two conditions of forming, namely by pure bending and by bending under tension, and to a simple idealised material.

Further work is necessary to establish experimentally and theoretically the free form of springs manufactured by winding with little or no back-tension followed by a tightening operation. In this case a comprehensive testing programme will be necessary to ascertain the behaviour of the material during unloading and reverse loading from plastic overstraining.

J. B. Whiteside's thesis [R.10] should prove helpful in establishing the necessary techniques which have been broadly outlined in Chapter 9 of this thesis.

Further study of the behaviour of the spiral spring during the winding-up and running-down processes might prove useful, particularly if coupled with the examination of the curvature-change curves as indicated in article 6.8, page 95.

11.4. Closure

The work described in this thesis has, it is hoped, contributed to the knowledge of spiral springs in that it has established that such springs are, approximately at least, of logarithmic form. New methods of examination and testing have been evolved and tried, giving satisfactory results, and new work has been proposed which, together with the work reported here, should give a complete understanding of the mechanics of the spring forming process for this particular type of spring however performed.

APPENDIX A1

A1.1 DERIVATION OF EQUATION 1.1

In figure A1.1 are depicted the forces and moments considered to be acting on a spiral spring. M_o is the external moment applied to the arbor, and M_1 is the external moment required to fix the direction of the strip at its outer end in the clamped condition. X and Y are external forces applied at the outer end of the strip to maintain its location. The distances c and d are self-explanatory.

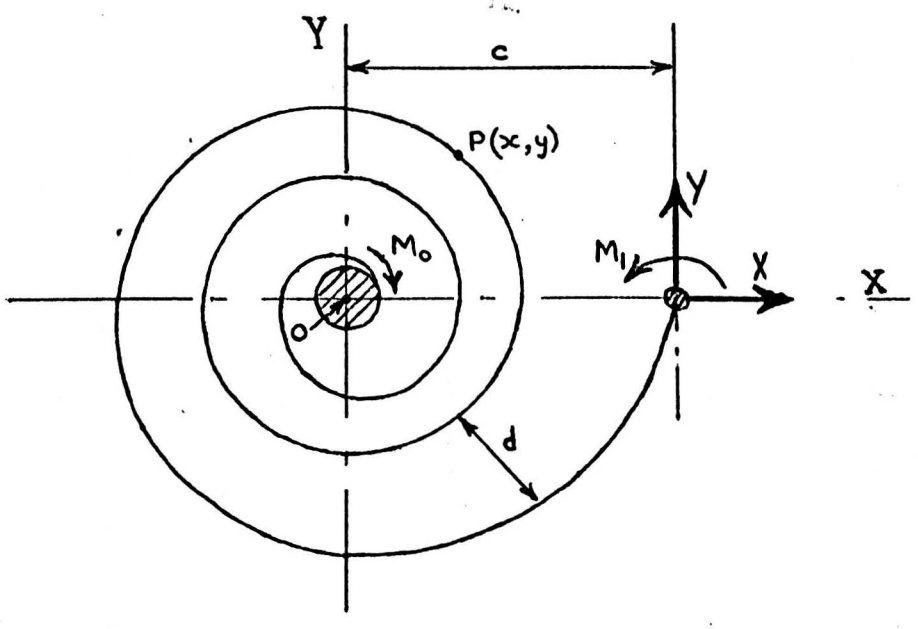

Fig A1.1. External forces and moments acting on a spiral spring.

A1.1.1 Case 1. Theoretical M-ϕ relationship for clamped outer end

If there is no friction between adjacent coils, equating of external moments gives :-

$$M_o = M_1 + Yc \qquad \text{——————(1.1)}$$

and taking M_1 positive as shown, the bending moment, M, at a point P (x,y) on a coil is :-

$$M = M_1 + Xy + Yc - x \qquad \text{——————(1.2)}$$

Substituting for Y from eq. 1.1 :-

$$M = M_o\left(1 - \frac{x}{c}\right) + Xy + M_1\frac{x}{c} \qquad \text{——————(1.3)}$$

The energy stored in the spring is now obtained as :-

$$V = \frac{\Psi}{2EI}\int_0^{\ell} M^2\, ds$$

in which Ψ is a function depending upon the product of the width to thickness ratio and the width to radius of curvature ratio. (See appendix A1.2). In the accepted theory for wide plates Ψ has the value

$$\psi = 1 - \nu^2$$

and in those cases where simple bending theory is acceptable $\Psi = 1$.

At the present stage ψ will be taken to be unity and corrections made later, if found necessary. Then

$$V = \frac{1}{2EI}\int_0^{\ell} M^2\, ds \qquad \text{——————(1.4)}$$

If the outer end is clamped neither M_1 nor X do work during either the winding-up process or the running-down process

i.e. $$\frac{\delta V}{\delta M_1} = \frac{\delta V}{\delta X} = 0 \qquad \text{——————(1.5)}$$

$$\therefore \frac{1}{2EI}\int_0^{\ell} M\frac{\delta M}{\delta M_1}\, ds = \frac{1}{2EI}\int_0^{\ell} M\frac{\delta M}{\delta X}\, ds = 0 \qquad \text{——(1.6)}$$

From eq. 1.3 :-

$$\frac{\delta M}{\delta M_1} = \frac{x}{c} \qquad \frac{\delta M}{\delta X} = y \qquad \text{——(1.7)}$$

Substituting the first of equations 1.7 with equation 1.3 into the first of equations 1.6 gives :-

$$\int_0^{\ell}\left[M\left(1 - \frac{x}{c}\right) + Xy + M_1\frac{x}{c}\right]\frac{x}{c}\, ds = 0 \qquad \text{——(1.8)}$$

whence

$$\int_0^{\ell}\frac{M_0}{c}x\, ds + \int_0^{\ell}\frac{(M_1 - M_0)}{c^2}x^2 ds + \int_0^{\ell}\frac{X}{c}xy\, ds = 0$$

Now, if the coil spacing, d, is small then

(i) $\int_0^\ell x\,ds \simeq 0$ since c. of g. lies on the x-axis

(ii) $\int_0^\ell y\,ds \simeq 0$ since c. of g. lies on the y-axis

(iii) $\int_0^\ell xy\,ds \simeq 0$ since c. of g. lies at 0, approx.

In this event equation 1.8 reduces to :-

$$\int_0^\ell \frac{(M_1 - M_0)}{c^2} x^2\,ds = 0$$

and, therefore,

$$\underline{M_0 = M_1}$$

The value of X is found by substituting the second of equations 1.7 with equation 1.3 into the second of equations 1.6 :-

$$\int_0^\ell \left[M_0\left(1 - \frac{x}{c}\right) + Xy + M_1\frac{x}{c}\right] y\,ds = 0$$

or $$\int_0^\ell M_0 y\,ds + \int_0^\ell \frac{(M_1 - M_0)}{c} xy\,ds + \int_0^\ell Xy^2 ds = 0$$

which gives

$$X = 0$$

Substituting these values into equation 3 indicates that the bending moment along the strip should be constant, i.e.

$$M = M_0$$

If we now equate the strain energy, V , to the work done by M_0 in turning the arbor through radian angle ϕ we obtain that

$$V = \frac{M_0}{2EI}\int_0^\ell ds = \frac{1}{2} M_0 \phi$$

whence

$$\phi = \frac{M_0 \ell}{E I} \qquad \text{(1.9)}$$

or more accurately

$$\phi = \Psi \cdot \frac{M \ell}{E I}$$

where Ψ is the function referred to above. It is implied here that Ψ is constant throughout the length of the spring but, in fact, this is not the case. This aspect of the problem is dealt with more fully in Appendix A1.2.

A1.1.2 Case 2. Theoretical M-ϕ relationship for pinned outer end

In this case $M_1 = 0$ in equations 1.1, 1.2 and 1.3 and equation 1.4 is unaltered. Therefore :-

$$M_o = Y c \qquad \text{——————} (2.1)$$
$$M = Xy + Y(c-x) \qquad \text{——————} (2.2)$$
$$M = M_o\left(1 - \frac{x}{c}\right) + Xy \qquad \text{——————} (2.3)$$

and, renumbering equation 1.4 for convenience

$$V = \frac{1}{2EI}\int_o^\ell M^2 \, ds \qquad \text{——————} (2.4)$$

then, since X does no work :

$$\frac{\delta V}{\delta X} = 0 \qquad \text{——————} (2.5)$$

and

$$\int_o^\ell M \frac{\delta M}{\delta X} \, ds = 0 \qquad \text{——————} (2.6)$$

Equation 2.2 with equation 2.6 gives :-

$$\int_o^\ell \left[Xy + Y(c-x)\right] ds = 0$$

which expands to

$$\int_o^\ell Xy^2 \, ds + \int_o^\ell Yc\,y\,ds - \int_o^\ell Yx\,y\,ds = 0 \qquad \text{——————} (2.7)$$

As before

$$X = 0$$ because

$$\int_0^{\ell} y\,ds = \int_0^{\ell} x\,y\,ds = 0$$

Equation 2.3 now gives :-

$$M = M_0\left(1 - \frac{x}{c}\right).$$

and equation 2.4. becomes :-

$$V = \frac{M_0^2}{2EI}\int_0^{\ell}\left(1 - \frac{x}{c}\right)^2 ds$$

i.e. $$V = \frac{M_0^2}{2EI}\left[\int_0^{\ell} ds - \int_0^{\ell}\frac{2x}{c}\,ds + \int_0^{\ell}\left(\frac{x}{c}\right)^2 ds\right]$$

and, since $\int_0^{\ell} x\,ds = 0$:-

$$V = \frac{M_0^2}{2EI} + \frac{M_0^2}{2EI}\int_0^{\ell} x^2\,ds$$

Now for a long close-coiled spiral of outer radius c,

$$\int_0^{\ell} x^2\,ds = \frac{\ell c^2}{4}$$

therefore,

$$V = \frac{5}{8}\,\frac{M_0^2\ell}{EI}$$

and equating to the external work done by M_0 during rotation of the arbor :-

$$\frac{5}{8}\,\frac{M_0^2\ell}{EI} = \frac{1}{2}\,M_0\phi$$

therefore

$$\phi = \frac{5}{4}\,\frac{M_0\ell}{EI} \qquad \text{——————(2.9)}$$

Equations 1.9 and 2.9 can be combined into the single equation

$$\phi = a\,\frac{M_0\ell}{EI}$$

which is equation 1.1 of the text and in which a = 1.0 for a clamped outer end and 1.25 for a pinned outer end.

A1.2 Distortion of transverse cross-section of a strip in bending

Ashwell[R4] shows that the shape of the transverse cross-section of a strip subjected to bending depends upon the dimensions of the strip (b = width, t = thickness) and the radius, R, to which the longitudinal neutral axis of the strip is bent. Three major types of distortion of the transverse cross-section may occur depending on the value of the quantity b^2/Rt as follows :

i) $0 < \frac{b^2}{Rt} < 1$ bent to circular arc radius $\frac{R}{\nu}$

ii) $1 < \frac{b^2}{Rt} < 100$ undulating, the undulations decreasing towards the centre of the cross-section

iii) $100 < \frac{b^2}{Rt}$ flat except near edges. The maximum 'lift' of edges tending to a value 0.102t

Ashwell deals with the theoretical determination of bending moment by applying a factor varying between 1.0 and 1.125, depending on the value of b^2/Rt, to the simple bending equation which, therefore, may be modified to the form

$$M = \frac{EI}{R} \psi_A \qquad \text{(A1.2.1)}$$

in which we will refer to ψ_A as Ashwell's factor which is given approximately by the table A1.2 constructed by the author from Ashwell's curve (R4 fig 7).

Table A1.2

b^2/Rt	0	10	20	30	50	100	300
ψ_A	1.0	1.07	1.09	1.10	1.105	1.112	1.12

In the manufacture of spiral springs a wide variety of strip widths and thicknesses are encountered, and the range of b^2/Rt through which a given spring may operate varies considerably. Therefore the correction to be applied to the moment equation will depend upon the instantaneous state of the spring. In other words, the value of Ashwell's factor is governed by the curvature of the active portion of the strip for a given point on the moment versus arbor rotation characteristic.

A chart showing the variation of Ashwell's factor ψ_A, for a range of width/thickness ratios, with the radius of curvature of the strip is given in Figure A1.1. A typical spring design might require the length of 1 in x 0.056 in strip to be 10,000t (t = thickness). The arbor diameter should be not less than 15t and, for best utilization of material, the barrel diameter will be approximately 150t. Under these conditions the value of b^2/Rt at the arbor will be about 30 and that at the barrel approximately 3. The 'working radius' will have a value nearer to 3 than to 30 i.e. a value of R/t of approximately 70 (Fig A1.1) which gives a correction factor, ψ_A= 1.02 to 1.03. It is seen therefore that the application of the theory of simple bending incurs an error of less than 5% in this instance.†

A1.3 Second Moment of Area of distorted cross-section

The curling of the edges of the strip during the manufacture of a spiral spring causes a change in the relevant second moment of area which should be taken into account when investigating the moment-rotation characteristic of the spring itself.

One of the springs tested was ultimately cut up into half-coils in order to ascertain the variation in shape of the cross-section throughout its length. At the inside coils the value

† see section A1.4 p.A9a.

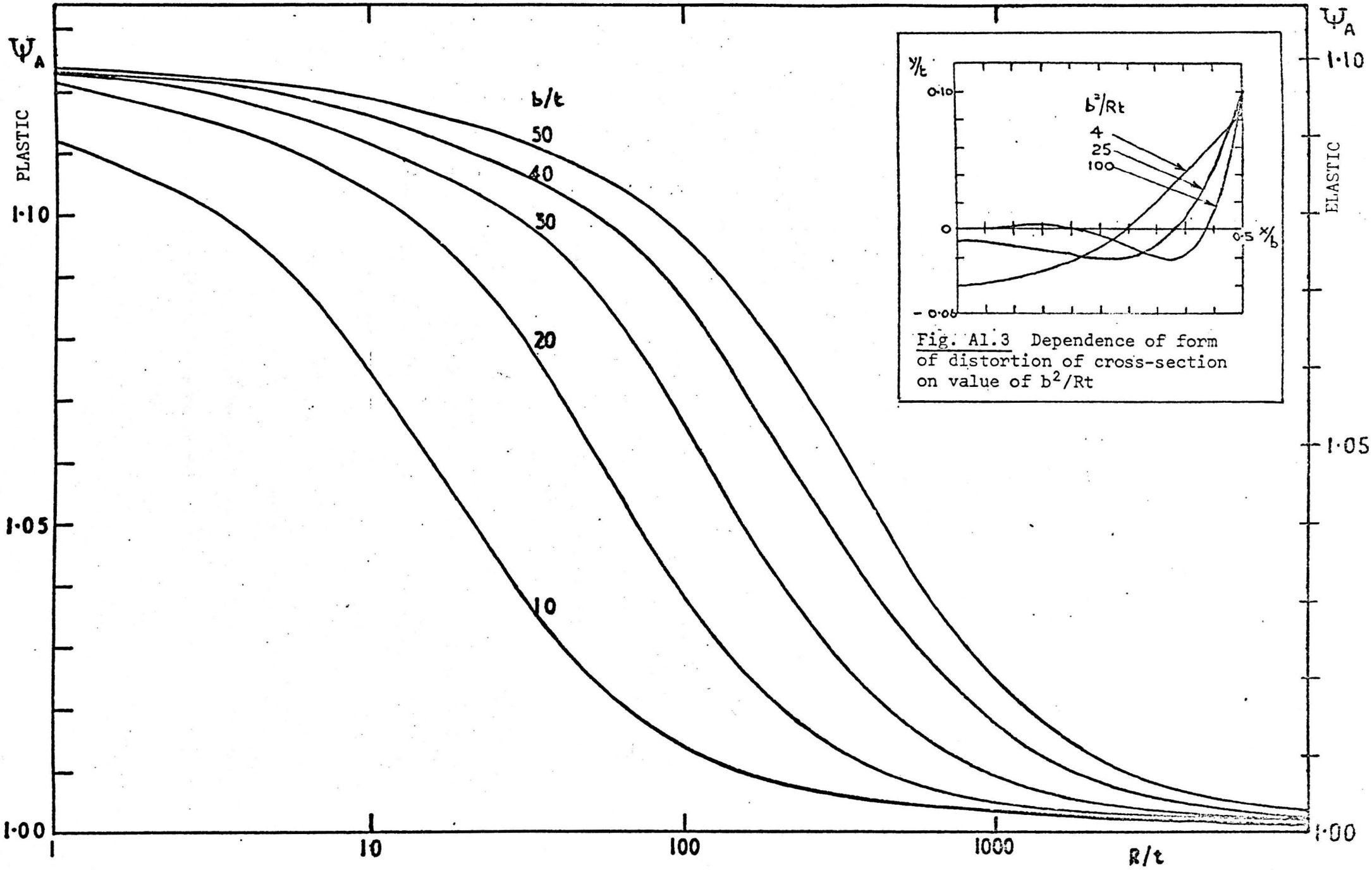

Fig. A1.3 Dependence of form of distortion of cross-section on value of b^2/Rt

Fig. A1.2 Ashwell factor for anticlasticity, ψ_A for width/thickness ratios 10-50

of b^2/Rt was approximately 25 and at the outside coil 6.5. The deformation of the cross-section was such that the central part appeared to be almost flat with the outer 1/8 in raised by 0.006 in at the outside coil and 0.009 in at the inside coil. These values are roughly in agreement with Ashwell's predictions. Fig A1.2 is a reproduction of Ashwell's Fig 4 showing the theoretical variation in cross-section to be expected.

The half-coils were next bent in a vice to half their initial radius and the 'lift' of the edges was measured again. The changes noted were of the order of 0.0005 in, in some cases an increase, in others a decrease. It is justified, therefore, to assume that the shape of the cross-section does not alter under the operating conditions of a spiral spring.

The relevant moment of inertia of the undeformed cross-section of the spring referred to was

$$I = \frac{1 \cdot 0.055^3}{12} = 1.39 \cdot 10^{-5} \text{ in}^4$$

The value for the distorted section can be estimated by approximating to two rectangles displaced relative to each other in the direction of the thickness by 0.005 in. The shift in the neutral axis amounts to 0.0013 in if the edge effect is 1/8 in wide. The relevant moment of inertia is

$$I^1 = 1.38 \cdot 10^{-5} + 0.75 \cdot 0.056 \cdot 0.0013^2 + 0.25 \cdot 0.056 \cdot 0.0037^2$$
$$= 1.389 \cdot 10^{-5} \text{ in}^4$$

which is less than 1% greater than the value for the undistorted cross-section. For the worst case the increase in I is unlikely to exceed 2%.

A1.4 Supporting Evidence

The author's experience supports that of Votta (Ref. B1.2.17). In the discussion of his paper with A.M. Wahl, Votta pointed out that the plate theory produced errors, in his, Votta's,case, greater than simple theory. The test results on his neg'ator springs were 10% lower than calculated results based on the simple bending expression but 20% lower than those calculated using the plate theory.

APPENDIX A2

A2.1. Derivation of equation 2.7

$$K = \frac{r^2 + 2\left(\frac{dr}{d\theta}\right)^2 - r\frac{d^2r}{d\theta^2}}{\left[r^2 + \left(\frac{dr}{d\theta}\right)^2\right]^{3/2}} \quad , \quad \text{and} \quad r = r_o e^{b\theta}$$

$$\therefore \quad K_o = \frac{r_o^2 e^{2b\theta} + 2b^2 r_o^2 e^{2b\theta} - b^2 r_o^2 e^{2b\theta}}{\left(r_o^2 e^{2b\theta} + b^2 r_o^2 e^{2b\theta}\right)^{3/2}}$$

$$= \frac{1}{r_o e^{b\theta}(1+b^2)^{1/2}} \quad - - - - - - - (A2.1)$$

$$\text{i.e.} \quad K_o = \frac{1}{r(1+b^2)^{3/2}}$$

A2.2. Derivation of equations 2.8 and 2.9

The length of a logarithmic spiral between angular positions θ_1 and θ_2 is given by:

$$s = \int_{\theta_1}^{\theta_2} \left(r^2 + \left(\frac{dr}{d\theta}\right)^2\right)^{1/2} d\theta$$

and $$r = r_o e^{b\theta} \quad ; \quad \frac{dr}{d\theta} = b r_o e^{b\theta}$$

$$\therefore \quad s = \int_{\theta_1}^{\theta_2} \frac{r_o e^{b\theta}}{b}(1+b^2)^{1/2} d\theta$$

$$\text{i.e.} \quad s = \left[\frac{r_o e^{b\theta}}{b}(1+b^2)^{1/2}\right]_{\theta_1}^{\theta_2}$$

Now if $\theta_1 = 0$ and $\theta_2 = \theta$

$$\text{then} \quad s = \frac{r_o}{b}(1+b^2)^{1/2}\left(e^{b\theta} - 1\right) \quad - - - - - - (A2.2)$$

A2.3 Derivation of equation 2.10

Equation A2.2 can be rewritten:

$$bs = r_0 e^{b\theta}(1+b^2)^{1/2} - r_0(1+b^2)^{1/2}$$

Substitute equation A2.1 and get

$$bs = \frac{1}{K_0} - r_0(1+b^2)^{1/2}$$

whence

$$K_0 = \frac{1}{bs + r_0(1+b^2)^{1/2}}$$

and if $b \rightarrow 0$

$$K_0 \simeq \frac{1}{bs + r_0}$$

APPENDIX A4

A4.1. Calibration of Torque Bars for use in the Testing Machine

A4.1.1. Apparatus

The machine used was an Avery torsion testing machine, the arrangement being as shown in the photograph (Fig. A4.1).

A4.1.2. Procedure

The arrangement of the dial gauges shown in the photograph is identical to that used in the spring testing machine. The four torsion bars, A, B, C and D, were designed for maximum torques of 200, 300, 500 and 1000 lbf.in. at a twist of approximately 3°. This allowed for a factor of safety of approximately 2, and provided a good range for the machine.

The torque was measured directly by the Avery machine and the dial gauge readings noted. A plot of torque against gauge differences was made for each bar. A second set of readings over the range of each torque bar was made as a check.

A4.1.3. Results

The resulting curves of torque against gauge differences are shown in Fig. A4.2. These all prove to be good straight lines, and allow the calculation of a factor for converting the dial gauge differences (in thousands of an inch) directly into torque in lbf.in.

From the curves the gradients are:

$$\text{grad A.} = \frac{207}{400}\text{lbf.in./0.001} \quad \text{so factor A} = 0.5175\text{lbf.in./0.001 in.}$$

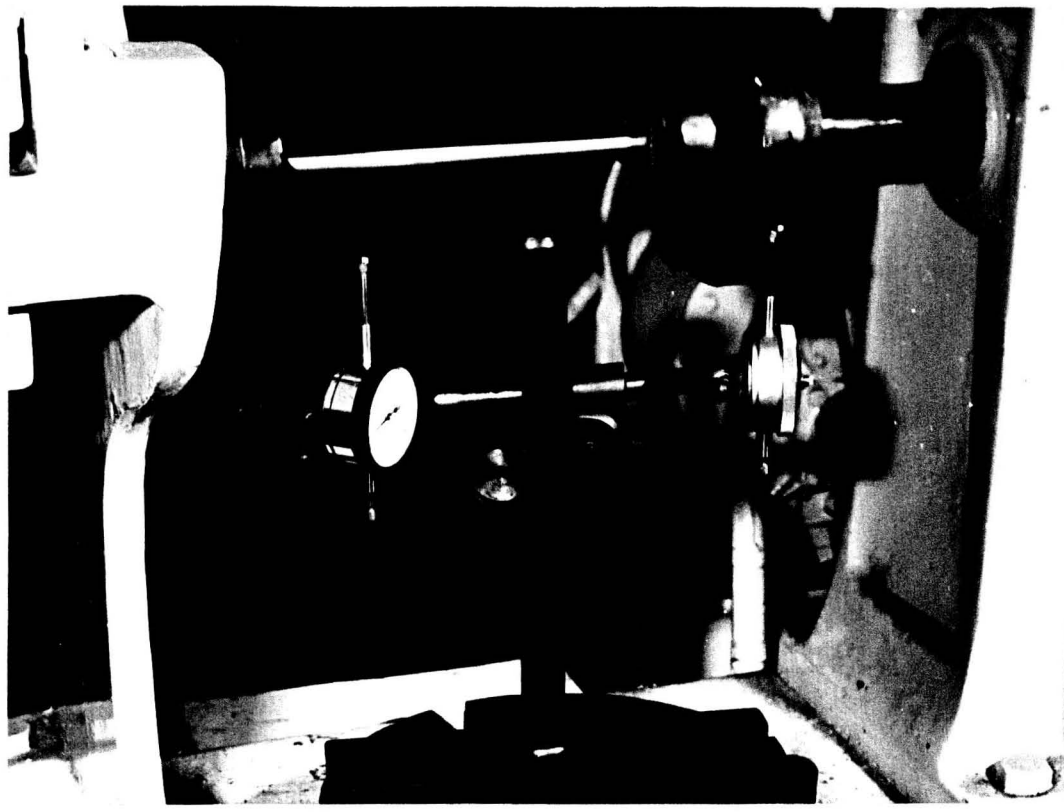

Fig. A4·1. Testing rig.

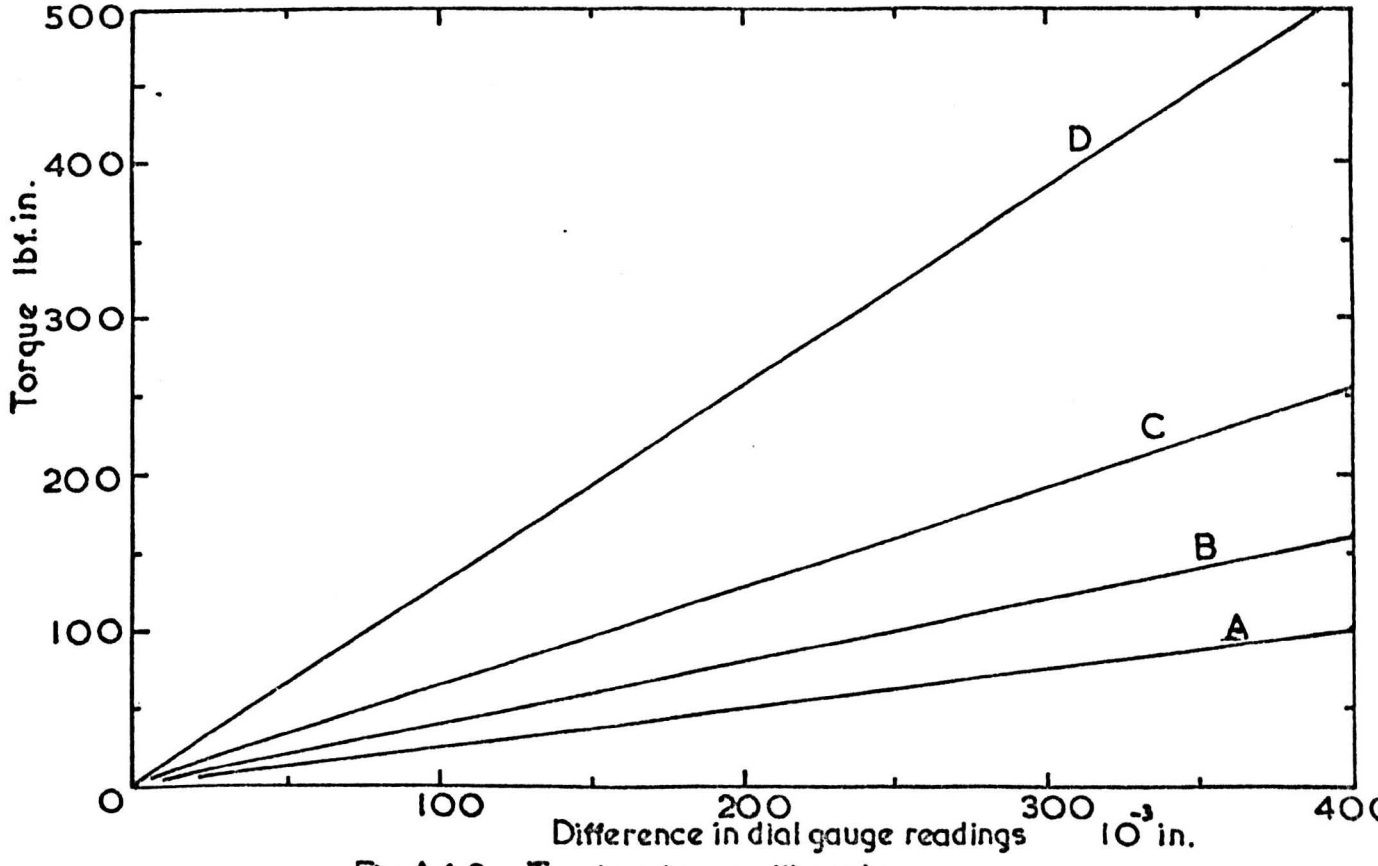

Fig. A4·2 Torsion bar calibration.

grad. B = $\frac{327}{400}$ lbf.in./0.001 so factor B =

0.8175 lbf.in./0.001 in.

grad. C = $\frac{510}{400}$ lbf.in./0.001 so factor C =

1.275 lbf.in./0.001 in.

grad. D = $\frac{1030}{400}$ lbf.in./0.001 so factor D =

2.575 lbf.in./0.001 in.

A4.1.4 Comments

The results obtained enable simple torque readings to be obtained on the machine.

A4.2. Notes on the use of Dial Gauges in the Testing Machine

The use of dial gauges for measuring the machine torque will incur inaccuracies if they are incorrectly aligned and positioned. It is required to estimate the maximum probably error due to this.

Consider the dial gauge and torque arm arrangement shown in fig. A4.3.

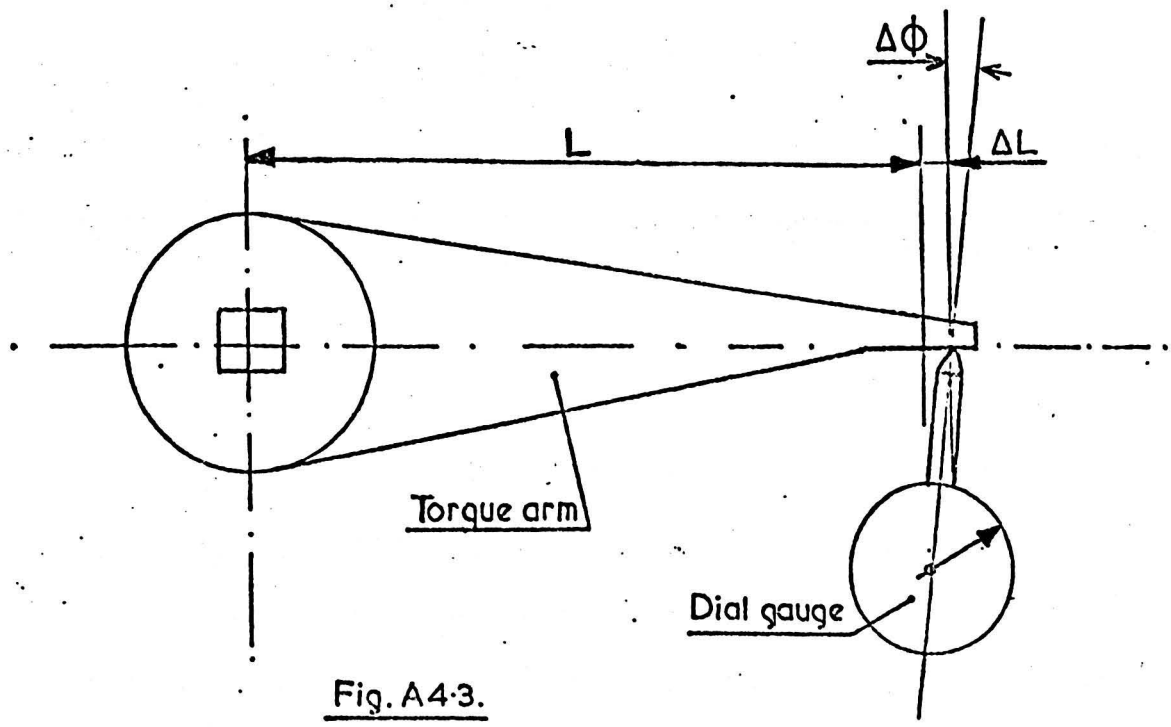

Fig. A4.3.

Assume an error in positioning of ΔL, and an incorrect perpendicular angle with error $\Delta\phi$, as shown.

(a) Considering first the angle error, let the twist of the torque arm be θ (this is necessarily small), so the true deflection of the gauge should be $L\theta$.

However, due to the error $\Delta\phi$ the actual gauge reading will be $L\theta$ sec. $\Delta\phi$, the error = $L\theta$(sec. $\Delta\phi$ - 1) and percentage error due to this error = (sec. $\Delta\phi$ - 1) x 100%. But siting inaccuracy will not be greater than $\pm 2^{o}$, so maximum percentage error = 0.0006 x 100 = 0.06%.

(b) Due to a positional error of ΔL as shown, the effective length of the arm is $L + \Delta L$, so the actual reading for a small twist θ is $(L + \Delta L)\theta$ whereas the true reading should be $L\theta$.

Hence the percentage error is given by $\frac{\Delta L\theta}{L}$ x 100 In the system to be used L = 7 in. and siting inaccuracy is of the order 0.025 in.

Hence the maximum percentage error due to positioning will be

$$\frac{0.025}{7} \times 100 = 0.3\%$$

The result of an angle error in the plane of the diagram will be the same as for the angle error discussed above, and the total effect of all these errors is additive. The total maximum error however, will not be greater than 0.5%, which is well within the required limits of the machine.

The torsion-bar calibration will itself involve inaccuracies but these are unavoidable in that it is impractical to design a torsion bar for which the torque-twist relationship can be simply and accurately calculated.

APPENDIX A5

Spring No. 1

Barrel $3\frac{3}{4}$" diameter, Arbor $1\frac{1}{4}$" diameter

Torsion Bar B factor = 0.8175.

Test 1

Rotn. θ	Dial Gauge 1	2	3	Δ	Loading Torque	1	2	3	Δ	Unloading Torque
0	0	0	0	0	0	3.5	11	15	.5	.4
1	1	1	43.5	41.5	34.0	8.0	17.5	60	34.5	28.2
2	1	3	74.5	70.5	57.6	12.0	19.5	92.5	61.0	49.9
3	2	6	101.0	93.0	76.1	9.0	20.0	110.5	81.5	66.6
4	3.5	10	130	116.5	95.4	15	21	140	140.0	85.1
5	-9.5	16	159	152.5	124.8	-13	20	130	123.0	100.6
6	10	20.5	212	181.5	148.3	18	22.5	186	145.5	119.0
7	-5	23	239	221.0	180.0					

Retest

θ	1	2	3	Δ	1	2	3	Δ
0	0	0	0	0	0	.5	.5	0
1	-0.5	12	52.5	41	0	16	50.5	34.5
2	2	14	87.5	71.5	3.5	18	82	60.5
3	3	16	111.5	92.5	1	18	100.5	81.5
4	4	17	138	117	7.5	19	131	104.5
5	-19	18	152	153	-26.5	17.5	114	123
6	1.5	20	202.5	181	-9	20.5	175.5	146
7	-16	21.5	226.5	221				

Test 2 (Spring lubricated)

θ	1	2	3	Δ	1	2	3	Δ
0	0	0	0	0	6	.5	1	.5
1	1	13	55	41	3.5	16.5	56	36
2	4	16.5	90.5	70	6	18	85.5	61.5
3	5	17	113.5	91.5	4	19	105	82
4	5.5	18	138	114.5	11	19	134	104
5	-20	18.5	146	148	-26	17.5	116.5	125
6	3	20	201	178	12.5	21	182	148.5
7	-16	21	222	217				

Units

θ - radians

Dial Gauge readings (1, 2 and 3) - 10^{-3} in.

Δ actual relative deflection of torque arms - 10^{-3} in.

Torque - lbf.in.

APPENDIX A6

A6.1. Spring A7 Test (a)

Experimental Results

Rotation (revs.)	2 dial gauges Torque (lb.in.) Up	2 dial gauges Torque (lb.in.) Down	3 dial gauges Torque (lb.in.) Up	3 dial gauges Torque (lb.in.) Down
0	0	0	0	0
½	5.7	11.4	8.2	6.73
1	12.9	11.4	13.2	11.4
1½	18.1	12.4	17.85	16.8
2	23.4	19.7	22.0	21.2
2½	26.3	22.5	25.85	24.8
3	31.6	24.1	29.5	28.2
3½	33.8	26.4	32.6	29.5
4	37.8	29.0	35.7	32.6
4½	40.1	32.1	37.5	36.5
5	43.6	34.7	40.4	38.6
5½	44.0	35.7	42.7	40.9
6	47.1	40.4	45.5	42.7
6½	50.5	41.4	47.6	45.5
7	53.4	47.6	50.5	48.9
7½	53.9	45.0	52.5	51.3
8	58.5	52.0	56.1	55.6
8½	59.5	50.0	58.5	55.6
9	69.8	56.2	64.2	58.0
9½	65.8	54.4	62.6	61.1
10	73.5	62.1	63.4	63.2
10½	75.0	60.0	67.5	67.0
11	81.7	-	68.1	69.4

Theoretical Results

Rotation (revs.)	Torque (lb.in.)
0	0
1.13	12.06
2.72	24.12
4.99	36.18
7.21	48.24
9.75	60.30
12.12	72.36
14.52	84.42
16.12	96.48
16.42	106.2

A6.1 (continued)

Spring A7 Test (b)

Experimental Results

Rotation (revs.)	Torque (lb.in.) Up	Torque (lb.in.) Down
0	0	1.0
½	9.6	4.1
1	10.1	6.7
1½	12.9	8.3
2	15.3	10.9
2½	16.6	13.7
3	18.9	16.5
3½	21.7	18.6
4	23.3	21.7
4½	26.6	24.1
5	28.2	26.1
5½	31.6	29.8
6	31.8	31.3
6½	36.2	35.2
7	36.2	35.4
7½	40.4	40.1
8	40.9	41.4
8½	46.0	45.3
9	47.9	46.8
9½	50.2	50.7
10	50.6	51.5
10½	55.2	55.9
11	55.6	55.1
11½	60.3	60.0
12	60.0	

Theoretical Results

Rotation (revs.)	Torque (lb.in.)
0	0
2.22	12.06
4.61	24.12
7.00	36.18
9.36	48.24
11.75	60.30
14.15	72.36
16.50	84.42
18.22	96.48
18.76	106.2

A6.1 (continued)

Spring A7 Test (c)

Experimental Results

Rotation (revs.)	Torque (lb.in.) Up	Torque (lb.in.) Down
0	0	.5
½	7.0	6.2
1	13.5	11.6
1½	18.1	
2	22.8	21.2
2½	26.6	24.8
3	30.5	28.2
3½	34.2	30.5
4	36.5	33.9
4½	39.3	36.5
5	41.9	39.6
5½	44.3	41.9
6	47.4	45.0
6½	47.4	47.6
7	54.9	53.5
7½	54.9	55.2
8	60.9	59.8
8½	58.0	58.8
9	64.7	62.1
9½	66.0	63.6
10	67.8	67.3
10½	83.4	

Theoretical Results

Rotation (revs.)	Torque (lb.in.)
0	0
1.02	12.06
2.36	24.12
4.37	36.18
6.55	48.24
8.61	60.30
10.45	72.36
10.95	79.50

A6.2. Proof of the equation for rotation of the arbor

The angle of rotation is given by the area between the ΔK_{20} and ΔK_{10} curves and the ΔK ordinate corresponding to the applied moment.

$$\phi = \Delta K(s) + \int \Delta K_{20} ds - \int \Delta K_{10} ds$$

Now $$\int \Delta K_{20} ds = \int \left\{ \frac{B}{\sqrt{c_2 + s}} - \frac{1}{bs + k_1} \right\} ds$$

where $k_1 = r_o(1 + b^2)^{\frac{1}{2}}$

$$= \left[2B\sqrt{c_2 + s} - \frac{1}{b} \ln \left(s + \frac{k_1}{b}\right) \right]^{\text{limits}}$$

Similarly $$\int \Delta K_{10} ds = \int \left\{ \frac{B}{\sqrt{c_1 + s}} - \frac{1}{bs + K_1} \right\}$$

$$= \left[2B\sqrt{c_1 + s} - \frac{1}{b} \ln \left(s + \frac{k_1}{b}\right) \right]^{\text{limits}}$$

$$\therefore \quad \phi = \Delta K(s)^{\text{limits}} + \left[2B\sqrt{c_2 + s} - \frac{1}{b} \ln \left(s + \frac{k_1}{b}\right) \right]^{\text{limits}} - \left[2B\sqrt{c_1 + s} + \frac{1}{b} \ln \left(s + \frac{k_1}{b}\right) \right]^{\text{limits}}$$

APPENDIX A7

A7.1 Equation of path on strip during winding

Refer to fig. 7.3, page 103, for a point (x, y) on the strip, the bending moment $\bar{M}$ is:-

$$\bar{M} = M + Ty - Rx$$

whence $$EI \frac{d^2y}{dx^2} = M + Ty - Rx$$

and $$(D^2 - n^2)y = -m^2x + p^2$$

where $$D^2 = \frac{d^2}{dx^2}$$

$$m^2 = \frac{R}{EI}$$

$$n^2 = \frac{T}{EI}$$

$$p^2 = \frac{M}{EI}$$

which has the solution:

$$y = A \sinh nx + B \cosh nx + \frac{R}{T}x - \frac{M}{T}y \quad \text{---- (A7.1)}$$

The boundary conditions are:-

(i) At $x = 0$, $y = 0$ (ii) at $x = L$, $y = -d$

(iii) at $x = 0$, $\frac{dy}{dx} = \beta$ (iv) at $x = L$, $\frac{dy}{dx} = -\alpha$

(i) in equation A7.1 gives $B = \frac{M}{T}$

(ii) in equation A7.1 gives $d = A \sinh nL + \frac{M}{T}(\cosh nL - 1) + \frac{RL}{T}$ ... (A7.2)

(iii) in $\frac{d}{dx}$ (A7.1) gives $\beta = An + \frac{R}{T}$ ------ (A7.3)

and

(iv) in $\frac{d}{dx}$ (A7.1) gives $\alpha = An \cosh nL + \frac{Mn}{T} \sinh nL + \frac{R}{T}$ ---(A7.4)

Substitute for $\frac{R}{T}$ from A7.3 into A7.2 then:

$$d = A\sinh nL + \frac{M}{T}(\cosh nL - 1) + L(\beta - An)$$

or $$d = A(\sinh nL - nL) + \frac{M}{T}(\cosh nL - 1) + L\beta \quad \text{-----(A7.5)}$$

Eliminate $\frac{R}{T}$ from A7.3 and A7.4:

$$\alpha = An(\cosh nL - 1) + \frac{Mn}{T}\sinh nL + \beta \quad \text{-----(A7.6)}$$

Eliminate $\frac{M}{T}$ from A7.4 and A7.6:

$$dn\sinh nL - \alpha(\cosh nL - 1) = An\sinh nL(\sinh nL - nL) - An(\cosh nL - 1)^2 + L\beta n\sinh nL - \beta(\cosh nL - 1)$$

whence $$A = \frac{n\sinh nL(d - L\beta) + (1 - \cosh nL)(\alpha - \beta)}{n\{\sinh nL(\sinh nL - nL) - (\cosh nL - 1)^2\}} \quad \text{-----(A7.7)}$$

Equations A7.2 and A7.3 give, on eliminating A,

$$dn(\cosh nL - 1) - \alpha(\sinh nL - nL) = \frac{M}{T}\times(\cosh nL - 1)^2 - \frac{Mn}{T}\sinh nL(\sinh nL - nL) + L\beta n(\cosh nL - 1) - \beta(\sinh nL - nL)$$

whence $$M = \frac{T}{n}\left\{\frac{n(\cosh nL - 1)(d - L\beta) - (\sinh nL - nL)(\beta - \alpha)}{(\cosh nL - 1)^2 - \sinh nL(\sinh nL - nL)}\right\} \quad \text{---(A7.8)}$$

Substituting for A, and $B = \frac{M}{T}$ in equation A7.5 gives

$$B = \frac{1}{n}\left\{\frac{n(\cosh nL - 1)(d - L\beta) - (\sinh nL - nL)(\beta - \alpha)}{(\cosh nL - 1)^2 - \sinh nL(\sinh nL - nL)}\right\} \quad \text{-----(A7.9)}$$

Now, from equation A7.3 we get

$$R = T(\beta - An) \qquad \text{and hence}$$

$$R = T\left\{\beta - \frac{n\sinh nL(d - L\beta) + (\alpha - \beta)(1 - \cosh nL)}{\sinh nL(\sinh nL - nL) - (\cosh nL - 1)^2}\right\} \quad \text{-----(A7.10)}$$

If we substitute in A7.1 for $\frac{R}{T}$ and $\frac{M}{T}$ we get

$$y = A\sinh nx + B(\cosh nx - 1) + (\beta - An)x$$

which requires only evaluation of A and B in order to obtain the path of a particle which is almost identical to the shape of the strip between O and P, fig. 7.3.

A7.2. PER CENT VARIATION OF EXPERIMENTAL VALUES FROM THEORETICAL

The simple per cent variation given by the expression

$$\% \text{ variation} = \frac{r_t - r_e}{r_t} \times 100\%$$

does not yield a true indication of the difference since the final radius depends heavily on the initial radius before spring-back. A better expression is yielded by using the spring-back ratios R/r_t and R/r_e :

$$\% \text{ variation} = \frac{R/r_t - R/r_e}{R/r_t} \times 100\%$$

Note that R cancels leaving reciprocal r's.

For example take material B, table 7.1, page 108, pressed with a $\frac{1}{2}$ in. radius tool.

$R = 0.510$, $r_t = 0.963$, $r_e = 0.937$ (table 7.2, page 118)

$$\% \text{ variation} = \frac{\frac{1}{0.963} - \frac{1}{0.937}}{\frac{1}{0.963}} \times 100\%$$

$$= 2.84\%$$

APPENDIX A8

STRETCH-FORMING OF SPRING STRIP

Assume an ideal elastic- perfectly plastic material.

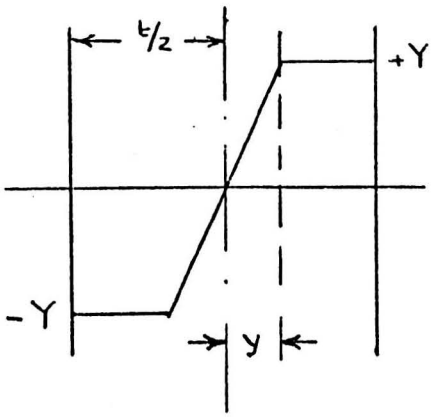

$$Y = \frac{Ey}{R}$$

$$\therefore \quad \frac{y}{t} = \frac{RY}{Et}$$

(i) Stress distribution with Pure Bending.

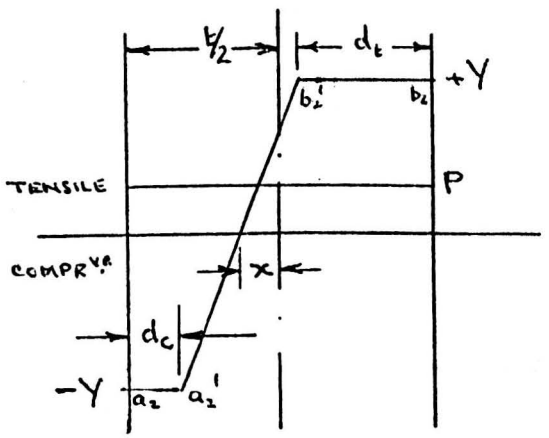

$$2xY = Pt$$

$$\therefore \quad x = \frac{Pt}{2Y}$$

$$\text{or} \quad \frac{x}{t} = \frac{P}{2Y}$$

(ii) Stress distribution with tensile stress P giving compressive yielding.

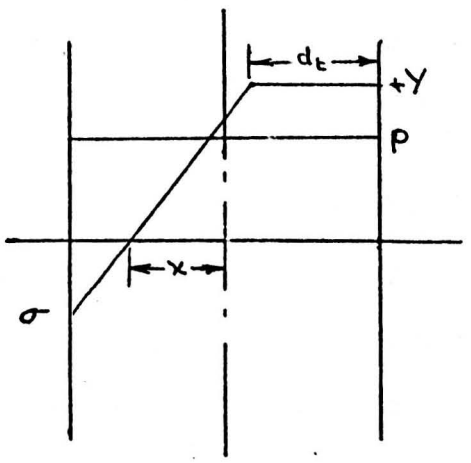

(iii) Stress distribution with tensile stress P giving no compressive yield.

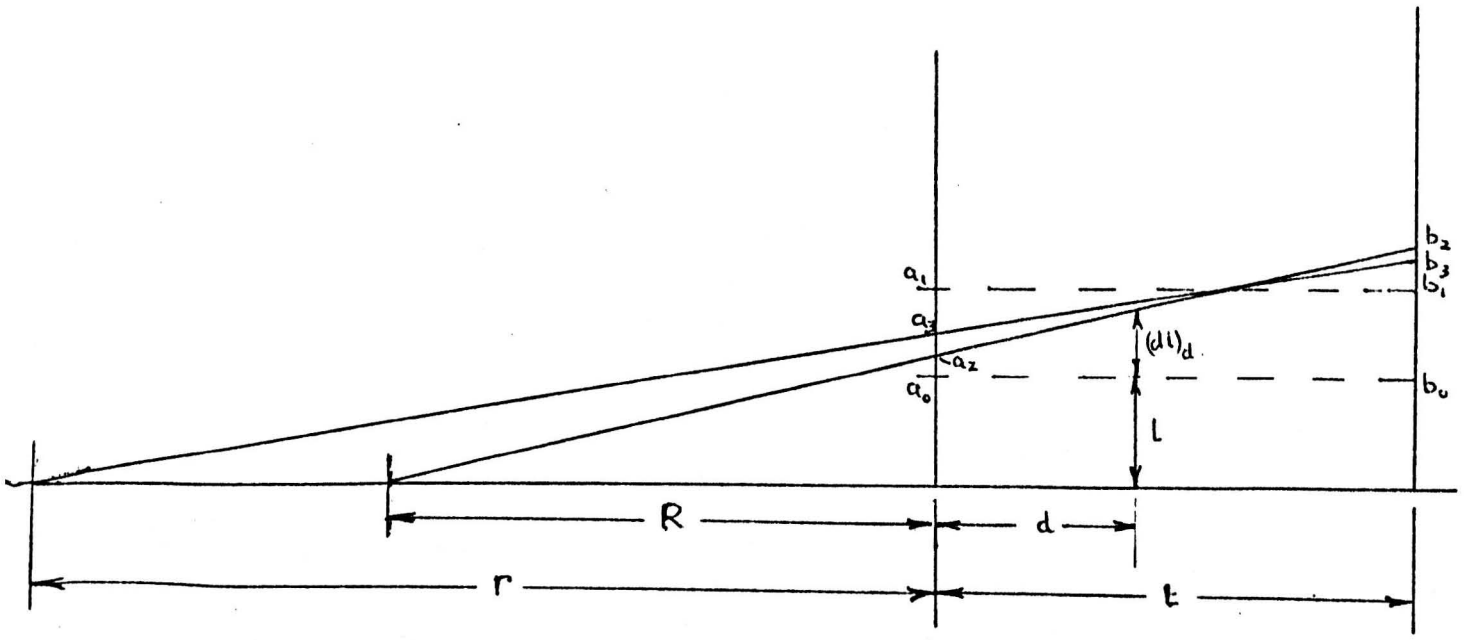

(iv) Strain diagram.

a_0b_0 position of unstrained fibre.

a_1b_1 position of fibre strained in tension only.

a_2b_2 position of fibre strained in tension and bent to radius R.

a_3b_3 position of fibre after stretch forming process.

Assume that strip is bent under constant tension. Two conditions may obtain depending on the magnitude of the tensile force and the radius of bend.

1) There may be compressive yielding at the inside edge (fig. ii) in which case the analysis is as follows:-

Let ε_a = strain at inside fibre = $\frac{(dl)_{a_2}}{l}$

strain at distance d from inside fibre is

$$\varepsilon_d = \frac{(dl)_d}{l} \quad \text{and} \quad \frac{l+(dl)_d}{R+d} = \frac{l+(dl)_{a_2}}{R}$$

$$\therefore \quad \frac{(dl)_d}{l} = \left(\frac{R+d}{R}\right)\left(\frac{L+(dl)_{az}}{l}\right) - 1$$

$$\text{or} \quad \varepsilon_d = \left(1+\frac{d}{R}\right)(1+\varepsilon_a) - 1 = \varepsilon_a + \frac{d}{R}(1+\varepsilon_a)$$

Depth of yield d_c:-

$$E.\,\varepsilon_{d_c} = -Y \qquad \therefore \quad \varepsilon_{d_c} = -\frac{Y}{E}$$

$$\text{Also} \quad \varepsilon_{d_c} = \varepsilon_a + \frac{d_c}{R}(1+\varepsilon_a)$$

$$\therefore \quad d_c = -\frac{\left(\frac{Y}{E}+\varepsilon_a\right)R}{1+\varepsilon_a}$$

$$\text{and} \quad \frac{d_c}{t} = -\frac{RY}{Et}\cdot\frac{1}{1+\varepsilon_a}\left[1+\frac{E}{Y}\varepsilon_a\right]$$

Depth of yield d_t:-

$$E\,\varepsilon_{d_t} = Y \qquad \therefore \quad \varepsilon_{d_t} = \frac{Y}{E}$$

$$\text{Also} \quad \varepsilon_{d_t} = \varepsilon_a + \left(\frac{t-d_t}{R}\right)(1+\varepsilon_a)$$

$$\therefore \quad d_t = -\frac{\left(\frac{Y}{E}-\varepsilon_a\right)R}{1+\varepsilon_a} + t$$

$$\text{and} \quad \frac{d_t}{t} = 1 - \left(\frac{d_c}{t} + 2\frac{RY}{Et}\cdot\frac{1}{1+\varepsilon_a}\right)$$

For zero resultant force on cross section:-

$$P_t = Y(d_t - d_c)$$

$$\text{i.e.} \quad P_t = Y\left(t + \frac{2R\varepsilon_a}{1+\varepsilon_a}\right)$$

$$\text{whence} \quad \frac{\varepsilon_a}{1+\varepsilon_a} = \left(\frac{P}{Y}-1\right)\frac{t}{2R}$$

$$\text{If} \quad 1+\varepsilon_a \longrightarrow 1 \quad \text{then} \quad \varepsilon_a \simeq \left(\frac{P}{Y}-1\right)\frac{t}{2R}$$

$$\text{or if} \quad \varepsilon_a' = \frac{-\left(1-\frac{P}{Y}\right)}{2\frac{RY}{Et}\cdot\frac{E}{Y}}$$

or

$$\text{then} \quad \varepsilon_a = \varepsilon_a' \Big/ 1-\varepsilon_a'$$

Stress condition across the section is:- (see diag ii)

$a_2 - a_2'$ $\qquad \sigma = -Y$

$a_2' - b_2'$ $\qquad \sigma = E\left[\varepsilon_a + (1+\varepsilon_a)\frac{d}{R}\right]$

$b_2' - b_2$ $\qquad \sigma = +Y$

Let radius after spring back be r then strain at any distance d from the inside fibre is:-

$$\varepsilon_d' = \varepsilon_{a_3} - \frac{d}{r}(1+\varepsilon_{a_3})$$

Change in strain is

$$\Delta\varepsilon = \varepsilon_d' - \varepsilon_d = (\varepsilon_{a_3} - \varepsilon_a) + \left(\frac{1+\varepsilon_{a_3}}{r} - \frac{1+\varepsilon_a}{R}\right)d$$

Residual stress is given by:-

$$\sigma_{res} = \sigma + E\Delta\varepsilon$$

For zero resultant force on any cross section in the final state, we have:-

$$\int_0^t \sigma_{res}\, dt = 0 \qquad \text{Let } t - d_t = d_t'$$

Then :—

$$\int_0^{d_c} -Y\,dt + \int_{d_c}^{d_t'} E\varepsilon_a + E(1+\varepsilon_a)\frac{d}{R}\,dt + \int_{d_t'}^{t} Y\,dt$$

$$+ \int_0^t \left[E(\varepsilon_{a_3} - \varepsilon_a) + E\left(\frac{1+\varepsilon_{a_3}}{r} - \frac{1+\varepsilon_a}{R}\right)d\right]dt = 0$$

$$\therefore\ -Yd_c + E\varepsilon_a(d_t' - d_c) + E(1+\varepsilon_a)\left(\frac{d_t'^2 - d_c^2}{2R}\right) + Yt - Yd_t'$$

$$+ E(\varepsilon_{a_3} - \varepsilon_a)t + E\left(\frac{1+\varepsilon_{a_3}}{r} - \frac{1+\varepsilon_a}{R}\right)\frac{t^2}{2} = 0$$

i.e. $$Y\left(t - (d_t' + d_c)\right) + E\varepsilon_a(d_t' - d_c - t) + \frac{E(1+\varepsilon_a)}{2R}\left(d_t'^2 - d_c^2 - t^2\right)$$

$$+ E\varepsilon_{a_3}t + E\frac{(1+\varepsilon_{a_3})t^2}{2r} = 0$$

and $$\varepsilon_{a_3}\left(Et + \frac{Et^2}{2r}\right) = Y\left(d_t' + d_c - t\right) - \frac{Et^2}{2r} + E\varepsilon_a\left(t - (d_t' - d_c)\right)$$
$$+ \frac{E(1+\varepsilon_a)}{2R}\left(t^2 - (d_t'^2 - d_c^2)\right)$$

$$\therefore\ \varepsilon_{a_3}\left(1 + \frac{t}{2r}\right) = \frac{Y}{Et}\left(d_t' + d_c - t\right) - \frac{t}{2r} + \frac{\varepsilon_a}{t}\left(t - (d_t' - d_c)\right)$$
$$+ \frac{(1+\varepsilon_a)}{2Rt}\left(t^2 - (d_t'^2 - d_c^2)\right) \quad \text{------} \quad (A8.1)$$

For zero resultant moment on any cross section in the final state we have:-

$$\int_0^b \sigma_{res}\, d\, dt = 0$$

$$\therefore \int_0^{d_c} -Yd\, dt + \int_{d_c}^{d_t'} E\varepsilon_a d\, dt + \int_{d_c}^{d_t'} E(1+\varepsilon_a)\frac{d^2}{R}dt + \int_{d_t'}^{t} Yd\, dt$$
$$+ \int_0^b E\left(\varepsilon_{a_3} - \varepsilon_a\right)d\, dt + \int_0^t E\left(\frac{1+\varepsilon_{a_3}}{r} - \frac{1+\varepsilon_a}{R}\right)d^2\, dt = 0$$

i.e. $$\frac{Y}{2}\left(t^2 - d_t'^2 - d_c^2\right) + \frac{E\varepsilon_a}{2}\left(d_t'^2 - d_c^2 - t^2\right) + \frac{E}{3R}(1+\varepsilon_a)\left(d_t'^3 - d_c^3 - t^3\right)$$
$$+ \frac{E\varepsilon_{a_3}}{2}t^2 + \frac{E}{3r}(1+\varepsilon_{a_3})t^3 = 0$$

whence $$\frac{E\varepsilon_{a_3}}{2}\left(t^2 + \frac{2t^3}{3r}\right) = \frac{Y}{E}\left(d_t'^2 + d_c^2 - t^2\right) + \frac{E\varepsilon_a}{2}\left(t^2 - (d_t'^2 - d_c^2)\right)$$
$$+ \frac{E(1+\varepsilon_a)}{3R}\left(t^3 - (d_t'^3 - d_c^3)\right) - \frac{Et^3}{3r}$$

$$\therefore\ \varepsilon_{a_3}\left(1+\frac{2t}{3r}\right) = \frac{Y}{Et^2}\left(d_t'^2 + d_c^2 - t^2\right) + \frac{\varepsilon_a}{t^2}\left(t^2-(d_t'^2-d_c^2)\right)$$

$$+ \frac{2(1+\varepsilon_a)}{3Rt^2}\left(t^3-(d_t'^3-d_c^3)\right) - \frac{2t}{3r} \quad \text{------ (A8.2)}$$

From page A26

$$d_c = \frac{-\left(\frac{Y}{E}+\varepsilon_a\right)R}{1+\varepsilon_a} \quad \text{and} \quad d_t' = d_c + \frac{2YR}{E(1+\varepsilon_a)} \quad \text{----- (A8.3)}$$

and $$\frac{\varepsilon_a}{1+\varepsilon_a} = \left(\frac{P}{Y}-1\right)\frac{t}{2R} \qquad \text{or if } \varepsilon_a \to 0 \text{ ie } 1+\varepsilon_a \to 1$$

then $$\varepsilon_a = \left(\frac{P}{Y}-1\right)\frac{t}{2R} \quad \text{- - - - - - - - - - (A8.4)}$$

If $1+\varepsilon_a \not\to 1$ then $$\varepsilon_a = \frac{\left(\frac{P}{Y}-1\right)\frac{t}{2R}}{1-\left(\frac{P}{Y}-1\right)\frac{t}{2R}}$$

also $$Y(d_t-d_c) = Pt \quad \text{or} \quad Y(t-d_t'-d_c) = Pt$$

and $$d_t'-d_c = \frac{2YR}{E(1+\varepsilon_a)} \; ; \; d_t'+d_c = \frac{-2R\varepsilon_a}{1+\varepsilon_a}$$

$$\therefore\ Y\left(t+\frac{2R\varepsilon_a}{1+\varepsilon_a}\right) = Pt$$

A8.1 now gives :—

$$\varepsilon_{a_3}\left(1+\frac{t}{2r}\right) = -\frac{P}{E} - \frac{t}{2r} + \frac{\varepsilon_a}{E}\left(t-\frac{2YR}{E(1+\varepsilon_a)}\right)$$

$$+ \frac{(1+\varepsilon_a)}{2Rt}\left(t^2+\frac{4YR^2\varepsilon_a}{E(1+\varepsilon_a)}\right)$$

i.e. $$\varepsilon_{a_3}\left(1+\frac{t}{2r}\right) = -\frac{P}{E} - \frac{t}{2r} + \varepsilon_a + \frac{t}{2R}(1+\varepsilon_a)$$

$$\therefore\ \varepsilon_{a_3}\left(1+\frac{t}{2r}\right) = -\frac{P}{E} - \frac{t}{2r} + \frac{(1+\varepsilon_a)t}{2R}\cdot\frac{P}{Y}$$

$$\text{or}\qquad \varepsilon_{a_3}\left(1+\frac{t}{2r}\right) = \varepsilon_a - \frac{P}{E} - \frac{t}{2r} + \frac{t}{2R}(1+\varepsilon_a) \quad \text{------(A8.5)}$$

Similarly with equation A8.2:-

$$\varepsilon_{a_3}\left(1+\frac{2t}{3r}\right) = -\frac{Y}{Et^2}\left(t^2 - \left(\frac{R}{E(1+\varepsilon_a)}\right)^2\left(2Y^2+2E^2\varepsilon_a^2\right)\right)$$
$$+ \frac{\varepsilon_a}{t^2}\left(t^2 + \frac{4YR^2\varepsilon_a}{E(1+\varepsilon_a)^2}\right)$$
$$+ \frac{2(1+\varepsilon_a)}{3Rt^2}\left(t^3 - \left(\frac{R}{E(1+\varepsilon_a)}\right)^2\left(2Y^2+6Y\varepsilon_a^2\right)\right)$$
$$- \frac{2}{3}\frac{t}{r}$$

Expanding right hand side

$$\varepsilon_{a_3}\left(1+\frac{2t}{3r}\right) = -\frac{Y}{E} + 2\left(\frac{Y}{E}\right)^3\left(\frac{R}{(1+\varepsilon_a)t}\right)^2 + \frac{2Y\varepsilon_a^2R^2}{E(1+\varepsilon_a)^2t^2}$$
$$+ \varepsilon_a + \frac{4Y}{E}\left(\frac{R}{(1+\varepsilon_a)t}\right)^2\cdot\varepsilon_a^2$$
$$+ \frac{2(1+\varepsilon_a)t}{3R} - \frac{4}{3}\left(\frac{Y}{E}\right)^3\left(\frac{R}{(1+\varepsilon_a)t}\right)^2 - \frac{4Y}{E}\varepsilon_a^2\left(\frac{R}{(1+\varepsilon_a)t}\right)^2$$
$$- \frac{2}{3}\frac{t}{r}$$

$$\varepsilon_{a_3}\left(1+\frac{2t}{3r}\right) = \varepsilon_a + \frac{2}{3}\frac{t}{R}(1+\varepsilon_a) - \frac{2}{3}\frac{t}{r}$$
$$- \frac{Y}{E}\left(1 + \left(\frac{R}{(1+\varepsilon_a)t}\right)^2\left(-\frac{2}{3}\left(\frac{Y}{E}\right)^2 - 2\varepsilon_a^2\right)\right)$$

$$= \varepsilon_a + \frac{2}{3}\frac{t}{R}(1+\varepsilon_a) - \frac{2}{3}\frac{t}{r} - \frac{Y}{E}(1-2A) \quad \text{------(A8.6)}$$

$$(A8.5)\times\left(1+\frac{2t}{3r}\right) = \varepsilon_a\left(1+\frac{2}{3}\frac{t}{r}\right) - \frac{P}{E}\left(1+\frac{2}{3}\frac{t}{r}\right) - \frac{t}{2r}\left(1+\frac{2}{3}\frac{t}{r}\right) + \frac{t}{2R}(1+\varepsilon_a)\left(1+\frac{2}{3}\frac{t}{r}\right) \quad \text{---- (A8.7)}$$

$$(A8.6)\times\left(1+\frac{t}{2r}\right) = \varepsilon_a\left(1+\frac{t}{2r}\right) + \frac{2}{3}\frac{t}{R}(1+\varepsilon_a)\left(1+\frac{t}{2r}\right) - \frac{2}{3}\frac{t}{r}\left(1+\frac{t}{2r}\right) - \frac{\gamma}{E}\left(1+\frac{t}{2r}\right) \quad \text{----(A8.8)}$$
$$+ \frac{2\gamma A}{E}\left(1+\frac{t}{2r}\right)$$

$$(A8.7)-(A8.8):- \quad \varepsilon_a\left(\frac{2}{3}\frac{t}{r}-\frac{t}{2r}\right) - \frac{P}{E}\left(1-\frac{2}{3}\frac{t}{r}\right) - \frac{t}{r}\left(\frac{1}{2}+\frac{1}{3}\frac{t}{r}-\frac{2}{3}-\frac{1}{3}\frac{t}{r}\right)$$
$$+(1+\varepsilon_a)\left(\frac{t}{2R}+\frac{1}{3}\frac{t^2}{Rr}-\frac{2}{3}\frac{t}{R}-\frac{1}{3}\frac{t^2}{Rr}\right)+\frac{\gamma}{E}\left(1+\frac{t}{2r}\right)-\frac{2\gamma A}{E}\left(1+\frac{t}{2r}\right)=0$$

$$\therefore \quad \varepsilon_a\frac{t}{6r} - \frac{P}{E}\left(1+\frac{2}{3}\frac{t}{r}\right)+\frac{t}{6r}-\frac{(1+\varepsilon_a)t}{6R}+\frac{\gamma}{E}+\frac{\gamma t}{2Er}-\frac{2\gamma A}{E}-\frac{\gamma A t}{Er}=0$$

and
$$\frac{t}{6r}(\varepsilon_a+1)+\frac{t}{r}\left(\frac{\gamma}{2E}-\frac{2P}{3E}-\frac{\gamma A}{E}\right)$$
$$= \frac{P}{E}+\frac{(1+\varepsilon_a)t}{6R}-\frac{\gamma}{E}+\frac{2\gamma}{E}A$$

$$\frac{t}{r}\left(\frac{\varepsilon_a+1}{6}-\frac{2}{3}\frac{P}{E}+\frac{\gamma}{2E}(1-2A)\right) = \frac{P}{E}-\frac{\gamma}{E}(1-2A)+\frac{t}{6R}(1+\varepsilon_a)$$

whence
$$\frac{R}{r} = \frac{\frac{1+\varepsilon_a}{6}+\frac{R}{t}\left(\frac{P}{E}-\frac{\gamma}{E}(1-2A)\right)}{\frac{1+\varepsilon_a}{6}-\frac{2}{3}\frac{P}{E}+\frac{\gamma}{E}(1-2A)}$$

in which
$$A = \left(\frac{R}{(1+\varepsilon_a)t}\right)^2\left(\frac{1}{3}\left(\frac{\gamma}{E}\right)^2+\varepsilon_a^2\right)$$

or
$$A \simeq \frac{1}{3}\left(\frac{R\gamma}{Et}\right)^2$$

But if $1 + \varepsilon_a \longrightarrow 1$

$$\text{then} \quad \frac{R}{r} = \frac{\frac{1}{6} + \frac{R}{E}\left(\frac{P}{E} - \frac{Y}{E}(1-2A)\right)}{\frac{1}{6} - \frac{2}{3}\frac{P}{E} + \frac{Y}{E}(1-2A)}$$

$$\text{And} \quad \therefore \quad \frac{R}{r} = \frac{\frac{1}{6} + \frac{RY}{EE}\left(\frac{P}{Y} - (1-2A)\right)}{\frac{1}{6} - \frac{2}{3}\frac{P}{Y}\cdot\frac{Y}{E} + \frac{Y}{E}(1-2A)} \qquad \text{------ (A8.9)}$$

2) No compressive yielding

$$E\varepsilon_d = Y \qquad \therefore \quad \varepsilon_d = \frac{Y}{E}$$

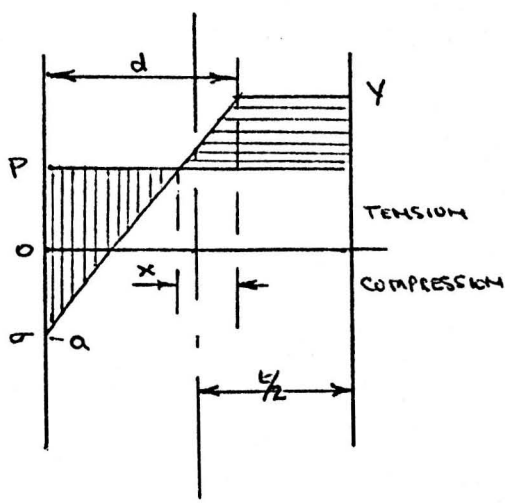

For any value of d:-

$$1 + (dl)_d = \frac{R+d}{R}\left(1 + (dl)_a\right)$$

$$1 + \frac{(dl)_d}{l} = \left(\frac{R+d}{R}\right)\left(1 + \frac{(dl)_a}{l}\right)$$

$$1 + \varepsilon_d = \left(\frac{R+d}{R}\right)\left(1 + \varepsilon_a\right)$$

$$1 + \varepsilon_d = 1 + \frac{d}{R}(1+\varepsilon_a) + \varepsilon_a.$$

$$\therefore \quad \varepsilon_d = \varepsilon_a + \frac{d}{R}(1+\varepsilon_a)$$

and $\frac{Y}{E} = \varepsilon_a + \frac{d}{R}(1+\varepsilon_a)$

$\therefore \quad d = \left(\frac{Y}{E} - \varepsilon_a\right)\frac{R}{1+\varepsilon_a}$

Equilibrium of cross section

area ≡ = area ////

x:-

$\frac{Y-P}{x} = \frac{P+\sigma}{d-x} \qquad \therefore \quad \frac{P+\sigma}{Y-P} = \frac{d-x}{x}$

$\therefore \quad x = \frac{d(Y-P)}{Y+\sigma}$

area ≡ = area ////

area ≡ + ▱ = area //// + ▱

$(Y-P)t = \frac{d}{2}(Y+\sigma)$

$2t\frac{(Y-P)}{(Y+\sigma)} = \left(\frac{Y}{E} - \varepsilon_a\right)\frac{R}{(1+\varepsilon_a)}$

$2t\frac{(Y-P)}{(Y-E\varepsilon_a)} = \left(\frac{Y}{E} - \varepsilon_a\right)\frac{R}{(1+\varepsilon_a)}$ and if $1+\varepsilon_a \longrightarrow 1$

then $\frac{2t}{E}\frac{(Y-P)}{\left(\frac{Y}{E} - \varepsilon_a\right)} \simeq \left(\frac{Y}{E} - \varepsilon_a\right)R$

$\therefore \quad \left(\frac{Y}{E} - \varepsilon_a\right)^2 \simeq \frac{2t}{ER}(Y-P)$

$$\therefore \quad \frac{Y}{E} - \varepsilon_a \simeq \pm\sqrt{\frac{2t}{ER}(Y-P)}$$

and $$\varepsilon_a \simeq \frac{Y}{E} - \sqrt{\frac{2t}{ER}(Y-P)}$$

or $$\varepsilon_a' = \frac{Y}{E} - \frac{Y}{E}\sqrt{\frac{2(1-\frac{P}{Y})}{\frac{RY}{Et}}}$$

where the dash is used to distinguish between the two cases ie case 1 and case 2.

Stress distribution across section

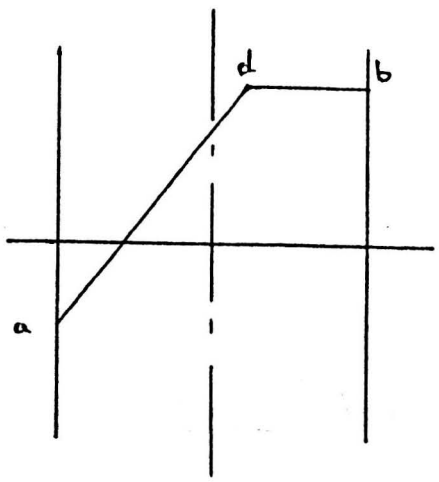

a - d:- $\sigma = E\varepsilon_d = E\left(\varepsilon_a + \frac{d}{R}(1+\varepsilon_a)\right)$

d - b:- $\sigma = +Y$

If radius after spring back is r then strain at distance d from inside fibres is

$$\varepsilon_d' = \varepsilon_a' + \frac{d}{r}(1+\varepsilon_a')$$

Change in strain is $\Delta\varepsilon = (\varepsilon_a' - \varepsilon_a) + \left(\frac{1+\varepsilon_a'}{r} - \frac{1+\varepsilon_a}{R}\right)d$

Residual stress is:- $\sigma_{res} = \sigma + E\Delta\varepsilon$

For zero resultant force in final state:-

$$\int_0^t \sigma_{res}\, dt = 0$$

$$a-d:- \quad \sigma_{res} = E\left(\varepsilon_a + \frac{d}{R}(1+\varepsilon_a)\right) + E\left(\varepsilon_a' - \varepsilon_a\right) + \frac{Ed}{r}(1+\varepsilon_a') - \frac{Ed}{R}(1+\varepsilon_a)$$

$$= E\left(\varepsilon_a' + \frac{d}{r}(1+\varepsilon_a')\right)$$

d - b:- $\quad \sigma_{res} = Y + E\left(\varepsilon_a' + \frac{d}{r}(1+\varepsilon_a')\right) - E\left(\varepsilon_a + \frac{d}{R}(1+\varepsilon_a)\right)$

$$\int_0^t \sigma_{res}\, dt = \int_d^t Y dt + \int_0^t E\left(\varepsilon_a' + \frac{d}{r}(1+\varepsilon_a')\right)dt - \int_d^t E\left(\varepsilon_a + \frac{d}{R}(1+\varepsilon_a)\right)dt$$

$$0 = Y(t-d) + E\varepsilon_a' t + \frac{E}{r}(1+\varepsilon_a')\frac{t^2}{2} - E\varepsilon_a(t-d) - \frac{E}{R}(1+\varepsilon_a)\left(\frac{t^2}{2}-d^2\right)$$

$$\varepsilon_a'\left(Et + \frac{Et^2}{2r}\right) = E\varepsilon_a(t-d) + \frac{E}{2R}(1+\varepsilon_a)(t^2-d^2) - \frac{Et^2}{2r} - Y(t-d) \quad \text{----} \quad (A8.10)$$

For zero resultant moment in final state:-

$$\int_0^t \sigma_{res}\, d\, dt = 0$$

$$\int_0^t \sigma_{res}\, d\, dt = \int_d^t Y d\, dt + \int_0^t E\left(\varepsilon_a' d + \frac{d^2}{r}(1+\varepsilon_a)\right)dt - \int_d^t E\left(\varepsilon_a d + \frac{d^2}{R}(1+\varepsilon_a)\right)dt$$

$$0 = \frac{Y}{2}(t^2-d^2) + \frac{E\varepsilon_a' t^2}{2} + \frac{Et^3}{3r}(1+\varepsilon_a') - \frac{E\varepsilon_a}{2}(t^2-d^2) - \frac{E(t^3-d^3)}{3R}(1+\varepsilon_a)$$

$$\varepsilon_a'\left(\frac{Et^2}{2} + \frac{Et^3}{3}\right) = \frac{E\varepsilon_a}{2}(t^2-d^2) + \frac{E}{3R}(t^3-d^3)(1+\varepsilon_a) - \frac{Et^3}{3r} - \frac{Y}{2}(t^2-d^2) \quad \text{----} \quad (A8.11)$$

Rewrite (A8.10):-

$$\varepsilon_a'\left(1 + \frac{t}{2r}\right) = \frac{\varepsilon_a}{t}(t-d) + \frac{1+\varepsilon_a}{2Rt}(t^2-d^2) - \frac{t}{2r} - \frac{Y}{Et}(t-d) \quad \text{- - - -} \quad (A8.12)$$

Rewrite (A8.11):-

$$\varepsilon_a'\left(1 + \frac{2t}{3r}\right) = \frac{\varepsilon_a}{t^2}(t^2-d^2) + \frac{2}{3Rt^2}(t^3-d^3)(1+\varepsilon_a) - \frac{2t}{3r} - \frac{Y}{Et^2}(t^2-d^2) \quad \text{----} \quad (A8.13)$$

(A8·12) can be written

$$\varepsilon_a'\left(1+\frac{t}{2r}\right) = \varepsilon_a + (1+\varepsilon_a)\frac{t}{2R} - \frac{t}{2r} - \left(\varepsilon_a\frac{d}{t} + (1+\varepsilon_a)\frac{d^2}{2Rt} + \frac{Y}{Et}(t-d)\right)$$

(A8·13) can be written

$$\varepsilon_a'\left(1+\frac{2t}{3r}\right) = \varepsilon_a + \frac{2t}{3R}(1+\varepsilon_a) - \frac{2t}{3r} - \left(\varepsilon_a\frac{d^2}{t^2} + \frac{2d^3}{3Rt^2}(1+\varepsilon_a) + \frac{Y}{Et^2}(t^2-d^2)\right)$$

$$= \varepsilon_a + \frac{2t}{3R}(1+\varepsilon_a) - \frac{2t}{3r} - \left(\frac{Y}{E} - \left(\frac{Y}{E}-\varepsilon_a\right)\frac{d^2}{t^2} + \frac{2(1+\varepsilon_a)d^3}{3Rt^2}\right)$$

$$= \varepsilon_a + \frac{2t}{3R}(1+\varepsilon_a) - \frac{2t}{3r} - A'$$

Now $\varepsilon_a\frac{d}{t} + (1+\varepsilon_a)\frac{d^2}{2Rt} + \frac{Y}{Et}(t-d) = \frac{Y}{E} + \left(\frac{Y}{E}-\varepsilon_a\right)\frac{d}{2t} - \frac{(1+\varepsilon_a)d^2}{Rt}$.

also $(Y-P)t = \frac{d}{2}(Y - E\varepsilon_a)$ $\therefore$ $\frac{d}{t} = \frac{2(Y-P)}{E\left(\frac{Y}{E}-\varepsilon_a\right)}$

whence $\left(\frac{Y}{E}-\varepsilon_a\right)\frac{d}{t} = \frac{2(Y-P)}{E} = \frac{2\left(1-\frac{P}{Y}\right)}{E/Y}$

and $\left(\frac{d}{t}\right)^2 = \frac{2RY}{Et}\left(1-\frac{P}{Y}\right) = \left(\frac{Y-P}{E}\right)\frac{2R}{t}$

$\therefore$ $\frac{d^2}{2Rt} = \frac{Y-P}{E}$

and $\varepsilon_a\frac{d}{t} + (1+\varepsilon_a)\frac{d^2}{2Rt} + \frac{Y}{Et}(t-d) = \frac{2Y}{E} - \frac{P}{E}$

$\therefore$ A8·12 becomes:-

$$\varepsilon_a'\left(1+\frac{t}{2r}\right) = \varepsilon_a + \frac{t}{2R}(1+\varepsilon_a) - \frac{t}{2r} + \frac{P}{E} - \frac{2Y}{E} \quad \text{---------- (A8·14)}$$

and A8·13 becomes:-

$$\varepsilon_a'\left(1+\frac{2t}{3r}\right) = \varepsilon_a + \frac{2t}{3R}(1+\varepsilon_a) - \frac{2t}{3r} - A' \quad \text{---------- (A8·15)}$$

where $A' = \frac{Y}{E} - \left(\frac{Y}{E}-\varepsilon_a\right)\frac{d^2}{t^2} + \frac{2}{3}(1+\varepsilon_a)\frac{d^3}{Rt^2}$

$$= \frac{1}{E/Y} - \left(\frac{1}{E/Y}-\varepsilon_a\right)\left(\frac{d}{t}\right)^2 + \frac{2}{3}(1+\varepsilon_a)\frac{\left(1-\frac{P}{Y}\right)}{E/Y}\frac{d}{t}$$

A 8·14 $$\left(1+\frac{2t}{3r}\right) = \varepsilon_a + (1+\varepsilon_a)\frac{t}{2R} - \frac{t}{2r} + \frac{P}{E} - \frac{2Y}{E} + \frac{2}{3}\varepsilon_a\frac{t}{r} + (1+\varepsilon_a)\frac{2t^2}{3Rr} - \frac{t^2}{3r^2} + \frac{2t}{3r}\frac{P}{E} - \frac{4t}{3r}\frac{Y}{E}$$

A 8·15 $$\left(1+\frac{t}{2r}\right) = \varepsilon_a + \frac{2t}{3R}(1+\varepsilon_a) - \frac{2t}{3r} - A' + \frac{\varepsilon_a t}{2r} + \frac{2t^2}{3Rr}(1+\varepsilon_a) - \frac{t^2}{3r^2} - \frac{A't}{2r}$$

whence $$\frac{R}{r} = \frac{\frac{1+\varepsilon_a}{6} + \frac{R}{t}\left(\frac{P}{E} - A'\right)}{\frac{1+\varepsilon_a}{6} - \frac{2}{3}\frac{P}{E} + \frac{A'}{2}}$$

or $$\frac{R}{r} = \frac{1+\varepsilon_a + \frac{6RY}{Et}\left(\frac{P}{Y} - \frac{E}{Y}A'\right)}{1+\varepsilon_a - 4\frac{P}{Y}\cdot\frac{Y}{E} + 3A'}$$

APPENDIX B1. BIBLIOGRAPHY.

The publications referred to in the text of the thesis appear in section B1.1 of this bibliography. Other works which might be consulted with advantage are listed in the sections B1.2 to B1.8. The section headings refer to the various aspects of the research reported in this thesis.

B1.1 References

Chapter 1

1. Wahl, A. M. - Mechanical Springs, McGraw-Hill 1963.
2. Chironis, N. (Ed.) - Spring Design and Application McGraw-Hill 1961.

3a. Timoshenko, S. - Strength of Materials, Pt.2, Van Nostrand, 1956.

3b. Timoshenko, S. - Strength of Materials, Pt.1, Van Nostrand, 1955.

4. Ashwell, D.G. - Anti-clastic Curvature of Rectangular Beams and Plates, J.R.Ae.Soc. V54, n 479, 1950, p.708.
5. Van Den Broek, J. A. - Spiral Springs, A.S.M.E. APM-53-18, 1931.
6. Gross, S. C. - The Spring Journal, No. 6, 1962.

Chapter 2

7. Timoshenko, S. & Woinowsky-Krieger, S. - Theory of Plates and Shells, McGraw-Hill; 1959.

Chapter 3

8. Kroon, R. P. & Davenport, C. C. - Journal of the Franklin Institute, Feb. 1938.
9. Associated Spring Corporation - Handbook of Mechanical Spring Design, 1958.

Chapter 7

10. Whiteside, J. B. - Ph.D. Thesis. The determination of residual stresses in torsion bars subjected to torsional overstrain. University of Sheffield, 1968.

11. Gardiner, F. J. - The spring-back of metals, Trans. A.S.M.E., Jan. 1957.

12. Woo, D. M. & Marshall, J. - Spring-back and stretch-forming of sheet metal, The Engineer, Aug. 1959.

Chapter 8

13. Sidebottom, O. M. & Chan, C. T. - Proc. 1st U.S. Cong. App. Mech., 1951, p.631.

14. Osgood, W. R. (Ed.) - Residual Stresses in Metals and Metal Construction;(Book), Reinhold, N.Y.

15. Symposium on Internal Stresses in Metals and Alloys, Inst. Metals, London, 1948.

16. King, R. - Ref. 15, p.13.

17. Greenough, G. B. - Ref. 14, p.285.

18. Hyler, W. S. & Jackson, L. R. - Ref. 14, p.297.

19. Thomas, D.E. - Ref. 15, p.25.

20. Cullity, B. D. - J. App. Phys., V35-6, 1964, p.1915.

21. Taira, S. & Arima, J. - Proc. 7th Jap. Cong. Test. Mat., 1964, p.21.

22. Kalakoutzky, N. - The Study of Internal Stresses in C.I. and Steel, London, 1888.

23. Howard, J. E. - Rept. 5992 of Tests of Metals, Watertown Arsenal, 1893, p.285 & 532.

24. Heyn, E. & Bauer, O. - J. Inst. Met., V12, 1914, p.3-37.

25. Mesnager, M. - Compt. Rend., V169, 1919, p.1391-93.

26. Sachs, G. - Internal Stresses in Piston Rods of a Large Diesel Engine, Trans. Am. Soc. Met., V27, 1939, p.821.

27. Fuchs, H. O. & Mattson, R. L. - Proc. S.E.S.A., V4, n 1, 1946, p.64.

28. Treuting, R. G. & Read, W. T. - J. App. Phys., V22, 1951, p.130-4.

29. Loxley, E.M. - Ph.D. Thesis, University of Sheffield, 1955.

30. Hill, P. V. - B.Eng. Thesis, University of Sheffield, 1956.

31. Taira, S. & Yoshioka, Y. - Bull. J.S.M.E., V8, n 31, 1965, p.307.

32. Jackson, J. S. - Ph.D. Thesis, University of Birmingham, 1951.

33. Botros, B. M. - Ph.D. Thesis, University of Sheffield, 1956.

Chapter 9

34. Sachs, G. & Espey, G. - The Measurement of Residual Stresses in Metals, Iron Age, V148, n 12, p.63 and n 13, p.36.

Chapter 11

35. Associated Spring Corporation - Handbook of Mechanical Spring Design, A.S.C., 1958.

B1.2 Literature on spiral springs

1. Alexander, B. - Methods of Spiral Spring Design, Airc. Eng., V23, no.266, 1951, p.113.
2. Berry, W. R. - Practical problems in spring design: P.I.M.E., 139, 1938, p.431.
3. Camm, F. J. - Newnes Engineer's reference book, 6 ed.
4. Davidenkov, N. N. (Haynes, R. ed.) - Problems in design, production and service life of springs, N.L.L. Boston Spa.
5. Gross, S. C. - Calculation and design of metal springs, Chapman Hall, 1966.
6. Gross, S. C. - Formula for clock springs, S.M.R.A. Records, May 1960.
7. Gross, S. C., Lehr, E. & Speer, P. - Die Federn. Ihre Gestaltung und Berechnung. Z.VDI, V82, 1938, p.1415.
8. Joerg, E. - The spiral spring as a means of driving in spring mechanisms and clocks, Feinwerktechnik, V58, no.3, 1954, p.81.
9. Keil, W. - The design of springs in the spring barrel of clocks, Z. f. Instrumentenkunde, V55, 1935, p.183.
10. Keitel, H. - The calculation of flat spiral springs with rectangular cross section, Draht 8, no.8, 1957, p.326.
11. Morley, A. - Strength of Materials, Longman's Green, 1923.
12. Phillips, E. - Mémoire sur le spiral réglant des chronomètres et des montres, Jour. de Math, Ser 2T, Paris, 1860, p.313.
13. also, same title, Annales des Mines, Tome XX, Paris, 1861, p.1.

14. Popplewell, W. C. & Carrington, H. - Properties of engineering materials, Methuen, 1923.

15. Redford, G. D. - Mechanical engineering design, Macmillan, 1966.

16. Roberts, J. A. - Spring Design and Calculations, 11 ed., H. Terry, 1961.

17. Ryder, G. H. - Strength of Materials, Cleaver-Hume, 1954.

18. S.A.E. - Manual on design and application of Helical and spiral springs, TR-9, S.A.E., 1958.

19. Salter, G. - Salter Springs, Salter Springs, 1943.

20. Schwarz, M. V. - Spiral Springs, Z.VDI V76, 1932, p.393.

21. Tatarinoff, V. - The design of spiral springs, Machinery, V71, no.1823, 1947, p.375.

22. Tatarinoff, V. - Graphical Spring Design, Machinery Pub. Co. 1954.

23. Todhunter, I. & Pearson, K. - A history of the theory of elasticity, V2, Dover, 1960.

24. Tuting, W. - What we need to know regarding driving springs, Draht 7, V1, 1956.

25. Votta, F. A. & Lansdale, P. A. - The theory and design of long-deflection constant-force spring elements, Trans. A.S.M.E.

26. Wadlow, E. C. - Spiral Springs, Machinery, V46, no.1197, 1935, p.775.

27. Wehr, G. - Calculation of flat spiral springs, A.G.T. Anzeiger - Die Maschine, V5/6, 1956.

B1.3 Mathematics of the spiral

1. Caunt, G. W. - Introduction to infinitesimal calculus, Oxford, 1949.

2. Edwards, J. - Differential calculus, Macmillan, 1942.

3. Martin, W. T. & Reissner, E. - Elementary Differential Equations, Addison-Wesley, 1961.

4. Rectorys, K. - Survey of Applicable Mathematics, Iliffe, 1969.

5. Wayland, H. - Differential Equations, Van Nostrand, 1958.

6. Wylie, C. R. - Advanced Engineering Mathematics, McGraw-Hill, 1960.

B1.4 Elastic and plastic properties of materials

1. Ball, C. S. - The mechanical properties of quenched and tempered spring steels, Coil Spring Jour., 12, Sept. 1948.

2. Brewer, G. A. - Measurement of strain in the plastic range, Proc. S.E.S.A., V1, n 2, 1944, p.105.

3. Coker, E. G. - Apparatus for measuring strain and applying stress, Phil. Trans. Roy. Soc. Ed., 40(II), 1901, p.263.

4. Dour, J. E. & Lat ter, J. E. - Stress-strain relations for finite elasto-plastic deformations. J. App. Mech., Sept. 1948.

5. Drucker, D. C. - A more fundamental approach to plastic stress-strain relations, Proc. 1st U.S. Cong. App. Mech., A.S.M.E., 1951, p.487.

6. Drucker, D. C. - A reconsideration of deformation theories of plasticity, Trans. A.S.M.E., 1949, p.587.

7. Dudukalenko, V. V. & Inley, D. D. - On the torsion of anisotropically work hardening prismatic rods, Izv. Akad. Nauk SSR, Otd Nauk, Mek, i. Mash, No.4, 1963, p.79-85.

8. Fields, D. S. & Backoffen, W. A. - Determination of strain - hardening characteristics by torsion testing, Proc. A.S.T.M., V57, 1957, p.1259.

9. Freudenthal, A. M. - General law of work-hardening, J. Frank. Inst., 1949.

10. Hill, R. - The plastic torsion of anisotropic bars, J. Mech. Phys. Solids, V2, 1954, p.87.

11. Johnson, W. & Mellor, P. B. - Plasticity for Mechanical Engineers, Van Nostrand, 1962.

12. Kuznetsov, A. I. - The problem of torsion and plane strain of non-homogeneous plastic bodies, Arch. Mech. Stos, V10, n 4, 1958.

13. Lubahn, J. D. & Felgar, R. P. - Plasticity and creep of metals, Wiley, 1961.

14. Marcal, P. V. & Prager, W. - A method of optimal plastic design, J. Mecan. V3, n 4, 1964, p.509.

15. Morrison, J. L. M. - The yield of mild steel with particular reference to the effect of size of specimen, P.I.M.E., V142, 1940, p.193.

16. Morrison, J. L. M. - The criterion of yield of gun steels, P.I.M.E., V159, 1948, p.81.

17. Nadai, A. - Plasticity, McGraw-Hill, 1931.

18. Neuber, H. - Anisotropic non-linear stress-strain laws and yield conditions, Int. J. Sol. & Struc., V5, 1969, p.1299.

19. Olszak, W., Mroz, Z. & Perzyna, P. - Recent trends in the development of the theory of plasticity, Perg. Press, 1963.

20. Osgood, W. R. - Stress-strain formulae, J. Aero. Sci., V13, n 1, 1946, p.43.

21. Oxley, P. L. B., Humphreys, A. G. & Larizaden, A. - The influence of strain hardening in machining, P.I.M.E., V175, n 8, 1961, p.881.

22. Prager, W. & Hodge, P. G. - Theory of perfectly plastic solids, Wiley, 1951.

23. Prager, W. - An introduction to the mathematical theory of plasticity, J. Appl. Phys., V18, 1947, p.375.

24. Prager, W. - The stress-strain laws of the mathematical theory of plasticity - a survey of recent progress, J. App. Mech., V70, 1948, p.226.

25. Prager, W. - Introduction to plasticity, Ad. Wes., 1959.

26. Ramberg, W. & Osgood, W. R. - Description of stress-strain curves by three parameters, N.A.C.A. Tech. Note 962, July 1943.

27. Richards, C. W. - Engineering Materials Science, Chapman & Hall, 1961.

28. Sachs, G. - Z. Metallkunde, V16, p.55, 1924

29. Shepherd, W. M. - Plastic stress-strain curves, P.I.M.E., V159, 1948, p.95.

30. Swainger. - Compatability of stress and strain in yielded metals, Phil. Mag., Ser 7, No.36, 1945, p.443.

31. Taylor, G. I. & Quinney, H. - The plastic distortion of metals, Trans. Roy. Soc., A, 230, 1931, p.323.

32. Thompson, E. G. - Plasticity equations on applications to working of metals in the work-hardening region, Trans. A.S.M.E., V78, 1956, p.407.

33. Watts, A. B. & Ford, H. - On the basic yield stress curve for a metal, P.I.M.E., V169, 1955, p.1141.

34. Whiteman, I. R. - A mathematical model depicting the stress-strain diagram and hysteresis loop, Trans. A.S.M.E., V26, 1959, p.95.

35. Wilshaw, T. R. - Review of special techniques for measuring plastic strain, AGARD rpt. 569, 1969.

36. Winger, A. & Prager, W. - On the use of power laws in stress analysis beyond the elastic range, J. App. Mech., 1947, p.281. Discussion - J. App. Mech., 1948, p.185.

37. Zener, C. & Holloman, J. H. - Problems in non-elastic deformation of metals, J. App. Phys. V17, 1946, p.69.

B1.5 Anti-clastic behaviour

1. Ashwell, D. G. - The anticlastic curvature of rectangular beams and plates, J.R.Ae.S., V54, n479, 1950, p.708.

2. Ashwell, D. G. - A characteristic type of instability in the large deflections of elastic plates, Proc. Roy. Soc. (A), V214, 1952, p.98.

3. Ashwell, D. G. - On the deformation of flat plates into cones, Q.J.Mech.Ap. Math., V16, n 2, 1963, p.163.

4. Ashwell, D. G. - The inextensional twisting of a rectangular plate, Q. J. Ap. Math., V15, n 1, 1962, p.91.

5. Ashwell, D. G. & Greenwood, E. D. - The pure bending of rectangular plates, Engineering, July 1950, p.51 & p.76.

6. Bellow, D. G., Ford, G. & Kennedy, J. S. - Anticlastic behaviour of flat plates, Paper 911, S.E.S.A. Annual Meeting, Oct. 1964.

7. Conway, H. D. & Nickola, W. E. - Anticlastic action of flat sheets in bending, Paper 895, S.E.S.A. Annual Meeting, Oct. 1964.

8. Conway, H. D. & Lo, C. F. - Further studies on the elastic stability of curved beams, Int. J. Mech. Sci., V9, n 10, 1967, p.707.

9. Friedrichs, K. O. - The edge effect in the bending of plates, Reissner Anniv. Volume. Ann Arbor, 1949.

10. Fung, Y. C. & Wittrick, W. H. - A boundary layer phenomenon in the large deflection of thin plates, Q. J. Mech. & App. Math. 1955.

11. Kelvin, W. T. & Tait, P. G. - A treatise on Natural Philosophy, 2 ed., Cambridge, 1890.

12. Lamb, H. - On the flexure of a flat elastic spring, Phil. Mag. 1891.

13. Nickola, W. E., Conway, H. D. & Farnham, K. A. - Moiré, Study of anticlastic deformation of strips with tapered edges, Exp. Mech., V7, 1967, p.168-175.

14. Pomeroy, R. J. - Effect of anticlastic bending on the curvature of beams, Int. J. Sol. Struc., V6, n 2, 1970.

15. Reissner, E. - Spannungen in Kugelschalen, Festschrift Mueller - Breslau (Leipzig) 1912.

16. Searle, G.F.C. - Experimental Elasticity, Cambridge, 1908.

Bl.6 Bending of strip and plate

1. Benedyk, J. C. & Newnham, J. A. - Springback of cold-rolled copper foil after bending under tension, J.I.M, V98, 1970.

2. Biot, M. A. - Mechanics of incremental deformations, Wiley, 1965.

3. Billard, A. - Theory of elasticity of a coiled circular wire, Mem. Artill. Fr., V37, n 3, 1963, p.605.

4. Bolz, R. W. - Metals Engineering Processes (A.S.M.E. Hdbk.) McGraw-Hill, 1958.

5. Bui, H. D. & Dangvan, K. - Stress rate boundary value problem of an elasto-plastic body, In. J. Sol. Struc., V6, n 1, 1970.

6. Gardiner, F. J. & Carlson, H. R. C. - The spring-back of coil springs, Mech. Eng., V80, p.74, 1958.

7. Goodier, J. N. & Griffin, D. S. - Elastic bending of pre-twisted bars, Int. J. Sol. Struc., V5, n 1, 1969.

8. Ingerle, K. - Flexural stiffness of rectangular bar component made of ideal elastic-plastic material, Oestereichische Ing-Z, V12, n 10, 1969.

9. Maunder, L. & Reissner, E. - Pure bending of pre-twisted rectangular plates, J. Mech. Phys. Sol., V5, 1957.

10. Prager, W. & Shield, R. T. - Optimal design of multi-purpose structures, Int. J. Sol. Struc., V4, n 4, 1968, p.469.

11. Shackell, K. K. & Welsh, I. K. - Plastic flexure of mild steel beams of rectangular cross-section, P.I.M.E., V166, 1952, p.112.

12. Sielaff, D. W. - Preforming. A cure for flats, Tool & Mfg. Eng. V62, n 10, 1969.

13. Swift, H. W. - Plastic bending under tension, Engg., V166, 1948, p.333 also p.357.

14. Tuba, I. S. - An elastic-plastic curved bar analysis, Trans. A.S.M.E., V87(D), n 4, 1965, p.894.

15. Woo, D. M. - Plastic deformation of sheet metal in axisymmetric forming processes, Ph.D. Thesis, Sheffield.

16. Woo, D. M. - On the variation of tension in stretch-forming a metal strip, J. App. Mech., V25, n 4, 1958, p.623.

17. Woo, D. M. - The analysis of axisymmetric forming of sheet metal and the hydrostatic bulging process, Int. J. Mech. Sci., V6, 1964.

B1.7 Residual Stress

1. Almen, J. O. - Effect of residual stress on the fatigue of metals, Prod. Eng., V14, June 1943, p.348.

2. Baldwin, W. M. - Residual stresses in metals, Edgar Marburg Lecture, 52nd annual meeting A.S.T.M., 1949.

3. Barret, C. S. - A critical review of various methods of residual stress measurement, Proc. S.E.S.A., V2, n 1, 1944, p.147.

4. Becker, M.L. & Phillips, C. E. - Internal stresses and their effect on the fatigue resistance of spring steels, J.I.S.I., V133, 1936, p.427.

5. Birger, I.A. - Determination of residual stresses in thin-walled tubes, Indust. Lab., V28, n 9, 1963, p.1182.

6. Blain, P. A. - The influence of residual stress on hardness, Met. Prog., Jan. 1957, p.99.

7. Blum, W. & Hogaboom, G. B. - Principles of electroplating and electroforming, 3 ed., McGraw-Hill, 1949.

8. Colwell, L. V., Sinnott, M.I. & Tobin, J. C. - The determination of residual stresses in hardened ground steel, Trans. A.S.M.E., V77, 1955, p.1099.

9. Corten, H. T. & Elsesser, T. M. - The effect of slightly elevated-temperature treatment upon microscopic and sub-microscopic residual stresses induced by small elastic strains in metals, Trans. A.S..M.E., V74, 1952, p.1297.

10. Davidenkov, N. N. - Bereschnung der Restspannungen in kaltgezogenen Rohren, Z f. Metallkunde, 1932.

11. Demorest, D. J. & Leeser, D. O. - A study of Residual Stresses in Flat Beams by Electro-polishing methods, Proc. S.E.S.A., V11, n 1, 1953, p.45.

12. Denton, A. A. & Alexander, J. M. - On the determination of residual stresses in tubes, J. Mech. Eng. Sci., V5, n 1, 1963, p.89.

13. Ferril, D. A., Juhl, P. B. & Miller, D. R. - Measurement of residual stresses in a heavy weldment, Weld. J., V45, n 11, 1966, p.504s

14. Foppl, H. - The evaluation of macroscopic residual stresses in cylindrical bars, J.I.S.I., V168, 1951, p.15.

15. Frisch, J. & Thomsen, E. G. - Residual stresses in cold extruded aluminium, Trans. A.S.M.E., V79, 1957, p.155.

16. Geller, Y. A. & Shrieber, G. K. - Effect of residual stresses on the limit of fatigue in tempered steel, J. Tech. Phys., V11, 1941, p.700.

17. Gencsoy, H. T. & O'Leary, J. P. - Residual stresses in a butt-welded flat plate, Weld. J., V44, n 2, 1965, p.56s.

18. Graham, A. K. - Electro-plating Engineering handbook, Reinhold, 1955.

19. Gray, A. G. - Modern electro-plating, Wiley, 1953.

20. Greaves, R. H. - Overstrain and elastic recovery in relation to pre-stressing, Coil Sp. J., V10, March 1948.

21. Greenough, G. B. - Residual lattice strains in plastically deformed polycrystalline metal aggregates, Proc. Roy. Soc., A197, 1949, p.556.

22. Henricksen, E. K. - Residual stresses in machined surfaces, Trans. A.S.M.E., V73, 1951, p.69 & p.461.

23. Huang, T. C. - Bibliography on Residual Stress, S.A.E., Sp.125, 1954.

24. Heindlhofer, K. - Evaluation of residual stress, McGraw-Hill, 1948.

25. Hetenyi, M. - Handbook of experimental stress analysis, Wiley, 1950.

26. Horger, O. J., Neifert, H. R. & Regen, R. R. - Residual stresses and fatigue studies, Proc. S.E.S.A., V1, n 1, 1943, p.10.

27. Horger, O. J. - Metals Engineering Design (A.S.M.E. hdbk.), McGraw-Hill, 1965.

28. Institute of Metals - Symposium on internal stresses in metals and alloys, Inst. Met. Monograph and rept. ser. No. 5, 1947.

29. Johnson, L. G. - The effect of shearing on the residual stress in plates, Ind. math. soc., V3, 1952, p.42.

30. Johnson, L. G. - Derivation of the fundamental equation of residual stress analysis by dissection, Ind. Math. Soc. V5, 1955, p.7.

31. Johnson, L. G. - The effect of residual stresses on indentation hardness, Ind. Math. Soc. V6, 1955, p.75.

32. Kobrim, M. M. & Dekhtyar, L. I. - Improved extrapolation and checking of incomplete curves in determining residual stresses by the Sachs method, Indust. Lab. V28, n 9, 1963, p.1188.

33. Lambert, J. W. - A method of deriving residual stress equations, Proc. S.E.S.A., V12, n 1, 1954, p.91.

34. Leaf, W. - Techniques in residual stress analysis, Proc. S.E.S.A., V9, n 2, 1952, p.133.

35. Leeser, D. O. & Daane, R. A. - Residual stresses in a strip in terms of strain changes during electropolishing, Proc. S.E.S.A., V XII, n 1, 1953, p.203.

36. Letner, H. R. - Application of optical interference to the study of residual surface stresses, Proc. S.E.S.A., V10, n 2, 1952, p.23.

37. Letner, H. R. - Residual grinding stresses in hardened steel, Trans. A.S.M.E., V77, 1955, p.1090.

38. Letner, H. R. - Influence of grinding fluids upon residual stresses in hardened steel, Trans. A.S.M.E., V79, 1957, p.149.

39. Loxley, E. M. - Residual stresses in cold-drawn tubes, Ph.D. Thesis, Sheffield, 1955.

40. Marcal, P. V. - A stiffness method for elastic-plastic problems, Int. J. Mech. Sci., V7, n 4, 1965, p.229.

41. Mathar, J. - Determination of initial stresses by measuring the deformation around drilled holes, Trans. A.S.M.E., V56, 1934, p.249.

42. Mattson, R. L. & Coleman, W. S. - Effect of shot peening variables and residual stress on the fatigue life of leaf spring specimens, S.A.E.Qu. Trans., V62, 1954, p.546.

43. Messnager, N. - Méthods de détermination des tensions existant dans un cylindre circulaire, Comp. Rendus, Acad. des Sci., V169, 1919, p.1391.

44. Pattinson, E. J. - The effect of residual stresses on fatigue strength, Ph.D. Thesis, U. of Wales, 1961.

45. Rembowski, J. L. - Theory for the calculation of the tangential residual stress distribution in curved beams, Proc. S.E.S.A., V16, n 1, 1958, p.195.

46. Richards, D. G. - A study of certain mechanically-induced residual stresses, Proc. S.E.S.A., V 3, n 1, 1945, p.40.

47. Sachs, G. - Residual stress in cylinders (German), Z. f. Metallkunde, V19, 1927, p.352.

48. Sachs, G. - Internal stresses in metals, Zeitschrift, V71, 1927, p.1511.

49. Sachs, G. - The determination of residual stresses in rods and tubes, Trans. A.S.M.E., V27, 1939, p.821.

50. Sachs, G. & Van Horn, K. R. - Practical metallurgy, A.S.M., Cleveland, 1940.

51. Schwaighofer, J. - Determination of residual stresses on the surface of structural parts, Exp. Mech., Feb. 1964, p.54.

52. Sopwith, D. G. - The production of favorable internal stresses in helical compression springs by pre-stressing, Symp. Int. Stress, Inst. Metals, Oct. 1947, p.195.

53. Taira, S. & Murakami, Y. - Effect of residual stress on fatique strength, 5th Jap. Cong. Test. Mat., 1962.

54. Watson, R. L. & Coleman, W. S. - Effect of shot peening variables and residual stress on the fatigue life of leaf spring specimens, Trans. S.A.E., V62, 1954, p.548.

55. Weinman, E. W., Hunter, J. E. & McCormack, D. D. - Determining residual stresses rapidly, Met. Prog., V96, n 1, 1969.

56. Zahn, J. J. - Residual stresses in curved laminated wood beams, Proc. A.S.C.E., V95, n ST12, 1969.

Bl.8 Bauschinger Effect

1. Baushis, I. P. - Device for studying stress relaxations, Ind. Lab., V29, n 9, 1964, p.1237.

2. Coffin, L. F. - The influence of mean stress on the mechanical hysterisis loop shift of 1100 aluminium, Trans. A.S.M.E., V86-D, 1964, p.673.

3. Elsesser, M., Sidebottom, O. M. & Corten, H. T. - The influence of aging on the Bauschinger effect in inelastically strained beams, Trans. A.S.M.E., V74, 1952, p.1291.

4. Milligan, R. V., Koc, W.H. & Davidson, T. E. - The Bauschinger effect in a high strength steel, Metals Eng. & Prod. Eng. Conference, N.Y. 1965.

5. Polakowski, N. H. - Bauschinger effect in single crystals, J.I.S.I., V172, 1952, p.369.

6. Sidebottom, O. M. & Chan, C. T. - Influence of the Bauschinger effect on inelastic bending of beams, 1st U.S. Nat. Cong. App. Mech., 1951, p.631.

7. Woolley, R. L. - The Bauschinger effect in some face-centred and body-centred cubic materials, Phil. mag., V44, n 353, 1953, p.597.